SYNTHESIS AND CHARACTERIZATION OF NOVEL MORTIA-BAYLIS HILLMAN COMPLEXES AND IT'S APPLICATION

A project submitted to

ST MARY'S COLLEGE (Autonomous), Thoothukudi

Affiliated to

Manonmaniam Sundaranar University,

Tirunelveli

In partial fulfilment of the award of the degree of

MASTER OF SCIENCE IN CHEMISTRY

Submitted by

M. Agnes Mary

Reg. No: 21SPCH01

Under the Supervision and Guidance of

Mrs. R. Pratheeba M.Sc. M.Phil.,

PG DEPARTMENT OF CHEMISTRY (SSC)

St. Mary's College (Autonomous),

Thoothukudi

April 2023

CERTIFICATE

This is to certify that this project work entitled **"SYNTHESIS AND CHARACTERIZATION OF NOVEL MORTIA-BAYLIS HILLMAN COMPLEXES AND IT'S APPLICATION"** is submitted to **St. Mary's College (Autonomous), Thoothukudi** affiliated to **Manonmaniam Sundaranar University**, Tirunelveli in partial fulfilment for the award of the **Degree of Master of Science in Chemistry** and this work done during the year 2022 - 2023 by **M. AGNES MARY (Reg. No: 21SPCH01)**

Signature of the Guide

15/4/23

Signature of the Coordinator

Dr. J. ANTONY RAJAM, M.Sc., M.Phil., Ph.D., SET.
Staff Coordinator & Associate Professor
Post Graduate Department of Chemistry
St. Mary's College (Autonomous)
Thoothukudi - 628 001.

Signature of the Director

Director
Self Supporting Courses
St. Mary's College (Autonomous)
Thoothukudi - 628 001.

Signature of Principal

Principal
St. Mary's College (Autonomous)
Thoothukudi - 628 001.

Signature of the Examiner

13/4/23

DECLARATION

I do hereby declare that the project entitled **"SYNTHESIS AND CHARACTERIZATION OF NOVEL MORTIA-BAYLIS HILLMAN COMPLEXES AND IT'S APPLICATION"** submitted for the degree of Master of Science in Chemistry is my original work carried out under the guidance of **Mrs. R. Pratheeba M.Sc., M.Phil., Assistant Professor, PG Department of Chemistry (SSC), St. Mary's College (Autonomous), Thoothukudi** and that it has not previously formed the basis for award of any Degree.

Station: Thoothukudi

M. Agnes Mary

Date: 05.04.2023 **M. Agnes Mary**

ACKNOWLEDGEMENT

I express my first and humble thanks to **GOD ALMIGHTY** for giving an opportunity to devote this work

I would like to express my sincere thanks to our Principal **Dr. Sr. A.S.J. LUCIA ROSE**, Secretary **Sr. FLORA MARY**, Deputy principal **Dr. Sr. S. KULANDAI THERESE**, Director of SSC **Sr. JOSEPHINE JEYARANI** and **Dr. J. ANTONY RAJAM M.Sc., M. Phil., SET, Ph.D,** (SSC Coordinator), St Mary's College (Autonomous), Thoothukudi for providing the permission to complete the project work

I find it difficult for me to write something in short to acknowledge my guide **Mrs.R**. **Pratheeba M.Sc., M.Phil**. , she taught me to think and solve the unconventional problems in a conventional way. Her constant inspiration, evaluable guidance tremendous patience and constructive criticism helped a lot to focus my views in the proper perspective I take this opportunity to express my deepest sense of gratitude and reference towards her for guiding me in the right direction throughout the course of this work.

I heartily express my sincere thanks to my parents and friends.

ABSTRACT

"SYNTHESIS AND CHARACTERIZATION OF NOVEL MORTIA-BAYLIS HILLMAN COMPLEXES AND IT'S APPLICATION"

Novel Mortia-Bayllis Hillman adduct has been synthesized. The Baylis– Hillman adducts and their derivatives have been extensively utilized for the generation of heterocyclic and other cyclic frameworks.The most common catalysts in synthetic use are DABCO (1, 4diazabicyclo [2.2. 2] octane), quinuclidine, and cinchona-derived alkaloids, all of which have a tertiary amine nucleophile. We chose the MBH reaction between Benzaldehyde derivatives and methyl acrylate derivatives using DABCO as catalyst.

The synthesized compound were characterized by mass spectroscopy , functional group present in it by IR spectroscopy, further UV and fluorescence spectra support the formation of complexes with metal ions.

The prepared MBH adduct forms complex with Zinc and Silver ions. The formation of metal complexes extend its application as antibacterial compound in the biological field.

Keywords

- Mortia-Baylis Hillman Adduct
- Metal Complexes
- Antibacterial Activity

Content

LIST OF ABBREVATIONS

MBH	Morita Baylis hillmann adduct
Hg^{2+}	Mercury ions
Zn^{2+}	Zinc ions
UV Spectroscopy	Ultra violet Visible Spectroscopy
FT-IR Spectroscopy	Fourier Transform Infrared Spectroscopy

CHAPTER – 1

INTRODUCTION

Introduction

1.1 Emergence of Organic Complexes as Antimicrobes and Anti-bacterial

Neglected tropical diseases (NTDs) are those that occur primarily in poor countries. Drugs to treat these diseases are few, and usually lead to severe side effects, since the buying power of these populations is very low, not being attractive to global pharmaceutical industries to invest money on the development of drugs for these diseases [1]. Due to inexistence of vaccines for humans and that the available chemotherapy is toxic and expensive, research aiming to obtain new efficient drugs is of great urgency.

Many of the diseases that affect the human health are associated with infectious agents. The microorganisms that colonize the target organisms contribute to the development of numerous clinical conditions: such as dental caries, periodontal, endodontic, and periapical diseases and others. The pathogenicity of microorganisms depends on their virulence and the state of the host. The microorganisms found in hospitals appear to be more resistant because they promote high morbidity and difficult eradication of these infections [2]. Due to excessive and indiscriminate use of first-generation drugs and the consequent growing increase of bacterial **[3]** and fungal [4] [5] resistance, the antimicrobial effects of many substances for clinical use are being intensely studied. Some new options for treatment of these diseases have been proposed including modified molecules. Morita-Baylis Hillman adducts (MBHA) are molecules derived from Morita-Baylis-Hillman reactions (MBHR), which consist of alkene group coupling between molecules containing electron attracting groups (EAG), and aldehydes, ketones and imines in the presence of a nucleophilic catalyst, typically a tertiary amine [6], such

as the 1,4- diazabicyclo-[2.2.2]-octane (DABCO) is an example of MBHR [7]. This reaction results in different molecules that can have biological effect. These MBHA have been employed in several applications as starting material for organic synthesis products, such as antiparasitics [6] [8], neoplastics [9] [10] [11], antioxidant [12] and anti-inflammatory [11] [13]. Although some molecules of MBHA have been previously evaluated in parasites and bacteria, different molecules need to be studied. In addition, there are no reports of the antimicrobial evaluation against pathogens including fungal species using simple organic compounds. Thus, the objective of this study was to evaluate the antimicrobial effect of Morita-Baylis-Hillman adducts against common pathogens, aiming at the future use of these compounds in antimicrobial therapy.

1.2 Baylis Hillmann reaction

The **Baylis–Hillman reaction** is a carbon-carbon bond forming reaction between the α-position of an activated alkene and a carbon electrophile such as an aldehyde. Employing a nucleophilic catalyst, such as a tertiary amine and phosphine, this reaction provides a densely functionalized product (e.g. functionalized allyl alcohol in the case of aldehyde as the electrophile) [14] [15]. It is named for Anthony B. Baylis and Melville E. D. Hillman, two of the chemists who developed this reaction while working at Celanese. This reaction is also known as the **Morita–Baylis–Hillman reaction** or **MBH reaction**, as K. Morita had published earlier work [16] on it.

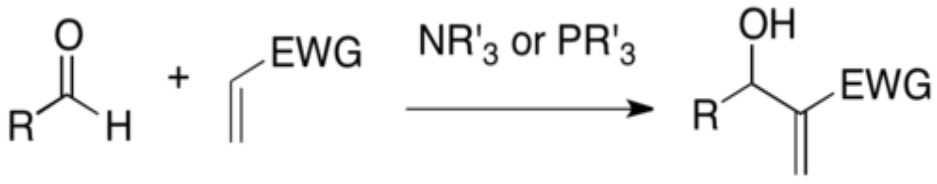

……Eq 1

Due to the presence of -OH group it acts as sensor of certain metal ions. Also, most of the Morita Baylis hillmann adduct act as antimicrobial or antibacterial agent by simple one pot synthesis.

DABCO is one of the most frequently used tertiary amine catalysts for this reaction. In addition, nucleophilic amines such as DMAP and DBU as well as phosphines have been found to successfully catalyze this reaction.

MBH reaction has several advantages as a useful synthetic method:

- It is an atom-economic coupling of easily prepared starting materials.
- Reaction of a pro-chiral electrophile generates a chiral centre, therefore an asymmetric synthesis is possible.
- Reaction products usually contain multiple functionalities in a proximity so that a variety of further transformations are possible.
- It can employ a nucleophilic organo-catalytic system without the use of heavy metal under mild conditions.

Several reviews have been written based on biological application of MBH adduct including antimicrobial activity, antihistamine agent and anticancer agent. [17][18][19][20][21]

1.3 DABCO

DABCO (**1,4-diazabicyclo[2.2.2]octane**), also known as **triethylenediamine** or **TEDA**, is a bicyclic organic compound with the formula $N_2(C_2H_4)_3$. This colourless solid is a highly nucleophilic tertiary amine base, which is used as a catalyst and reagent in polymerization and organic synthesis.[22] It is similar in structure to quinuclidine, but the latter has one of the nitrogen atoms replaced by a carbon atom.

The PK_a of $[HDABCO]^+$ (the protonated derivative) is 8.8, which is almost the same as ordinary alkylamines. The nucleophilicity of the amine is high because the amine centers are unhindered. It is sufficiently basic to promote C–C coupling of terminal acetylenes, for example, phenylacetylene couples with electron-deficient iodoarenes.

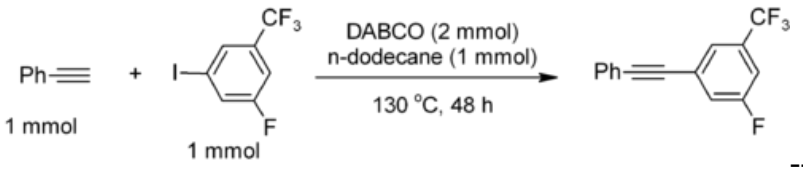

----------Eq 2

Catalyst

DABCO is used as a base-catalyst for- Formation of polyurethane from alcohol and isocyanate functionalized monomers and pre-polymers [23]. Baylis-hillmann adduct of aldehydes and unsaturated ketones and aldehydes.[24]

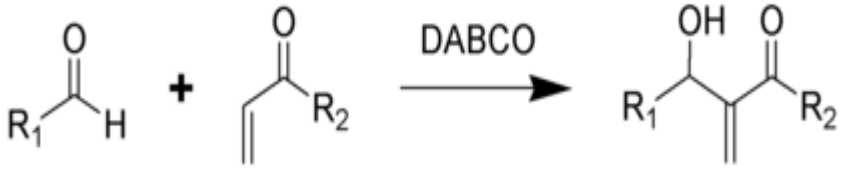

……Eq 3

Lewis base

As an unhindered amine, it is a strong ligand and lewis base. It forms a crystalline 2:1 adduct with hydrogen peroxide [25] and sulfur dioxide [26].

Quencher of singlet oxygen

DABCO and related amines are quenchers of singlet oxygen and effective antioxidants, [27] and can be used to improve the lifetime of dyes. This makes DABCO useful in dye lasers and in mounting samples for fluorescence microscopy (when used with glycerol and PBS) [28]. DABCO can also be used to dimethylate quaternary ammonium salts by heating in dimethyl formamide (DMF). [29]

Production

It is produced by thermal reactions of compounds of the type $H_2NCH_2CH_2X$ (X = OH, NH_2, or NHR) in the presence of zeolitic catalysts. An idealized conversion is shown for the conversion from ethanolamine. [30]

$3\ H_2NCH_2CH_2OH \rightarrow N(CH_2CH_2)_3N + NH_3 + 3\ H_2O$

Advantage of DABCO as Organic Catalyst

DABCO has more advantages than other organic catalysts because it is an inexpensive, nontoxic base, an ecofriendly and a highly reactive catalyst for building of organic frameworks, which

produce the desired products in excellent yields with high selectivity. In chemical and biological defense, activated carbon is impregnated with DABCO for use in filters for collective protection system. [31]

1.4 Application as Antimicrobials

The Morita-Baylis-Hillman adducts (MBHAs) are being explored as drug candidates against several diseases, one of them being leishmaniasis [32]. These compounds are prepared from the Morita-Baylis-Hillman reaction [33,34] in green conditions from aldehydes (among other electrophiles) or alkenes connected to electron attractor groups (EAG, like methyl acrylate, acrylonitrile, and others) under basic catalysis (DABCO being the most common base, **Scheme 1** and the MBHA (**3**) resulting in the development of a chalcone-like compound (**1**) that is more active as a leishmanicide than corresponding precursors [35]. In 2016 we also described the synthesis of a new hybrid (**5**) from an analgesic and anti-inflammatory eugenol (**4**) that presents a stronger leishmanicidal activity than compound **1** [36] (**Figure 1**).

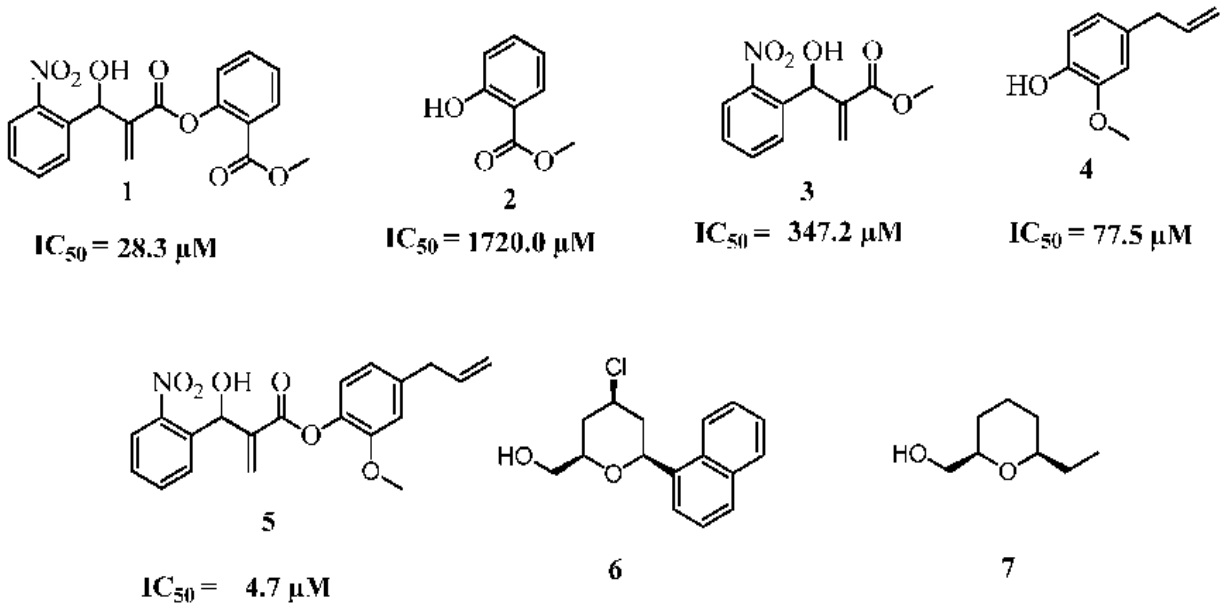

Figure 1. The leishmanicidal activity of hybrids **1** and **5** and their precursors. The analgesic/anti-inflammatory **6** and **7**.

In a different line of research from our group, synthesis and in vivo experiments were described that demonstrate that tetrahydropyran derivative **6** is very efficient and is a non-toxic analgesic/anti-inflammatory [37, 38].

1.5 Application as Organic complexes

FLUORESCENCE

Fluorescence occurs when an orbital electron of a molecule, atom or nanostructure relaxes to its ground state by emitting a photon of light after being excited to a higher quantum state by some type of energy [39].

Excitation: $S_0 + h\nu_{ex} \rightarrow S_1$

Fluorescence: $S_1 \rightarrow S_0 + h\nu_{em}$ + heat

Where hν is a generic term for photon energy with h = Planck's constant and ν = frequency of light, S_0 is called the ground state of the fluorophore (fluorescent molecule) & S_1 is its first (electronically) excited state.

A molecule,S_1, can relax by various competing pathways. It can undergo non-radiative relaxation in which the excitation energy is dissipated as heat (vibrations) to the solvent. Excited organic molecules can also relax via conversion to a triplet state, which may subsequently relax via phosphorescence by a secondary non-radiative relaxation step. Relaxation of an S_1 state can also occur through interaction with a second molecule through fluorescence quenching. Molecular oxygen (O_2) is an extremely efficient quencher of fluorescence just because of its unusual triplet ground state. In must cases, the emitted light has a longer wavelength, and therefore lower energy, than the absorbed radiation. However, when the absorbed electromagnetic radiation is intense, it is possible for one electron to absorb two photons; this two-photon absorption can lead to emission of radiation having a shorter wavelength than the absorbed radiation. The emitted radiation may also be of the same wavelength as the absorbed radiation, termed "resonance fluorescence" [40]. Molecule that are excited through light

absorption or via a different process (e.g. as the product of a reaction) can transfer energy to a second ‘sensitized’ molecule, which is converted to its excited state and can then fluoresce.

OCCURRENCE OF FLUORESCENCE

Electrons prefer residing in ground-state orbitals, those excited to the excited states will return to the ground states, accompanied by energy release. According to the different ways of energy release, those in the form of light are called luminescence. The occurrence of fluorescence is best explained by the Jabalonski diagram where all the process associated with the emission can be well understood. The various mechanisms behind the emission process is nothing but the relaxation of excited fluorophores from the excited state to ground state.

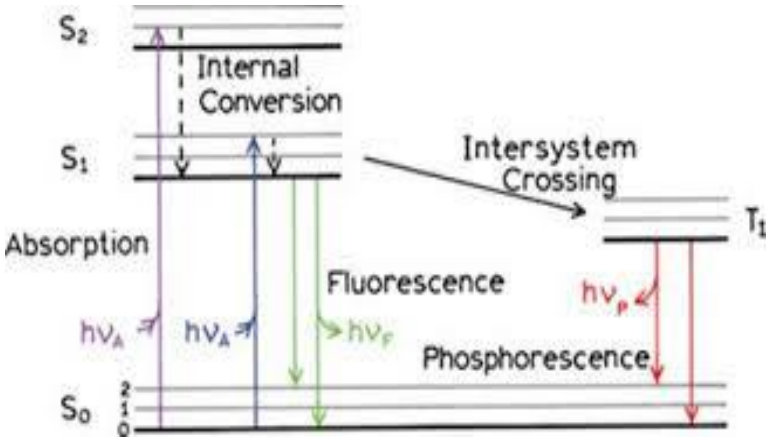

Fig 1.1 Jablonski diagram showing various energy transitions in common optical events

Fluorescence occurs, accompanied by the transformation of an electron from its excited state (S_1) to its ground state (S_0) .Another emission pathway similar to that of fluorescence where electrons are transferred from its triplet state (T_1) to the ground state calls phosphorescence. Jablonski diagrams (Fig.1.1) showed the difference of these two pathways. Then they quickly relax to the lowest vibrational level of S_1through internal conversion: Electrons will be excited to the excited states such as S_1 and S_2 after absorbing a certain wavelength of light. The decay of the excited electron from a singlet excited state (S_1) to the ground state (S_0) is a spin-allowed process as it has opposite spin to the electron in the ground-

state orbital. Thus, typical fluorescence lifetime is about 10 ns [41]. However, some excited electrons also undergo a spin conversion process and transfer to the first triplet state T_1. The decay from T_1 to S_0 is typically with longer lifetime as it is spin-prohibited. Some phosphorescence could last a few hours.

There are several unique characteristics of fluorescence, such as the Stokes shift, maximum emission wavelength, and fluorescent intensity. Due to internal conversion, the wavelength where fluorescence emission occurs is often longer than that at which absorption happens. The wavelength shift is called Stokes shift. Another property of fluorescence is that the maximum emission wavelength remains the same when changing the excitation wavelength. As whichever level the molecule is excited to, internal conversion will quickly remove the excess energy and fluorescent emission always takes place at the lowest vibrational state of S_1 state. Since emission is the opposite process to absorption, the emission spectrum is often the mirror image of absorption, though there are some exceptions.

FLUOROPHORE

The fluorophore absorbs light energy of a specific wavelength and re-emits light at a longer wavelength. The absorbed wavelengths, energy transfer efficiency, and time before emission depend on both the fluorophore structure and its chemical environment, as the molecule in its excited state interacts with surrounding molecules.

Main characteristics of fluorophores are:

- **Maximum excitation and emission wavelength** (expressed in nanometers(nm)): corresponds to the peak in the excitation and emission spectra (usually one peak each),
- **Extinction Coefficient** (or molar absorption, in Mol^{-1} cm^{-1}): links the quantity of absorbed light, at a given wavelength, to the concentration of fluorophore in solution.
- **Quantum yield**: efficiency of the energy transferred from incident light to emitted fluorescence (= number of emitted photons per absorbed photons)

- **Lifetime** (in picoseconds): duration of the excited state of a fluorophore before returning to its ground state. It refers to the time taken for a population of excited fluorophores to decay to 1/e (≈0.368) of the original amount.
- **Stokes shift**: difference between the maximum excitation and maximum emission wavelengths.

CHAPTER – 2

REVIEW OF LITERATURE

2.1. Literature review

- Panmella Pereira Maciel et.al (2021) studied, "Antimicrobial effect of Morita-Baylis-Hillman adducts against oral pathogens and cellular viability in human leukocytes" The aim of their work was to evaluate Morita-Baylis-Hillman adduct (MBHA) antimicrobial effect against oral pathogens and related cell viability in human leukocytes. Minimum inhibitory concentration (MIC) was determined using microdilution method. Cell viability was assessed in human peripheral blood mononuclear cells (PBMCs) using the resazurin assay. For S. aureus (ATCC 15656) and S. mutans (UA 159) MIC values of 2,000 μg/mL were reported for the A1 Morita-Baylis-Hillman adducts. The MICs of the A2 and A3 adducts were not found for the bacterial strains. MIC values for the A1 adduct was 125 μg/mL, A2 1,000 μg/mL and A3 to 15.6μg/mL against the C. albicans strain (ATCC 11006). PBMCs showed cell viability greater than 50 % when in contact with concentrations 10x higher than MIC of MBHA. It was concluded that MBHA A1, A2 and A3 present potential antimicrobial effects against C. albicans without presenting

substantial cytotoxic effects in human cells, highlighting adduct A3 for future therapeutic applications.

- Yue Wang et.al (2021) studied, "Auto-tandem palladium/phosphine cooperative catalysis: synthesis of bicycle [3.1.0] hexenes by selective activation of Morita–Baylis–Hillman carbonates" Herein they report a new palladium/phosphine cooperative catalytic system for the synthesis of bicyclo [3.1.0]hexene derivatives, particularly useful structural motifs in numerous biologically active entities. By application of their palladium/phosphine cooperative catalytic system, they accomplish the first selective intermolecular activation of Morita–Baylis–Hillman carbonates, where the phosphine species leads to a zwitterionic allylic ylide and the Pd catalyst generates a π-allylpalladium complex. Experimental results indicate that both the Pd and phosphine play crucial roles in the sequential annulation reaction. This strategy opens up a new avenue for efficient and economical metal/Lewis base dual catalytic systems and provides valuable clues on solving the limitations of selective activation.

- Fernando Coelho et.al (2020) studied, "Catalyst-free conjugate addition of indolizines to in situ generated oxidized Morita–Baylis–Hillman adducts" A sequential one-pot 2-Iodoxybenzoic acid (IBX) oxidation of Morita–Baylis–Hillman (MBH) adducts followed by catalyst-free indolizine conjugate addition was developed. The wide scopes of MBH adducts and indolizines were investigated, and densely functionalized adducts were obtained in yields of up to 94%. The conjugate addition step occurred in less than a minute at room temperature with total regioselectivity toward indolizine C3 carbon. Less nucleophilic C1 carbon was also alkylated when C3-substituted indolizines were employed as the substrate.

- Pambingal Rajan Sruthi et.al (2020) studied, "Palladium Catalyzed Annulation of Morita-Baylis-Hillman Adducts: Synthesis of Indene and Indanone Derivatives"

Concise and efficient methods for the syntheses of functionalized Indene and Indanone derivatives from Morita-Baylis Hillman (MBH) alcohols via Palladium catalyzed annulations are described. The formation and nature of the product was based on the MBH adduct used and the reaction conditions established after detailed optimization studies. The reaction of Baylis-Hillman alcohols (1a–m) in presence of Pd(OAc)2 (5 mol%), P(o-Tol)3 (20 mol%), AgOAc (1 eq.) and Na2CO3 (2 eq.) in Dioxane at 120°C under Nitrogen atmosphere provided substituted indenes (2a–m) in good to excellent yields. While, Indanone derivatives (4a–f) are obtained from o-halo substituted MBH adducts (3a–l) when subjected to reaction with Pd (OAc) 2 (3 mol %) and K3PO4 (2.5 eq.) in DMA at 140°C in the absence of any ligand or additive.

- Dinesh K. Jangid1 et.al (2019) studied, "DABCO as a Base and an Organocatalyst in Organic Synthesis: A Review" One of the organocatalysts 1, 4-diazabicyclo [2.2.2] octane (DABCO) is an excellent solid catalyst in a number of reactions. It was also a good nucleophile and a base in numerous reactions for the synthesis of heterocycles. DABCO catalyzes many reactions like cycloaddition reactions, coupling reactions, Baylis-Hillman reaction, Henry reaction, ring opening reactions, etc. One more advanced feature of these reactions is that they proceed through environmentally friendly pathway. DABCO has more advantages than other organic catalysts because it was an inexpensive, nontoxic base, an ecofriendly and a highly reactive catalyst for building of organic frameworks, which produce the desired products in excellent yields with high selectivity. Many catalytic applications of DABCO have been reported for the synthesis of an organic framework which has been discussed in their review.

- Hongxing Jin et.al (2019) studied, "Phosphine-Catalyzed Domino [3 + 3] Cyclization of para-Quinamines with Morita−Baylis−Hillman Carbonates: Access to Hydroquinoline Derivatives" A phosphine-catalyzed [3 + 3] cyclization strategy between para-quinamines and HCHO Morita− Baylis−Hillman (MBH) carbonates was discovered, delivering a series of highly functionalized hydroquinoline derivatives in moderate to

good yields and excellent diastereoselectivity. Moreover, mechanistic insights, gram-scale experiments, and synthetic manipulations of the products were also discussed.

- Peng Chen et.al (2019) studies, "Auto-Tandem Cooperative Catalysis Using Phosphine/Palladium: Reaction of Morita–Baylis–Hillman Carbonates and Allylic Alcohols" Auto-tandem catalysis (ATC), in which a single catalyst promotes two or more mechanistically different reactions in a cascade pattern, provides a powerful strategy to prepare complex products from simple starting materials. Reported here was an unprecedented auto-tandem cooperative catalysis (ATCC) for Morita–Baylis–Hillman carbonates from isatins and allylic carbonates using a simple Pd(PPh3)4 precursor. Dissociated phosphine generates phosphorus ylides and the Pd leads to p-allylpalladium complexes, and they undergo a g-regioselective allylic–allylic alkylation reaction. Importantly, a cascade intramolecular Heck-type coupling proceeds to finally furnish spirooxindoles incorporating a 4-methylene-2-cyclopentene motif. Experimental results indicate that both Pd and phosphine play crucial roles in the catalytic Heck reaction. In addition, the asymmetric versions with either a chiral phosphine or chiral auxiliary are explored, and moderate results are obtained.

- Sheng-Jiao Yan et.al (2019) studied, "Cascade reaction of Morita–Baylis–Hillman acetates with 1,1-enediamines or heterocyclic ketene aminals: Synthesis of highly functionalized 2-aminopyrroles" A new strategy for the construction of two kinds of fully substituted pyrroles, including 2-aminopyrroles and bicyclic pyrroles from Morita–Baylis–Hillman (MBH), acetates with 1,1-enediamines (EDAMs) or heterocyclic ketene aminals (HKAs) via base-promoted tandem Michael addition, elimination, and aromatization sequence has been developed, affording the expected products in moderate to excellent yields. This methodology was a highly efficient, concise way to access 2-aminopyrroles or bicyclic pyrroles with diversity in molecular structures from accessible building blocks under moderate reaction conditions.

- Ying-Chun Chen et.al (2019) studied, “Sequential Assembly of Morita−Baylis−Hillman Carbonates and Activated ortho-Vinylbenzaldehydes To Construct Chiral Methanobenzo[7]annulenoneThe α-regioselective asymmetric [3 + 2] annulation reaction of Morita−Baylis−Hillman carbonates from isatins and activated ortho-vinylbenzaldehyses was developed by the catalysis of a chiral tertiary amine. The sequential N-heterocyclic carbene-mediated intramolecular Stetter reaction was conducted to finally furnish the bridged 5,8-methanobenzo[7]annulen-9-one architectures incorporating a spirooxindole motif with excellent stereoselectivity Frameworks”

- Haitham Elleuch et.al (2018) studied, “Potential antioxidant activity of Morita-Baylis-Hillman adducts”. The wide variety of potent biological activities of Morita–Baylis–Hillman adducts (MBH) encouraged us to synthesize new series of products belonging to their class of compounds, possessing different functionalities and exhibiting potential antioxidant activity. As part of their on-going program on targeting molecules with antioxidant activity, they describe herein different DPPH (2, 2-diphenyl-1-picrylhydrazyl) scavenging activities of MBH alcohols and their derivatives including acetates, phosphonates and hydrazonophosphonates. The obtained results showed that the strongest DPPH radical scavenging activity was observed in the case of hydrazonophosphonates in comparison to the other MBH derivatives.

- Jian-Qiang Zhao et.al (2018) studied, “Organocatalyzed Dearomative Cycloaddition of 2-Nitrobenzofurans and Isatin-Derived Morita−Baylis−Hillman Carbonates: Highly Stereoselective Construction of Cyclopenta[b]benzofuran Scaffolds” The first organocatalyzed asymmetric dearomative cycloaddition between 2-nitrobenzofurans and isatin-derived Morita−Baylis−Hillman carbonates has been developed. Using a modified cinchona alkaloid as the catalyst, a series of structurally diverse cyclopenta[b]benzofuran derivatives with three contiguous stereocenters, including a spiro-quaternary chiral center, could be smoothly obtained in excellent results (all cases

>20:1 dr, up to 99% yield and 98% ee). The utility of this method was showcased by the versatile transformations of the product

- Vaidya Jayathirtha Rao et.al (2018) studied, “Importance of Baylis-Hillman adducts in modern drug discovery” The Baylis-Hillman (BH) reaction plays a fascinating role in the field of synthetic and medicinal chemistry. BH adducts and their derivatives have been used as crucial synthons for the synthesis of various pharmaceutically useful natural products and compounds with carbocyclic or heterocyclic frameworks. Their digest letter aims to discuss some key ideas for the synthesis of biologically active scaffolds using BH reaction and raise the awareness of their emerging research domain in modern drug discovery. In their review, we will present and discuss recent reports of various biologically active scaffolds derived from BH reaction, and their reported biological activities.

- Belen Levenfeld et.al (2017) studied, “DABCO-Functionalized Polysulfones as Anion-Exchange Membranes for Fuel Cell Applications: Effect of Crosslinking”: A series of DABCO-functionalized polysulfones were synthesized and characterized. The effect that crosslinking has on the membrane properties containing different degrees of functionalization was evaluated. These polymers showed good thermal stability below the fuel cell operation temperature, T < 100 8C, reflected by the TOD, TFD, and thermal durability. The water uptake increased as the percentage of DABCO groups increased and the crosslinked membranes showed lower capacity to absorb water than the non-crosslinked ones favoring thus the dimensional stability of the first ones. Membranes in the chloride form containing low degree of functionalization exhibited the highest tensile strength values. The ionic conductivity of non-crosslinked membranes varied as a function of the functionalization degree until a value of around 100% achieving a maximum value at 86%. However, the crosslinked ones showed satisfactory ionic conductivities for values higher than 100%. The behavior of these polymeric materials in alkaline solutions revealed a great alkaline stability necessary to be used as solid

electrolytes in fuel cells. VC 2017 Wiley Periodicals, Inc. J. Polym. Sci., Part B: Polym. Phys. 2017, 55, 1326–1336.

- Thirumal Yempala et.al (2012) studied, "Molecular hybridization of bioactives: Synthesis and antitubercular evaluation of novel dibenzofuran embodied homoisoflavonoids via Baylis–Hillman reaction". A novel series of natural product like dibenzofuran embodied homoisoflavonoids [(E)-3-(dibenzo [b, d]- furan-2-ylmethylene) chroman-4-ones] designed by molecular hybridization were synthesized in very good yields via a sequence of reactions involving base catalyzed Baylis–Hillmann (BH) reaction of 2-dibenzofuran carboxaldehyde and methyl acrylate; bromination of BH adduct; condensation of resulted allylic bromide with substituted phenols or 2-dibenzofuranol followed by cyclization. Among the all 11 new compounds screened for in vitro antimycobacterial activity against Mycobacterium tuberculosis H37Rv (MTB), (E)-3-(dibenzo [b, d] furan-2-ylmethylene)-6-fluorochroman-4-one (7f) and (E)-3-(dibenzo [b, d] furan-2-ylmethylene)-6-fluorochroman-4-one (7g) were found to be active with MIC 12.5 lg/mL.

- Mário L.A.A. Vasconcellos et.al (2012) studied, "Morita–Baylis–Hillman adducts: Biological activities and potentialities to the discovery of new cheaper drugs" Their review aims to present by the first time the Morita–Baylis–Hillman adducts (MBHA) as a new class of bioactive compounds and highlight its potentialities to the discovery of new cheaper and efficient drugs. Now, most these compounds can be prepared fast and on a single synthetic step (one-pot reaction) in high yields and using ecofriendly synthetic protocols. They highlight here the aromatic MBHA, which have shown diverse biological activities as anti-Leishmania chagasi and Leishmania amazonensis (parasites that cause cutaneous and visceral leishmaniasis), anti-Trypanosoma cruzi (parasite that cause Chagas disease), anti-Plasmodium falciparum and Plasmodium berghei (parasites that cause malaria), lethal against Biomphalaria globate (the snail transmitter of schistosomiasis), antibacterial, antifungal, herbicide and actives against some human

tumor cell lines. Understanding of the biological mechanisms of action of their new class of molecules was still in the infancy stage. However, they report here which has been described to date on the possibilities of biological mechanisms of action, and they present new analyzes based on literature in their area. The academic and industrial interest in selecting green and cheaper experiments to the drugs development has been the prime mover of the growth on the subject.

- T. H. Suresha Kumara et.al (2009) studied, "An expeditious, bidirectional synthesis of furofuranones: a new application of Morita–Baylis–Hillman adducts" A concise, flexible approach of general utility to the furo[3,2-b] furanones from readily available Morita– Baylis–Hillman adducts was delineated. In an expeditious variant of their approach, a four-step cascade process was executed in a one-pot operation to generate the furofuranoid framework containing two quaternary centers.

- Min Shi et.al (2007) studied, "Aza-Baylis–Hillman Reactions and Their Synthetic Applications" Aza-Baylis–Hillman reactions have attracted much attention over the past decade. This review concentrates on discussion of the origins of and progress in aza-Baylis–Hillman reactions, including the development of catalysts and substrate scopes, mechanistic study, asymmetric reactions, and further transformations of the products.

- Ranjan Jana et.al (2007) studied, "Chemo-, regio- and stereoselective addition of triorganoindium reagents to acetates of Baylis–Hillman adducts: a new strategy for the synthesis of (E) and (Z)-trisubstituted alkenes" The addition of several trialkyl or triarylindium reagents to the acetates of Baylis–Hillman adducts proceeds readily under the catalysis of copper and palladium derivatives. The reactions of trialkylindiums are catalyzed efficiently by CuI whereas additions of triarylindiums produce better results with Pd (PPh3)4. The reactions with 3-acetoxy-2-methylenealkanoates provide (E)-alkenes, whereas similar reactions with 3-acetoxy-2-methylenealkanenitriles lead to (Z)-alkenes. All the reactions are highly regio- and stereoselective and high yielding.

- V. Jayathirtha Raoa et.al (2006) studied, “Synthesis of multisubstituted quinolines from Baylis–Hillman adducts obtained from substituted 2-chloronicotinaldehydes and their antimicrobial activity” Baylis–Hillman acetates were synthesized from substituted 2-chloronicotinaldehydes and were conveniently transformed into multisubstituted quinolines and cyclopenta[g]quinolines on reaction with nitroethane or ethyl cyanoacetate via a successive SN20 –SNAr elimination strategy. Thus, synthesized quinolines were evaluated for antimicrobial activity and found having substantial antibacterial and antifungal activity.

- Jamjanam Srivardhana Rao et.al (2005) studied, “Applications of Baylis–Hillman adducts: a simple, convenient, and one-pot synthesis of 3-benzoylquinolines” —A simple and convenient synthesis of 3-(2-hydroxybenzoyl) quinoline derivatives via the treatment of 3-[hydroxy(2-nitroaryl) methyl]-4H-chromen-4-ones, derived from chromones and various 2-nitrobenzaldehydes, with Fe/AcOH, in a one-pot operation, was described.

CHAPTER – 3

SCOPE OF THE INVESTIGATION

3.1 SCOPE OF THE INVESTIGATION

The aim of this research is to synthesize and evaluate some properties of Baylis hillmann adduct using various metal ions. In recent years, many researchers have focused on Baylis hillmann adduct due to their applications in several chemical reaction as intermediate, specifically in biological activities such as antimicrobial, antioxidant studies and other applications, including the sensors and the gas sensors. Therefore, the present investigation was made to synthesize Baylis hillmann adduct by using simple method.

The objectives of this investigation are:

- To utilize simple available chemicals for the synthesis of Baylis hillmann adduct, this hopefully will replace expensive chemical previously used.
- To engage synthesis with biological properties of Baylis hillmann adduct.
- To analyse the functional groups of synthesized adduct by Fourier Transform Infrared Spectroscopy (FT-IR).
- To study the structural properties of the adduct by Mass spectroscopy (MS).
- To determine transitions occurring using UV Visible spectrophotometer.
- To analyse the complex formation with Fluorescence Spectroscopy
- To evaluate the antimicrobial properties of the synthesized Baylis hillmann adduct against selected bacteria.

CHAPTER – 4

MATERIALS AND METHODS

4.1 MATERIALS REQUIRED

All chemical and reagents were purchased from Sigma-Aldrich and Merck used as received without any further purification.

- p- hydroxybenzaldehyde

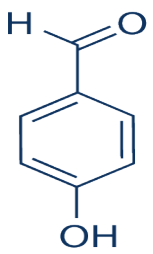

- DABCO (1,4-diazabicyclo[2,2,2]octane

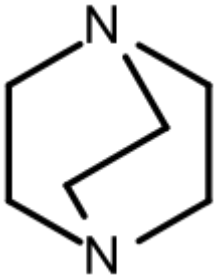

- Methyl acrylate

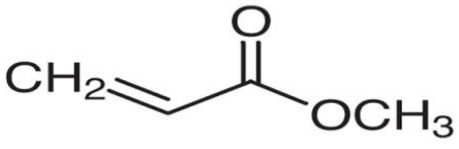

- Silica gel(SiO_2)

- Ethanol (C_2H_5OH)
- Zinc chloride ($ZnCl_2$)
- Mercuric chloride ($HgCl_2$)

4.2 METHODS

4.2.1. SYNTHESIS OF COMPOUNDS

For the synthesis of MBH adduct, 5ml of methyl acrylate in presence of 2g of DABCO and stirred in magnetic stirrer for 30 minutes. Along with silica gel 5g of p-hydroxybenzaldehyde is added and slightly heated at 50℃ for about 30 minutes. The product was filtered to remove silica gel. The white precipitate is then recrystallized with ethanol, results in yield of 80%.

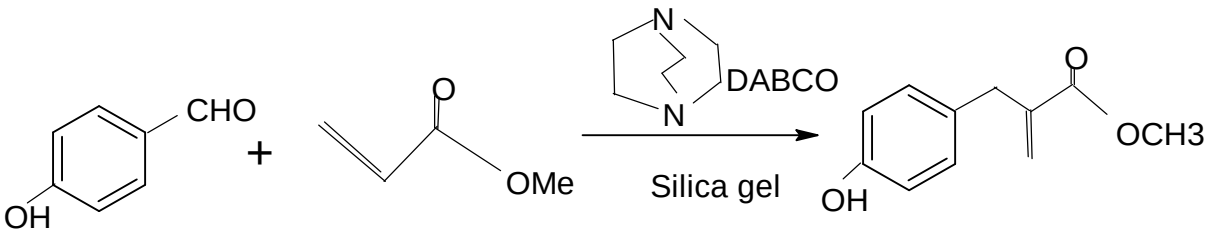

4.2.2 Preparation of complex using MBH adduct

Preparation of MBH-Hg^{2+}complex

The recrystallized MBH adduct is reacted with $HgCl_2$, the ratio of 1:1 mole using ethanol as solvent and refluxed for about 1hour at 60^oC forms MBH-Hg^{2+} complex. The white precipitate obtained was recrystallized using ethanol.

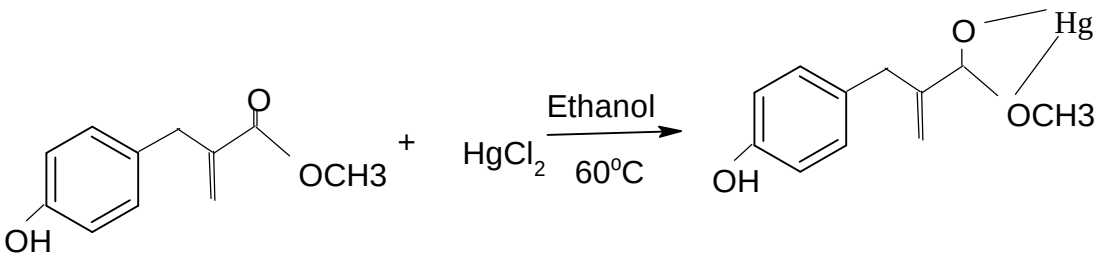

Based on the stoichiometric ratio, the assumed structure of the complex is represented by the above equation, which is proved by fluorescence spectra and its calculations

Preparation of MBH-Zn^{2+}complex

The recrystallized MBH adduct is reacted with $ZnCl_2$, the ratio of 1:1 mole using ethanol as solvent and refluxed for about 1hour at 60^{o}C forms MBH- Zn^{2+} complex. The white precipitate obtained was recrystallized using ethanol.

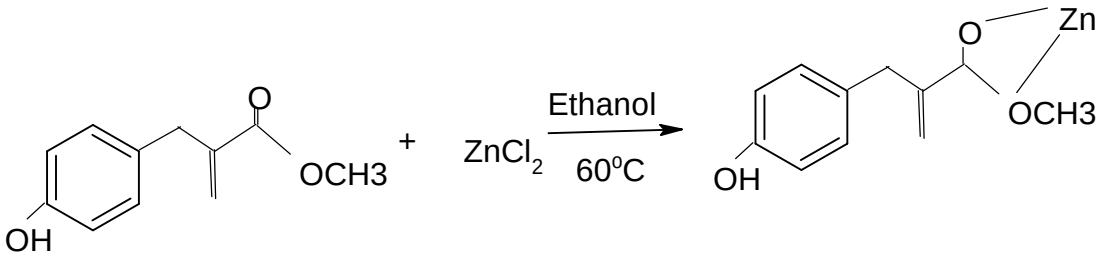

Based on the stoichiometric ratio, the assumed structure of the zinc complex is represented by the above equation, which is proved by fluorescence spectra and its calculations.

4.3 INSTRUMENTATION

4.3.1 Mass spectroscopy

Mass spectroscopy is a powerful analytical technique used to quantify known material, to identify unknown compounds within a sample, and to elucidate the structure and chemical properties of different molecule. The complete process involves the conversion of the sample into gaseous ions, with or without fragmentation, which are then characterized by their mass to charge ratios (m/z) and relative abundances. This technique basically studies the effect of ionizing energy on molecule. It depends upon chemical reactions in the gas phase in which sample molecule are consumed during the formation of ionic and neutral species.

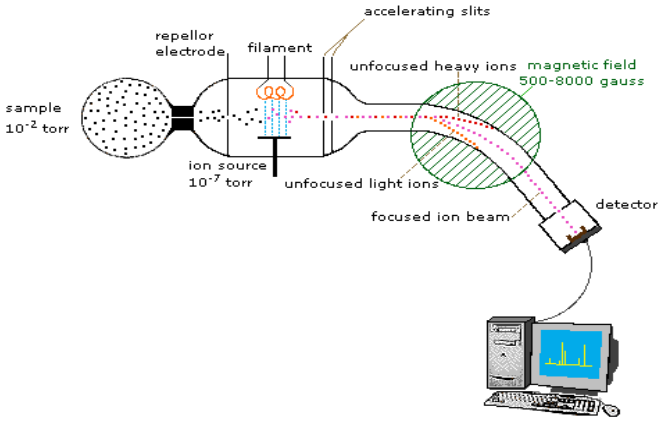

Fig. 4.1 Mass Spectroscopy

4.3.2 UV-VISIBLE SPECTROSCOPY

The principle of UV-Vis spectroscopy is based on Beer-Lambert law which states that the absorbance of a solution is directly proportional to the concentration of the absorbing species in the solution and the path length. Thus, for a fixed path length, UV – VIS spectroscopy can be used to determine the concentration of the absorber in a solution. The presence of an analyte gives a response which can be assumed to be proportional to the concentration. An ultraviolet-visible spectrum is essentially a graph of light absorbance versus wavelength in a range of ultraviolet or visible regions. Such a spectrum can often be produced directly by a more sophisticated spectrometer, or the data can be collected one wavelength at a time by simpler instruments. The UV-Vis spectral measurements have been carried out in a quartz cuvette of 1 cm using JASCO 530 UV-Vis spectrophotometer. The UV-Visible absorption spectra were recorded on a JASCO variant 630 spectrometer at V. O. Chidambaram College, Tuticorin.

Fig. 4.2 UV-Visible spectrophotometer

4.3.3 FOURIER TRANSFORM INFRARED SPECTROSCOPY (FTIR)

When infrared light is passed through a sample of compound some of the frequencies are absorbed while frequencies are transmitted through the sample without being absorbed. In order for molecules to absorb infrared radiation as vibrational excitation energy, there must be change in the dipole moment of the molecule as it vibrates. Consequently, the stretching of homo nuclear diatomic molecules will not give rise to IR absorption. According to the selection rule, any change in direction or magnitude of the dipole during a vibration gave rise to an oscillation electric field component of the IR radiation giving rise to absorption of radiation. The plot of percent absorbance or percent transmittance against frequency resulted in infrared spectrum. The infra-red spectra of the complexes have been recorded in a JASCO spectrophotometer in solid phase, as KBr pellets. The FTIR spectra were recorded by using Nicolet Si 5 at V.O.Chidambaram College, Tuticorin.

Fig.4.3 Fourier transform infrared spectroscopy

4.3.4 FLUORESCENCE SPECTROSCOPY

Fluorescence spectroscopy is one of the most widely used spectroscopic techniques in the fields of biochemistry and molecular biophysics today. Although fluorescence measurements do not provide detailed structural information, the technique has become quite popular because of its acute sensitivity to changes in the structural and dynamic properties of biomolecules and biomolecular complexes. Like most biophysical techniques, fluorescence spectroscopic studies can be carried out at many levels ranging from simple measurement of steady-state emission intensity to quite sophisticated time resolved studies. The information content increases dramatically as various fluorescence observables are time resolved and combined in global analyses of the phenomena of interest. Nonetheless, quite a good deal of information is available from steady-state measurements for which the requirements in instrumentation are quite modest. Consequently, steady-state fluorimeters are routinely used to measure complexation and conformational phenomena of biological molecules. The fluorescence emission spectrum were recorded with JASCO FP-6300 at V.O.C. College at Tuticorin.)

Fig.4.4 Spectrofluorometer

4.3.5 THE FLUORESCENCE PROCESS

Fluorescence is the result of a three-stage process that occurs in certain molecules called fluorophores or fluorescent dyes. A fluorescent probe is a fluorophore designed to localize within a specific region of a biological specimen or to respond to a specific stimulus. The

process responsible for the fluorescence of fluorescent probes and other fluorophores is illustrated by the simple electronic-state diagram (Jablonski diagram) shown in Figure 4.5

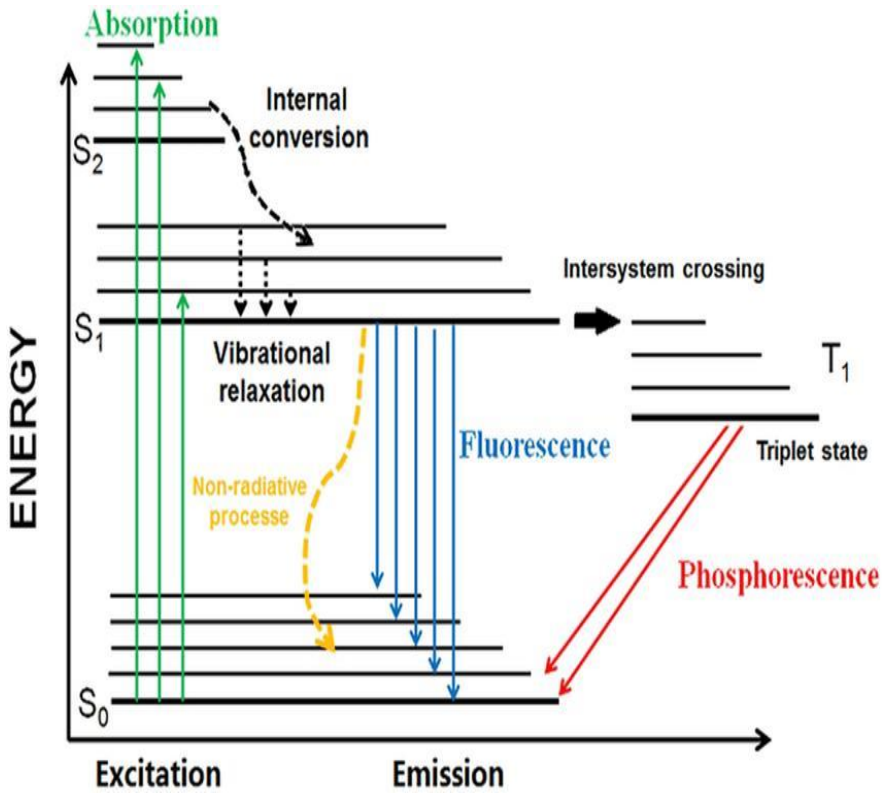

Fig.4.5 Jablonski diagram

A photon of energy hv_{EM} is emitted, returning the fluorophore to its ground state S_0. Dueto energy dissipation during the excited-state lifetime, the energy of this photon is lower, and therefore of longer wavelength, than the excitation photon hv_{EX}. The difference in energy or wavelength represented by $(hv_{EX} - hv_{EM})$ is called the Stokes shift. The Stokes shift is fundamental to the sensitivity of fluorescence techniques because it allows emission photons to be detected against a low background, isolated from excitation photons. In contrast, absorption spectrophotometry requires measurement of transmitted light relative to high incident light levels at the same wavelength.

4.3.6 FLUORESCENCE SPECTRUM

The entire fluorescence process is cyclical. Unless the fluorophore is irreversibly destroyed in the excited state (an important phenomenon known as photobleaching), the same fluorophore can be repeatedly excited and detected. The fact that a single fluorophore can generate many thousands of detectable photons is fundamental to the high sensitivity of fluorescence detection techniques. For polyatomic molecules in solution, the discrete electronic transitions represented by hv_{EX} andhv_{EM} in Fig.6 are replaced by rather broad energy spectra called the fluorescence excitation spectrum and fluorescence emission spectrum, respectively.

The bandwidths of these spectra are parameters of particular Importance for applications in which two or more different fluorophores are simultaneously detected. With few exceptions, the fluorescence excitation spectrum of a single fluorophore species in dilute solution is identical to its absorption spectrum. Under the same conditions, the fluorescence emission spectrum is independent of the excitation wavelength, due to the partial dissipation of excitation energy during the excited-state lifetime, as illustrated in Fig.4.5. The emission intensity is proportional to the amplitude of the fluorescence excitation spectrum at the excitation wavelength (Figure 4.6).

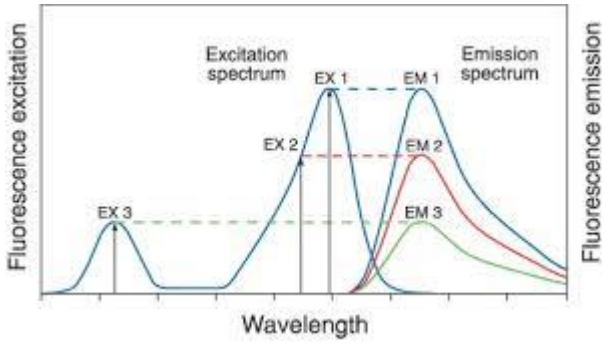

Fig. 4. 6. Fluorescence excitation spectrum

4.3.7 Antibacterial activity

Procedure

The test bacteria was inoculated in peptone water and incubated for 3 – 4 hours at 35 ºC. Mueller hinton agar plates was prepared and poured in sterile petriplates. 0.1 ml of bacterial culture was inoculated on the surface of Mueller hinton agar plates and spread by using L-rod. The inoculated plates was allowed to dry for five minutes. The disk loaded with samples concentration 1000 µg/ml was placed on the surface of inoculated petriplates using sterile technique. The plate was incubated at 37 ºC for 18-24 hours. The plate was examined for inhibitory zone and the zone of inhibition was measured in mm. we have examined MBH complexes with five different bacterial (E.coli, Staphylococcus aureus, Bacillus subtilis, Bacillus cereus, Pseudomonas aeruginosa).

CHAPTER-5

RESULTS AND DISCUSION

5.1 Mass spectra

The Electron spray Ionisation Mass Spectrometry (EMI-MS) was recorded in HP Agilent 5973, Chennai and the ESI-MS was performed in negative ion mode. The collision voltage and ionization voltage were -70 V and -4.5 kV, respectively, using nitrogen as atomization and desolvation gas. The desolvation temperature, was set at $300^{O}C$. The scan range of mass spectrum was 300-200 m/z. The relative amount of each component of each compound was LC- MS chromatogram, using the area normalization method. The mass spectra of the MBH adduct are recorded in CH_3CN shown in Fig 5.1. The mass spectra reveal that the peak with m/z values corresponds to the fragmentation of receptors.

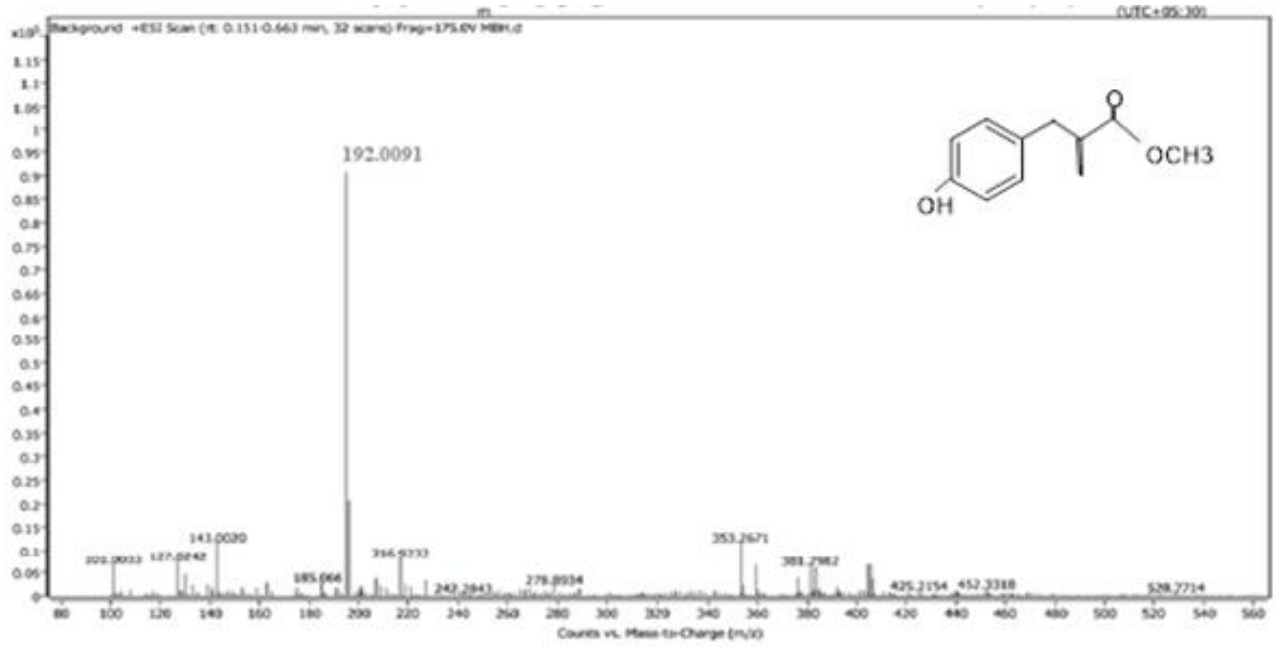

Fig 5.1. Mass spectrum of MBH

The mass spectra of the MBH was recorded in negative mode and the mass values were similar to that of the formula weight and are presented in the table 5.1 as given below. Thus, it is experimentally conformed the prepared sample is MBH adduct.

Table 5.1 Mass spectral data for receptors

Receptors	Molecular weight calculated	ESI-MS (found)
MBH adduct	192	192.0091

5.2 IR SPECTRA

The FT-IR spectra of MBH complex with Hg^{2+} and MBH Zn^{2+} as shown in Fig. 5.2. The data on the important infrared spectra bands of the MBH adduct, complexes such as MBH- Hg^{2+} and Zn^{2+}

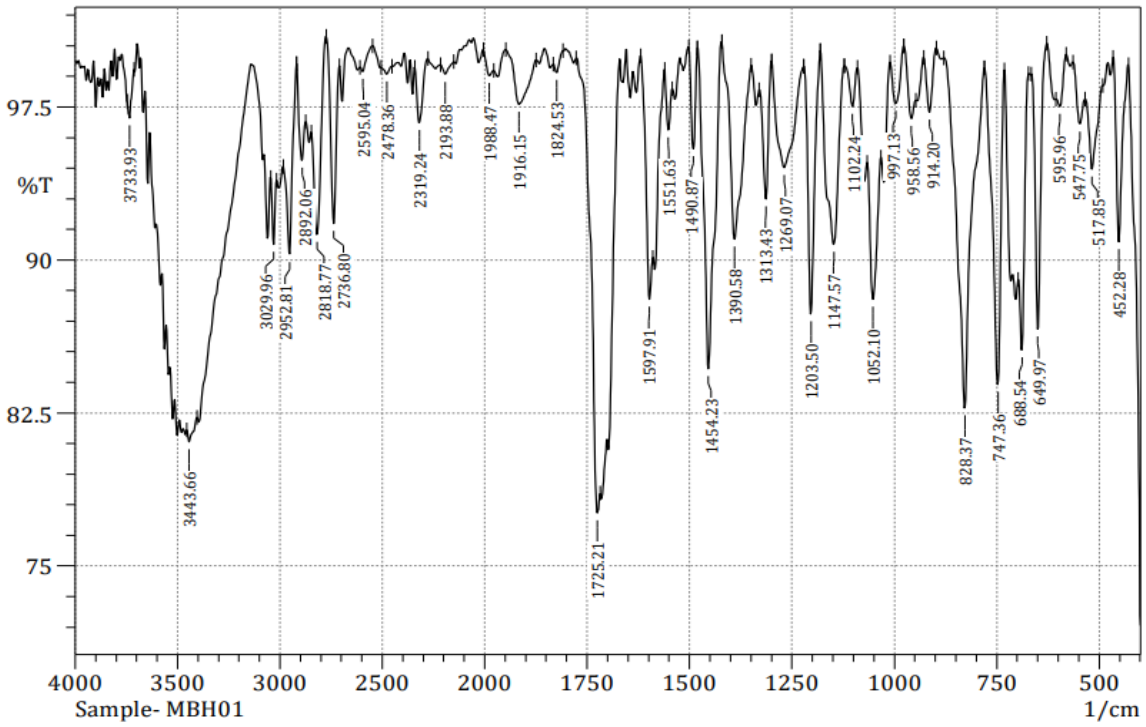

Fig. 5.2 FT-IR spectrum of MBH

The characteristic band situated at 3029.96 cm^{-1} can be ascribed to the =C-H vibrations of the aromatics. The characteristic peak at 1597.91 cm^{-1} is assigned to the v(C=O) stretching mode. The bands in the region 1250-1000 cm^{-1} is due to carbon-carbon stretching vibrations in the aromatic ring.

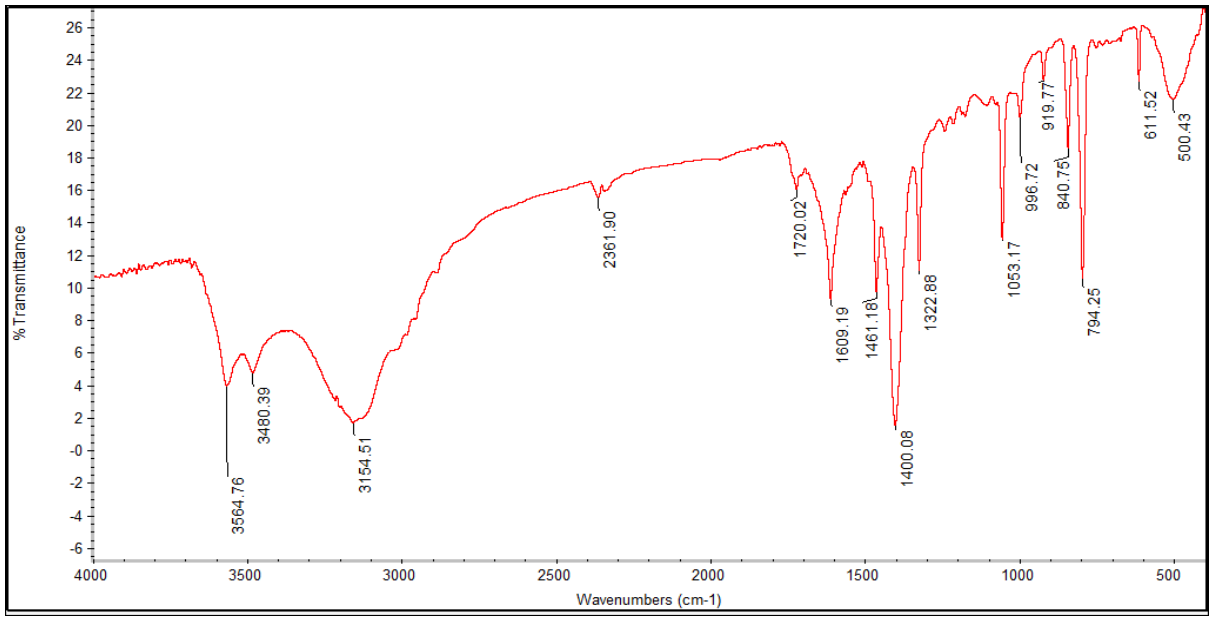

Fig.5.3 FT-IR spectrum of MBH-Hg^{2+} complex

The FT-IR spectrum of MBH complexes in Hg^{2+} is shown in Fig.5.3. The characteristic band situated at 3154.51 cm^{-1} can be ascribed to the =C-H vibrations of the aromatics. The characteristic at 1609.19 cm^{-1} is assigned to the v(C=O) stretching mode. The band in the region 1250-1000 cm^{-1} corresponds to carbon – carbon stretching vibrations in the aromatic ring. The band at 500.43cm^{-1} represent metal presence in our complexes.

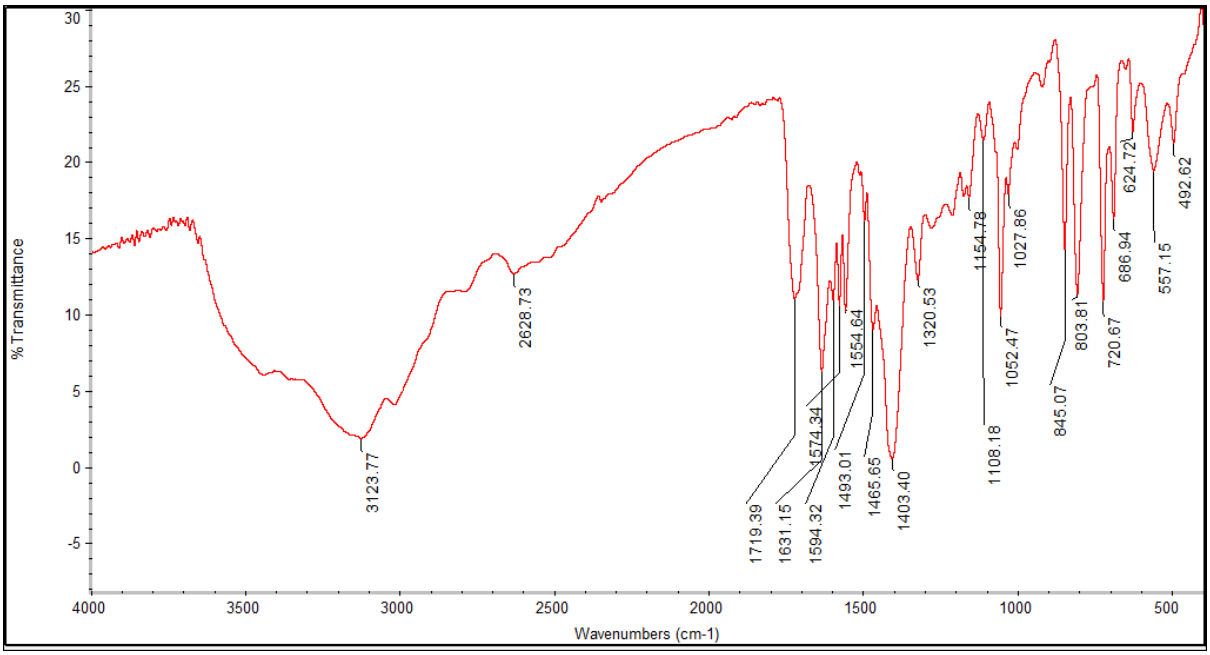

Fig. 5.4 FT-IR spectrum of MBH – Zn^{2+} complex

The characteristic band situated at 3123.77 cm^{-1} can be ascribed to the =C-H vibrations of the aromatics. The characteristic at 1631.15 cm^{-1} is assigned to the v(C=O) stretching mode. The band in the region 1250-1000 cm^{-1} indicates carbon – carbon stretching vibrations in the aromatic ring. The band 492.62 cm^{-1} corresponds to Zn^{2+} complexes with MBH adduct.

Table 5.2: FT-IR spectral data for complex

Receptor	**v(C=O)** **cm^{-1}**	**v(C-C)** **cm^{-1}**	**V(O-M)** **cm^{-1}**
MBH adduct	1597.91	1250-1000	-
Hg^{2+}	1609.19	1250-1000	500.43
Zn^{2+}	1631.15	1250-1000	492.62

5.3 UV spectra

The absorption spectrum of MBH are shown in fig. 5.5

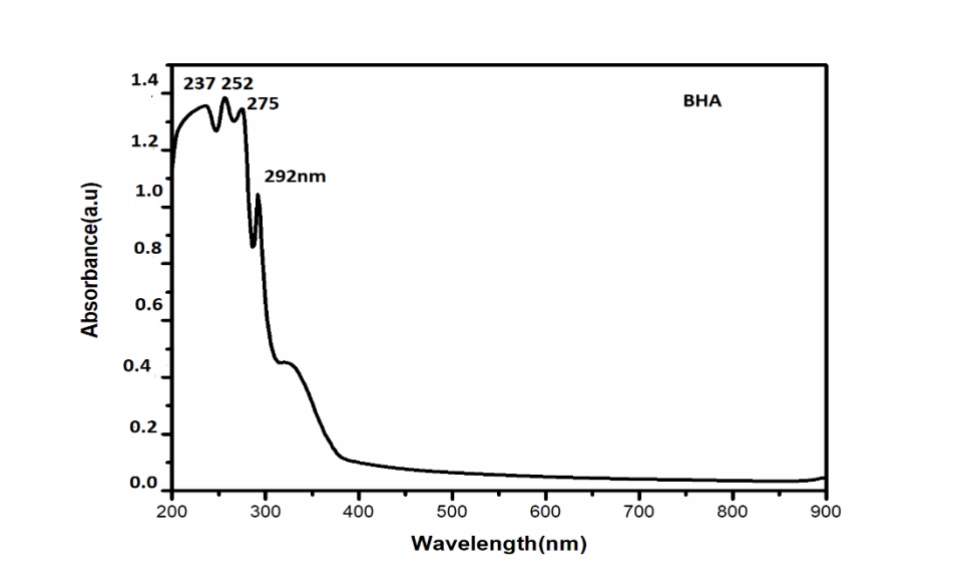

Fig. 5.5 UV-visible spectra of MBH

The UV-vis absorption spectrum of the MBH is shown in the Fig.5.5 which reveals that the spectrum region 230-240 nm corresponds to the π-π^* transition of C=C in aromatic chromophore and the intense absorption band is observed around 292-410 nm can be attributed to the π-π^* transition resulting from the extended conjugation between the aromatic ring.

The UV-Vis data of MBH shows peak at 237,252,275,292nm

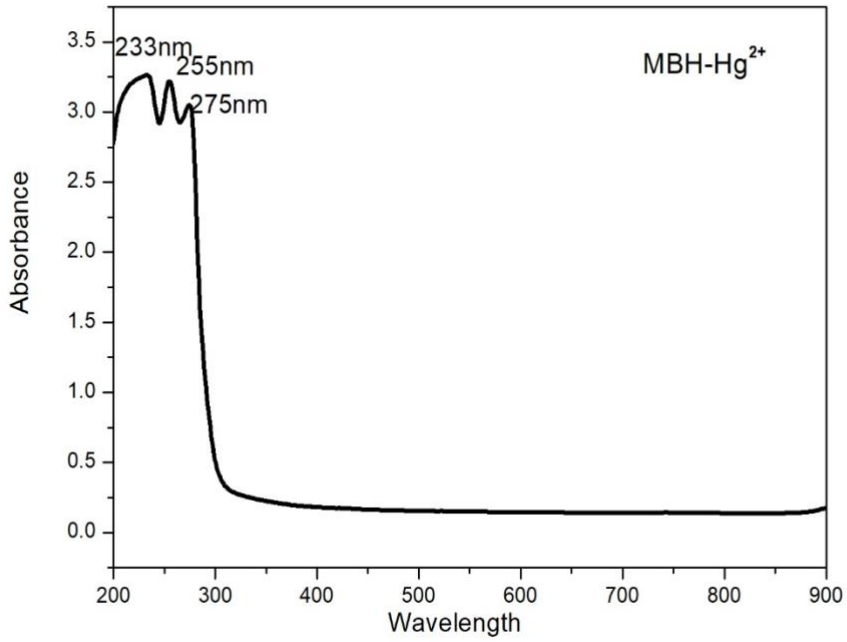

Fig 5.6 UV-Visible spectrum of MBH – Hg^{2+}

The UV-Vis absoption spectrum of the MBH-Hg2+ is shown in the Fig 5.6 . After the complex formation of complex MBH –Hg^{2+} , the UV-Visable spectrum obtained a bathochromic shift due to the lone pair of electron present in the oxygen atom get bonded with Hg^{2+} ions.

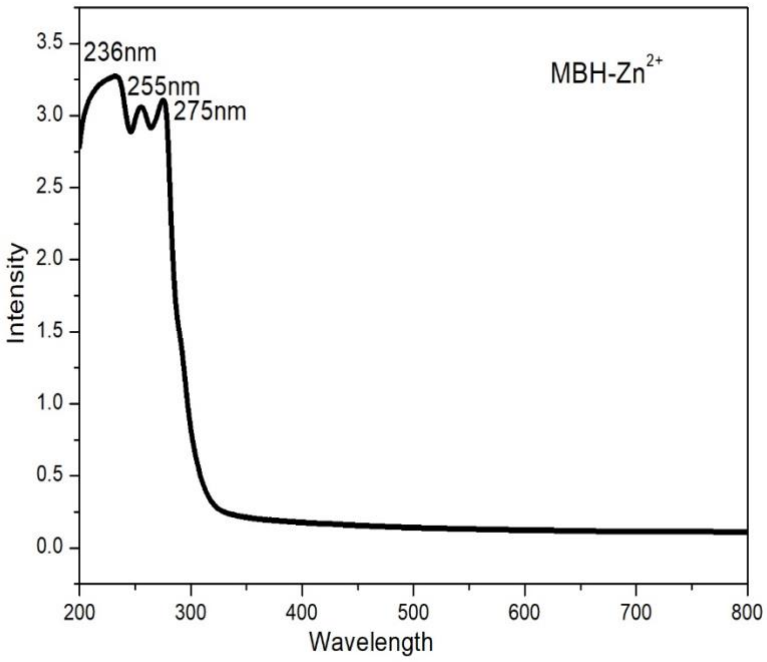

Fig 5.7 UV-Visible spectrum of MBH- Zn^{2+}

The UV-Vis absorption spectrum of the MBH-Zn^{2+} is shown in the Fig 5.7 which reveals that the spectral region 230-280 nm corresponds to the n-π^* transition of carbonyl atom present in the aromatic ing. After the complex formation of complex MBH –Zn^{2+} , the UV-Visable spectrum obtained a bathochromic shift due to the lone pair of electron present in the oxygen atom get bonded with Zn^{2+} ions.

Table 5.3: UV-Vis data of MBH complex

Receptor	**λmax**
MBH adduct	237,252,275,292
MBH-Hg^{2+}	233,255,275
MBH-Zn^{2+}	232,256,275

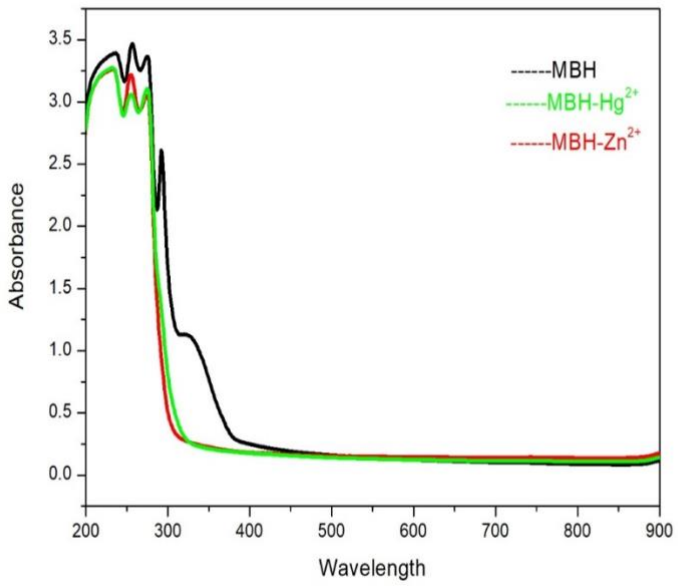

Fig 5.8 UV-Vis spectrum of MBH complexes for stack graph

The comparison of UV-Visable spectrum of MBH adduct with MBH – Hg^{2+} and MBH-Zn^{2+} clearly shows the shift occurs after the complex formation.

5.3.1 Job's plot in MBH-$Hg^{2+}$and Zn^{2+}complexes

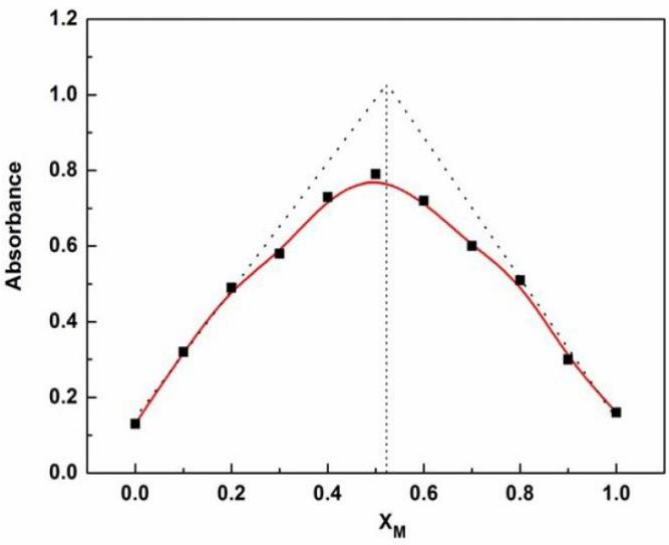

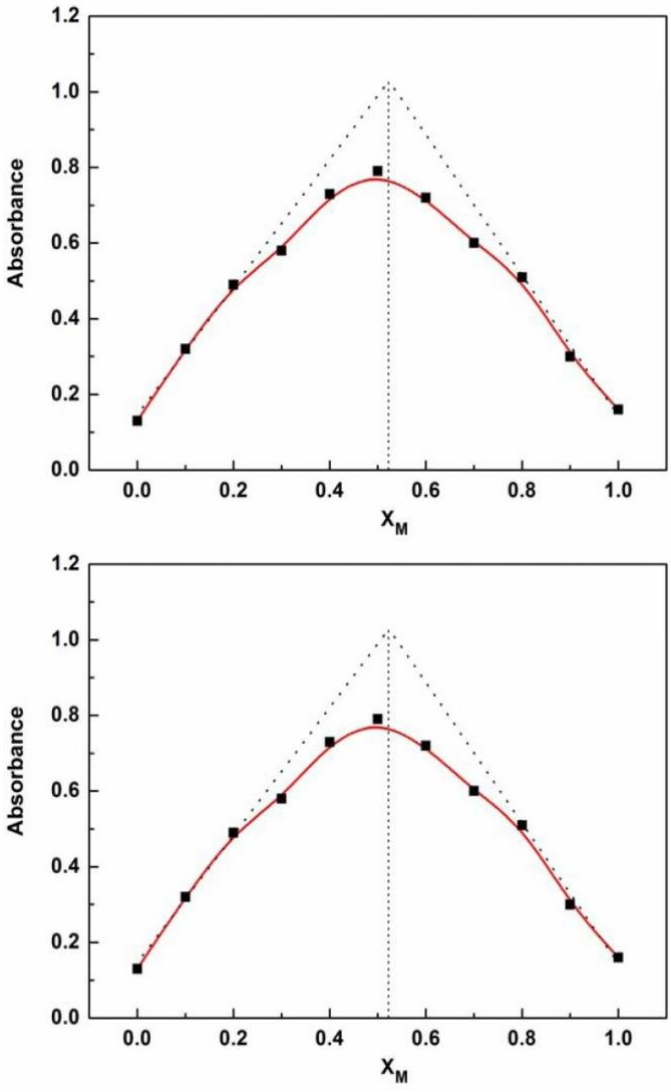

5.3.2Job's plot for complex formation

- For 2.5 milli Mole(mM) of MBH and Hg^{2+} ions from ($HgCl_2$), it forms a complex MBH-Hg^{2+} in the ratio 1: 1 which is proved by Job's plot (Absorbance Vs Mole fraction of MBH – Hg^{2+} complex). A value of 0.5 mole fraction from jobs plot indicates 1:1 ratio of ligand and metal complex.
- In the case of 2.5 milli Mole(mM) of MBH and Zn^{2+} ions from ($ZnCl_2$), it forms a complex MBH- Zn^{2+} in the ratio 1: 1 which is proved by Job's plot (Absorbance Vs

Mole fraction of MBH – Zn^{2+} complex). A value of 0.5 mole fraction from jobs plot indicates 1:1 ratio of ligand and metal complex.

5.4 Fluorescence Spectrum

The cations binding behaviour of the MBH was also investigated by using fluorescence emission spectral studies. There was a strong emission band centered at range of 475 nm, when excited at λ_{ex} = 320 nm. By the addition of various cations, there was a significant increase in the emission intensity of MBH. This fluorescence enhancement could be ascribed to the increased photoinduced electron transfer (PET) process between the MBH moiety and the binding site [42].

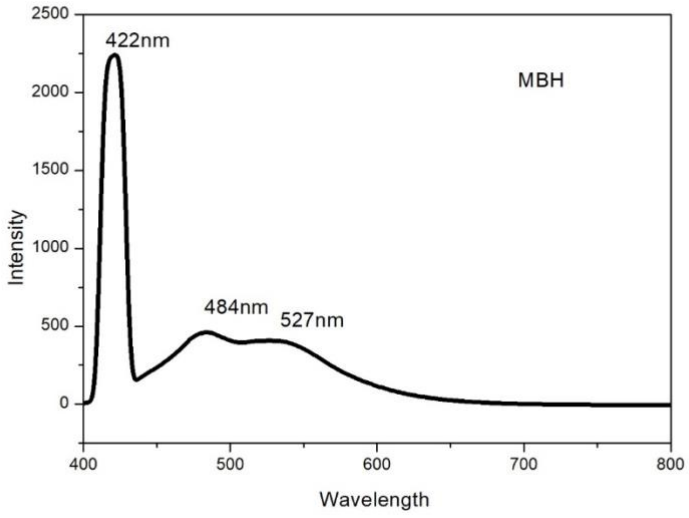

Fig 5.9 Fluorescence spectrum of MBH adduct

Fluorescence spectrum shows peak at 420 nm and a hump at 484 nm, 527 nm when excited at 320 nm, which indicates the emission occurs at 422 nm and a broad spectrum around 484nm.

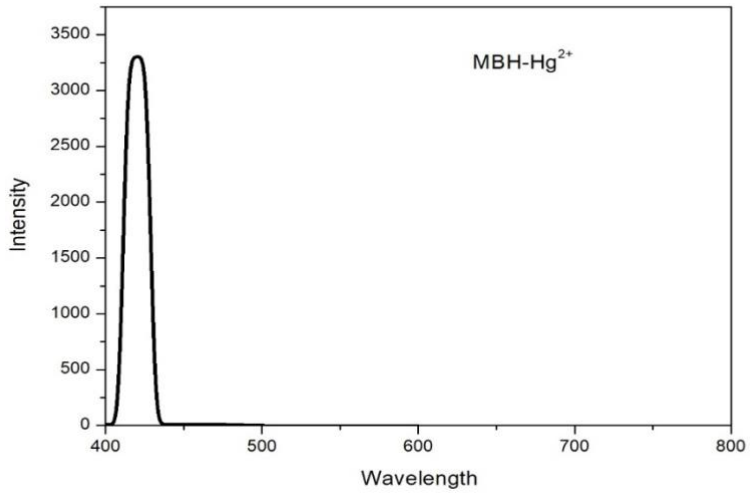

Fig 5.10 Fluorescence spectrum of MBH complex for Hg^{2+}

Once the Hg^{2+} ions forms a complex with MBH adduct, when excited at 320 nm, gives a emission spectrum with increased intensity 2250 to 3250 due to photoinduced electron transfer process. And the absence of hump at 484 nm, which indicates the complex formation of oxygen (lone pair of electrons) with Hg^{2+} ions.

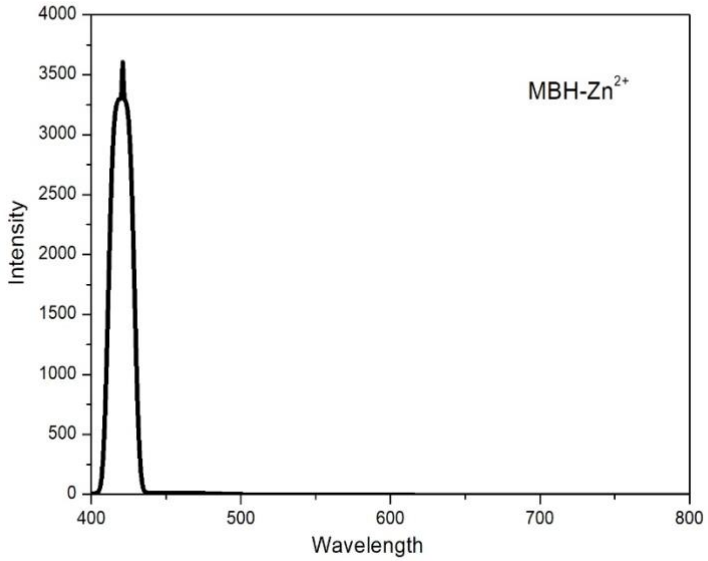

Fig 5.11 Fluorescence spectrum of MBH complex for Zn^{2+}

Once the Zn^{2+} ions forms a complex with MBH adduct, when excited at 320 nm, gives a emission spectrum with increased intensity 2250 to 3250 due to photoinduced electron transfer process. And the absence of hump at 484 nm, which indicates the complex formation of oxygen (lone pair of electrons) with Zn^{2+} ions.

5.4.1 Stack graph of Fluorescence spectrum

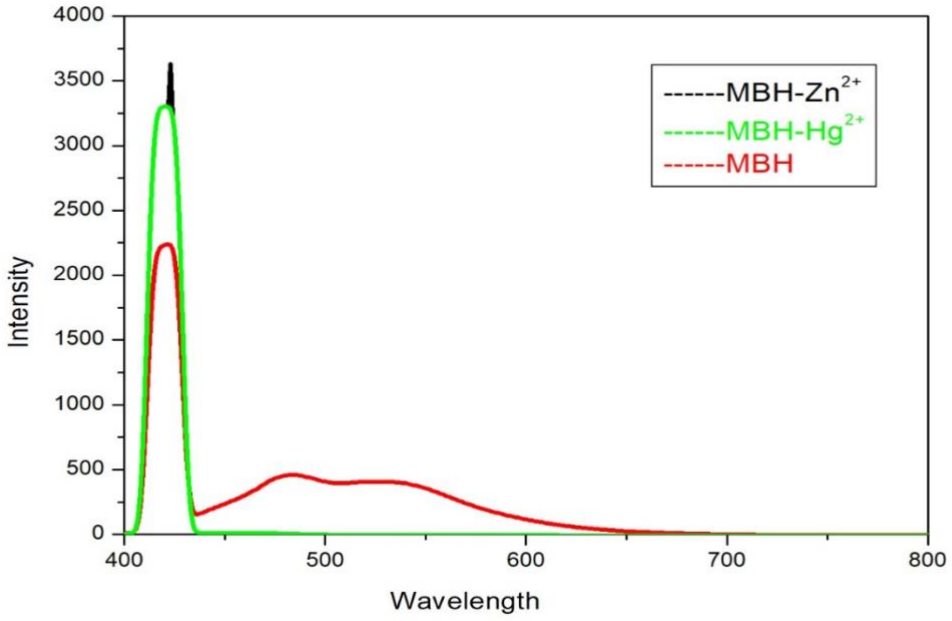

Fig 5.12 Fluorescence spectrum of MBH complex in stack graph

Comparative fluorescence spectrum of MBH, MBH-Hg^{2+} and MBH-Zn^{2+} indicates an increased emission intensity of complexes than MBH adduct. Also, the fluorescence nature of compound get enhanced after complex formation.

5.5 Antibacterial activity

The compound generated during the study gave satisfactory results against the susceptible Gram positive and the Gram negative bacteria including **E.coli, Staphylococcus aureus, Bacillus subtilis, Bacillus cereus, Pseudomonas aeruginosa.**

5.5.1Antibacterial activity of MBH-Hg^{2+}Complexes

Among the evaluated bacteria, mercury complex shows elicit significant antibacterial activity against both **E.coli and Pseudomonas aeruginosa.**

Bacteria	**Inhibition zone in mm**	
	Ab	**MBH-Hg^{2+}**
E.coli	13.5	28
Staphylococcus aureus	15	27
Bacillus subtilis	14	27
Bacillus cereus	19	29
Pseudomonas aeruginosa	14.5	28

Table 5.4: Antibacterial activity of MBH-Hg^{2+} complexes against the bacteria

5.5.2Antibacterial activity of MBH-Zn^{2+}Complexes

Among the evaluated bacteria, zinc complex shows elicit significant antibacterial activity against both ***Bacillus subtilis*** **and** ***Pseudomonas aeruginosa.***

Bacteria	**Inhibition zone in mm**	
	Ab	**MBH- Zn^{2+}**
E.coli	13.5	14.5
Staphylococcus aureus	15	16.5
Bacillus subtilis	14	19
Bacillus cereus	19	15
Pseudomonas aeruginosa	14.5	24

Table 5.5: Antibacterial activity of MBH-Zn^{2+} complexes against the bacteria

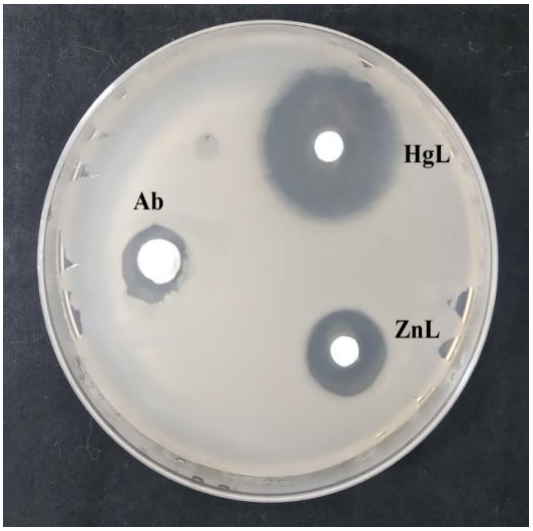

Fig 5.5 (a) E.coli

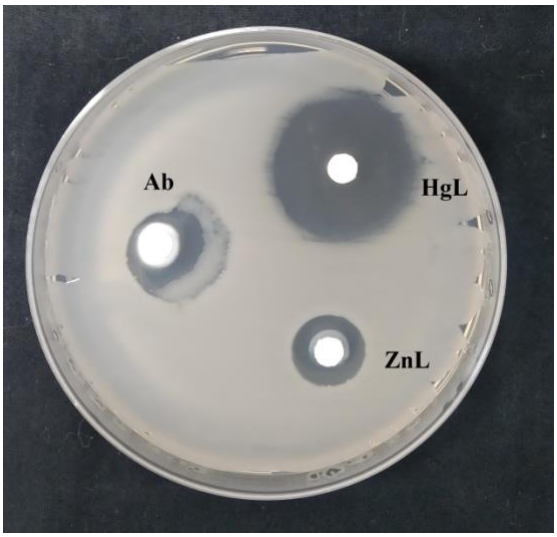

Fig 5.5 (b) Staphylococcus aureus

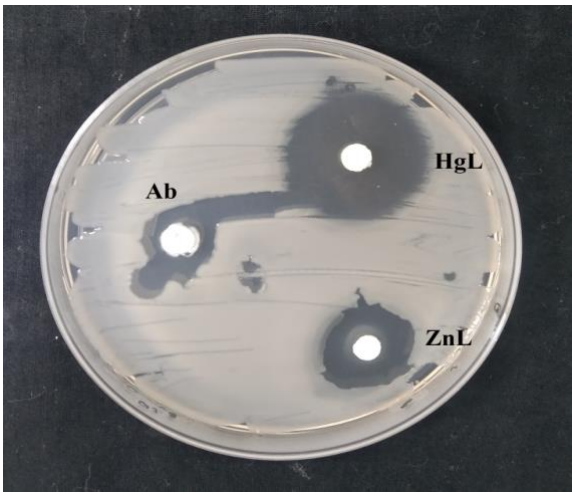

Fig 5.5 (c) Bacillus subtilis

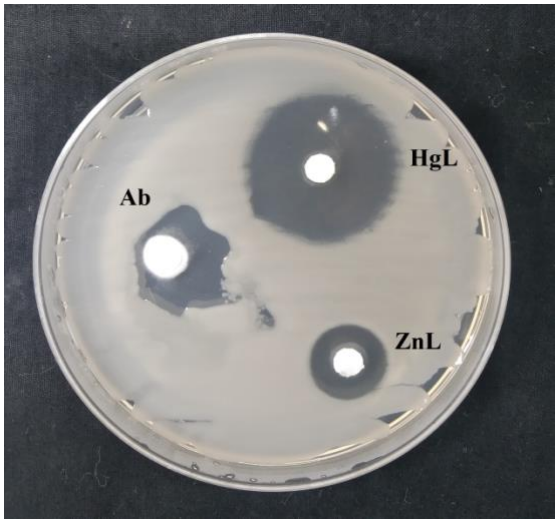

Fig 5.5 (d) Bacillus cereus

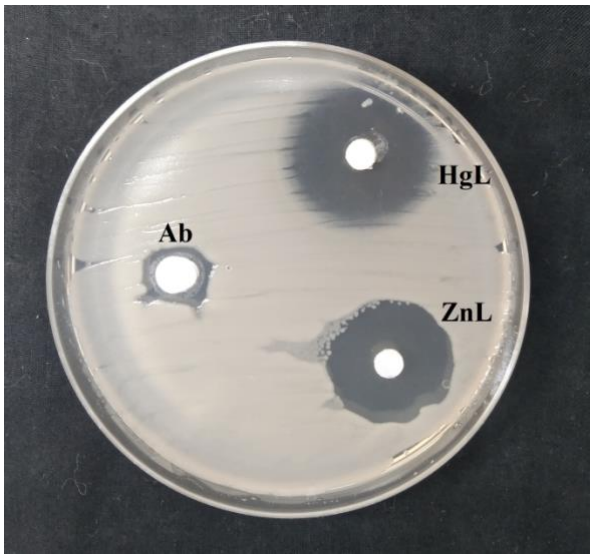

Fig 5.5 (e) Pseudomonas aeruginosa

Table.5.6 Comparitive Antibacterial activity of both MBH-Hg^{2+} and MBH –Zn^{2+} complexes

Bacteria	**Inhibition zone in mm**		
	Ab	**HgL**	**ZnL**
E.coli	13.5	28	14.5
Staphylococcus aureus	15	27	16.5
Bacillus subtilis	14	27	19
Bacillus cereus	19	29	15

Pseudomonas aeruginosa	14.5	28	24

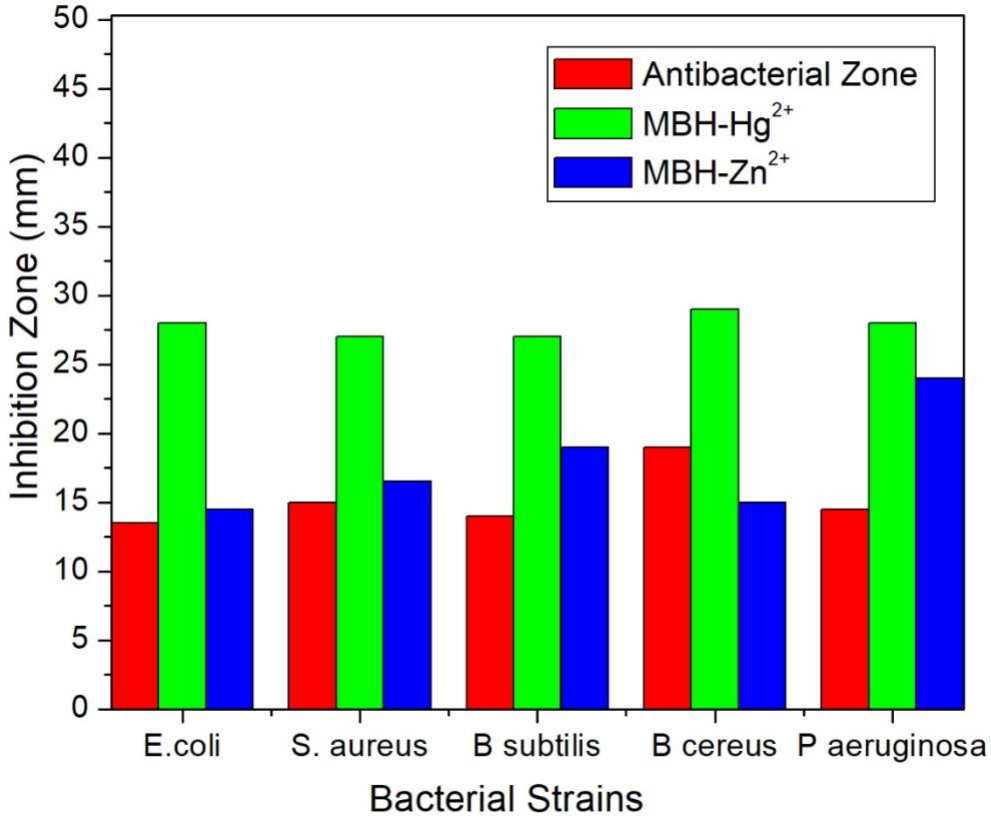

CHAPTER – 6

CONCLUSION

Conclusion

The Hg and Zn complex was synthesis using Morita baylis hillmann adduct. The prepared MBH characterized using several techniques such as UV-Visible, FT-IR, Mass Spectroscopy, and Fluorescence Spectroscopy. The application of the antibacterial activity.

- The UV-Visible absorption peak 252 nm, 255 nm, 236nm and the synthesized baylis hillmann adduct the complexes of Hg^{2+} and $Zn^{2+.}$
- The FT-IR studies showed an absorption peak at 500.43 cm^{-1}, 492.62 cm^{-1} which indicates the formation of baylis hillmann adduct the complexes of Hg^{2+} and Zn^{2+}.
- The mass spectroscopy studies is relatively simple : A compound is ionised, the ions are separate on the basis of their mass / charge ratio and the number of ions representing each mass / charge unit is recorded as a spectrum. The molecular weight of the MBH adduct is 192.
- The fluorescence spectroscopy studies the cations binding behaviour of the MBH was also investigated.

CHAPTER-7

REFERENCES

References

1. Feasey, N.; Wansbrough-Jones, M.; Mabey, D.C.W.; Solomon, A.W. Neglected tropical diseases. Br. Med. Bull. **2010**, 93, 179–200. [**Google Scholar**] [**CrossRef**] [**PubMed**]
2. Singh S, Bhat S **(2011)** Antimicrobial potential of 3-hydroxy-2-methylene-3-phenylpropionic acid derivatives. Acta Pharm 61(4): 447–455. https://doi.org/10.2478/v10007-011-0034-2
3. Toma A, Deyno S **(2015)** Overview on mechanisms of acetic acid resistance in acetic acid bacteria. Int J Res Pharm Bio Sci 2(1): 1–12
4. Cuenca-Estrella M **(2014)** Antifungal drug resistance mechanisms in pathogenic fungi: From bench to bedside. Clin Microbiol Infect 8: 54–59. https://doi.org/10.1111/1469-0691.12495
5. Scorzoni L, de Paula e Silva ACA, Marcos CM, Assato PA, de Melo WCMA, de Oliveira HC, Costa-Orlandi CB, Mendes-Giannini MJ, Fusco-Almeida, A. M. **(2017)** Antifungal Therapy: New Advances in the Understanding and Treatment of Mycosis. Front Microbiol 8: 1–23. https://doi.org/10.3389/fmicb.2017.00036
6. Barbosa TP, Lima-Junior CG, Silva FPL, Lopes HM, Figueiredo LRF, Sousa SCO, Batista GN, Silva TG, Silva TMS, Oliveira MR, Vasconcellos MLAA **(2009)** Improved synthesis of seven aromatic Baylis-Hillman adducts (BHA): Evaluation against Artemia salina Leach. and Leishmania chagasi. Eur J Med Chem 44(4): 1726–1730. https://doi.org/10.1016/j.ejmech.2008.03.016

7. Basavaiah D, Reddy BS, Badsara SS **(2010)** Recent contributions from the BaylisHillman reaction to organic chemistry. Chem Rev 110(9): 5447–5674. https://doi.org/10.1021/cr900291g
8. Lima-Júnior CG, Assis PAC, Silva FPL, Sousa SCO, Andrade NG, Barbosa TP, Nerís PLN, Segundo LVG, Anjos IC, Carvalho GAU, Rocha GB, Oliveira MR, Vasconcellos MLAA **(2010).** Efficient synthesis of 16 aromatic Morita-Baylis-Hillman adducts: Biological evaluation on Leishmania amazonensis and Leishmania chagasi. Bioorg Chem 38(6): 279–284. https://doi.org/10.1016/j.bioorg.2010.08.002
9. Kohn LK, Pavam CH, Veronese D, Coelho F, Carvalho JE, Almeida WP **(2006)** Antiproliferative effect of Baylis-Hillman adducts and a new phthalide derivative on human tumor cell lines. Eur J Med Chem 41: 738–744. https://doi.org/10.1016/j.ejmech.2006.03.006
10. Lima-Júnior CG, Faheina-Martins GV, Bomfim CCB, Dantas BB, Silva EP, Araújo DAM, Filho EB, Vasconcellos MLAA **(2016)** Synthesis, Cytotoxic Activity on Leukemia Cell Lines and Quantitative Structure-Activity Relationships (QSAR) Studies of MoritaBaylis-Hillman Adducts. Med Chem 12(7): 602–612. http://www.ncbi.nlm.nih.gov/pubmed/27150963
11. Faheina-Martins GV, Leite JA, Dantas BB, et al. Morita-Baylis-Hillman Adducts Display Anti-Inflammatory Effects by Modulating Inflammatory Mediator Expression in RAW264.7 Cells **(2017)** Mediators Inflamm 2017:6898505. https://doi.org/10.1155/2017/6898505
12. Elleuch H, Mihoubi W, Mihoubi M, Ketata E, Gargouri A, Rezgui F. Potential antioxidant activity of Morita-Baylis-Hillman adducts **(2018)** Bioorg Chem 78:24-28. https://doi.org/10.1016/j.bioorg.2018.03.004.
13. França JS, de Sales-Neto JM, Carvalho DCM, de Almeida Lima É, Olegário TR, Mendes RKS, Lima-Junior CG, de Almeida Vasconcellos MLA, Rodrigues-Mascarenhas S. Morita-Baylis-Hillman Adduct 2-(3-Hydroxy-2-oxoindolin-3-yl) acrylonitrile (ISACN) Modulates Inflammatory Process In vitro and In vivo **(2021)** Inflammation 44(3):899- 907. https://doi.org/10.1007/s10753-020-01385-9.
14. Baylis, A. B.; Hillman, M. E. D. German Patent 2155113, **1972**.

15. Ciganek, E. Org. React. **1997**, *51*, 201. doi:10.1002/0471264180.or051.02
16. K. Morita, Z. Suzuki and H. Hirose, Bull. Chem. Soc. Jpn. **1968**, 41, 2815.
17. Jump up to:[a] [b] *Recent Advances in the Baylis−Hillman Reaction and Applications* Deevi Basavaiah, Anumolu Jaganmohan Rao, and Tummanapalli Satyanarayana Chem. Rev., **2003**, 103 (3), pp 811–892 2003 (Article) doi:10.1021/cr010043d
18. Masson, G., Housseman, C. and Zhu, J. (**2007**), *The Enantioselective Morita–Baylis–Hillman Reaction and Its Aza Counterpart*. Angewandte Chemie International Edition, 46: 4614–4628. doi:10.1002/anie.200604366
19. *aza-Baylis−Hillman Reaction* Valerie Declerck, Jean Martinez and Frederic Lamaty Chem. Rev., **2009**, 109 (1), pp 1–48, 2009 (Review) doi:10.1021/cr068057c
20. *Recent Contributions from the Baylis−Hillman Reaction to Organic Chemistry* Deevi Basavaiah, Bhavanam Sekhara Reddy and Satpal Singh Badsara Chemical Reviews **2010** 110 (9), 5447-5674 doi:10.1021/cr900291g
21. *The Baylis–Hillman reaction: a novel concept for creativity in chemistry* Deevi Basavaiah and Gorre Veeraraghavaiah Chem. Soc. Rev., **2012**, Advance Article doi:10.1039/C1CS15174F
22. Uppuluri V. Mallavadhani, Nicolas Fleury-Bregeot. "1,4-Diazabicyclo[2.2.2]octane". In Encyclopedia of Reagents for Organic Synthesis, **2010**, John Wiley & Sons, Ltd. doi:10.1002/047084289X.rd010m.
23. *"Polyurethane additives guide" (PDF). Air Products & Chemicals. Archived from the original (PDF) on* **2016-03-06.**
24. Baylis, A. B.; Hillman, M. E. D. German Patent 2155113, **1972**.
25. P. Dembech, A. Ricci, G. Seconi, and M. Taddei "Bis(trimethylsilyl) Peroxide" Org. Synth. **1997**, volume 74, pp. 84. doi:10.15227/orgsyn.074.0084
26. Ludovic Martial and Laurent Bischoff "Preparation of DABSO from Karl-Fischer Reagent" Org. Synth. **2013**, volume 90, pp. 301. doi:10.15227/orgsyn.090.0301
27. *Ouannes, C.; Wilson, T.* **(1968).** *"Quenching of singlet oxygen by tertiary aliphatic amines. Effect of DABCO (1,4-diazabicyclo[2.2.2]octane)". Journal of the American Chemical Society. **90** (23): 6527–6528. doi:10.1021/ja01025a059.*

28. *Valnes, K.; Brandtzaeg, P.* **(1985).** *"Retardation of immunofluorescence fading during microscopy". Journal of Histochemistry and Cytochemistry. **33** (8): 755–761. doi:10.1177/33.8.3926864. PMID 3926864.*
29. *Ho, T. L.* **(1972).** *"Dealkylation of Quaternary Ammonium Salts with 1,4-Diazabicyclo[2.2.2]octane". Synthesis. **1972** (12): 702. doi:10.1055/s-1972-21977.*
30. Karsten Eller, Erhard Henkes, Roland Rossbacher, Hartmut Höke "Amines, Aliphatic" in Ullmann's Encyclopedia of Industrial Chemistry, Wiley-VCH, Weinheim, 2005. doi:10.1002/14356007.a02_001
31. *Mahle, J.; et al.* **(2010)**. *"Role of TEDA as an Activated Carbon Impregnant for the Removal of Cyanogen Chloride from Air Streams: Synergistic Effect with Cu(II)". Journal of Physical Chemistry C. **114** (47): 20083–20090. doi:10.1021/jp106730j. Retrieved 2022-03-17.*
32. Basavaiah, D.; Reddy, B.S.; Badsara, S.S. Recent Contributions from the Baylis−Hillman Reaction to Organic Chemistry. Chem. Rev. **2010**, 110, 5447–5674. [**Google Scholar**] [**CrossRef**] [**PubMed**]
33. Santos, M.S.; Coelho, F.; Lima-Junior, C.G.; Vasconcellos, M.L.A.A. The Morita-Baylis-Hillman Reaction: Advances and Contributions from Brazilian Chemistry. Curr. Org. Synt. **2015**, 12, 830–852. [**Google Scholar**] [**CrossRef**] [**PubMed**]
34. Viegas-Junior, C.; Danuello, A.; Bolzani, V.S.; Barreiro, E.J.; Fraga, C.A.M. Molecular Hybridization: A Useful Tool in the Design of New Drug Prototypes. Curr. Med. Chem. **2007**, 14, 1829–1852. [**Google Scholar**] [**CrossRef**] [**PubMed**]
35. Barbosa, T.P.; Sousa, S.C.O.; Amorim, F.M.; Rodrigues, Y.K.S.; de Assis, P.A.C.; Caldas, J.P.A.; Oliveira, M.R.; Vasconcellos, M.L.A.A. Design, synthesis and antileishmanial in vitro activity of new series of chalcones-like compounds: A molecular hybridization approach. Bioorg. Med. Chem. **2011**, 19, 4250–4256. [**Google Scholar**] [**CrossRef**] [**PubMed**]
36. Xavier, F.J.S.; Rodrigues, K.A.F.; Oliveira, R.G.; Lima-Junior, C.G.; Rocha, J.C.; Keesen, T.S.L.; Oliveira, M.R.; Silva, F.P.L.; Vasconcellos, M.L.A.A. Synthesis and In Vitro Anti Leishmania amazonenses Biological Screening of Morita-Baylis-Hillman

Adducts Prepared from Eugenol, Thymol and Carvacrol. Molecules **2016**, 21, 1483. [**Google Scholar**] [**CrossRef**] [**PubMed**]

37. Capim, S.L.; Carneiro, P.H.P.; Castro, P.C.; Barros, M.R.M.; Marinho, B.G.; Vasconcellos, M.L.A.A. Design, Prins-cyclization reaction promoting diastereoselective synthesis of 10 new tetrahydropyran derivatives and in vivo antinociceptive evaluations. Eur. J. Med. Chem. **2012**, 58, 1–11. [**Google Scholar**] [**CrossRef**] [**PubMed**]
38. The 2D-NOESY spectrum of compound **6** described on reference 11, presented significant signals of correlation between Ha/ Hb, Ha/Hc and Hb/Hc that determine unequivocally the 2,4,6-cis geometry of tetrahydropyran ring. Thus, the relative configuration of the C2 -C4-C6 in the compounds **8a-8h** in the tetrahydropyran ring are the same as those determined for **6**. However, the relative configuration in the carbinolic carbon in **8a-8h** has not been determined in this article.
39. Lakowicz, JR **2006**. Principles of fluorescence spectroscopy (3rd ed.) springer., p 954
40. Holler, F. James; Skoog, Douglas A., crouch, stanely R**. 2006.** Principles of Instrumental Analysis.
41. J.R. Lakowicz, Principles of Fluorescence spectroscopy, **2006.**
42. Gunnlaugsson, T., Bichell, B., Nolan, C. Tetrahedron 60, 5799-5806, **2004**.

THE MOLECULAR DOCKING ANALYSIS OF ANTIHYPERTENSION DIURETIC

A project submitted to

St. Mary's College (Autonomous), Thoothukudi

Affiliated to

MANONMANIUM SUNDARNAR UNIVERSITY

TIRUNELVELI

In partial fulfilment of the award of the degree of

MASTER OF SCIENCE IN CHEMISTRY

Submitted by

ASHMITHA.K

Reg. No: 21SPCH02

Under the Supervision and Guidance of

Dr. Mrs. C. ZOZIMUS DIVYA LOBO M.Sc., M.Phil, Ph.D.,

PG DEPARTMENT OF CHEMISTRY (SSC)

St. Mary's College (Autonomous), Thoothukudi

APRIL 2023

CERTIFICATE

This is to certify that this project work entitled **" THE MOLECULAR DOCKING ANALYSIS OF ANTIHYPERTENSION DIURETIC** "is submitted to St. Mary's College (Autonomous), Thoothukudi affiliated to **Manonmaniam Sundaranar University, Tirunelveli** in partial fulfilment for the award of the **Degree of Master of Science in Chemistry** and this work done during the year 2022 - 2023 by ASHMITHA.K (Reg. No: 21SPCH02)

Signature of the Guide

Dr. C. ZOZIMUS DIVYA LOBO
M.Sc., M.Phil, Ph.D.,
ASSISTANT PROFESSOR
DEPARTMENT OF CHEMISTRY
ST. MARY'S COLLEGE (AUTONOMOUS)
THOOTHUKUDI-628001. TAMILNADU

Signature of the Director
Director
Self Supporting Courses
St. Mary's College (Autonomous)
Thoothukudi - 628 001.

Signature of the Coordinator

Dr. J. ANTONY RAJAM, M.Sc. M.Phil. Ph.D. SET.
SSC Co-ordinator & Asst. Professor
PG Department of Chemistry
St. Mary's College (Autonomous)
Thoothukudi - 628 001.

Signature of Principal
Principal
St. Mary's College (Autonomous)
Thoothukudi - 628 001.

Signature of the Examiner

13/4/23

DECLARATION

I do hereby declare that the project entitled**“ THE MOLECULAR DOCKING ANALYSIS OF ANTIHYPERTENSION DIURETIC"** submitted for the degree of Master of Science in Chemistry is my original work carried out under the guidance of **Dr. Mrs. C. ZOZIMUS DIVYA LOBO M.Sc., M.Phil., Ph.D., Assistant Professor, PG Department of Chemistry (SSC), St. Mary's College (Autonomous), Thoothukudi** and that it has not previously formed the basis for award of any Degree.

Station: Thoothukudi

Date: 05.04.23

K. Ashmitha

K.ASHMITHA

ACKNOWLEDGEMENT

I express my first and humble thanks to **GOD ALMIGHTY** for giving an opportunity to devote this work

I would like to express my sincere thanks to our Principal Dr. Sr. A.S.J. Lucia Rose, Secretary Dr.Sr. C. Shibana, Deputy principal Dr. Sr. S.Kulandi Therese, Director of SSC Sr. Josephine Jeyarani and Dr. J. Antony Rajam (SSC Coordinator), St Mary's College (Autonomous), Thoothukudi for providing the permission to complete the project work

I find it difficult for me to write something in short to acknowledge my guide **Dr. C. ZOZIMUS DIVYA LOBO** she taught me to think and solve the unconventional problems in a conventional way. Her constant inspiration, evaluable guidance tremendous patience and constructive criticism helped a lot to focus my views in the proper perspective I take this opportunity to express my deepest sense of gratitude and reference towards her for guiding me in the right direction throughout the course of this work.

I heartily express my sincere thanks to my parents and friends.

ABSTRACT

Diuretics was a medication prefered in management and treatment of oedema,water retension,fluidretension,dropsy,swelling edematous and other non-edematous disease conditions. Diuretics drugs shows about the indications, action and symptoms for diuretics as a valuable agent in treating heart failure, hypertension, abdominal dropsy, etc.,. Diuretics is used in the treatment of patients with heart failure and related conditions.Diuretic. In the current investigation, the ability of separated phytochemicals to bind to the intended protein was tested. In order to achieve this, the 3D structure of the current investigation, the ability of separated phytochemicals to bind to the intended protein was evaluated. For this, PyRx was used to replicate the target protein's (3-dimensional) structure. To predict the binding mechanisms of these drug-like compounds, the molecular docking of 24 phytochemicals described as Diuretics inhibitors was carried out using the PyRx software together with reference compounds. The findings showed that they were similar to reference ligands and had remarkable interactions with the target protein's active site residues. In summary, the current work gave the tested - blocker inhibitors a computational foundation. The discovery of innovative medicinal compounds for the treatment of should be aided by this information.

KEYWORDS: Molecular docking, Protein, Ligand, Diuretics, PyRx

Content

CHAPTER 1

INTRODUCTION

DIURETICS

Diuretics was a medication prefered in management and treatment of oedema, water retension, fluid retention, dropsy, swelling edematous and other non-edematous disease conditions. Diuretics is a class of drugs.[1] This activity shows about the indications, action, and symptoms for diuretics as a valuable agent in treating heart failure, hypertension, abdominal dropsy, etc..[2] Diuretics are used in the treatment of patients with heart failure and related conditions. Diuretic medication can help the person who are all suffering from high blood pressure, heart failure, renal failure, pulmonary edema, nephritic syndrome etc [3]

Any chemical that enhances urine flow and consequently, water excretion is referred to as a diuretic. The word diuretic is derived from the Greek diu (through) retic (to urinate) [4] The majority of diuretics work by lowering salt chloride reabsorption at various sites in the nephron, which increases urine sodium and as a result, water loss. Diuretics are among the most widely used medication [5]

The mercurials were the most efficient diuretics from 1919 to the 1960s and were the cornerstone of treatment; however, they are no longer utilised due to their toxicity [6] Other possibilities at the time included acidifying salts like Ammonium Chloride, Osmotic Diuretics like Urea, Mannitol and Sucrose, Xanthine derivatives and digoxin, which has both an inotropic and diuretic action [7]

ADVERSE EFFECT

The usual adverse effect for all type of diuretic is mild hypovolemia, which can lead to temporary dehydration and increased thirst. When there is an over-treatment with a diuretic, this could lead to severe blood disorder, causing hypotension, dizziness and loss of consciousness. Generalized side-effects of diuretic agents include headache, urinary frequency,

restlessness, weakness, fatigue and lethargy. GI disturbances like nausea, vomiting, constipation, diarrhea, anorexia and abdominal pain can occur with loop diuretics and PSDs than any other diuretic group. Hyponatraemia is very oftenly used [8].

CLASSIFICATION

Based on their action in the kidneys, diuretics are classified into loop, thiazide, and potassium sparing diuretics.

LOOP DIURETICS

Loop or high-ceiling diuretics have more than 95% albumin-bound and reach peak concentrations in 30 min to 2 hours as they are absorbed .Loop diuretics are threshold drugs that is no diuretic effect. It will occur below the threshold drug concentration [9]. The threshold level also based on different clinical conditions and could be different for one patients to another patient. To gain effective diuresis, different doses might be required to achieve the threshold level. The lowest dose that is clinically effective should be chosen for HF treatment. Loop diuretics have been approved by the Food and Drug Administration (FDA) for treating conditions of edema related with heart failure, liver cirrhosis and renal disease, including glomerular disease [10]

The ascending limb of the Henle loop is where the effects of loop diuretics are felt. They are used to treat edoema related to liver cirrhosis, renal illness, particularly nephrotic syndrome, and pulmonary and peripheral edoema brought on by heart failure [11] they are the first-line therapy for these conditions. Furosemide is the most well-known agent. Torsemide, ethacrynic acid, and bumetanide are further medications in this group. There are numerous oral and intravenous versions of loop diuretics [12]

THIAZIDE DIURETICS

Thiazide diuretics come in oral tablet form. Patients should take these medications with breakfast. For the uses that have been approved by the FDA and are described above, HCTZ and chlorthalidone require different dosages [13] These medications typically need to be used in lower doses for the treatment of hypertension, starting at 25 mg daily and increasing as needed to 50 mg or 100 mg. Based on the patient's individual therapeutic needs, the dosage should be raised. Dosing ranges for patients with fluid retention and edoema are 50 mg to 100 mg and 50 mg to 200 mg, respectively [14]. Thiazide diuretics have been a cornerstone of the

management of hypertension ever since they were discovered in 1957, when they offered the first opportunity to effectively lower blood pressure. Additionally, thiazide diuretics, whether administered alone or in combination with blockers, have been shown to reduce CardioVascular (CV) morbidity and mortality in placebo-controlled clinical studies a benefit that is comparable to that seen with other Antihypertensive drug classes, such as Angiotensin-Converting Enzyme (ACE) inhibitors and calcium antagonists[15] In this article, we go over a variety of subjects related to thiazide diuretics' use in the management of hypertension.

POTASSIUM- SPARING DIURETICS

Potassium-sparing diuretics are drugs that boost urination without causing potassium loss during dieresis [16]. They function as antagonists at the aldosterone receptor or as mild diuretics by interfering with sodium-potassium exchange in the distal convoluted tubule of the kidneys. When potassium-sparing diuretics are used to counteract the impact of aldosterone, more sodium and water can pass into the collecting ducts of the kidneys, resulting in an increase in diuresis [17]. Potassium-sparing diuretics do not produce hypokalemia because they do not encourage the secretion of potassium during diuresis (low potassium levels). When combined with medications that also retain potassium, like ACE inhibitors, they can cause hyperkalemia (high potassium levels). Diuretics that conserve potassium can be used on their own or in combination with loop or thiazide diuretics [18].

DIURETIC IN DIAGNOSES

Diuretic has found a specific purpose in the diagnosis of distal renal tubular acidosis (RTA), often known as type I RTA. Diuretics are typically thought of as therapeutic drugs[19] The furosemide-fludrocortisone test is a speedier and more palatable way to detect urine acidity than the ammonium chloride test [20]. The ammonium chloride loading test has several inherent issues, one of which is that it frequently results in vomiting, necessitating the termination of the test. None of the participants in Walsh *et al.*, report suffered negative side effects, and the concurrent administration of furosemide and the mineralocorticoid fludrocortisone was well tolerated [21].

FUTURE DEVELOPEMENT

An intriguing challenge for medical science has lately been presented by the discovery of a new family of diuretics. They are known as AQP modulators, and since a patent application

for the first in their class, AqB013, has just been made, it seems likely that they will be used commercially [22]. Long had physiologists debated the possibility of "gates" allowing quick water absorption by renal tubular cells. The lipid bilayer of the cell membrane, which was first described as a hydrophobic barrier by the Danielli-Davson model in 1935, can only be crossed via diffusion in a very small amount [23].

TREATMENT

Diuretics should be taken into consideration for heart failure patients who have dyspnea, ankle or pulmonary oedema, according to other research and guidelines released by the National Institute for Health and Clinical Excellence (NICE) in 2003[24]. Both should be started before the beginning of -blockers, either simultaneously or before ACE inhibitors. Diuretics are administered on an individual basis to lessen fluid retention, despite the lack of clear evidence that they have a positive impact on mortality. With loop diuretics in particular, overtreatment can cause renal impairment as well as dehydration [25].

Unfortunately, people sometimes decide to use diuretics improperly when there isn't really a clinical reason to. The hypokalaemia that can develop is typically linked to an eating disorder (anorexia nervosa or bulimia), and it may be lethal. Diuretics have been added to The World Anti-Doping Agency's (WADA) list of prohibited substances since they are also abused in sports [26]. Both during and after competition, the use of diuretics is prohibited and antidoping laboratories routinely check for their presence.

DRUG DISCOVERY

In the fields of medicine, biotechnology and pharmacology, drug discovery is the process by which new candidate medications are discovered [27]. Historically, drugs were discovered by identifying the active ingredient from traditional remedies or by serendipitous discovery, as withpenicillin. More recently, chemical libraries of synthetic small molecules, natural products or extracts were screened in intact cells or whole organisms to identify substances that had a desirable therapeutic effect in a process known as pharmacology[28]. After sequencing of the human genome allowed rapid cloning and synthesis of large quantities of purified proteins, it has become common practice to use high throughput screening of large compounds libraries against isolated biological targets which are

hypothesized to be disease-modifying in a process known as reverse pharmacology. Hits from these screens are then tested in cells and then in animals for efficacy [29].

Modern drug discovery involves the identification of screening hits, medicinal chemistry and optimization of those hits to increase the affinity, selectivity (to reduce the potential of side effects), efficacy/potency, metabolic stability (to increase the half-life) and oral bioavailability. Once a compound that fulfills all of these requirements has been identified, the process of drug development can continue. If successful, clinical trials are developed [30].

Modern drug discovery is thus usually a capital-intensive process that involves large investments by pharmaceutical industry corporations as well as national governments [31]. Despite advances in technology and understanding of biological systems, drug discovery is still a lengthy, "expensive, difficult and inefficient process" with low rate of new therapeutic discovery. In 2010, the research and development cost of each new molecular entity was about US$1.8 billion. In the 21st century, basic discovery research is funded primarily by governments and by philanthropic organizations, while late-stage development is funded primarily by pharmaceutical companies or venture capitalists[31]To be allowed to come to market, drugs must undergo several successful phases of clinical trials, and pass through a new drug approval process, called the New Drug Application in the United States.

Discovering drugs that may be a commercial success, or a public health success, involves a complex interaction between investors, industry, academia, patent laws, regulator exclusivity, marketing and the need to balance secrecy with communication [32]. Meanwhile, for disorders whose rarity means that no large commercial success or public health effect can be expected, the orphan drug funding process ensures that people who experience those disorders can have some hope of pharmacotherapeutic advances [33].

PHYTOMEDICINE

Phytomedicine is primarily a therapy-oriented Journal. *Phytomedicine* publishes innovative studies on efficacy, safety, quality and mechanisms of action of specified plant extracts, phytopharmaceuticals and their isolated constituents. This includes *pharmacological, pharmacokinetic, and toxicological studies* of specified herbal medicinal products, herbal preparations and purified compounds which have a defined and consistent quality assuring activity[34].

Phytomedicine was founded in 1994 to focus and stimulate research in this particular field and

to set internationally accepted scientific standards for pharmacological studies, proof of clinical efficacy and safety of phytomedicines.The directions are known to provide profound scientific background in Herbal Medicinal Products, their reproducible Quality and evidence based therapeutic efficacy[35] Since then quality criteria and standardization methods were defined and the European Medical Agency has elaborated numerous guidelines for the conduction of clinical studies and preparation of Herbal Medicinal Products[36] In total 107 ESCOP monographs have been produced and submitted to EMA. Many new analytical methods and instruments were implemented both for analysis and standardization of herbal Substances, herbal preparations and their bioassays and tremendous work has been carried out to remain aligned with these intentions during the last 18 years.

Nowadays important topics remain to be approached, such as harmonization of the regulatory frameworks in Europe, America, Asia and Australia or the legislation of various "botanicals", where strict differentiation of requirements for health claims of herbal medicinal product, dietary supplements and nutraceuticals are required [37]

MOLECULAR DOCKING

A computer technique called molecular docking is used to assess how well certain molecules attach to their active site residue. Molecular docking is a quick method for determining how well ligands will attach to a target (a receptor), making it possible to choose active compounds, foresee how they will operate and improve lead structures. In the field of structure-based drug development, QSAR analysis and docking-based scoring are frequently combined.

Docking processes are essentially a fusion of scoring systems and search algorithms. There are the most available search algorithms and scoring mechanisms. The ligand binding orientation and conformations, also known as posing, are predicted using search methods. Monte Carlo methods, genetic algorithms, fragment-based methods, point complementary methods, distance geometry methods, tabu searcher, and fragment-based methods are a few examples of common search algorithms [38]

REMEDIES

Some plants, like parsley and dandelion are regarded as natural diuretics. The fact that caffeine is a natural diuretic is fortunate for those who like coffee and tea, black and green teas make the finest diuretic beverages because you can control how much you consume. Exercise is one of the simpler natural diuretics since it increases your heart rate, which will help the fluid that has accumulated in your body circulate. Fruits and vegetables that contain water not only contain vitamins and minerals but also act as natural diuretics. Another common natural diuretic is weight loss; after all, over 60% of your body is water, so doing so is one approach to lessen fluid retention [39]

There are a tonne of diuretics available to treat issues with water retention. Western medical professionals will typically recommend a water pill or other synthetic drug to treat the issues. Because they are not built to cooperate with how the body normally functions, many man-made substances can be harsh on the body. Naturopaths, Chinese traditional doctors and herbalists typically recommend plant-based remedies instead. This might be offered as a tablet, tincture, or herbal tea. Any medication or tea derived from a plant or other substance found in nature is considered a natural diuretic. Basically, any treatment that isn't created by a machine is usually regarded as natural [40]

CHAPTER 2

LITERATURE REVIEW

- *Radwan Alnajjar et al., (2020)*studied the Drug repurposing is the most rapid and economic way nowadays to rapidly provide effective drugs for our pandemic corona virus disease 2019 (COVID-19). It was a great debate about ARBs whether to be stopped or continued for patients using them especially at the beginning of the COVID-19 pandemic. In this study, we carried out a virtual screening for almost all members of ARBs (nine) against COVID-19 main protease. Molecular docking as one of the important computational techniques was performed in this work. Interestingly, the tested compounds showed variable binding affinities in the order of N3 inhibitor (10, docked) were additionally estimated through molecular dynamic simulations monitored via computing the binding free energy using MM-GBSA. The results are promising for rapidly repurposing such drugs after further preclinical and clinical studies either alone or in combination with others for the treatment of COVID-19 virus especially known to cause vasodilatation (to prevent blood coagulation) and to reduce inflammation and fibrosis (to prevent pulmonary fibrosis), with well-known safety profiles. In vitro, the virtual findings were consistent with the experimental testing of four representative ARBs. Out of the tested compounds, showed the most promising anti-SARS-CoV-2 activity with high selectivity index (308.4) against SARS-CoV-2 in Vero E6 cells. This work may clarify and approve not only the safety of ARBs used by a large group of patients worldwide but also their possible effectiveness against the COVID19 virus either as a prophylactic or treatment option.

- *Syed Sikander Azam et al., (2013)*studied three melatoninergic inhibitors were docked with acetyl serotonin-Omethyl transferase in order to identify the potent inhibitor against the enzyme. The chemical nature of the protein and ligands greatly influence the performance of docking routines. Keeping this fact in view, critical evaluation of

the performance of four different commonly used docking routines: AutoDock/Vina, GOLD, Flex and FRED were performed. An evaluation criterion was based on the binding affinities/docking scores and experimental bioactivities. Results and conclusion: Results indicated that both hydrogen bonding and hydrophobic interactions contributed significantly for its ligand binding and the compound selected as potent inhibitor is having minimum binding affinity, maximum GoldScore and minimum FlexX energy. The correlation value of r2 = 0. 66 may be useful in the selection of correct docked complexes based on the energy without having prior knowledge of the active site. This may lead to further understanding of structures, their reliability and Biomolecular activity especially in connection with bipolar disorders.

- *Koushik Nandan Dutta et al., (2014)*studied Medicinal herbs are the significant source as Diuretics. Mono and poly-herbal preparations have been used as diuretics. According to one estimate, more than 650 mono and poly-herbal preparations in the form of decoction, tincture, tablets and capsules from more than 75 plants are in clinical use. There exist a large number of studies which supports the diuretic effects of traditional herbal medicines. This article reviews the various herbal plants used traditionally as diuretics and the identification of chemical constituent of the plant promoting diuresis. The present paper also involves various plant drugs and their pharmacological profile which focus on the dose administered, bioactive extract involved in diuresis mechanism. This work may mark an important milestone for the researchers in the selection of medicinal plant for carrying their work on diuretics

- *Kero Jemal (2019)* studied Allophylus serratus is a medicinal plant used traditionally as anti-inflammatory agent. The main objectives of this study are to identify phytochemical compounds that have anti-inflammatory properties from the leaf extracts of Allophylus serratus and to search for cyclooxygenase-2 (COX-2) enzyme inhibitors through molecular docking. From the GC-MS analysis of leaf extracts of this plant, various phytochemicals were identified. About 10of these phytochemical compounds were analyzed for their drug likeliness based on Lipinski's rule of five and inhibitor property against the cyclooxygenase (COX-2) enzyme, a protein responsible for inflammation The phytochemical compounds which satisfy the Lipinski's rule such as 1H-Benzocycloheptene and Sulfurous acid, dipentyl ester were subjected to docking

experiments using AutoDock Vina. The results from molecular docking study revealed that 1H-Benzocycloheptene, 2,4a,5,6,7,8-hexahydro-3,5,5,9-tetramethyl-, (R)-, Sulfurous acid, dipentyl ester and 1,2-Benzenedicarboxylic acid, bis(2-methylpropyl) ester bind effectively to the active site region of COX-2 with a binding energy of -8.9, -8.4, and -7.9, respectively. The binding energy of the phyto-compounds were compared with the known antiinflammatory drug Diclofenac that inhibit COX-2 enzyme. It was found that the phytochemical compounds from leaf extracts of Allophylus serratus have strong inhibitory effect on COX-2 enzyme and as a result they have potential anti-inflammatory medicinal values. Thus the study under aCC-BY 4.0 International license not certified by peer review) is the author/funder, who has granted bioRxiv a license to display the preprint in perpetuity. It is made available bioRxiv preprint this version posted December 5, 2019.

- *Shuyue Wang et al., (2020)*studied the Hypertensive vascular remodeling (HVR) is the pathophysiological basis of hypertension, which is also an important cause of vascular disease and target organ damage. Treatment with Fructus Tribuli (FT), a traditional Chinese medicine, has a positive effect on HVR. However, the pharmacological mechanisms of Flare still unclear. (Therefore, this study aimed to reveal the potential mechanisms involved in the effects of FT on HVR based on network pharmacology and molecular docking. Materials and Methods. We selected the active compounds and targets of FT according to the Traditional Chinese Medicine Systems Pharmacology Database and Analysis Platform (TCMSP) and the Swiss Target Prediction database, and the targets of HVR were collected from the Online Mendelian Inheritance in Man (OMIM), GeneCards, and DrugBank databases. (e protein-protein interaction network (PPI) was established using the STRING database. Moreover, Gene Ontology (GO) and Kyoto Encyclopedia of Genes and Genomes (KEGG) pathway analyses and network analysis were performed to further explore the potential mechanisms. Finally, molecular docking methods were used to evaluate the affinity between the active compounds and the main target. Results. Seventeen active compounds of FT and 164 potential targets for the treatment of HVR were identified. Component-target and PPI networks were constructed, and 12 main active components and 33 main targets were identified by analyzing the topological parameters. Additionally, GO analysis indicated that the potential targets were enriched in 483 biological processes, 52 cellular components, and 110 molecular functions. KEGG analysis revealed that the potential

targets were correlated with 122 pathways, such as the HIF-1 signaling pathway, ErbB signaling pathway, and VEGF signaling pathway. Finally, molecular docking showed that the 12 main active components had a good affinity for the top five main targets. Conclusion. (Study demonstrated the multiple compounds, targets, and pathway characteristics of FT in the treatment of HVR

- *Fang Liu et al., (2021)* studied the role of traditional Chinese medicine Prunella vulagaris L in the treatment of tumors and inflammation has been widely confirmed. We found that some signaling pathways of Prunella vulgaris L action can also regulate diabetes and hypertension, so we decided to study the active ingredients, potential targets and signaling pathway of Prunrlla vulgaris L, and explore the "multi-target, multi-pathway" molecular mechanism of Prunella vulgaris L on diabetes mellitus complicated with hypertension(DH). Methods. Based on TCMSP (Traditional Chinese Medicine Systems Pharmacology Database and Analysis Platform) and CNKI (China National Knowledge Infrastructure), the components and action targets related to Prunella vulgaris L were screened. The OMIM (Online Mendelian Inheritance in Man) and GeneCards (The human gene database) were used to search for targets related to DH. The "gene - drug - disease" relationship map was drawn by Cytoscape_v3.7.2 plug-in. The target was amplified by the STRING platform, and the "protein - protein" interaction relationship (PPI) network of the interacting target was obtained by the STRING online analysis platform and the Cytoscape_v3.7.2 plug-in. Finally, GO enrichment analysis and KEGG pathway enrichment analysis were conducted on David and Metascape platform to study the co-acting targets. Results. 11 active components, 41 key targets and 16 significant signaling pathways were identified from Prunella vulgaris L. The main active components of Prunella vulgaris L against DH were quercetin and kaumferol, etc, and potential action targets were IL-6 and INS, etc and signaling pathways were AGE-RAGE signaling pathway, TNF signaling pathway, MAPK signaling pathway, PI3K-AKT signaling pathway, etc. It involves in biological processes such as cell proliferation, apoptosis and inflammatory response. Conclusions. The main molecular mechanism of Prunella vulgaris L against DH is that sterols and flavonoids play an active role by affecting TNF signaling pathway, AGE-RAGE signaling pathway, MAPK pathway, PI3K-Akt pathway related targets such as IL-6 and INS.

- *Daddam Jayasimha Rayalu et al.,(2012)*studied about the cardiovascular system, activation of Endothelin receptors causes vasoconstriction which leads to Pulmonary Arterial Hypertension (PAH). Endothelin receptor antagonism has emerged as an important therapeutic strategy in pulmonary arterial hypertension. Bosentan is intended to affect vasoconstriction, hypertrophic and fibrotic effects by blocking the actions of receptors ETA and ETB. In this study we identified the action of Bosentan on endothelin B receptor using docking studies with homology modeled endothelin B receptor. Through the modeled protein, the flexible Docking study was performed with Bosentan and its derivatives with theoretically predicted active sites. The results indicated that amino acid ARG82, ARG84 and HIS197 present in endothelin B receptor are core important for binding activities and these residues are having strong hydrogen bond interactions with Bosentan. We have investigated the Bosentan and its derivatives interactions and scoring parameters using gold docking package. Among the docked compounds, one of the Bosentan derivatives BD6 shows better interaction than Bosentan with endothelin B receptor. Our results may be helpful for further investigations in both in vivo and in vitro conditions.
- *Tian-Qiong Lang et al.,(2020)*studied the three compounds with diuretic potential were identified from the 95% ethanol extract of Pyrrosia petiolosa (Christ) Ching. Among them, one was a new benzanilide named petiolide (1), and the other two were phenolic derivatives barbatic acid (2) and kaempferol (3). Their structures were elucidated based on extensive spectral analyses and comparison with the literature data. The docking experiments of all compounds into the active site of the With-No-Lysine kinase 1 (WNK1) domain demonstrated that kaempferol (3) was the most effective component with diuretic potential for its comparative diuretic effect to that of an orally bioavailable WNK inhibitor WNK463.
- *Zhaowei Zhai et al.,(2021)* studied the hypertension is a cardiovascular disease that causes great harm to health and life, affecting the function of important organs and accompanied by a variety of secondary diseases, which need to be treated with drugs for a long time. P. ternata alone or combination with western medicine has played an important role in traditional Chinese medicine. Although P. ternata is used clinically to treat hypertension, its functional molecular mechanism and pharmacological mechanism have not been elucidated. Therefore, in this study, the potentially effective components, and targets of P. ternata in the treatment of hypertension were screened by the method of network pharmacology, and the mechanism of P. ternata in the treatment

of hypertension was analyzed by constructing a component-target relationship network, PPI interaction network, targets' function analysis, and molecular docking. In the study, 12 potentially effective components and 88 targets were screened, and 3 potential protein modules were found and analyzed after constructing a PPI network using targets. In addition, 10 targets were selected as core targets of the PPI network. After that, the targets were analyzed by Gene Ontology (GO) enrichment analysis and Kyoto Encyclopedia of Genes and Genomes (KEGG) pathway analysis. Finally, the molecular docking method is used to study the interaction between the targets and the active components. The above evidence shows that the mechanism of P. ternata in the treatment of hypertension is complicated, as it acts in many ways, mainly by affecting nerve signal transmission, cell proliferation, and apoptosis, calcium channels, and so on. The binding between targets and active components mainly depends on Pi bonds and hydrogen bonds. Using the method of network pharmacology and molecular docking to analyze the mechanism of P. ternata in the treatment of hypertension will help to provide a better scientific basis for the combined use of traditional Chinese medicine and western medicine, and will better help to improve the quality of P. ternata and point out its direction.

- *Syed Awais Attique et al., (2019)* studied the cardiovascular diseases (CVDs) have become the leading cause of disability and death worldwide, particularly in low- and middle-income countries. Hypertension, a major cause of CVD progression, is widely attributable to genetic, behavioral, and environmental risk factors. Among the genetic reasons, angiotensin II enzyme, produced as a result of abnormal functioning of the renin–angiotensin system, is reported as the foremost cause of hypertension. A cascade of genes, including those encoding for WNK kinases (WNK1 and WNK4), Bp1, Bp2, angiotensinogen, and other enzymes, is involved in the conversion of angiotensin I to angiotensin II. However, the angiotensin-converting enzyme (ACE) plays a crucial role in this pathway. Therefore, ACE could be a potential therapeutic target in regulating the conversion of angiotensin I to angiotensin II and eventually controlling hypertension. In this study, a molecular docking-based approach was utilized for identifying and evaluating potential inhibitors of ACE present in herbs, other natural sources, and synthetic sources, on the basis of these compounds' binding affinities and other physicochemical features. In addition, the suitability of these inhibitors as drugs for biological systems, considering their adsorption, distribution, metabolism, and

excretion (ADME), was predicted using Lipinski's rule. In conclusion, our study provides a novel and clearer insight into the interaction properties of known putative inhibitors of ACE.

- *Vivek Kumar Gupta et al., (2011)* studied the most ancient Indian traditional system of medicine (Ayurveda) diuretics are called as Muttra- virechanya dravya. These agents were widely explored in Indian ancient system of medicine. Diuretics cause increase in the rate of urine flow rate thus employed in numerous disorders like hypertension, anxiety, cardiovascular disorders, diabetes mellitus and liver degeneration diseases. The aim of this review is to highlight the work on diuretics of plant origin. The selection of papers was made using the most relevant databases for the biomedical sciences on the basis of their traditional use. The numerous diuretic plants with their active phytoconstituents have been explored. The present paper also involves various plant drugs and their pharmacological profile which focus on the dose administered, bioactive extract involved in diuretic mechanism. This work may prove a milestone in selection of medicinal plant for carrying their work on the diuretics.

- *Lina Perekhoda et al., (2010)* studied the diuretics are the first-line therapy for widespread cardiovascular and non-cardiovascular diseases. Traditional diuretics are commonly prescribed for treatment in patients with hypertension, edema and heart failure, as well as with a number of kidney problems. They are diseases with high mortality, and the number of patients suffering from heart and kidney diseases is increasing year by year. The use of several classes of diuretics currently available for clinical use exhibits an overall favorable risk/benefit balance. However, they are not devoid of side effects. Hence, pharmaceutical researchers have been making efforts to develop new drugs with a better pharmacological profile. High-throughput screening, progress in protein structure analysis and modern methods of chemical modification have opened good possibilities for identification of new promising agents for preclinical and clinical testing. In this review, we provide an overview of the medicinal chemistry approaches toward the development of small molecule compounds showing diuretic activity that have been discovered over the past decade and are interesting drug candidates. We have discussed promising natriuretics/aquaretics/osmotic diuretics from such classes as: vasopressin receptor antagonists, SGLT2 inhibitors, urea transporters

inhibitors, aquaporin antagonists, adenosine receptor antagonists, natriuretic peptide receptor agonists, ROMK inhibitors, WNK-SPAK inhibitors, and pendrin inhibitors.

- *Yajun Zheng et al.,(2020)*studied the sargassum maclurei is a potential protein resource because of its high protein content and relatively balanced amino acid composition. To promote its usage in food, medical, or other industries, S. maclurei protein was hydrolyzed by pepsin and papain to obtain bioactive peptides. The S. maclurei protein hydrolysates (SMPHs) were purified using gel chromatography and reversed-phase high performance liquid chromatography (RP-HPLC), and 12 major fractions were obtained. The fraction D11 with the highest angiotensin I-converting enzyme (ACE) inhibition (61.59%, at 1 mg/mL) was subjected to liquid chromatography-mass spectrometry (LC-MS/MS) analysis, and about 17 peptides were identified, of which the RWDISQPY (1063.5 Da) was chosen to be synthesized based on in silico analysis. The RWDISQPY demonstrated high ACE inhibition ability (IC50: 72.24 μM) with competitive inhibition mode, and could effectively ($p < 0.05$) lower the systolic blood pressure and diastolic pressure of spontaneously hypertensive rats at the concentration of 150 mg/kg body weight. The results of the molecular docking simulation demonstrated that RWDISQPY could bind with the active sites S1 and S2 of ACE via short hydrogen bonds. Moreover, RWDISQPY showed acceptable endothelin-1 suppressing capacity (26.21% at 1.5 mg/mL). These results indicate that S. maclurei could be developed into functional foods such as antihypertensive product.

- *Min Li1 et al., (2020)* studiedurea transporters (UTs) are transmembrane proteins selectively permeable to urea and play an important role in urine concentration. UT-knockout mice exhibit the urea-selective urine-concentrating defect, without affecting electrolyte balance, suggesting that UT-B inhibitors have the potential to be developed as novel diuretics. In this study, we characterized a novel compound 5-ethyl-2-methyl-3-amino-6-methylthieno [2, 3-b]pyridine-2,5-dicarboxylate (CB-20) with UT inhibitory activity as novel diuretics with excellent pharmacological properties. This compound was discovered based on high-throughput virtual screening combined with the erythrocyte osmotic lysis assay. Selectivity of UT inhibitors was assayed using transwell chambers. Diuretic activity of the compound was examined in rats and mice using metabolic cages. Pharmacokinetic parameters were detected in rats using LC–MS/MS. Molecular docking was employed to predict the potential binding modes for

the CB-20 with human UT-B. This compound dose-dependently inhibited UT-facilitated urea transport with IC50 values at low micromolar levels. It exhibited nearly equal inhibitory activity on both UT-A1 and UT-B. After subcutaneous administration of CB-20, the animals showed polyuria, without electrolyte imbalance and abnormal metabolism. CB-20 possessed a good absorption and rapid clearance in rat plasma. Administration of CB-20 for 5 days did not cause significant morphological abnormality in kidney or liver tissues of rats. Molecular docking showed that CB-20 was positioned near several residues in human UT-B, including Leu364, Val367, and so on. This study provides proof of evidence for the prominent diuretic activity of CB-20 by specifically inhibiting UTs. CB-20 or thienopyridine analogs may be developed as novel diuretics.

- *Ying Li et al., (2019)* studied abnormal wound healing by pulmonary artery smooth muscle cells (PASMCs) promotes vascular remodeling in hypoxia-induced pulmonary hypertension (HPH). Increasing evidence shows that both the mammalian target of rapamycin complex 1 (mTORC1) and nuclear factor-kappa B (NF-κB) are involved in the development of HPH. In this study, we explored the crosstalk between mTORC1 and NF-κB in PASMCs cultured under hypoxic condition and in a rat model of hypoxia-induced pulmonary hypertension (HPH). We showed that hypoxia promoted wound healing of PASMCs, which was dose-dependently blocked by the mTORC1 inhibitor rapamycin (5−20 nM). In PASMCs, hypoxia activated mTORC1, which in turn promoted the phosphorylation of NF-κB. Molecular docking revealed that mTOR interacted with IκB kinases (IKKs) and that was validated by immunoprecipitation. In vitro kinase assays and mass spectrometry demonstrated that mTOR phosphorylated IKKα and IKKβ separately. Inhibition of mTORC1 decreased the level of phosphorylated IKKα/β, thus reducing the phosphorylation and transcriptional activity of NF-κB. Bioinformatics study revealed that dipeptidyl peptidase-4 (DPP4) was a target gene of NF-κB; DPP4 inhibitor, sitagliptin (10−500 μM) effectively inhibited the abnormal wound healing of PASMCs under hypoxic condition. In the rat model of HPH, we showed that NF-κB activation (at 3 weeks) was preceded by mTOR signaling activation (after 1 or 2 weeks) in lungs, and administration of sitagliptin (1−5 mg/kg every day, ig) produced preventive effects against the development of HPH. In conclusion, hypoxia activates the crosstalk between mTORC1 and NF-κB, and

increased DPP4 expression in PASMCs that leads to vascular remodeling. Sitagliptin, a DPP4 inhibitor, exerts preventive effect against HPH.

- *Hao Su et al., (2014)* studied pulmonary hypertension (PH) is a devastating disease characterized by progressive elevation of pulmonary arterial pressure and vascular resistance due to pulmonary vasoconstriction and vessel remodeling. The activation of RhoA/Rho-kinase (ROCK) pathway plays a central role in the pathologic progression of PH and thus the Rho kinase, an essential effector of the ROCK pathway, is considered as a potential therapeutic target to attenuate pH. Objective: In the current study, a synthetic pipeline is used to discover new potent Rho inhibitors from various natural products. Materials and methods: In the pipeline, the stepwise high-throughput virtual screening, quantitative structure–activity relationship (QSAR)-based rescoring, and kinase assay were integrated. The screening was performed against a structurally diverse, drug-like natural product library, from which six identified compounds were tested to determine their inhibitory potencies agonist Rho by using a standard kinase assay protocol. Results: With this scheme, we successfully identified two potent Rho inhibitors, namely phloretin and baicalein, with activity values of 0.95 mM, respectively. Discussion and conclusion: Structural examination suggested that complicated networks of nonbonded interactions such as hydrogen bonding, hydrophobic forces, and van der Waals contacts across the complex interfaces of Rho kinase are formed with the screened compounds.

CHAPTER 3

SCOPE OF INVESTIGATION

- A diuretic is a substance that promotes diuresis, the increased production of urine
- To find out target protein for Diuretics
- To find the inhibitors for phytochemical compounds for Diuretis
- To know the detail about Diuretics and its adverse effect of the world.
- To identify a natural phytochemical compounds
- To find the high binding efficiency for protein ligand complex

- To recognize the good pharmacological activities of the phytochemical compounds in future

CHAPTER 4

MATERIALS AND METHODS

TARGET SELECTION

The X-ray crystal structure of 1Z9X was retrieved from Protein Data Bank. The protein energy was analysed through Ramachandra Plot and conjugate by using SMILES of Swiss PDB Viewer and final energy minimized model was used for further docking studies.

PROTEIN PREPARATION

Load the protein and apply the force field. For docking studies, the protein 1Z9X loads from RCSB protein data bank (www.rcsb.org/pdb) and apply the force field. Field refers to the functional form parameter sets which are used to find out potential energy of a system. It includes parameter which is obtained through experimental works and quantum mechanics calculations. All molecules in a molecule system are made up of a number of components. Covalently bonded atoms take into consideration several parameters such as bond length, bond angle, dihedral angles etc., similarly there exist non bonded interactions such as Vanderwaals interactions, electrostatic interactions. Thus, the total potential energy of the system is calculated as follows.

$E1 = [E_{bond} + Eangle + Evanderwaals + Eelectronic]$

LIGAND SELECTION

The SMILES notation of fifty seven phytochemical compounds from various medicinal plants were obtained by drawing their 2D structures in ACD-Chemsketch. The 3D structures of these compounds were generated and converted into SDF format by using on online converter and structure file generator.

LIGAND PREPARATION

The chemically synthesized individual ligand compounds were sketched using ACD/ChemSketch (12.0) software and saved in (.mol) file format. The saved ligand compounds were later imported in PyRx and go to Minimization studies using minimize. After minimized ligands go to ligand preparation, then go for docking studies with ligand fit.

BINDING SITE AND SITE PARTITION

The active site of a receptor can be represented in many ways, for example a sphere or a list of residues. The Binding Site definition is one such representation. A binding site is a set of points on a grid that in a cavity. This definition is allowing the size and shape of the active site to be quantified. Docking algorithms such as Vina Search space can use this to both screen out in compatible ligands and quickly create shape-based alignments of candidate poses. The location, volume and shape of the binding site or all used in docking.

To define a binding site, the receptor is first mapped to a grid. Grid points within a given distance of the receptor atoms are marked as occupied by receptors and as undesirable as locations for ligand atoms. Two methods exist to identify a Binding Site. The first uses an "eraser" algorithm to identify sites based on the shape of the receptor. The second uses the volume occupies by the known ligand force already in an active site.

VIRTUAL SCREENING

The 3D structures of all the selected twenty threephytochemical compounds were virtually screened to reveal their binding efficiencies through docking in the predicted binding site usingPyRx-Python Prescription (version 0.8). The docking was performed with the default parameters such as triangle matching base placements, zero, full score and no score contributions and threshold for full score and no score contributions of 30 and 70 respectively. Clash handling values of 2.9 Å and 0.6 for protein ligand clashes with maximum allowed overlap volume and in a ligand clash factors while considering the hydrogen in internal clash tests and 200 as the default docking values for maximum number of solutions per iteration and also per fragmentations.

DOCKING INTERACTION

The docking interactions revealing H-bond and Vanderwaals forces among the phytochemical compounds and the amino acid residues of were analyzed by PyRx-Python Prescription (PyRx).

PYRX DOCKING

PyRx is a Virtual Screening software for Computational Drug Discovery that can be used to screen libraries of compounds against potential drug targets. PyRx enables Medicinal Chemists to run Virtual Screening from any platform and helps users in every step of this process. From data preparation to job submission and analysis of the results. While it is true that there is no magic button in the drug discovery process, PyRx includes docking wizard with an easy-to-use user interface which makes it a valuable tool for Computer-Aided Drug Design. PyRx also includes chemical spreadsheet-like functionality and powerful visualization engine that are essential for structure-based drug design.

DOCKING ALOGRITHM

Select upper left button Load molecule to load your protein and ligand into PyRx workspace. Right click on ligands and click PYRX to make ligand. Right click on protein and click AutoDock to Make Macromolecule. Now the protein and ligands files are ready for docking. Click on Start Here button under Vina Wizard. Select Local button under Vina execution Mode. Click Start button. Select protein and ligands by simply clicking on them. Click forward to Run Vina. The grid box (white box with spherical handles) in the 3D scene as shown below. This grid box allows to select search space (Part of the protein, where the docking performs and it is typically known binding site) in the protein. To help locating the binding site (or active site) use binding site amino acids. Click molecules button under Navigator panel, then click on + button located in front of protein tab. After selecting the amino acids (use shift button to select multiple amino acids) click on the Toggle selection Spheres button to see the selected amino acids. Make sure you select the grid box size big enough to allow the ligand to move freely in the search space. Use the search space (Vina search space) values close the ones mentioned in the picture below, to get better results. Click the forward button to start Vina calculations. Once, the calculations are done, results will be populated as seen in the below table with the Binding Affinity (kcal/mol) values

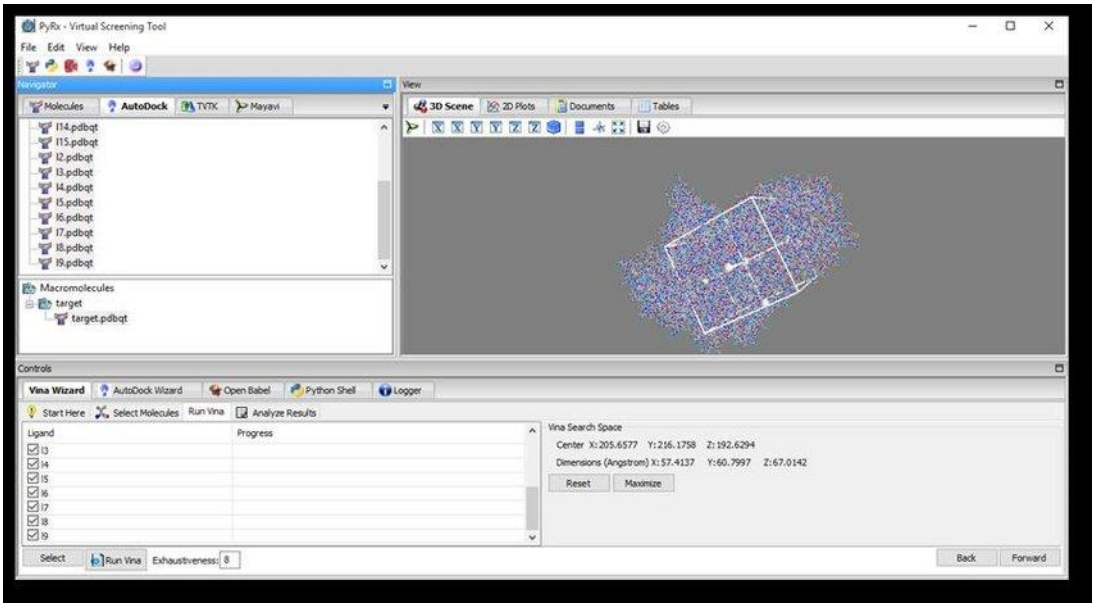

Fig:1 Vina Search Space

More negative the binding affinity better the orientation of the ligand in the binding site. Results can be exported to other software programs likePyMol or Discovery Studio for analysis. Click on Edit, go to Preferences. A pop-up window is opened. All your results will be saved in location specified as workspace. The protein folder contains three files (protein .pdbqt, ligand1_out.pdbqt and conf.txt), if you use only one ligand for docking. The ligand1_out.pdbqt contains 10 best poses (or orientations) of the ligand1 and conf.txt file contains search space (or grid box) parameters. Save this protein folder at your convenient location for further analysis with Discovery studio. You are done with PyRx, now let's analyse the results by using Discovery studio. Open protein .pdbqt file followed by ligand1_out.pdbqt to analyse the results. Select the ligand by using upper sequence bar and click on select A(action :)>find>Polar contacts >to any atoms..Now the result of PyRx docking is screened.

RESULT AND DISCUSSION

TARGET SELECTION

The X- ray crystal structure of 1Z9X was retrieved from Protein Data Bank .The protein energy was analysed through Ramachandra Plot.The protein energy minimized through SWISS PDB minimizer and used for further docking studies.

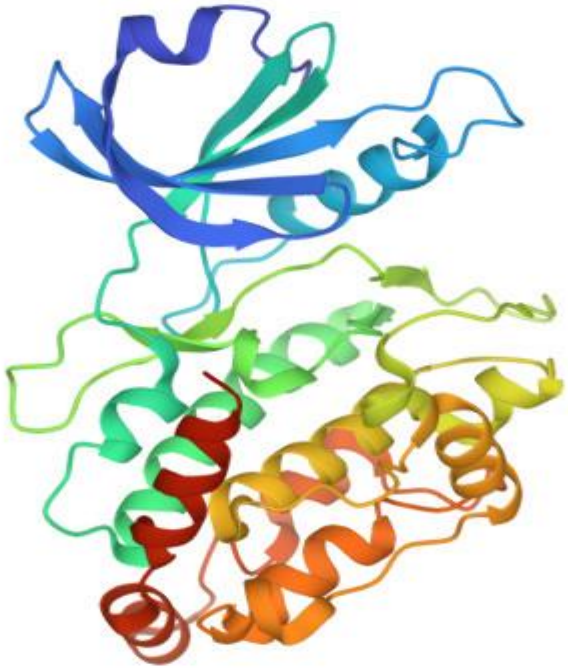

Fig.2 Protein structure of 1Z9X

LIGAND SELECTION

The SMILES notation of phytochemical compounds including alkaloids and flavonoids from various medicinal plants were obtained by drawing their 2D structures in ACD-Chemsketch (version 12.01). The 3D structures of these compounds were generated and converted into SDFformatby using Open Babel convertor and structure file generator' server.

A Phytochemical Compounds from different Plant Sources

COMPOUND NAME	CID NO.	PLANT SOURCE
Niazirinin	10426197	*Moringa oleifera*
Sterol	1107	*Abutilon indicum*
Xanthines	1188	*Camellia sinesis*
Lactucopicrin	102242110	*Lagenaria siceraria*

Avenasterol	12795736	*Centratherum punctatum*
Niazirin	129556	*Moringa oleifera*
Hentriacontane	12410	*Iopomoea aquatica*
Allantoin	204	*Zeamays*
Beta-Sistosterol	222284	*Zeamays*
Coumarin	323	*Lagenaria siceraria*
Gallic acid	370	*Abutilon indicum*
Glycoprotein	439212	*Zeamays*
Lactucin	442266	*Lagenaria siceraria*
Quercetin	5280343	*Camellia sinesis*
Luteolin	5280445	*Cuscutareflexa*
Kaempferol	5280863	*Camellia sinesis*
Glucoapparin	5281133	*Capparis spinosa*
Glucocleomin	5281134	*Capparis spinosa*
Glucoside	64689	*Terminala arjun*
Epigallocatechin Gallate	65064	*Combertacea asica*
Bergenin	66065	*Cuscutareflexa*
n-hexacosanol	68171	*MThymifolia*
Xanthone	7020	*Boerhaavia diffusa*

Structure of Phytochemical Compound

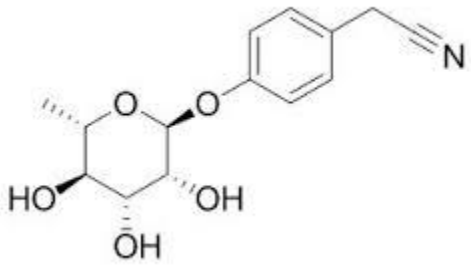

Niazirinin

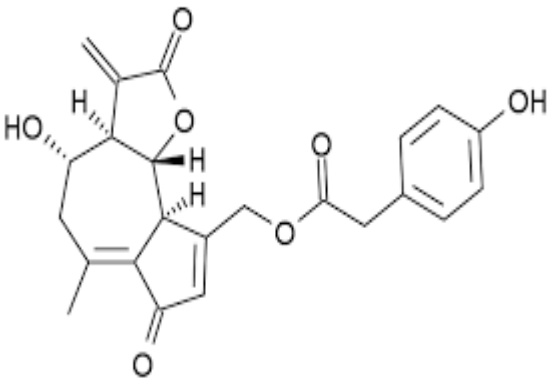

Lactucopicrin

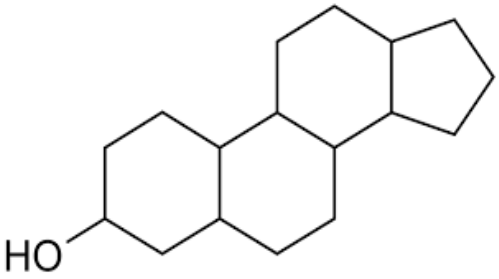

Sterol

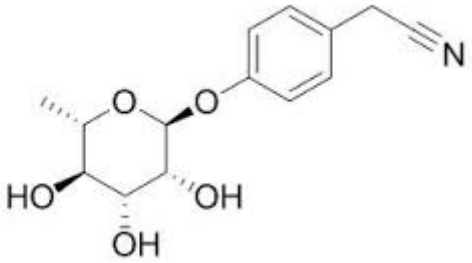

Niazirin

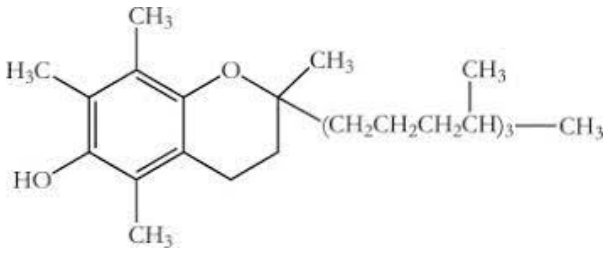

Hentriacontane

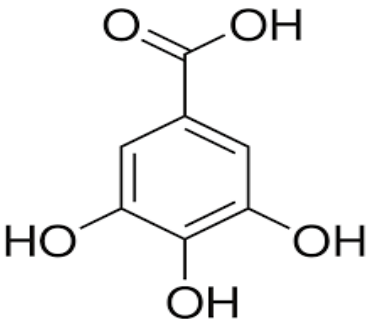

Gallic acid

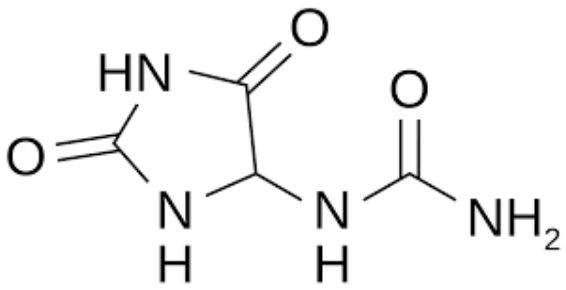

Allantoin

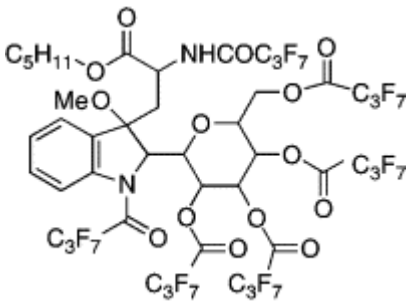

Glycoprotein

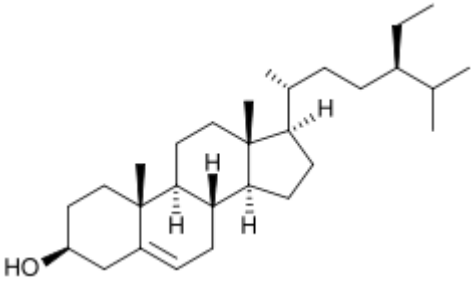

Beta-Sistosterol

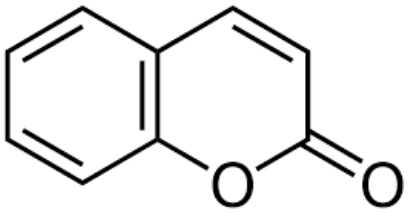

Coumarin

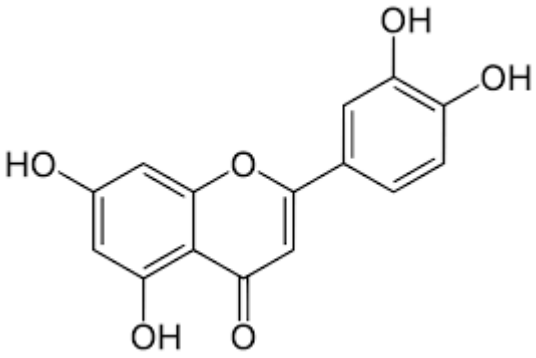

Kaempferol

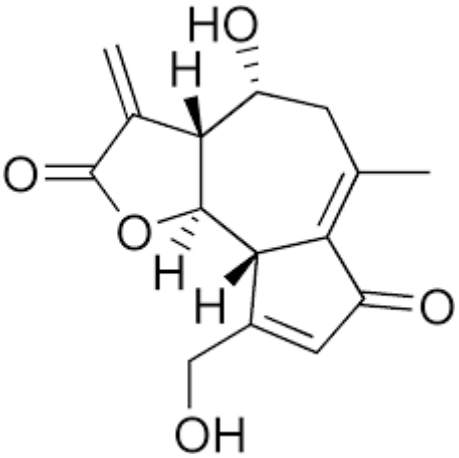

Lactucin

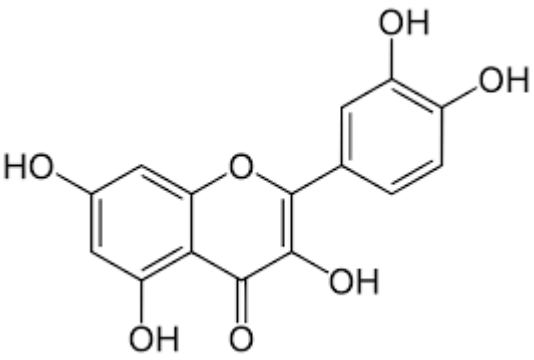

Quercetin

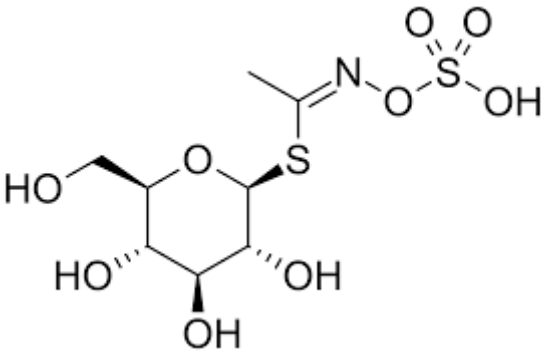

Glucoapparin

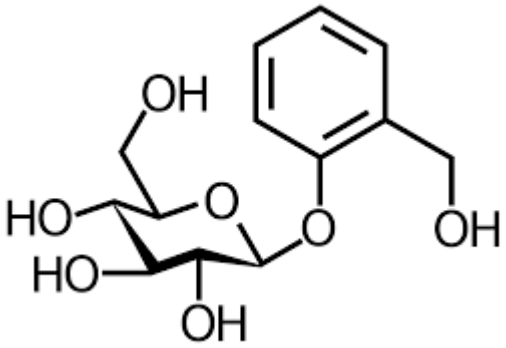

Glucoside

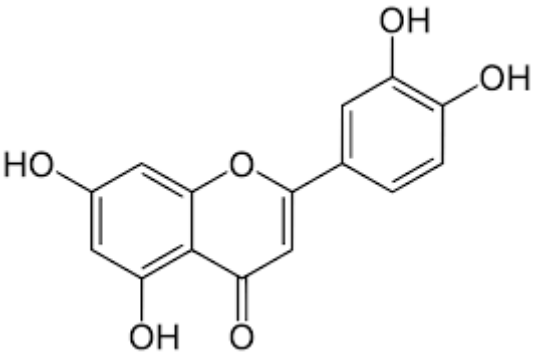

Luteolin

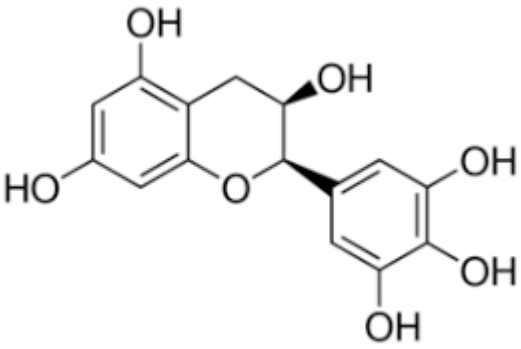

Epigallocatechin Gallate

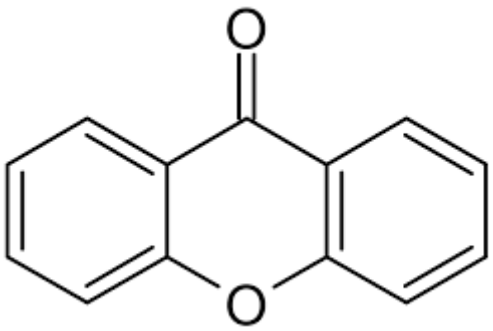

Xanthone

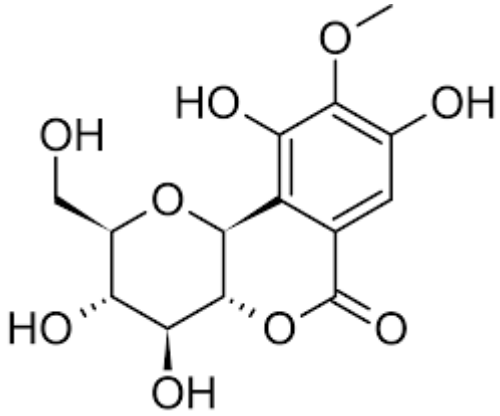

Bergenin

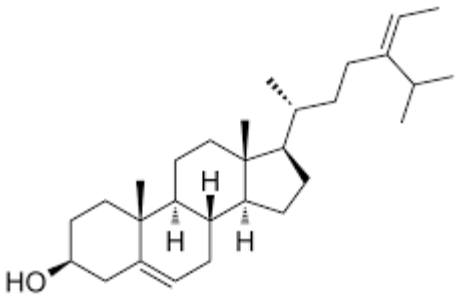

Avenasterol

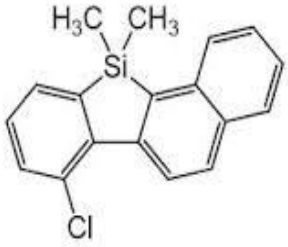

n-hexacosanol

BINDING SITE PREDICTION

The amino acid residues in binding site of 1Z9X protein is defined by using the reference ligand complexed in the retrieved PDB file. The amino acid residues within 6 Å radius ofference ligand was included in the predicted binding site by using PyRx-Python Prescription (version 0.8).

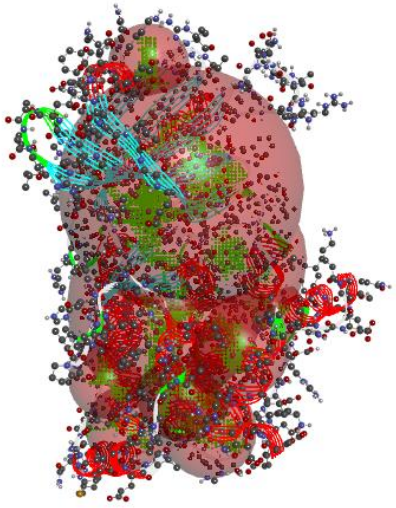

FIG: 3 Binding Site Prediction Of 1Z9X

VIRTUAL SCREENING

The 3D structures of all the selected phytochemical compounds were virtually screened to reveal their binding efficiencies through docking in the predicted binding site using PyRx Python Prescription. Docking values for maximum number of solutions per interaction and also per fragmentations. The binding affinity with their docking scores are given in table.

BINDING AFFINITIY OF PHYTOCHEMICAL BY USING PyRX

LIGAND	BINDING ENERGY (Kcal/mol)
Niazirinin	-9
Sterol	-10.9
Xanthines	-5.6
Lactucopicrin	-1.1
Avenasterol	-12
Niazirin	-8.6
Hentriacontane	-6.6
Allantoin	-5.4
Beta-Sistosterol	-12
Coumarin	-6.8
Gallic acid	-5.9
Glycoprotein	-12.1
Lactucin	-9.4
Quercetin	-9.2
Luteolin	-9.4
Kaempferol	-9.1
Hentriacontane	-8
Glucocleomin	-9.4
Glucoside	-5.8
Epigallocatechin Gallate	-10.3
Bergenin	-8.4
n-hexacosanol	-5.9
Xanthone	-8.7

Docking Complex and interaction of Glycoprotein (CID 439212)

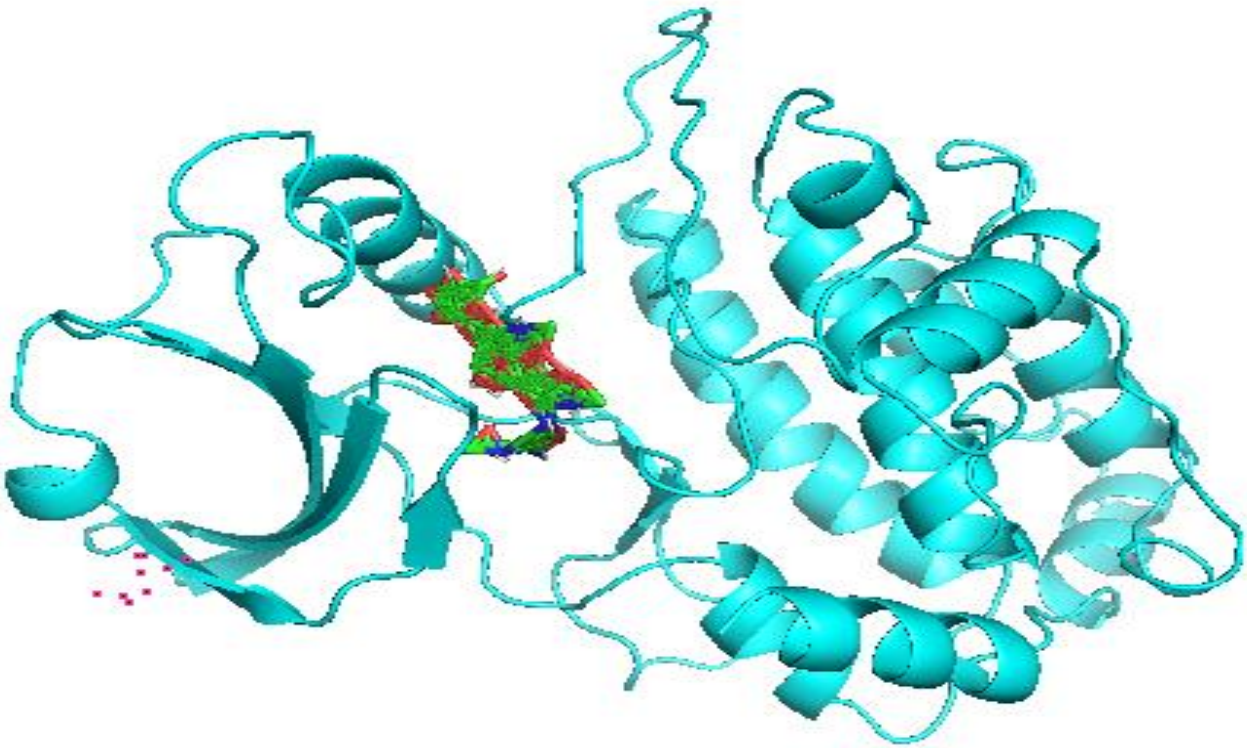

Docking complex and interaction of Avenasterol (CID12795736)

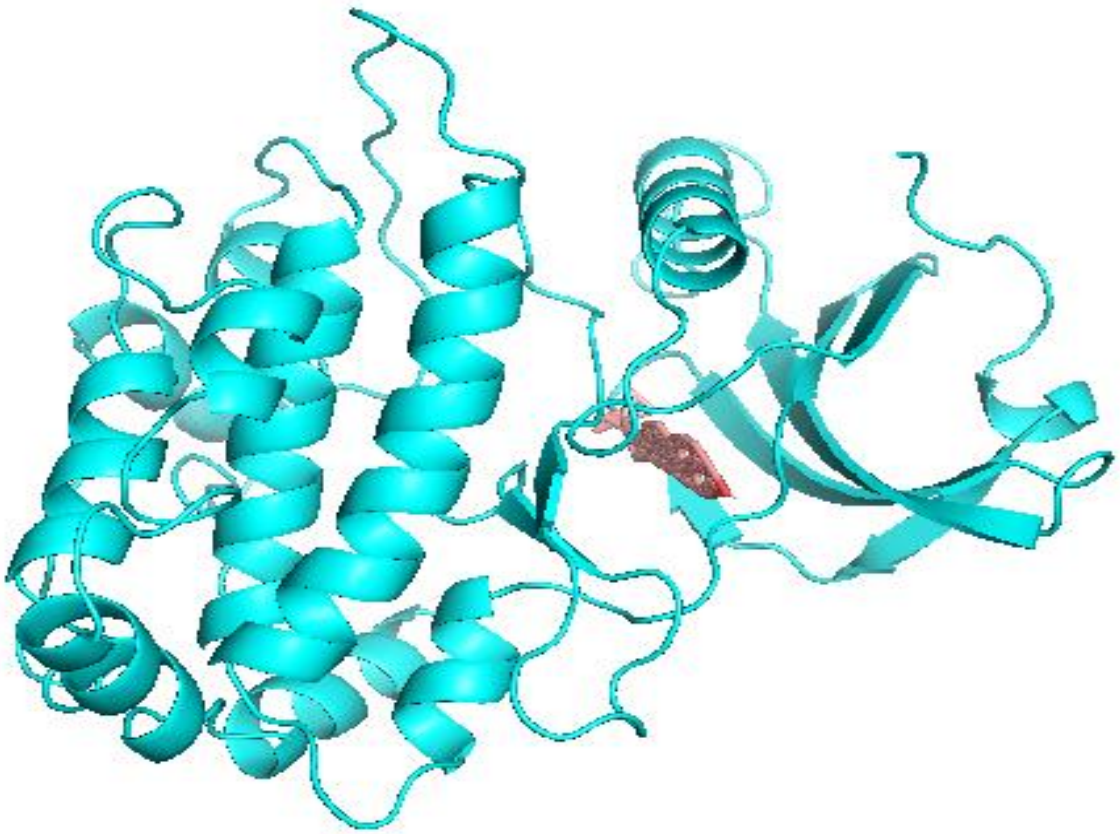

Docking complex and interaction of Lactucopicrin (CID102242110)

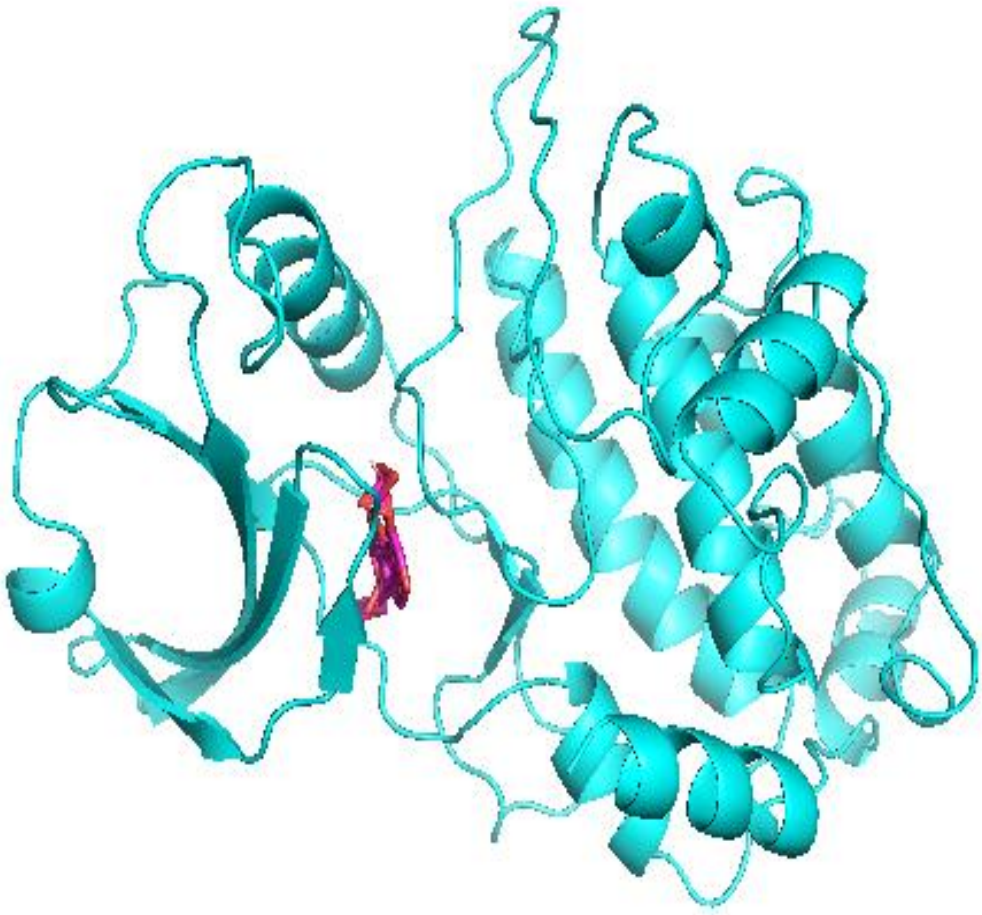

Docking complex and interaction of (CID1107)

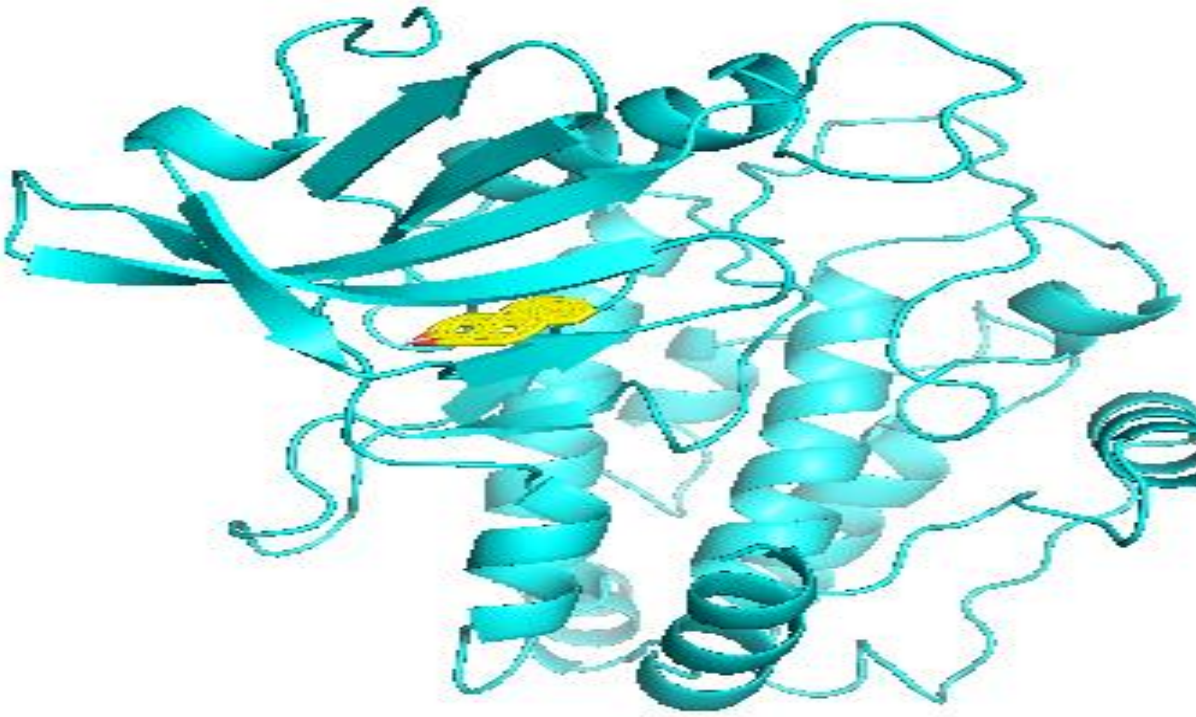

Docking complex and interaction of Epigallocatechin Gallate (CID6506

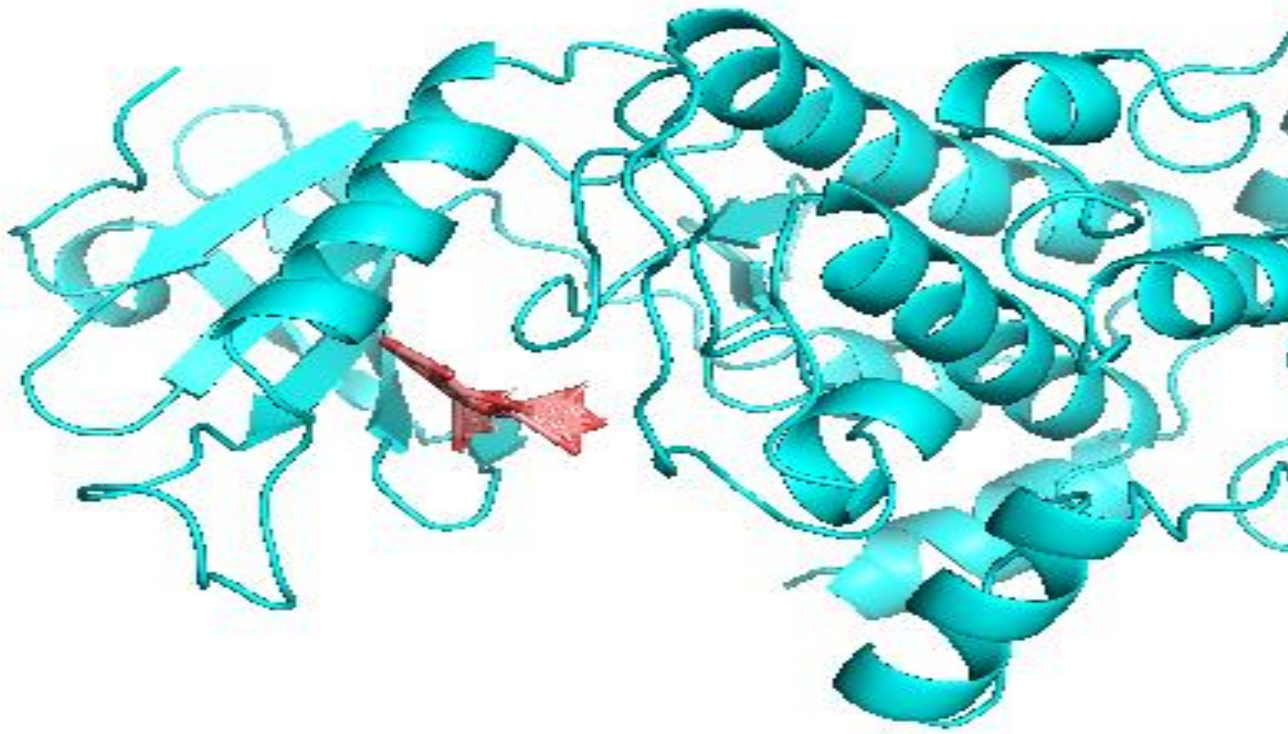

Docking complex and interaction of Glucocleomin (CID5281134)

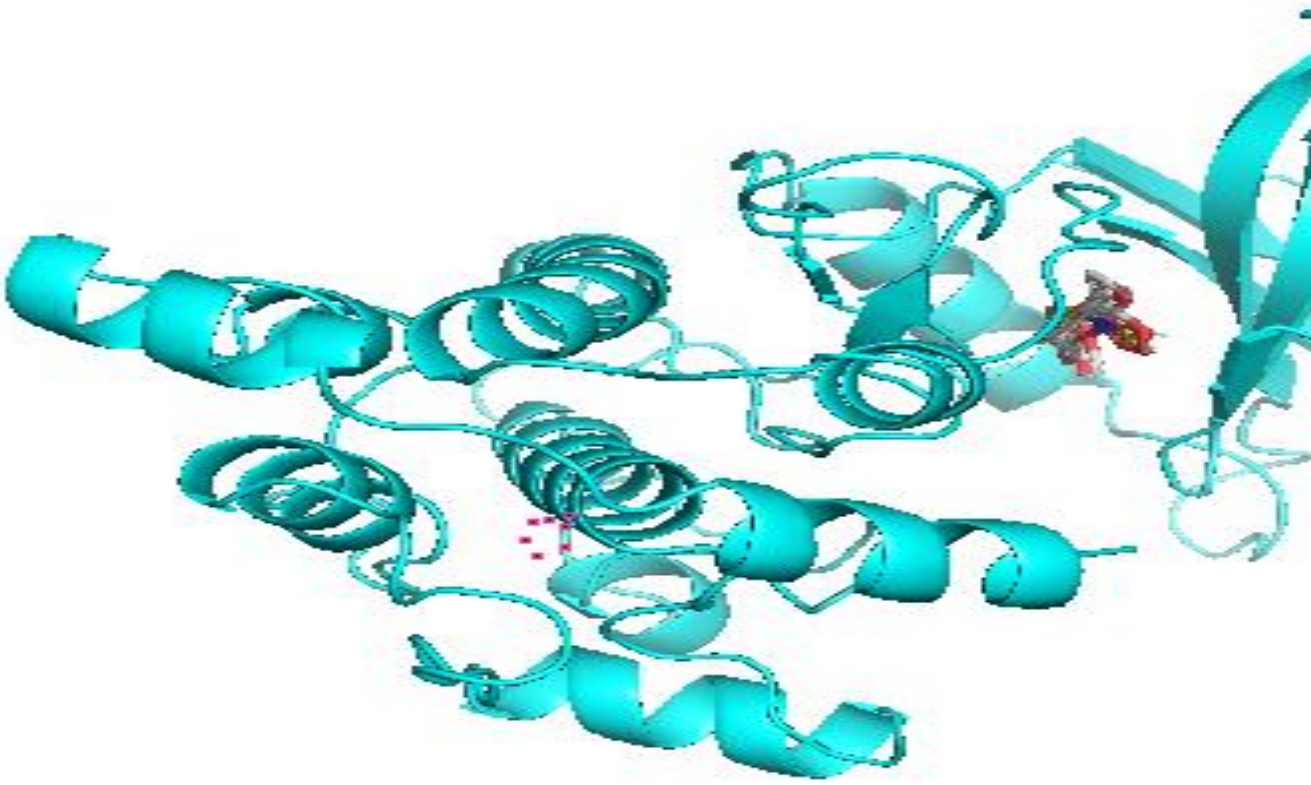

Docking complex and interaction of Luteolin (CID5280445)

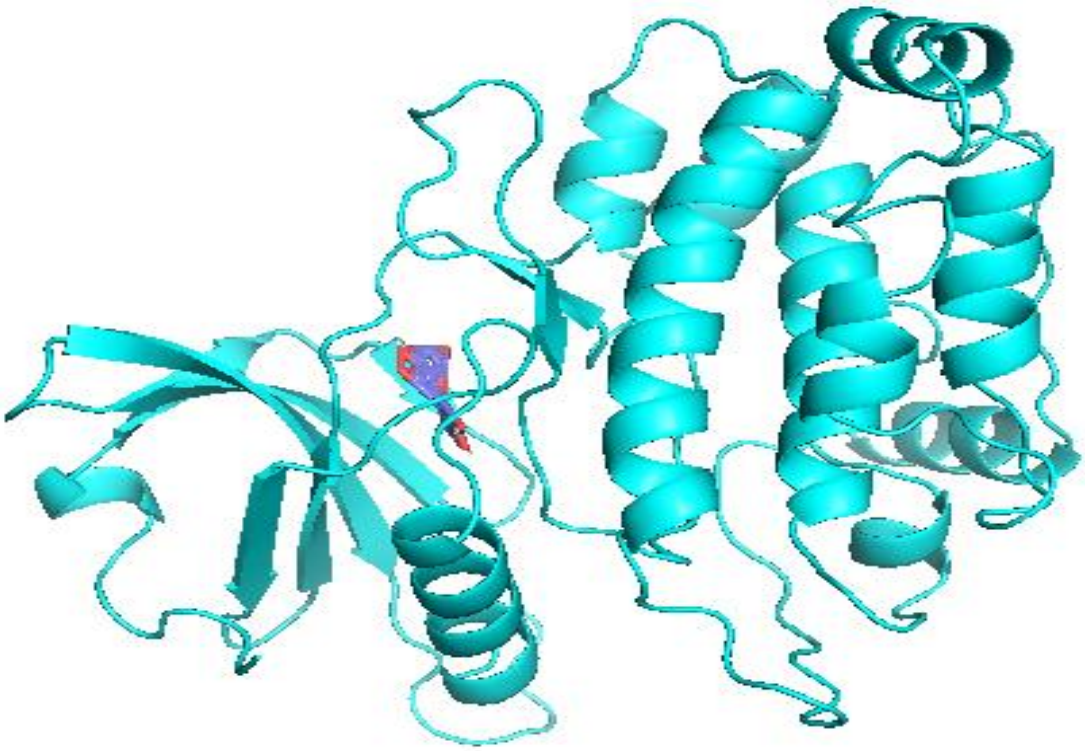

Docking complex and interaction of Quercetin (CID5280343)

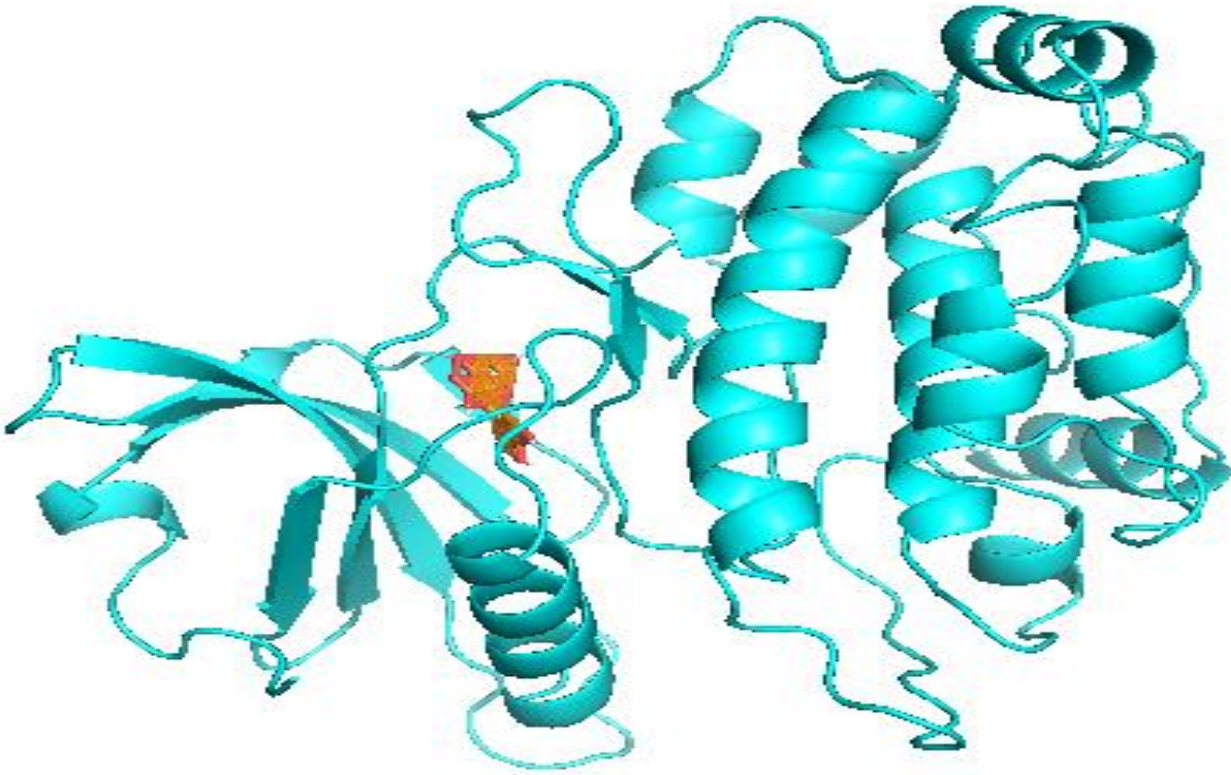

Docking complex and interaction of Kaempferol (CID5280863)

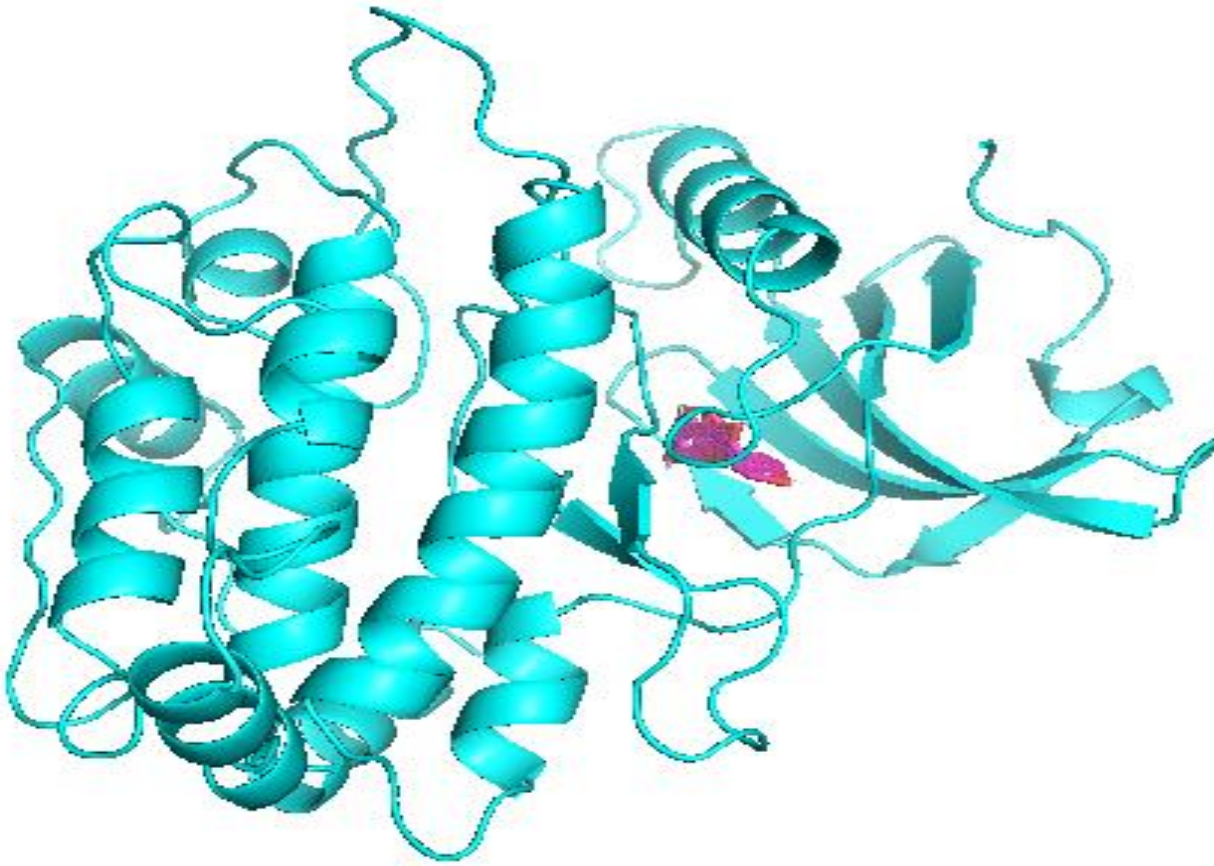

Docking complex and interaction of Niazirinin (CID10426197)

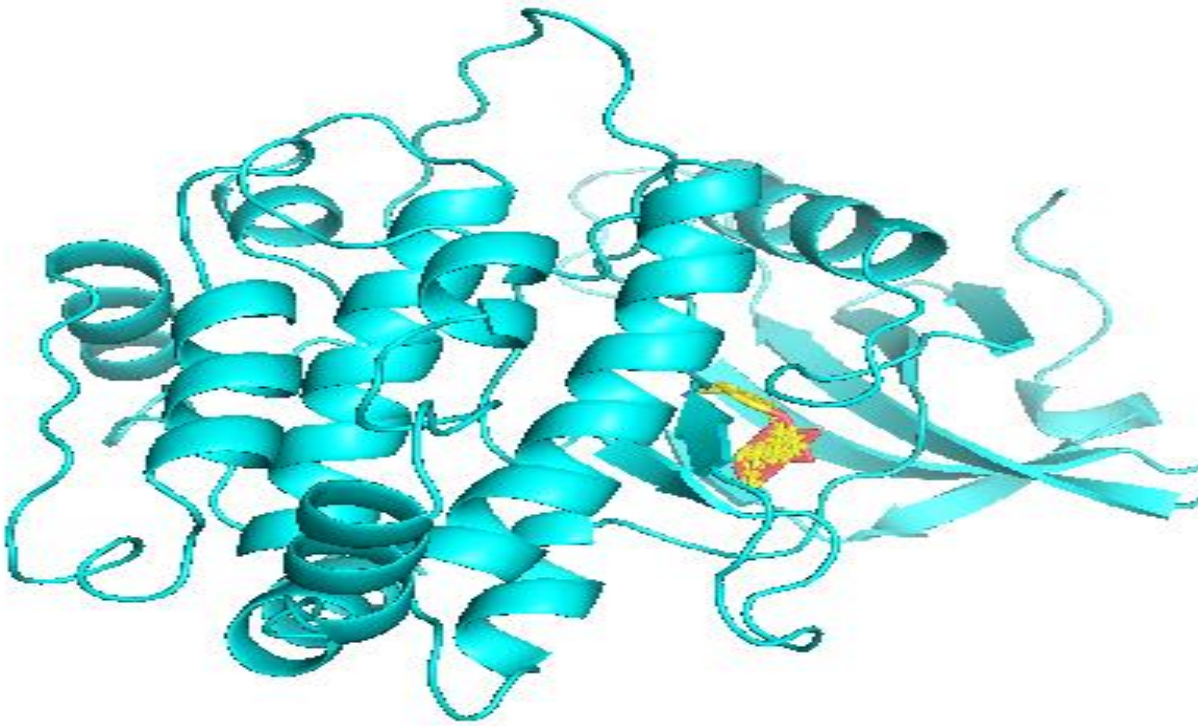

CHAPTER 6

CONCLUSION

The 1Z9X a part of insulin that significantly controls sugars serves as a drug target for diuretics. Insulin receptor kinase complexed with an inhibitor 1Z9X was used explore the diuretic activity of 23 pthytochemical compounds. In the present molecular modeling study results clearly demonstrated that Glycoprotein (-12.1kcal/mol), Avenasterol(-12kcal/mol), Lactucopicrin (-11kcal/mol) have similar binding sites and interaction with 1Z9X taken for the study and prove that dietary phytochemical compounds may possess properties of diuretic regulation.

CHAPTER 7

REFERENCE

1. Golik.M *et al., "QSAR analysis and molecular docking study of pyrrolo- and pyridoquinolinecarboxamides with molecular docking*"doi.org/10.15587/2519-4852.2021.234493,2020.
2. Radwan Alnajja *et al., "Molecular docking, molecular dynamics, and in vitro studies reveal the potential of angiotensin II receptor blockers to inhibit the COVID-19main protease "*doi.org/10.1016/j.heliyon.2020.e05641,2020.
3. Kero Jemal et at., "*Molecular Docking Studies of Phytochemicals of Allophylus serratus AgainstCyclooxygenase-2 Enzyme*"doi.org/10.1101/866152,2019
4. Shuyue Wang *et al.,"Study on the Potential Mechanism of Fructus Tribuli in the Treatment of Hypertensive Vascular Remodeling Based on Network Pharmacology and Molecular docking*"doi.org/10.1155/2021/8862176,2021
5. Xinyi Jiao *et al., "Study on the Mechanism of Prunella Vulgaris L on Diabetes MellitusComplicated with Hypertension Based on Network Pharmacology and Molecular Docking Analyses"*doi.org/10.1155/2021/9949302,2021
6. Wu-De Yang *et al., "Characterization of chemical components with diuretic potential from Pyrrosia petiolosa"*https://doi.org/10.1080/10286020.2020.1786065,2020
7. Zhaowei Zhai *et al.,"Network Pharmacology and Molecular Docking Combined to Analyze the Molecular and Pharmacological Mechanism of Pinellia ternata in the Treatmentof Hypertension*"doi.org/10.3390/cimb 43010006, 2021
8. Li Yang *et at.,"Natural phenylethanoid glycosides diuretics derived from* Lagopsis *supina: Biological activity, mechanism, molecular docking, and structure-activity relationship*"doi.org/10.1016/j.bioorg.2022.106165,2022
9. Muhammed Alzweiri *et al., "Ethnopharmacological survey of medicinal herbs in Jordan, the Northern Badia region*"doi.org/10.1016/j.jep.2011.02.007,2011.
10. Tian-Qiong Lang *et al., "Characterization of chemical components with diuretic potential from Pyrrosia petiolosa"* doi.org/10.1080/10286020.2020.1786065,2022

11. Elton Migliati *et al.,* "*Inhibition of Aquaporin-1 and Aquaporin-4 Water Permeability by a Derivative of the Loop Diuretic Bumetanide Acting at an Internal Pore-Occluding Binding Site"* doi.org/10.1124/mol.108.053744,2009.
12. **Sumanta Mondal *et al.,* "***Evaluation of Toxicological, Diuretic, and Laxative Properties of Ethanol Extract from Macrothelypteris Torresiana (Gaudich) Aerial Parts with In silico Docking Studies of Polyphenolic Compounds on Carbonic Anhydrase II: An Enzyme Target for Diuretic"* doi.org/10.1124/mol.108.053744,2018.
13. Md. Nazmul Islam *et al.,* "*Identification of Potential Diuretic and Laxative Drug Candidates from Avicennia officinalis L. Bark through In Vivo Mice Model Studies and In Vitro Gas Chromatography-Mass Spectrometry and Molecular Docking Analysis"* doi.org/10.1124/mol.108.053744,2009.
14. Sadia_Malik *et al., "Unravelling the inhibitory and cytoprotective potential of diuretics towards amyloid fibrillation"* doi.org/10.1016/j.ijbiomac.2019.10.137, 2020.
15. V. Shyni *et al., "Density functional theoretical study, spectroscopic characterization and molecular docking of the diuretic drug, spironolactone, adsorbed on AuNPs surface and in-vitro studies based on anticancer activity studies against A549 lung cancer cell line"*
16. S.Sobha *et al., "Pharmacological Evaluation and Molecular Docking Studies of Sorghum bicolor for Diuretic Activity"* DOI: 10.1007/978-981-16-1941-0_54, 2021
17. Nura Ershad Naznin *et al., "Molecular docking supported investigation of antioxidant, analgesic and diuretic effects of Costus speciosus rhizome"* DOI: 10.4314/bcse.v36i3.12, 2022
18. Boyle.K et *al., "An open chemical tool box Cheminform"* doi.org/10.1186/1758-2946-3-33,2011
19. Harder *etal.,"A force field providing broad coverage of drug-like small molecules and proteins".* 281–296,doi.org/10.1021/acs.jctc.5b00864,2016
20. Storer, J.W. *et al., "A new semi empirical approach in quantum chemistry*". J. Comput. Aided Mol. Des 9, 87–110, doi.org/10.1007/BF00117280,1995.
21. Madhavi, S.G *et al., "Proteinand ligand preparation: parameters, protocols, and influence on virtual screeningenrichments",* J. Comput. Aided Mol. Des. 27, 221–234,doi.org/10.1007/s10822-013-9644-8,2013
22. Dr. John Botomwito, the department of family medicineand Primary health care, Medunsa, University of Limpopo.

23. Ms. Bharathi and R.H. Singh, Constitutional study of Patients of Diabetes Mellitus VIS-A-MADHUMEHA, Ancient science of life, Vol No.XV No.1 July 1995.
24. Huang *et al., "Adverse childhood experiences and risk of type 2 diabetes: A systematic review and meta-analysis*". Metabolism – Clinical and Experimental. 64 (11): 1408–1418. doi:10.1016/j.metabol.2015.08.019. ISSN 0026-0495. PMID 26404480.
25. Disorders of Carbohydrate Metabolism: Merck Manual Professional". Merck Publishing. April 2010. Archived from the original on 2010-07-28. Retrieved 2010-07-30.
26. National Diabetes Statistics 2011. U.S. Department of Health and Human Services. Archived from the original on 17 April 2014. Retrieved 22 April 2014.
27. Abirami.S *et al., "Maturity onset diabetes of the Young(MODY) Genes"* Vol.No.1, pp.4-11. 2012
28. Prakash.P *et al.,. "Diagnosis and management of maturity onset diabetes of the young"* doi:10.1136/bmj.d6044. PMID 22012810.S2CID 44891167,2011
29. www.rcsb.org/pdb.
30. Prabakar.P *et al., "Antidiabetic Phytochemicals: A comprehensive Review on Opportunities and Challenges in Targeted Therapy for Herbal Drug Development*" ISSN 0975-2366. DOI:10.3183/ijpr/2020.SP1.242.
31. Hamidreza Ardalani *et al*., "*Potential antidiabetic phytochemicals in plant roots: a review of in vivo studies, Journal of Diabetes & Metabolic Disorders"* (2021) doi.org/10.1007/s40200-021-00853-9.
32. Sudhanshu Kumar Bharti *et al., "Antidiabetic phytoconstituents and their mode of action on metabolic pathways*" Ther Adv Endocrinol Metab 2018, Vol. 9(3) 81–100. DOI: 10.1177/2042018818755019.
33. Ngan Tran *et al.,Bioactive Compounds in Anti-Diabetic Plants:From Herbal Medicine to Modern Drug Discovery* 2020.
34. Patrick emeka Aba *et al.,"Mechanism of action of some bioactive anti-diabetic principles from phytochemical compounds of Medicinal Plants. Indian Journal Of Natural Products and Resources"* 2018.
35. Andreas and their Leiherer *et al.,"Phytochemicals impact on adipose tissue inflammation and diabetes"*2012.
36. Gopalsamy Rajiv Gandhi et al., (2021) "*Citrus Flavonoids as Promising Phytochemicals Targeting Diabetes and Related Complications:A Systematic Review of In Vitro and In Vivo Studies*" Doi: 10.3390/nu12102907.

37. Axelle Septembre *et al.,* June 2017 *"Fruits and vegetables, as a source of nutritional compounds and phytochemicals: Changes in bioactive compounds during lactic fermentation"* PII:S0963-9969(17)30598-7, DOI:10.1016/j.foodres.2017.09.031.
38. Muhammad Tahaa *et al., "Diuretic II inhibitors andmolecular docking studies. Bioorganic & Medicinal Chemistry*"27 (2019) 4081–4088. Received 7 May 2019; Received in revised form 17 July 2019; Accepted 19 July 2019. . et C https://doi.org/10.1016/j.bmc.2019.07.035.

SYNTHESIS AND CHARACTERIZATION OF BIOPLASTICS FROM *ORYZA SATIVA L.INDICA*AND *SETARIA ITALICA*

A project submitted to

ST. MARY'S COLLEGE (AUTONOMOUS), THOOTHUKUDI

Affiliated to

Mononmaniam sundaranar university, Thirunelveli

In partial fulfilment of the award of the degree of

MASTER OF SCIENCE IN CHEMISTRY

Submitted by

P. JEMIMA

Reg. No. 21SPCH03

Under the supervision and guidance

Dr. J. Antony Rajam M.Sc., M.Phil. SET, Ph.D.,

PG DEPARTMENT OF CHEMISTRY (SSC)

St. Mary's College (Autonomous), Thoothukudi

April 2023

CERTIFICATE

This is to certify that this project work entitled **"SYNTHESIS AND CHARACTERIZATION OF BIOPLASTIC FROM *Oryza sativa L.indica and Setaria italica* "** is submitted to St.Mary's College (autonomous), Thoothukudi affiliated to Mononmaniam sundaranar university, Thirunelveli in partial fulfilment for the award of the degree of Master of science in chemistry and this work done during the year 2022-2023by P. JEMIMA (Reg.No:21SPCH03)

Signature of the Guide

Signature of the Coordinator

Signature of the Director
Director
Self Supporting Courses
St. Mary's College (Autonomous)
Thoothukudi - 628 001.

Signature of Principal
Principal
St. Mary's College (Autonomous)
Thoothukudi - 628 001.

Signature of the Examiner

DECLARATION

I do hereby declare that the project entitled **″SYNTHESIS AND CHARACTERIZATION OF BIOPLASTIC FROM *Oryza sativa L.indica and Setaria italica ″*** submitted for the degree of Master of Science in chemistry is my original work carried out under the guidance of Dr.J. Antony Rajam M.Sc. M.Phil., SET., Ph.D., Assistant professor, PG Department of chemistry (SSC), St.Mary′s college (Autonomous), Thoothukudi and that it has not previously formed the basis for award of any degree.

Station: Thoothukudi.

P. Jemima.

Date: 05.04.25 P.JEMIMA

ACKNOWLEDGEMENT

I express my first and humble thanks to **GOD ALMIGHTY** for giving an opportunity to devote to this work.

I would like to express my sincere thanks to our secretary **Dr.Sr.C.Shibana**, our Principal **DR.Sr.A.S.J. Lucia rose**, Director of SSC **Sr.Josephine Jeyarani** and coordinator of SSC **Dr.J. Antony Rajam M.Sc. M.Phil., SET., Ph.D.,**Assistant professor, PG Department of chemistry (SSC), St.Mary′s College (Autonomous), Thoothukudi for providing the permission to complete the project work.

I find it difficult for me to write something in short to acknowledge my guide**Dr.J. Antony Rajam M.Sc. M.Phil., SET., Ph.D.,** She taught me to think and solve the unconditional problems in a conventional way .Her constant inspiration, evaluable guidance tremendous patience and constructive critism helped a lot of focus my views in the proper perspective I take this opportunity to express my deepest sense of gratitude and reference towards her for guiding me in the right direction throughout the course of this work. My deep personal regards are due for her forever.

I heartly express my sincere thanks to my parents and friends.

CONTENT

LIST OF ABBREVIATION

UV Spectroscopy	Ultra-violet visible spectroscopy
FT-IR Spectroscopy	Fourier transform infrared spectroscopy
XRD	X- ray diffraction
TGA	Thermo gravimetric Analysis
BRB	Black rice bioplastic
FMB	Foxtail millet bioplastic

ABSTRACT

Bioplastics are plastics that can be used just like conventional plastics but will disintegrate by the activity of microorganisms into water and carbon dioxide. Starch is a natural polymer material that can be used for bioplastic production. Due to the bio-degradability and renewability of biopolymers, petroleum-based plastics can be replaced with bio-based polymers in order to minimize the environmental risks. Bioplastics are biodegradable and biocompatible with humans and non-toxic to marine organisms. In this article, bioplastic was synthesized from Black rice (*Oryza Sativa)* and Foxtail millet (*Setaria Italica)* using vinegar and glycerol. This work focuses on the performance analysis of synthesized bioplastic from black rice and foxtail millet by using solubility test in water and various solvents. Degradability in the natural soil and in the marine environment was also carried out. Further characterization was done by using UV spectroscopy, XRD, FT-IR and TGA analysis.

Keywords: Bioplastic, degradation, bio polymer, marine environment, swelling ratio, starch, elongation, solubility

CHAPTER1
INTRODUCTION

1.1 Plastic everywhere:

Plastics were introduced approximately 100 years ago, and today are one of themost used and most versatile materials. Yet society is fundamentally ambivalenttoward plastics, due to their environmental implications, so interest in bioplasticshas sparked.According to the petrochemical market information provider ICIS, theEmergence of bio-feedstocks and bio-based commodity polymers production, inTandem with increasing oil prices, rising consumer consciousness and improvingEconomics, has ushered in a new and exciting era of bioplastics commercialization.However, factors such as economic viability, product quality and scale of operationwill still play important roles in determining a bioplastics place on the commercializationSpectrum.The annual production of synthetic polymers (‘‘plastics’’), most of which areDerived from petrochemicals, exceeds 300 million tons, having replacedTraditional materials such as wood, stone, horn, ceramics, glass, leather, steel, Concrete, and others. They are multitalented, durable, cost effective, and easy toProcess, impervious to water, and have enabled applications that were notpossible before the materials' availability. Plastics, which consist of polymers and additives, are defined by their set of Properties such as hardness, density, thermal insulation, electrical isolation, andprimarily their resistance to heat, organic solvents, oxidation, and microorganisms.There are hundreds of different plastics; even within one type, variousGrades exist (eg, low viscosity polypropylene (PP) for injection molding, highViscosity PP for extrusion, and mineral-filled grades Applications for polymeric materials are virtually endless; they are used as Construction and building material, for packaging, appliances, toys, and furniture, in cars, as colloids in paints, and in medical applications, to name but a few.Plastics can be shaped into films, fibers, tubes, plates, and objects such as bottles or boxes. They are sometimes the best available technology. Many plastic productsare intended for a short-term use, and others have long-term applications (eg, Plastic pipes, which are designed for lifetimes in excess of 100 yrs.).

1.2 Bioplastic

The environmental problems caused by discarded synthetic plastics have paved the way for the search for substitutes. Bioplastics, which are both functionally similar to synthetic plastics and environmentally sustainable, are touted as promising new materials to address these problems. Bioplastics is a term used to refer to plastics that are biodegradable, such as PCL or PBS; or may or may not be degradable but are produced from biological materials or renewable feedstocksuch as starch, cellulose, vegetable oils, and vegetable fat. Like any other polymeric material, the degradability of bioplastics is also a factor of their composition, degree of crystallinity and environmental factors, leading to degradation times ranging from several days to several years. For these reasons, the development of biodegradable bioplastics has gained attention in recent years. Based on degradation mechanisms, there are two main categories of biodegradable bioplastics, namely Oxo-biodegradable and hydro-biodegradable. Oxo-biodegradable plastics are made of petroleum-based polymers mixed with a pro-degrading additive that catalyzes the plastic's degradation process . The additive is a metal salt (manganese or iron salts), which enhances the abiotic degradation process of the Oxo-biodegradable plastic in the presence of oxygen. Presently, Oxo-biodegradable plastics are mainly produced from naphtha, a by-product of oil or natural gas. Interestingly, the time taken by biodegradable Oxo products to degrade can be 'programmed' at manufacture, like the methane or nitrous oxide industrial processes. The degradation of Oxo-biodegradable plastics usually takes months to years. On the other hand, hydro-biodegradable plastics decompose hydrolytically at a rate faster than Oxo-degradable plastics. These plastics can be converted to synthetic fertilizers. Examples include bioplastics produced from plant sources (such as starch), and polylactic acid (PLA). Forthcoming paragraphs summarize the most recent literature on different types of bioplastics that have been or are currently being developed.

1.3 Thermoplastic starch:

Starch is a biodegradable, cheap, renewable, easily modifiable biopolymer acquired from renewable plant resources. It consists of two main constituent polymers, amylose, and amylopectin. Amylose is a linear polysaccharide composed of α-D-glucose monomers linked by α-1, 4-glycosidic linkages, whereas amylopectin has the same composition but is highly branched through another type of linkage, the α-1, 6-glycosidic linkage. It should be noted that starch chains bind

together via strong hydrogen bonding, which results in a rigid structure composed of highly ordered crystalline regions .Starch can be formulated into suitable thermoplastic material that can be readily processed into useable forms. Starch's thermal processing involves a change in its microstructure, phase transitions and rheology. Furthermore, starch can be chemically modified and blended with other biopolymers to reduce its brittleness. Starch-based bioplastics are used for packaging materials and for producing food utensils such as cups, bowls, bottles, cutlery, egg cartons, and straws

1.4 Plastics and the environment

The global consumption of plastics has increased over the years, particularly because they are lightweight, resilient, relatively low-priced, and long-lasting. The plastic industry generates approximately 300 million tons of plastics annually, which are used once and discarded after use. Discarded plastic waste, owing to the durability and low degradability of these polymers, may take hundreds to thousands of years to decompose .Moreover, of the total produced quantity of plastics, only 7% is recycled, while about 8% is incinerated and the residual landfilled. The National Academy of Sciences in 1975 assessed that 14 billion pounds of garbage was dumped every year, either buried underground or buried in the oceans. Consequently, oceans and landmass are infested with plastics. In fact, more than 10 million tons of plastic waste is dumped in the oceans alone, so that the majority of anthropogenic debris littering the oceans is composed of human-made plastics. Reports suggest that plastics can now be used as a geological stratigraphic indicator of anthropogenic era. This anthropogenic debris threatens ocean safety, integrity, and sustainability . Overall, plastic waste contributes to a pressing environmental problem is as yet unsolved.

1.5 Advantage of bioplastic

- Bioplastics produce significantly fewer greenhouse gases than conventional plastics over their lifespan. From manufacturing to disposal, fewer emissions are generated than other forms of plastic; less energy is required to produce bioplastics, and less carbon is produced

when bioplastic waste is processed, especially when compared to generic mixed plastic waste. As a carbon-neutral packaging supplier**.**

- Bioplastics will biodegrade naturally over time under the right conditions, unlike other plastics. Bioplastics will naturally decompose in three to six months, but the average plastic takeaway container may take around 450 years to disintegrate. Even when it does, conventional plastics release toxins back into the environment, further damaging the planet.
- **Bioplastics are compostable at commercial facilities**meaning less recycling orgeneral waste to manage. All that's left behind after using a **bioplastic cup** or a **PLA-lined takeaway container**are its natural components since bioplastic packaging is derived from natural substances.
- Biodegradable products are made using naturally occurring substances. As, they don't contain harmful chemicals or pose any risks to intended users. The plastic used to create water bottles bioplastics don't attract harmful bacteria or leach a result chemicals back into the environment, making them practical, eco-friendly options as food and drink packaging.
- The bioplastics can avoid some of the environmental problems like uncontrolled.
- Bio-plastics biopolymers as base material attracted the interest of many researchers and industry because it is environmental friendly and is a substitute packaging material derived from petroleum raw materials such as polystyrene and polyethylene which is not decomposed material.

1.6 Starch Based Bioplas

Starch is one of the most common raw materials used for bio-plastic fabrication in replacing plastic polymers. The hoi-plastic produced from starch has a high biodegradability (quickly decomposes) in the soil. The first bioplastic was invented with maize starch substituted plastics and sold under names such as Ever Corn and Nature Works. These plastic were manufactured by the blending of petrochemical plastic polymer with biodegradable starch polymeric compounds. Currently, the starch-based polymer can be produced from potato, com. wheat, and tapioca during the disposal of this bioplastics, the starch molecules occurring in the polymer will be degraded by the microorganisms and thereby the plastic polymer will be Daunte grated. However, the physical and chemical properties of this starch substituted bioplastics are not suitable for practical usage

further, the accumulation of non-degradable plastic residue in soil and water may cause environmental pollution. This type of bioplastics manufactured directly from the starch, which will affect the stability of the products during the exposure to moisture Starch is one of the most common raw materials used for bio-plastic fabrication in replacing plastic polymers. The bio-plastic produced from starch has a high biodegradability (quickly decomposes) in the soil. The first bioplastic was invented with maize starch substituted plastics and sold under names such as Ever Corn and Nature Works. These plastic were manufactured by the blending of petrochemical plastic polymer with biodegradable starch polymeric compounds. Currently, the starch-based polymer can be produced from potato, com. wheat, and tapioca during the disposal of this bioplastics, the starch molecules occurring in the polymer will be degraded by the microorganisms and thereby the plastic polymer will be Daunte grated. However, the physical and chemical properties of this starch substituted bioplastics are not suitable for practical usage further, the accumulation of non-degradable plastic residue in soil and water may cause environmental pollution. This type of bioplastics manufactured directly from the starch, which will affect the stability of the products during the exposure to moisture.

1.7 Sources of starch

1.7.1 Black rice

Black rice, also known as purple rice or forbidden rice, is a range of rice types of the species *Oryza sativa*, some of which are rice. There are several varieties of black rice available today. These include Indonesian black rice, Philippine heirloom balatinaw black rice and pirurutong black glutinous rice, and Thai jasmine black rice. Black rice is known as *chak-hao* in Manipur, India. In Bangladesh, it is known as *kalo dhaner chaal* (black paddy rice) and used to make polao or rice-based desserts. The bran hull (outermost layer) of black rice contains one of the highest levels of anthocyanins found in food. The grain has a similar amount of fiber to brown rice and like brown rice, has a mild, nutty taste. Black rice has a deep black color and usually turns deep purple when cooked. Its dark purple color is primarily due to its anthocyanin content, which is higher by weight than that of other colored grains. It is suitable for creating porridge, dessert, traditional Chinese black rice cake, bread, and noodles.

Fig.1.1. Black rice *(Oryza sativa L.indica)*

1.7.2 FOXTAIL MILET

Foxtail millet, scientific name *Setaria italica* (synonym *Panicum italicum* L.), is an annual grass grown for human food. It is the second-most widely planted species of millet, and the most grown millet species in Asia. The oldest evidence of foxtail millet cultivation was found along the ancient course of the Yellow River in Cishan, China, carbon dated to be from around 8,000 years before present. Foxtail millet has also been grown in India since antiquity. Other names for the species include dwarf setaria, foxtail bristle-grass, giant setaria, green foxtail, Italian millet, German millet, and Hungarian millet.

Fig.1.2.Foxtail millet *(Setaria italica)*

1.8 Need of plasticizer in bioplastic

In the basic knowledge, by using the pure starch, it is able to absorb humidity. Thus it is a suitable material for production in pharmaceutical sector in the making of drug capsules to produce bioplastic from starch glycerol should be added in the heating process. The elasticity characteristic of bioplastic can be fabricated by adding glycerol as plasticizer Hence, the flexibility of the plastic is provided When used alone in packaging applications, starchi exhibits a poor performance because of us brittleness and hydrophilic nature Very important to find the perfect plasticizer that imparts flexibility

1.9Market demand for bioplastic

Importance of the bioplastics was not known for the past two decades, however, recently the bioplastics have become an integral part of our society. The continuous research and developmental activities towards bioplastics and growing awareness towards environmental conservation have led to a remarkable growth of the overall bioplastics market further, the stringent regulatory reforms by the several governments towards the reduction of plastic usage have augmented the demand for bioplastics. At present, the contribution of bioplastics products in the total plastics market is around only I percent However, the results of European Bioplastics annual market data update, presented at 12th European Bioplastics Conference held on 29 November 2017 in Berlin, confirmed that steady growth of the global bioplastics industry. The growth rate of bioplastics is around 20-25 per cent per year but the growth rate for conventional plastics is only 4-

9 per cent per year The European bio-plastics market reported that the global bioplastics market is to be growing at more than 20% per year. The only disadvantage of the global bioplastics market is high production cost over conventional plastics however, it can be overcome by the technology advancement Moreover, and the increasing price of crude oil has also boosted the manufacturer towards the production of bioplastics over petroleum based plastics.

1.10 Energy Generation from bio plastic

The energy is generated from the bioplastic wastes through different processes viz., anaerobic digestion, pyrolysis, incineration. But it would be carried out after complete recovery of all the recyclable materials from the bioplastic wastes. Since, the bioplastics having a high caloric value, it can be used to generate energy in general conventional plastic waste incineration facilities. Even though some of the bioplastics such as natural cellulose fibre and starch having the property of lower gross calorific values (GCV), they are a resemblance to wood, and hence the energy recovery is feasible and viable from these bioplastic wastes through incineration . The incineration of the bioplastic wastes will emit large quantities of carbon dioxide which will be captured and may be used to develop new biobased products. This will make the practice of incineration of bioplastic wastes as a sustainable practice.

1.11 Waste Management Options for Bioplastics

The bioplastics are suitable for a wide range of end-of-life options viz., reuse, mechanical recycling, chemical recycling, organic recycling and energy recovery. Recycling is the preferred and viable options for the sustainable management of bioplastics, and then incineration with energy recovery is the most suitable method over land-filling All the recycling methods including material, chemical, and organic recycling are viable for bioplastics management Another option for recycling of the bioplastics is chemical recycling, in which the biopolymer wastes will be remelted and regranulated for the development of a new product. In certain cases, the biopolymer wastes also converted into the chemical building blocks i.e., monomers which can be used again for the production of the biopolymer. This type of recycling is also called as feedstock recycling.

CHAPTER 2

REVIWE OF LITERATURE

- *Trien Khoa Nguyen* et al. (2022) Development of Starch-Based Bioplastic from Jackfruit Seed" In this article, jackfruit seed starch plasticized with common plasticizers was developed and characterized. At the first step, the research papers that dealt with the fabrication and characterization of starch-based bioplastics were synthesized and analyzed. Next, jackfruit seeds were selected as a source for starch because of their large availability, low price or even free, and high starch capacity. Afterward, a starch-based bioplastic fabrication procedure was proposed. From preliminary tests, plasticizers were sufficiently selected including water, glycerol, natri bicarbonate, and acid citrie. Using different combinations of these plasticizers, four types of bioplastics were then fabricated to study the effect of the plasticizers as well as to characterize the properties of the corresponding bioplastics a cutting tool for ASTM D412 type a standard tensile testing specimen was then designed and fabricated. Using these dog-bone specimens, tensile results showed that the hardness of the fabricated bioplastic was positively proportional to the ratio of the starch. Furthermore, from SEM characterization, the bioplastic specimens were fully plasticized although the fabricated bioplastic has lower mechanical properties than petroleum-based plastics, its environmental friendliness and high potential added value promise to be a material of the future.
- *Maria Alonso-González* et al. (2021) Effects of Mould Temperature on Rice Bran- Based Bioplastics Obtained by Injection Moulding" The high production rate of conventional plastics and their low degradability result in severe environmental problems, such as plastic accumulation and some other related consequences One alternative to these materials is the

production of oil-free bioplastics, based on wastes from the agro-food industry, which are biodegradable. Not only is rice bran an abundant and non-expensive waste, but it is also attractive due to its high protein and starch content, which can be used as macromolecules for bioplastic production. The objective of this work was to develop rice-bran-based bioplastics by injection moulding. For this purpose, this raw material was mixed with a plasticizer (glycerol), analyzing the effect of age Mould temperatures (100 130 and 150 in the mechanical and microstructural properties and water absorption capacity of the final matrices. The obtained results show that rice bran is a suitable raw material for the development of bioplastics whose properties are strongly influenced by the processing conditions. Thus, higher temperatures produce stiffer and more resistant materials (Young's modulus improves from 127 MPa to 236 and 33+6 MPa when the temperature increases from 100 to 150 and 150 C. respectively), however, these materials are highly compact and consequently, their water absorption capacity diminishes. On the other hand, although lower mould temperatures lead to materials with lower mechanical properties; they exhibit a less compact structure, resulting in enhanced water absorption capacity.

- *Fong Chul Nee and Siti Amira Othman* (2021), Preparation and Characterization of Irradiated Bioplastic from Cassava Peel- A Review The conventional plastic beats unavoidable responsibility for the massive scale generation of garbage. The bulk of the market is mostly made up of fossil-based plastics and the worldwide environmental pollution generated by them is growing increasingly problematic: Agro-waste product is probably a good way to make bioplastic In fact, biodegradable plastic is indeed a good alternative to replace the petroleum-based plastics Besides, making good use of agriculture waste can assist in diminishing waste accumulation Cassava peel is a type of waste from cultivating activities that has the potential in making bio-based plastics. This research will focus on the preparation and characterization of bioplastic from cassava peel. Several related characterization methods such as XRD, SEM. FTIR. TGA will be discussed. The main purpose of this review is to fabricate and produce bioplastic samples from cassava peel with the addition of different ratios of sorbitol and chitosan.

- *Jianlei Yang* et.al, (2021) modified starch and empty fruit bunch-based bioplastic composites with epoxidized palm oil (EPO) or citric acid-epoxidized palm oil (CEPO) oligomer using melt blending in order to improve the mechanical and water resistance properties. As evidenced by the FTIR, CEPO generated strong interactions with starch/fibers via citric acid-inspired esterification reaction. The X-ray diffraction patterns of the composites were apparently changed by CEPO because of the crosslinking effect. The SEM micrographs showed that EPO was immiscible with starch and hence migrated to the composite's surface. The compatibility between starch and CEPO was obviously improved. EPO contributed to a noticeable decrease in melting temperature (*Tm*) of the composites, while CEPO improved *Tm* due to its crosslinking effect. The water sensitivity and permeability of the composites were also slightly reduced upon the addition of both oils. This study proposed a simple and effective modification technique by utilizing the CEPO oligomer to fabricate the bioplastic composites with superior properties.
- *Mirko Cucina* et.al, (2021) assessed the effects of high concentrations (10 % w/w, data projected for 2030) of commercial bioplastics, i.e. starch based shopping bags (SBSB) and polylactic acid (PLA) tableware, in the organic fraction of municipal solid wastes (MSW) on compost quality obtained by pilot-scale dry mesophilic anaerobic digestion and subsequent composting of the digestate. After the biological processes, 48.1 % total solids (TS) of SBSB and 15 % TS of PLA degraded, resulting in a high bioplastics content (about 18 % TS) in compost. Subsequent compost incubation in soils indicated that bioplastics degraded by pseudo-zero order kinetics (0.014 and 0.010 mg C $cm^{-2}d^{-1}$ for SBSB and PLA, respectively), i.e. complete degradation was expected in 1.6 years (SBSB) and 7.2 years (PLA), confirming the intrinsic biodegradability of bioplastics. Nevertheless, enhancing the rate and amount of bioplastics degradation during waste management represents a goal to decrease the amount of bioplastics reaching the environment.
- *C. Lim* et.al, (2021) analyzed the practicability of forming seaweed films and their viability of enhancing the bioplastic market using new green technologies. Seaweeds can form films either directly or using their derivatives like agar, carrageenan, and alginate. Seaweeds films that are formed directly without chemical treatment are a promising approach but

currently, the field is still new and more research are needed. Seaweeds have numerous advantages compared to other biomass, where they do not need pesticide or wide land use while can grow fast, easy to harvest, and cheap. Seaweeds can also be mixed with other seaweed species or materials to improve their characteristics and properties. Hence, using seaweeds as biomass material is a promising approach to replace conventional plastic that can not only contribute to the economy but also eco-friendly. Green production methods are more viable to produce seaweed films Compared to conventional extraction methods as they are more eco-friendly and economic.

- *Emma M.N. Polman* et.al, (2021) made biodegradable plastics from biopolymers (made in nature) or from bio-based polymers (made in a factory) are becoming increasingly important in replacing the massive amounts of conventional, non-degradable fossil based plastics that have been produced and disposed over the past decades. In this review we compare the biodegradation rates and mechanisms of the bioplastics thermoplastic starch, cellulose acetate and lignin based bioplastics with the biodegradation rates and mechanisms of starch, cellulose and lignin, which are the unmodified biopolymers from which these bioplastics are produced. With this comparison we aim to determine to what extent the extensive knowledge on unmodified biopolymer biodegradation can be applied to the biodegradation of bioplastics (modified biopolymers) in the terrestrial environment.. We found that the similarities and differences in biodegradation are dependent on the structural changes imposed on a biopolymer during the bioplastic production process. A change in higher level structure, as found in thermoplastic starch, only resulted in a limited number of differences in the biodegradation process. However, when the chemical structure of a polymer is changed, as for cellulose acetate, different microorganisms and enzymes are involved in the biodegradation. Based on the cellulose acetate biodegradation process, a conceptual model was proposed that can be used as a starting point in predicting biodegradation rates of other chemically modified biopolymers used as bioplastics. Future bioplastic biodegradation research should focus on conducting long-term field experiments, since most studies are conducted in a study.
- *Noorul Hidayah Yusoffa* et.al, (2021) large quantities of disposable plastic products affected and threaten the extinction of living organisms, this research conducted to develop

bioplastics composite material made of Polylactic Acid (PLA) incorporated with tapioca starch (TS) to investigate the effect of TS as the filler towards the mechanical properties of this bioplastic. This study purposely conducted to develop material for food packaging usage limitation of usage and application below the 160 o of temperature application. The amount of loading percentage of TS and PLA between 10 to 50 wt. %. Sample from this composite material has been prepared through melt blending extrusion process and injection molding method. The result showed that tensile strength was improved significantly with the addition of TS with the maximum reading was at 30 wt. % loading, and then it had gradually decreased with the additional TS. Hence, the highest tensile strength has been obtained at 9.7 MPa while plain PLA recorded at 7.7 MPa only. The outcome data from the analysis of impact testing explained that the reduction in impact when loading of TS has been increased. The addition of TS in this composite system gives better results in tensile modulus and decreased in the value of crashed impact.

- *Yacouba zoungranan* et.al, (2020) use of petrochemical plastics has become a real problem for health and the environment. This problem is related to the non-biodegradable character of a great majority of these plastics and to the presence of certain chemical substances sometimes toxic in their internal structures. The development of biodegradable and less dangerous plastics thus represents an alternative to the petrochemical plastics. Two types of bioplastics were elaborated from cassava starch and corn starch. The simple bioplastics were obtained from starch only. The composite bioplastics were obtained by adding a natural ingredient extracted from the species Cola cordifolia to the starch. The biodegradability was assessed through burial tests in soil. The biodegradation was confirmed by the burial soil pH measurement. The burials in soil were also carried out taking into account the influence of abiotic (humidity, temperature) and biotic (enrichment in microorganisms) factors. The study showed that biodegradability of bioplastics is linked to the nature of the starch used. The simple cassava-based bioplastic degraded faster than those based on corn. The addition of the Cola cordifolia natural ingredient, significantly improves the biodegradability of composite bioplastics compared to simple bioplastics. However, variability of environmental factors can improve or disadvantage biodegradability. Humidity promotes the biodegradability of bioplastics.

- *Katrin jogi* et.al, (2020) global plastic production is reaching new altitudes every year. Growing production of petroleum-based plastics has incurred in disposal issues raising the concerns of plastic pollution and impact to the environment. These issues have encouraged innovation and research activities in the field of bioplastics, offering alternatives for conventional plastics. In recent years, global bioplastic production has also witnessed tremendous growth and expansion. Some of the main drivers of this growth are innovative biopolymers such as Polylactic acid (PLA) and Polyhydroxyalkanoates (PHAs). However, industrial expenses to produce bioplastics are much higher when compared to petroleum-derived plastics (e.g. industrial PHA production is estimated to be 5–10 times more expensive than petroleum-derived polymers). In this regard, globally many researchers have investigated for more environmentally friendly and cost-effective alternatives to produce plastics. One potential option to pursue would be to explore agri-food wastes and by-products for bioplastic production.
- *Wen Yi Chia* et.al, (2020) Increased global demand for plastic materials has led to severe plastic waste pollution, particularly to marine environment. This critical issue affects both sea life and human beings since micro plastics canenter the food chain and cause several health impacts. Plastic recycling, chemical treatments, incineration and landfill are apparently not the optimum solutions for reducing plastic pollution. Hence, this review presents two newly identified environmentally friendly approaches, plastic biodegradation and Bioplastic production using algae, to solve the increased global plastic waste. Algae, particularly Microalgae, can degrade the plastic materials through the toxins systems or enzymes synthesized by microalgae itself while using the plastic polymers as carbon sources. Utilizing algae for plastic biodegradation has been critically reviewed in this paper to demonstrate the mechanism and how micro plastics affect the algae. On the other hand, algae-derived bioplastics have identical properties and characteristics as petroleum-based plastics, while remarkably being biodegradable in nature. This review provides new insights into different methods of producing algae-based bioplastics (e.g., blending with other materials and genetic engineering), followed by the discussion on the challenges and further research direction to increase their commercial feasibility

- *Ebrahimian* et.al, (2020) Municipal solid waste is an environmental threat worldwide; however, the organic fraction of municipal solid waste (OF-MSW) has a great potential for the generation of fuels and high-value products. In the current study, OF-MSW was utilized for the production of ethanol, hydrogen, as well as 2, 3-butanediol, an octane booster, by using Enterobacter aerogenes. Furthermore, a promising alternative to nonbiodegradable petrochemical Farinaz -based polymers, Polyhydroxyalkanoates (PHAs), was produced..
- *João Medeiros Garcia lcântara* et.al, (2020) Plastics and microplastics is stimulating intense research towards more environmentally friendly materials, preserving the remarkable application characteristics of the currently available polymers. Among these, polyhydroxyalkanoates (PHAs) have been hailed as the solution to replace conventional, oil-based plastics. Given their biodegradable nature and mechanical properties, their use can be envisioned in a wide range of applications reducing the environmental footprint. Several types of processes have been proposed for their production, which can be grouped in three main classes: (i) microbiological, (ii) enzymatic and (iii) chemical processes. Given the significant amount of literature available on this topic, this review aims to critically analyze what has been proposed so far in each of these classes, with specific reference to their potential to provide bioplastics that can actually replace the currently available materials.
- *Vimudha Muralidharan* et.al, (2020) the untanned proteinaceous trimming waste from tanneries was used to prepare highly flexible and transparent bioplastic films. Composite bioplastic films were fabricated by blending trimming hydrolysate powder and polyvinyl alcohol using the solution casting method. In addition, a non-toxic and relatively inexpensive bio-cross linker – citric acid was used as a plasticizer / crosslinking agent. The effects of citric acid concentration on the mechanical properties, thermal stability, transparency and anti-microbial properties of the Bioplastic films were investigated. Crosslinking interactions by the citric acid on the Constituents of the bioplastic were confirmed using FTIR/ATR. Also, the surface Microstructure of the films was studied using SEM. The resultant bioplastic films were Smooth, uniform and defect-free. Citric acid used in the bioplastic blend formulation clearly acted as a plasticizer at higher concentrations the trimming waste-based Bioplasticwith the citric acid concentration of 40% exhibited an outstanding tensile strength above 20 MP Extremely high elongation at break value greater

than 343%.The Bioplastic degraded to an extent of 62% within 70 days under the soil burial test.

- *Caesar Javier Lopez Rocha* et.al, (2020) World population is in need of creating alternative materials that can replace conventional plastics, microalgae biomass may be identified as a viable source for producing more environmentally friendly materials. *Scenedesmus* sp and *Desmodesmus* sp are the main components (~80%) of a microalgae consortium (MC) that first has been used to remove Nitrogen and Phosphorus from wastewater. The potential to develop bioplastic materials from MC considering its relatively high protein content (~48%) has been assessed in the present manuscript, using as a reference a commercial biomass rich an *Arthrospira* specie (AM) also present in the studied consortium. Bioplastics were obtained through injection moulding of blends obtained after mixing with different amounts of glycerol, and eventually characterized using Dynamic Mechanical Thermal Analysis (DMTA), water immersion and tensile tests. All bioplastics displayed a glass transition temperature around 60 C, showing a thermoplastic behavior which is less pronounced in the CM based bioplastics. This would imply a greater thermal resistance of bioplastics produced from the biomass harvested in wastewater. Moreover, these bioplastics showed a lower ability to absorb water when immersed, due to the lower deformability displayed in the tensile tests. The mechanical properties of all samples, independently of the nature of the biomass, were improved when the presence of the biomass was higher.
- *Masanori Yamada* et.al, (2020) Soybean one of the most abundant plants, has been cultivated around the world as a familiar crop. Especially, most of the soybean is globally used as a crop to obtain the oil. The degreased soybean contains a lot of proteinin it. The part of the degreased soybean is used for the food of human consumption and livestock feed, howevermost of this are discarded as industrialwaste throughout the world. Therefore, we demonstrated the preparationof bioplastics consisting of soy protein. Although the soy protein without the cross-linking reaction by formaldehyde (HCHO) was collapsed in water, bioplastics were stable in water. Additionally, the bending strength of thebioplastic increased with the HCHO concentration and showed the maximum value of approximately 35MPa at a1% HCHO concentration. Surprisingly, this bending strength value was the same as that of polyethylene. In contrast, the infrared spectra indicated the formation ofmethylene cross-

linking between the basic amino acids, such as lysine and arginine. Finally, we estimated the biodegradable property of the bioplastic by pronase, one of theproteolytic enzymes. As a result, this bioplastic showed the weight loss of approximately 30% after the incubationtime of 6 days. These results suggested that the bioplastic consisting of soy protein possesses a biodegradable property. Therefore, the bioplastic consisting of soybean may have the potential to be used as a biodegradable material, such as agricultural materials, industrial parts, and disposable items.

- *O. Oluwasina* et.al, (2020) Oxidized starch was produced and its effect on starch-based bioplastic film has been evaluated. The produced oxidized starch was coarse, brownish with 15.68% carbonyl content, insoluble in cold water and has a positive influence on bioplastic films. The film thickness increased with increase in the amount of added oxidized starch from 0.21% to 0 .23%. The film moisture content dropped from 7.93% to 5.36%, likewise the film water solubility decreased from 13.48% to 5.75%. Addition of oxidized starched to longer biodegradability and enduring water absorption kinetics. The mechanical property was improved by the addition of oxidized starch. The derivative thermogravimetry analysis indicates five degradation stages for all the bioplastic films, while films surface roughness was shown by AFM. The research has revealed that oxidized Starch can be used to improve the physic mechanical properties of starch based bioplastic film.
- *M. Jim enez-Rosado* et.al, (2019) Bioplastic have generated an increasing interest as an alternative to conventional plastics. For this reason, their manufacture using the traditional techniques used for the production of plastics, such as extrusion, would help transferring bioplastics production to an industrial scale. In this way, the preparation of wheat gluten bioplastics by extrusion was the main objective of this research, modifying their structure by varying the pH value or by incorporating additives (glyoxal or xanthan gum). These bioplastics were characterized by the measurement of their mechanical properties and their water uptake capacity, proving that the modification of bioplastics cause variations in their properties. Thus, extrusion resulted in a greater gluten-plasticizer compatibility compared to compression, as denoted the temperature ramp tests, especially in the presence of additives (i.e. Xanthan gum, glyoxal). Moreover, tensile strength was enhanced at pH 9, probably due

to bonding promotion at alkaline conditions. These results demonstrate the great potential of these materials for the replacement of conventional plastics.

- *Martina Nevoralov* et.al, (2019) Preparation and characterization of biodegradable materials based a good alternative for starch based packaging production. On plasticized and chemically modified starch. During the experiments, the morphology, properties and biodegradability of the starch materials were influenced by the functionalization (acetylation, propionation) of the starch, different processing procedures and the use of plasticizers. The starch materials were prepared by either solution casting or melt mixing or by the combination of the two procedures, which strongly affected the degree of the material plasticization, its homogeneity, and the final morphology. FTIR spectroscopy qualitatively proved the esterification of starch by the intensity of signals associated with esters groups. The thermogravimetry analysis confirmed a gradual reduction in the water content proportional to the acetylation of starches, as well as noticeable changes in their thermal properties at the higher degree of substitution (DS). Signal intensities and weight losses derived from FTIR and TGA, respectively, were well correlated with DS.
- *Shazia Tabasuma* et.al, (2018) Maize or corn is considered as very distinctive plant. Corn having better capability of utilizingsun light, is a noble way of getting a natural polymer known as starch. Amylopectin and amylase composition in the starch firmly affects the properties of the polysaccharide. Despite of application of CS as food for living being including the human and animals it has many other applications in industry. No doubt it has many flaws which can be controlled by adopting different modifications. Nowadays bio-degradable polymers are useful which are produced by corn starch. Starch based plastics and composites are not cheap but produce less waste which ultimately reduces the plastic pollution. Different types of natural and synthetic polymers and Nano clay can be blended with starch. Some of these polymers are tailor made for some special purposes. Natural polymers like chitosan, cellulose, gelatin, collagen, zein, alginate, kappaphycus alvarezii seaweed, various amino acids, and synthetic polymers like polybutylene, polyacrylic acid, polyethylene, polyvinyl chloride, polyvinyl alcohol, polycaprolactone, and acrylic acid are utilized to modify starch to yield starch base completely bio-decomposable polymers. These

biopolymers have the capability to substitute the petroleum base polymers, and can be used for different environmental, industrial and medical applications.

SCOPE OF THE INVESTIGATION

Bioplastic are plastics made from natural sources. They can possess biodegradability, elongation, good solubility, thermal stability that can make them desirable in replacement for plastics.

OBJECTIVES

- To synthesis bioplastic from natural sources like black Rice Starch and Foxtail millet.
- To determine the solubility of the bioplastic in various solvents.
- To determine the water solubility of the bioplastic.
- To find the swelling ratio of the bioplastic.
- To find out the biodegradability of the bioplastic in soil as well as marine environment.
- To study optical properties by using UV-visible spectrophotometer.
- To identify the stretching frequencies for bonding FT-IR spectroscopy.
- To find out the nature of bioplastic using X-ray diffraction studies.

CHAPTER 3

MATERIALS AND METHODS

4.1. Materials used

- Black rice starch.
- Foxtail millet starch.
- Synthetic vinegar
- Glycerol
- Aluminum sheet
- Distilled water
- 50mL beaker
- 250mL beaker
- Glass rod
- Blender
- Muslin cloth

4.2 Preparation of bioplastics

4.2.1 Extraction of starch from Black rice:

50 g of good quality Black rice was powdered finely in a blender. The powdered black rice was then mixed with 100 mL of distilled water and stirred well, till the powder mixed well with water. It was then filtered through the muslin cloth to remove the larger particles in the filtrate. The filtrate was then allowed to stand for more than 6 hours. After that the clear solution at the top was separated by decantation, leaving the sediment starch in the bottom of the beaker. It was then dried for an hour at 120º C in a hot air oven, the fine starch was thus extracted from the black rice.

4.2.3 Preparation of bioplastic

3.5g of black rice starch was dissolved in 10mL of distilled water in a 50mL beaker. Similarly 3.5g of foxtail Starch was dissolved in 10mL of distilled water in a 50mL beaker. To this, 5mL of vinegar was added and stirred well. The beaker was then heated to 40°C in a hot plate. To this mixture, 4mL of the plasticizer, glycerol was added and the mixture was heated in a hot plate for about3 - 4 hours. The heating process was stopped when the mixture becomes thick paste. It was immediately poured and spread over the aluminum sheet, when it was hot. The care was taken to make the sheet with uniform thickness. After this, the sheet was exposed to sunlight for 2 days, so that it was dried completely. Finally the bioplastic film thus formed were peeled off from the aluminum sheet. The prepared bioplastic from Black rice was named as BRB.

4.2.3 Extraction of starch from Foxtail millet

The starch was extracted from Foxtail milletas per the same procedure mentioned above and it was dried.

4.2.4 Preparation of bioplastic

Similarly 3.5g of foxtail Starch was dissolved in 10mL of distilled water in a 50mL beaker. To this, 5mL of vinegar was added and stirred well. The beaker was then heated to 40°C in a hot plate. To this mixture, 4mL of the plasticizer, glycerol was added and the mixture was heated in a hot plate for about3 - 4 hours. The heating process was stopped when the mixture becomes thick paste. It was immediately poured and spread over the aluminum sheet, when it was hot. The care was taken to make the sheet with uniform thickness. After this, the sheet was exposed to sunlight for 2 days, so that it was dried completely. Finally the bioplastic film thus formed were peeled off from the aluminum sheet. The prepared bioplastic from Black rice was named as FMB.

4.3 solubility test

4.3.1 Water solubility test

The ORP samples were cut into square sections of 2.0 cm and the dry film mass was weighed accurately and recorded. The sample was immersed in 100 mL. Distilled water and the solubility was checked every 4 hours. It was dried and weighed. It was noted up to 24 hours. Glycerol has a good water solubility range from 18% to 25% the percentage of total soluble matter (% solubility) was calculated as

Water solubility (%) = [(Wo-Wf) Wo]×100

Where, W_o is the weight at the initial weight of the ORP and Wf is the final weight of the ORP.

4.3.2 Solubility test in various solvents:

The ORP samples were cut into 5 equal pieces. It was immersed in various solvents like water. Benzene, Acetone, Toluene and Ethanol in the beakers. It was left aside for 24 hours. The samples were taken out and dried at oven. The samples were weighed before and after the testing

Solubility = $[(W_o-W_f)/W_o] \times 100$

Where, W_o is the initial weight of the ORP and $W_f$is the final weight of the ORP.

4.4 Swelling test

The dried ORP were cut into equal pieces and immersed in ultrapure water for 10 minutes and the weight of these swelling materials was measured. The swelling ratio of bioplastic was estimated by

Swelling ratio (%) $= Ws / Wo \times 100$

Where, W_o and Ws, are the initial and swelling weights of ORP respectively. The value of swelling ratio was expressed as an average of five measurement.

4.5 Elongation test

Elongation at break is the ratio between the initial length and changed length of specimen after breakage when an external stress is applied. The values were measured and results documented.

4.6 biodegradability test

4.6.1 Biodegradability test in the soil:

The BRB and FMB samples were cut into equal pieces. Garden soil was collected, moistened and stored in a container. The samples were buried 2 cm inside the soil and kept at room temperature. They were monitored for 30 days. The weight of the samples was measured before (day zero) and after the testing (day 30).

The biodegradability was measured by:

$$\text{Weight Loss (\%)} = [(Wi - W_f) / Wi] \times 100.$$

Where Wi and W_f are the weights of samples before and after the test.

4.6.2 Biodegradability in the marine environment:

The ORP were cut into equal pieces. It was then kept inside the marine environment and monitored every two days. After 12 days, the sample were taken out and weighed. The samples were weighed before and after the testing (12 days). The biodegradability was measured by

$$\text{Weight Loss (\%)} = [(Wi-W_f)/Wi] \times 100$$

Where, Wi and Wf are the weights of samples before and after the test.

4.7 Characterization

The prepared bioplastic were characterized by various studies such as ultraviolet-visible spectroscopy, Fourier transform infrared spectroscopy-Ray diffraction, Thermo gravimetric analysis**.**

4.7.1 Ultraviolet-visible spectroscopy

Principle:

When a beam of monochromatic light is passed through a solution of an absorbing substance, the rate of decrease of intensity of radiation with thickness of the absorbing solution isProportional to the incident radiation as well as the concentration of the solution.

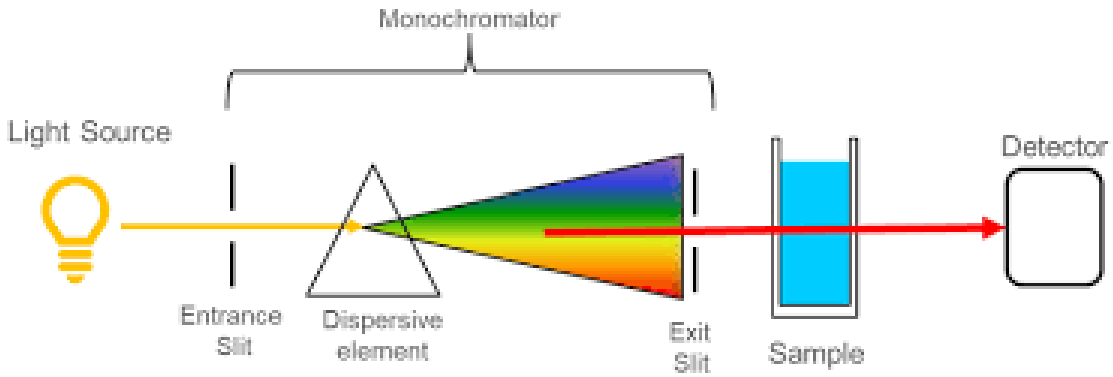

Instrumentation:

Light source:

Tungsten filament lamps and Hydrogen-Deuterium lamps are the most widely used and suitable light sources as they cover the whole UV region. Tungsten filament lamps are rich in red radiations; more specifically they emit the radiations of 375 nm, while the intensity of Hydrogen-Deuterium lamps falls below 375 nm.

Monochromator:

Monochromator generally composed of prisms and slits Most of the spectrophotometers an doable beam spectrophotometers The radiation emitted from the primary source is dispersal with the help of rotating prisms: The various wavelengths of the light source which are separated by the prism are then selected by the slits such the rotation of the prism results in a series of continuouslyincreasing wavelengths to pass through the slits for recording purposes. The bear selected by the slit is monochromatic and further divided into two beans with the help of another prism.

Sample and reference cells:

One of the two divided beams is passed through the sample solution and the second beam n passes through the reference solution. Both sample and reference solution is contained in the calls. These cells are made of either silica or quartz Glass can't be used for the cells as it also absorbs light in the UV region.

Detector

Generally, two photocells serve the purpose of the detector m UV spectroscopy. One of the photocells receives the beam from the sample cell and the second detector receives the beam from the reference. The intensity of the radiation from the reference cell is stronger than the beam of the sample cell. This results in the generation of pulsating or alternating currents in the photocells.

Amplifier

The alternating current generated in the photocells is transferred to the amplifier. The amplifier is coupled to a small servo meter. Generally, the current generated in the photocells is of very low intensity, the main purpose of the amplifier is to amplify the signals many times so can get clear and recordable signals.

Recording device

Most of the time amplifier is coupled to a pen recorder which is connected to the computer. The computer stores all the data generated and produces the spectrum of the desired compound.

4.7.2. Fourier Transform Infrared Spectroscopy (FTIR):

Fourier transform infrared spectroscopy (FTIR) is a technique which is used to obtain red spectrum of absorption, emission, and photoconductivity of solid, liquid, and gas. It is used to detect different functional groups in PHB. FTIR spectrum is recorded between 4000 and con FTIR method is used to obtain the infrared spectrum of transmission or absorption of a fuel sample. FTIR identifies the presence of organic and inorganic compounds in the sample. Depending on the infrared absorption frequency range 600-4000 cm^{-1} the specific molecular groups prevailing in the sample will be determined through spectrum data in the automated system.

Instrumentation

1) The Source:

Infrared energy is emitted from a glowing black body source. This beam passes through an aperture which controls the amount of energy presented to the sample (and, ultimately, to the detector).

2) The Interferometer:

The beam enters the interferometer where the "spectral encoding" takes place. The resulting interferogram signal then exits the interferometer.

3) The Sample:

The beam enters the sample compartment where it is transmitted rough or reflected off of the surface of the sample, depending on the type of analysis being accomplished. This is where

specific frequencies of energy, which are uniquely characteristic of the sample, are absorbed.

4) The Detector:

The beam finally passes to the detector for final measurement. The detectors used are specially designed to measure the special interferogram signal

5) The Computer:

The measured signal is digitized and sent to the computer where the Fourier transformation takes place .The final infrared spectrum is then presented to the user for interpretation and any further manipulation.

4.8.2 X-ray Diffraction (XRD):

X-ray powder diffraction (XRD) is a rapid analytical technique primarily used for phase identification of a crystalline material and can provide information on unit cell dimensions. The analyzed material is finely ground, homogenized, and average bulk composition is determined.

Fig 4.8.2 instrumentation of XRD

Instrumentation:

X-ray diffract meters consist of three basic elements: an X-ray tube, a sample holder, al an X-ray detector. X-rays are generated in a cathode ray tube by heating a filament to dace electrons, accelerating the electrons toward a target by applying a voltage, and barding the target material with electrons. When electrons have sufficient energy to dislodge inner shell electrons of the target material, characteristic X-ray spectra are produced. These spectra consist of several components,

the most common being Kα and Kβ.. The specific engths are characteristic of the target material (Cu, Fe, Mo, and Cr). Filtering, by foils or yal Monochromator, is required to produce monochromatic X-rays needed for diffraction. K$\alpha^1 and$ Kα_2 are sufficiently close in wavelength such that a weighted average of the two is used. Copper is the most common target material for single-crystal diffraction, with Cu K, radiation = 15418A. These X-rays are collimated and directed onto the sample. As the sample and detector used, the intensity of the reflected X-rays is recorded. When the geometry of the incident X-rays impinging the sample satisfies the Bragg Equation, constructive interference occurs and an al to a count rate which is then output to a device such as a printer or computer monitor. The geometry of a beam at an X-ray diffractometer is such that the sample rotates in the path of collimated X-ray beam at an angle θ while the X-ray detector is mounted on an arm to collect the diffracted X-rays and rotates at an angle of 2θ. The instrument used to maintain the angle and rotate the sample is termed a goniometer. For typical powder patterns, data is collected at 2θ from$\sim 5\ to\ 70°$, angles that are present in the X-ray scan

4.8.3. Thermo gravimetric analysis:

Thermo gravimetric analysis (TGA) measures weight changes in a material as a function of temperature (or time) under a controlled atmosphere. Its principle uses include measurement of a material's thermal stability, filler content in polymers, moisture and solvent content, and the percent composition of components in a compound.

Principle

A TGA analysis is performed by gradually raising the temperature of a sample in a furnace as its weight is measured on an analytical balance that remains outside of the furnace. In TGA, mass loss is observed if a thermal event involves loss of a volatile component Chemical reactions, such as combustion, involve mass losses, whereas physical changes, such as melting do not. The weight of the sample is plotted against temperature or time to illustrate thermal transitions in the material such as loss of solvent and plasticizers in polymers, water of hydration in morganic materials, and, finally, decomposition of the material.

Instrumentation

The instrument used in thermogravimetry (TG) is called a thermo balance. It consists of several basic components in order to provide the flexibility necessary for the production of useful analytical data in the form of TGA Curve as shown Basic components of a typical thermo balance are listed below: i) Balance ii) Furnace heating device ii) Unit for temperature measurement and control (Programmer) iv) Recorder, automatic recording unit for the mass and temperature changes.

Balance

The basic requirement of an automatic recording balance are includes accuracy. Sensitivity reproducibility, and capacity. Recording balances are of two types, null point and deflection type. The null type balance, which is more widely used, incorporates a sensing element which detects a deviation of the balance beam from its null position. A sensor detects the deviation and triggers the restoring force to bring the balance beam to back to the null position. The restoring force is directly proportional to the mass change. Deflection balance of the beam type involve the conversion of the balance beam deflection about the fulcrum into a table mass- change trace by (a) photographic recoding i.e. change in path of a reflected beam of light available of photographic recording, (b) recording electrical signals generated by an appropriate displacement measurement transducer, and (c) using an electrochemical device. The different balances used in TG instruments are having measuring range from 0.0001 mg to 1g depending on sample containers used.

Furnace

The furnace and control system must be designed to produce linear heating at over the whole working temperature range of the furnace and provision must be made to maintain any fixed temperature. A wide temperature range generally-150 °C to 2000 °C of furnaces is used in different instruments manufacturers depending on the models. The range of furnace basically depends on the types of heating elements are used.

Temperature Measurement and Control

Temperature measurement are commonly done using thermocouples, chromal - alumel thermocouple are often used for temperature up to 1100 °C whereas Pt/(Pt-10% Rh) is employed for temperature up to 1750 °C. Temperature may be controlled or varied using a program controller with two thermocouple arrangement, the signal from one actuates the control system whilst the second thermocouple is used to record the temperature.

Recorder

Graphic recorders are preferred to meter type recorders. X-Y recorders are commonly used as they plot weight directly against temperature. The present instrument facilitate microprocessor controlled operation and digital data acquisition and processing using personal computer with different types recorder and plotter for better presentation of data. There is a control mechanism to regulate the flow of inert gas to provide inert atmosphere and water to cool the furnace. The temperature sensor of furnace is linked to the programme to control heating rates, etc. The balance output and thermocouple signal may be fed to recorder to record the TGA Curve.

CHAPTER 5

RESULTS AND DISCUSSION

5.1 Water solubility test

The solubility of BRB and FMB was checked every 4 hours and the sample was weighed. The solubility was calculated and tabulated.

Table 5.1.1Solubility % of BRB and FMB in water

S.NO	Time (hour)	Solubility%	
		BRB	FMB
1	4	8.35	7.25
2	8	17	15
3	12	33	30
4	16	42	45
5	20	55	57.15
6	24	68	70

The solubility of BRB and FMB in water increases every 4 hours. At BRB initial the weight was 0.65g After 4 hours the solubility BRB was 8.35%. After 24 hours the solubility of BRB was 68% andinitial the weight was 0.60g After 4 hours the solubility FMB was 7.25%. After 24 hours the solubility of T was 70% the water solubility was plotted against the time. It was shown in fig 5.1.1 and 5.1.2.

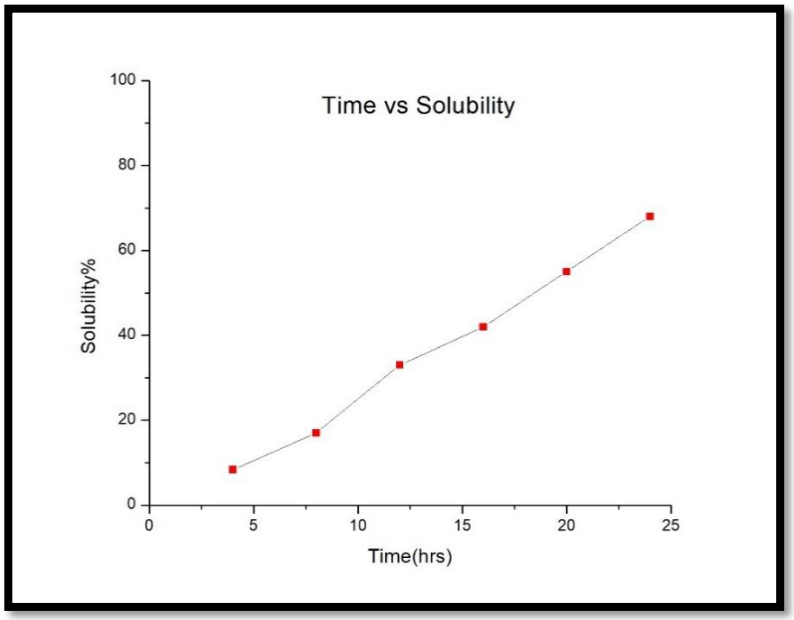

5.1.1 Solubility of BRB in water

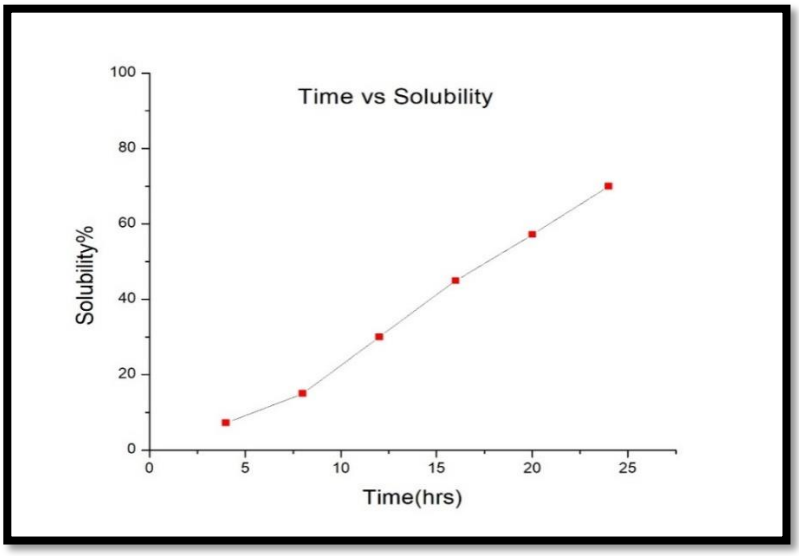

5.1.2. Solubility of FMB in water

From this we concluded that the BRB and FMB have a good solubility in water.

5.2 Solubility in various solvents:

The solubility of BRB and FMB in various solvents like water, Benzene, Toluene, Ethanol and Acetone, HCl were tested after 24 hours.

Table.5.2.1 Solubility % of BRB and FMB in various solvents.

S.NO	Name of the solvents	Solubility%	
		BRB	FMB
1	Water	67.2	64
2	Benzene	35	29
3	HCL	49	44
4	Toluene	26	20
5	Ethanol	1.25	1
6	Acetone	13	10.2

BRB and FMB immersed in various solvents were taken out after 24 hours and weighed. It was compared their initial weights. It was found that BRB has high solubility value of 67.2% in water, very low solubility of 1.25% of ethanol and medium solubility value of 35% in benzene.FMB has high solubility value of 64% in water, very low solubility of 1% in benzene and medium solubility value of 29% in benzene.

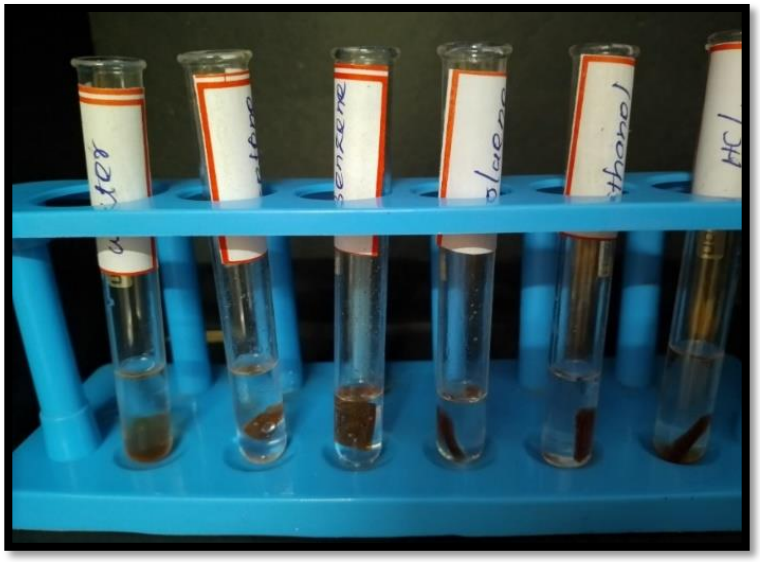

Fig 5.2.3 solubility test in various solvents

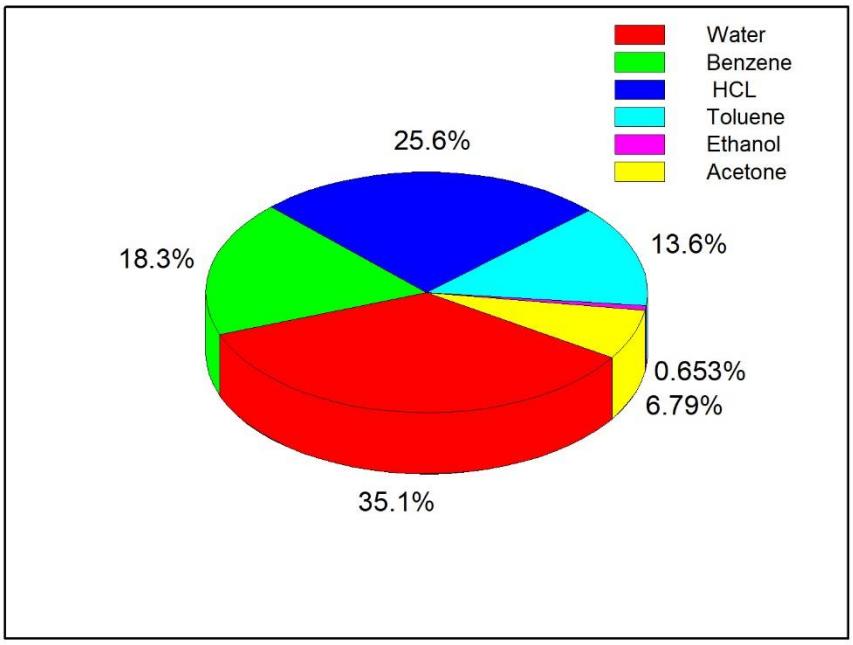

Fig.5.2.4 solubility % of BRB in various solvents

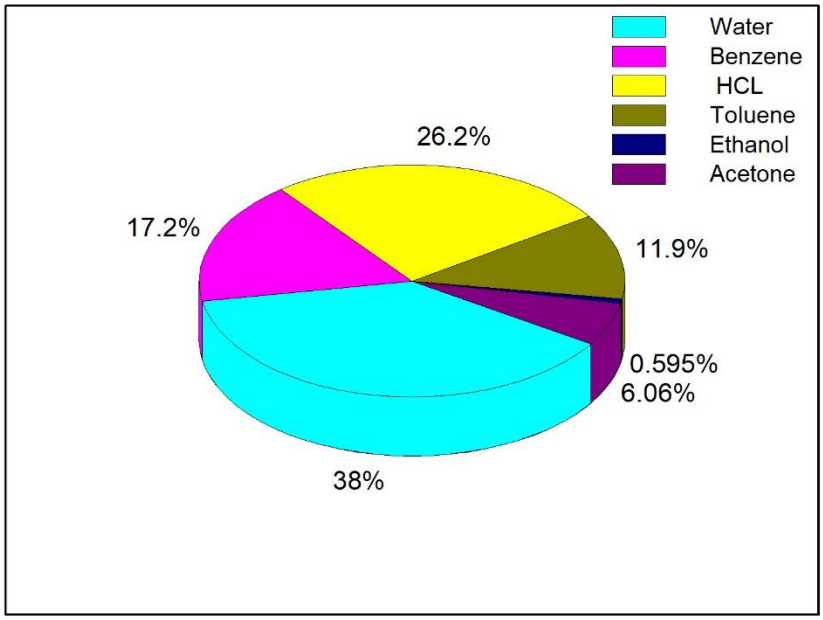

Fig.5.2.5 solubility % of FMB in various solvents

5.3 Swelling Ratio Test

Swelling ratio was calculated for five measurements for BRB and FMB.

S.NO	SWELLING RATIO%	
	Black rice	Foxtail millet
1	93.7	91.4
2	96.2	95.6
3	92.1	96.7
4	97.3	92.9
5	95.5	91.3

Table.5.3 swelling test for BRB and FMB

From the average of the reading the swelling ratio for BRB in 94.96% and FMB in 93.58.

5.4 Elongation test:

The elongation test was conducted for five samples of BRB and FMB .From the average of the measurements, the elongation of BRB and FMB was calculated.

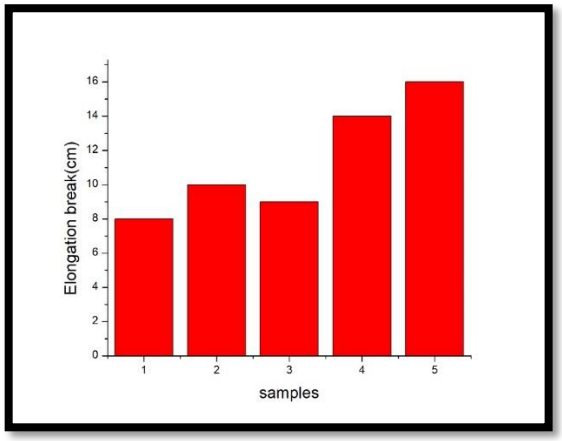

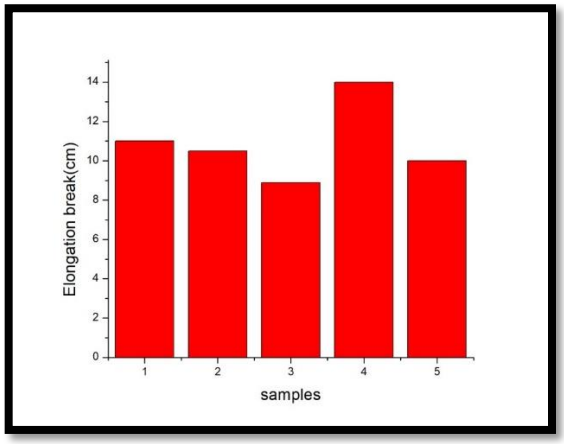

5.4.1 Elongation at break of BRB5.4.2 Elongation at break of FMB

Hence the elongation at break of BRB was found to be 15.6 cm and FMB was found to be 13.8 cm.

5.5 Biodegradability of BRP and FMB in soil

The biodegradability in the soil was determined after 30 days.

Table.5.5 Biodegradability of BRB and FMB in soil

S.NO	Number of days	Biodegradability %	
		BRB	FMB
1	7	24	22.2
2	10	31.7	30.15
3	15	42.8	41.2
4	20	55.5	57.14
5	25	76.19	77.7
6	28	92.06	93
7	30	100	100

This result shows the mass reduction of BRB and FMB in soil. Based on Fig.5.5.1 and 5.5.2 the biodegradability behavior reduced the mass of BRB and FMB.The initial mass was BRB and FMB was 0.63g on day 0 and reduced to 0.03 on day 28 with the optimum rate of weight loss of BRB was 92.06% and FMB was 93%. The BRB and FMB completely decomposed after 30days.

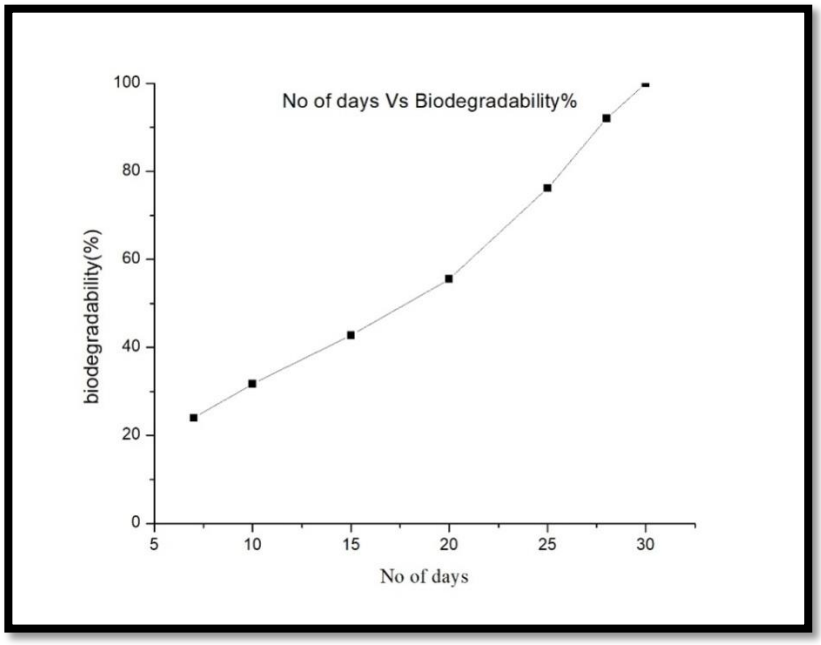

Fig.5.5.1 Biodegradability of BRB in the soil

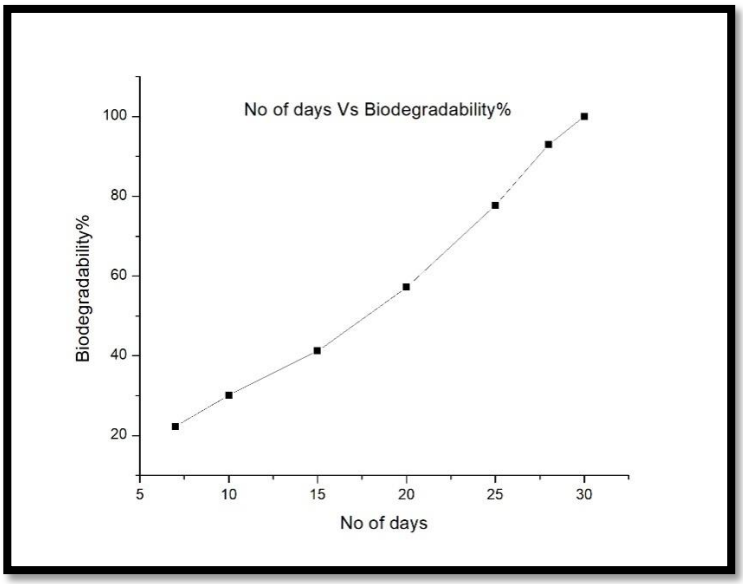

Fig 5.5.2 Biodegradability of FMB in soil

Hence the BMB and FMB have a good stability to decompose under the natural soil. From this we concluded that the BMS and FMB are good biodegradability behavior in the soil.

5.6 Biodegradability in the marine environment

The biodegradability of the BRB and FMB in the marine environment was tested after 12

days.

Table.5.6 Biodegradability in the marine environment

S.NO	Number of days	Degradability%	
		BRB	FMB
1	2	25.39	22.2
2	4	33.3	36.5
3	6	60.3	57.14
4	8	73	74.6
5	10	88.8	90.4
6	12	100	100

The test shows the BRB and FMB mass reduction in the marine environment. The biodegradability behavior the mass of BRB and FMB. The initial mass of BRB and FMB was 0.63g on day 0 and reduced to 0.03g on day with the optimum rate of weight loss of BRB was 88.8% and FMB was 90.4%.The BRB and FMB completely decomposed with after 12 days.

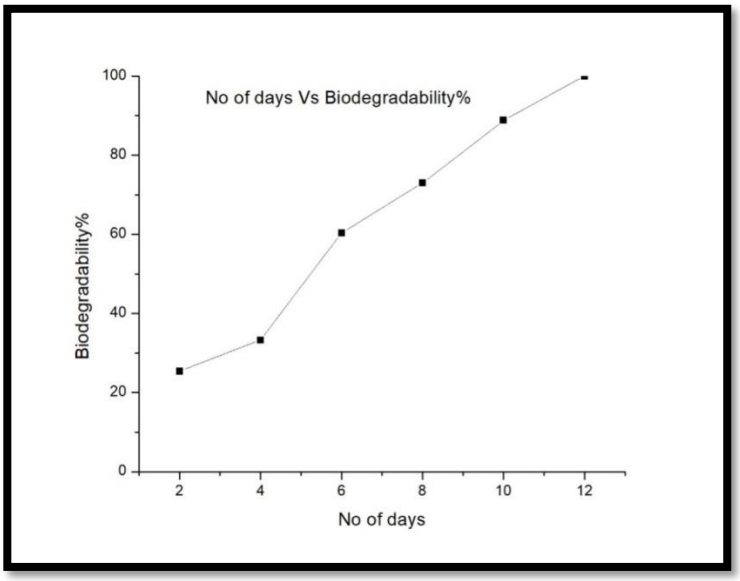

Fig 5.6.1 Biodegradability of BRB in marine soil

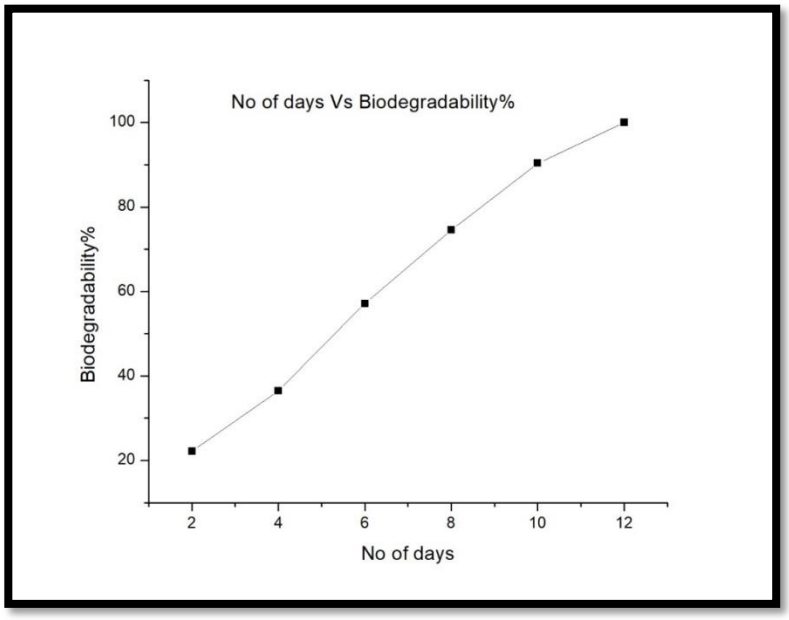

Fig .5.6.2 Biodegradability of FMB in marine soil**.**

The BRB and FMB a good ability to decompose in the marine environment. From this we concluded that the BRB and FMB a very good degradability behavior in the marine environment.

5.7 UV-Visible spectroscopy

The UV Visible spectrum of ORP was shown in fig. The spectrum was recorded in the range 200-900nm. For BR sample the maximum absorbance obtained at 560mm and the T sample the maximum absorbance obtained at 274nm this is similar to the UV absorption of starch based bioplastics. This indicates that the bioplastic absorbed UV light especially in the UV-A region

Table 5.7.1 UV-visible spectroscopy of BRB and FMB

Sample	Absorbance	Wavelength	Energy
FMB	0.410218	218	5.6880
	0.929904	274	4.5255
	0.928621	414	2.9951
	0.742192	234	5.2991

BRB	0.979327	276	4.4927
	1.07762	560	2.2142

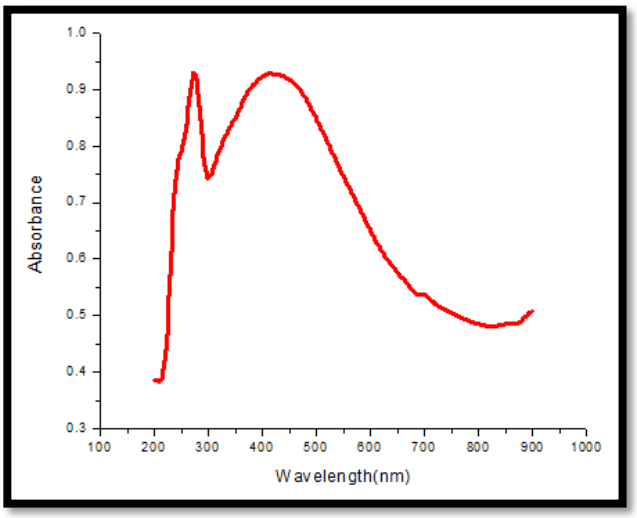

Fig.5.7.1 UV Visible spectrum of FMB (foxtail millet)

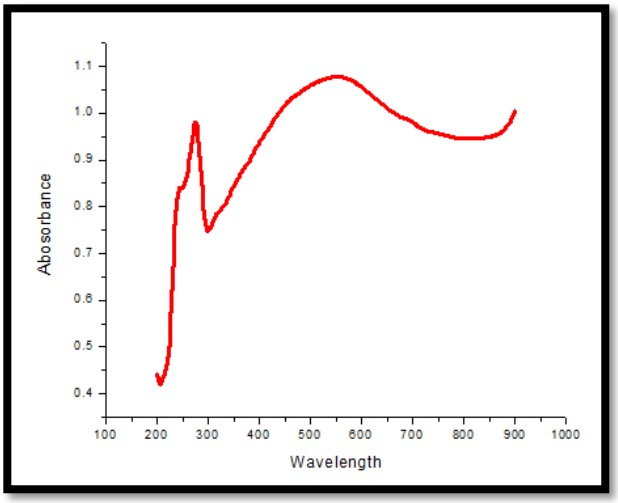

Fig.5.7.2 UV Visible spectrum of BRB (black rice)

5.8 FT-IR absorption spectroscopy

The FT-IR spectrum of BRB and FMB was shown in the fig.5.8.1 and 5.8.2 in the spectrum the sharp band at 1033.85 cm and 1018.41cm¹ corresponding to the stretching vibration C-O bond. The band around 3294.42cm¹ and 3302.13 is O-H stretching vibration for carbohydrate protein and polyphenols. The band around 2939.52 and 2931.80 cm¹ can be referred to the C-H

stretching vibration in presence of alkane.

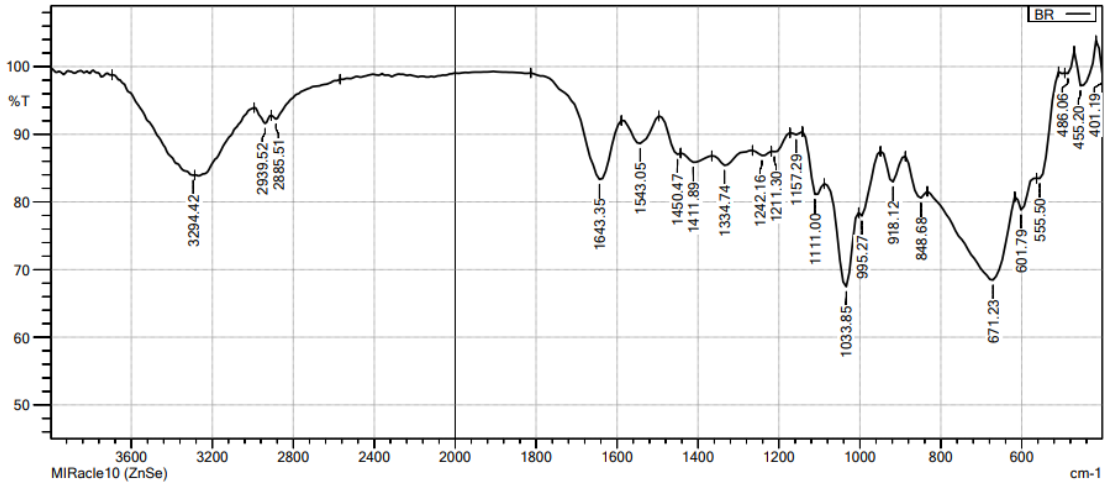

Fig.5.8.1 FT-IR Spectrum of BRB

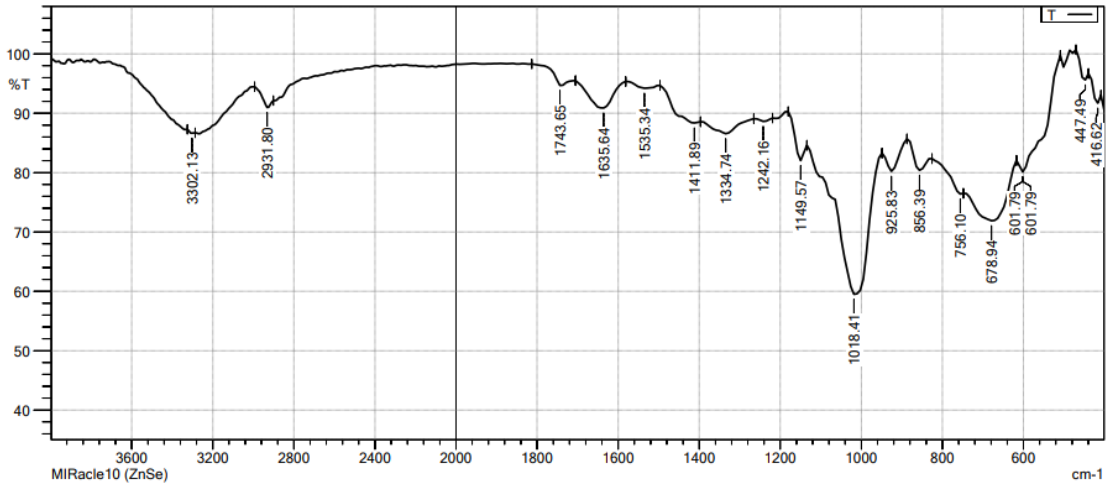

Fig.5.8.2 FT-IR Spectrum of FMB

5.9 Thermogravimetric analysis

TGA is a precise method for examining the decomposition pattern and thermal stability of bioplastic. The TGA and DTG, DTA of BRB and FMB were revealed in Fig Useful data from

TGA results include handling, storage, and shelf life of BRB and FMB at various temperatures. The sample weight loss is displayed as a function of temperature on the TGA curve. From the observation, the weight loss was generally associated with two stages. In BRB (Fig .a) the first stage of weight loss 35.1% at 30–300 °C and the second stage of weight loss 43.9% at 300°C and 650 °C.For the initial phase of FMB (Fig 5.3.b) weight loss with a significantly average rate of weight loss and a total weight reduction of about 36.5%, the second stage of weight loss occurs between 10 to 270°C. Occurs, with a higher loss of 46.8%.The main cause of first-stage weight loss is the evaporation of some of the free water included in sample BRB and FMB. Thus the BRB and FMB possess good thermal stability.

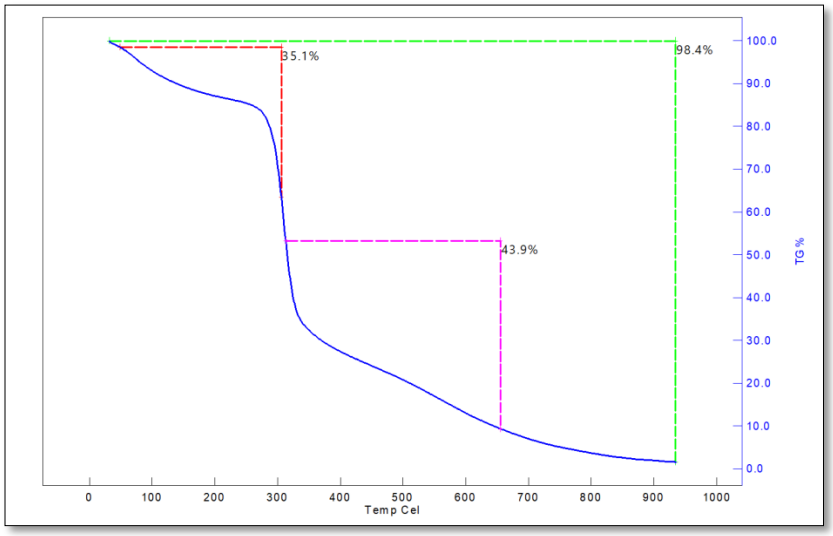

Fig.5.9.1 TGA of BRB curve

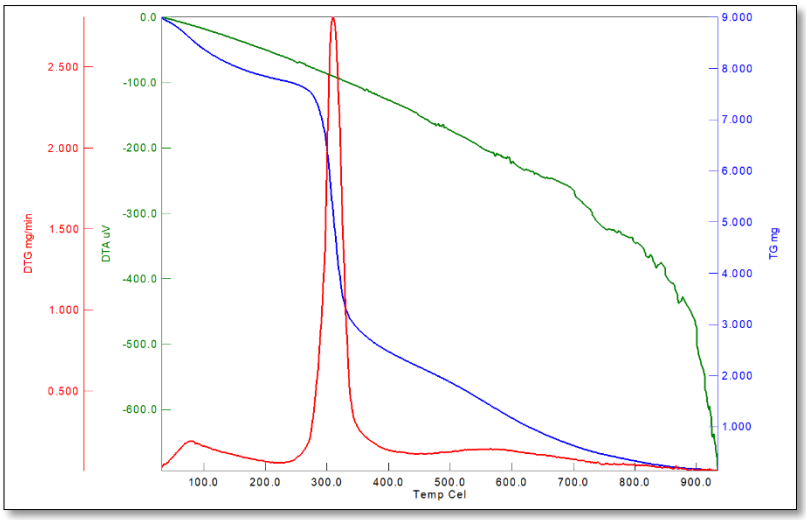

Fig.5.9.2 Comparison of TGA, DTA and DTG in BRB

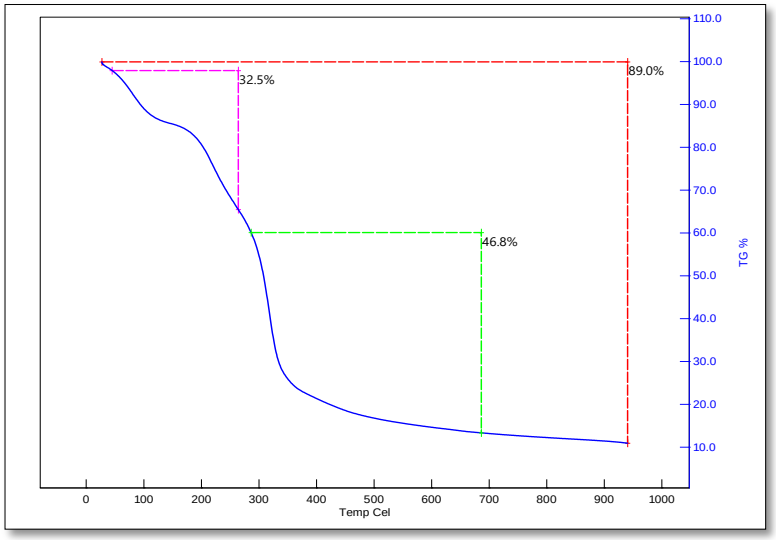

Fig.5.9.3 TGA of FMB curve

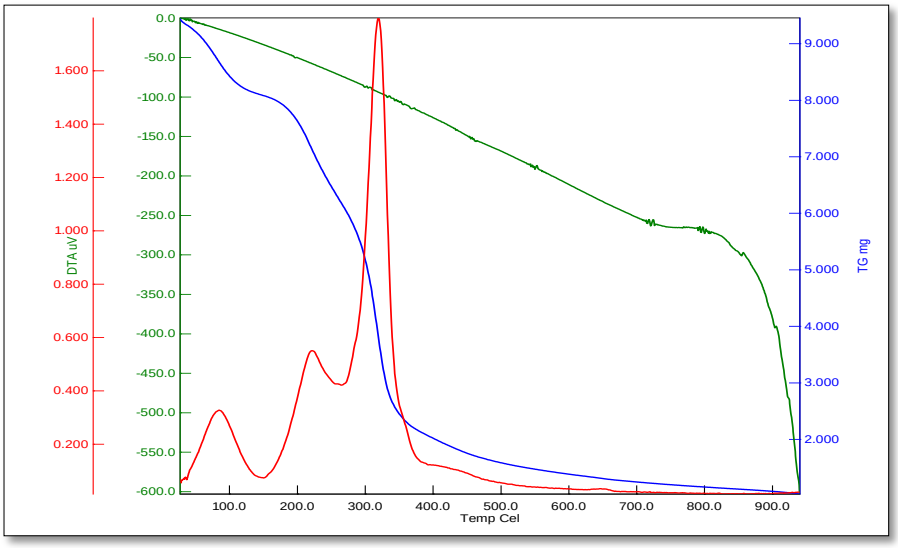

Fig5.9.4 Comparison of TGA, DTA and DTG.

5.10 X-Ray diffraction

X-ray diffraction (XRD). This test was performed to information about the crystallinity by using Shimadzu 7000 X-ray diffractometer with CuKα radiation (λ = 1.5405 Å) was recorded between 15° ≤ 2θ ≤ 60°, operates at 30 kV and 10 mA.There are two components in sago starch namely amylose which has a linear chain structure and amylopectin which has a branch chain structure [16]. Branch structures make a major contribution in the formation of amorphous structures. Chitosan has a linear polymer chain structure that contributes to the formation of crystalline phases by

connecting with each other to form polymer chains regularly. Starch is a semi-crystalline which consisting of crystal unit and amorphous units Starch granules can take amorphous and amylopectin .they are destroyed by heat and shear forces from the mixing during the manufacturing process of the bio composite resulting in a linear amylose polymer. Thermoplastic starch is characterized by strong peaks. The X-ray diffraction pattern of BRB and FMB was shown Fig.5.10.1 & 2 the BRB and FMB is low peak intensity. The diffraction peaks are narrower indicating lower crystallinity .The strongest peak of BRB was 20.5750, 16.2000, and 44.1000 are evident and FMB was 20.9363,9.3250,38.2800 are evident. The diffraction pattern is probably due to strong interaction between the hydroxyl group of the starch molecules are replaced by hydrogen bonds formed between plasticizer and starch during processing .Hence the BRB and FMB possess amorphous form.

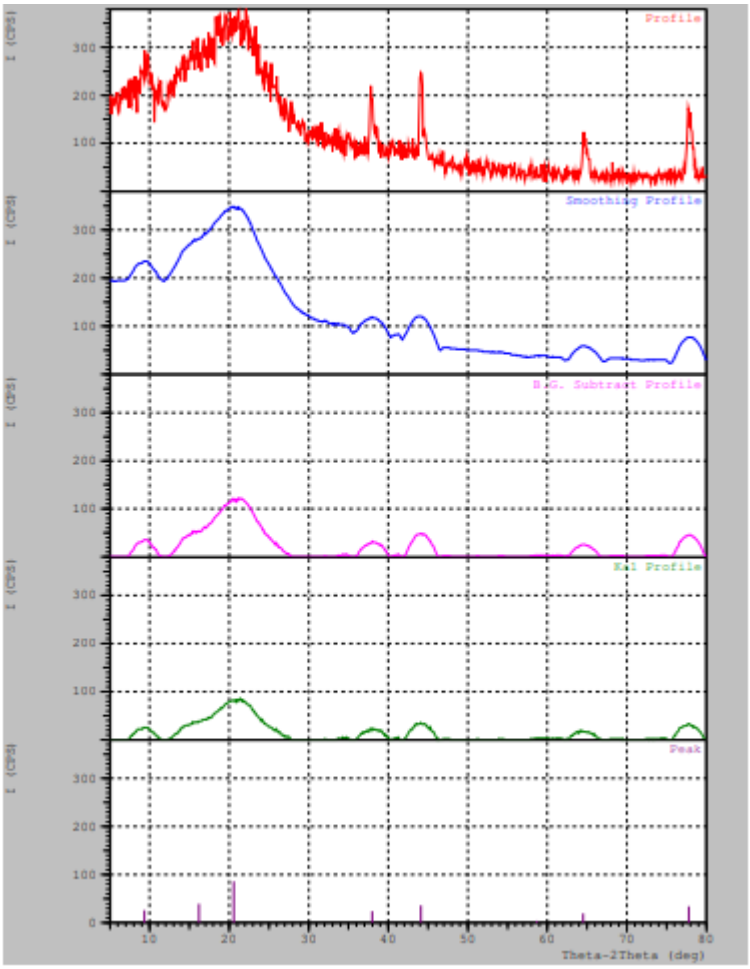

Fig 5.10.1 XRD for BRB

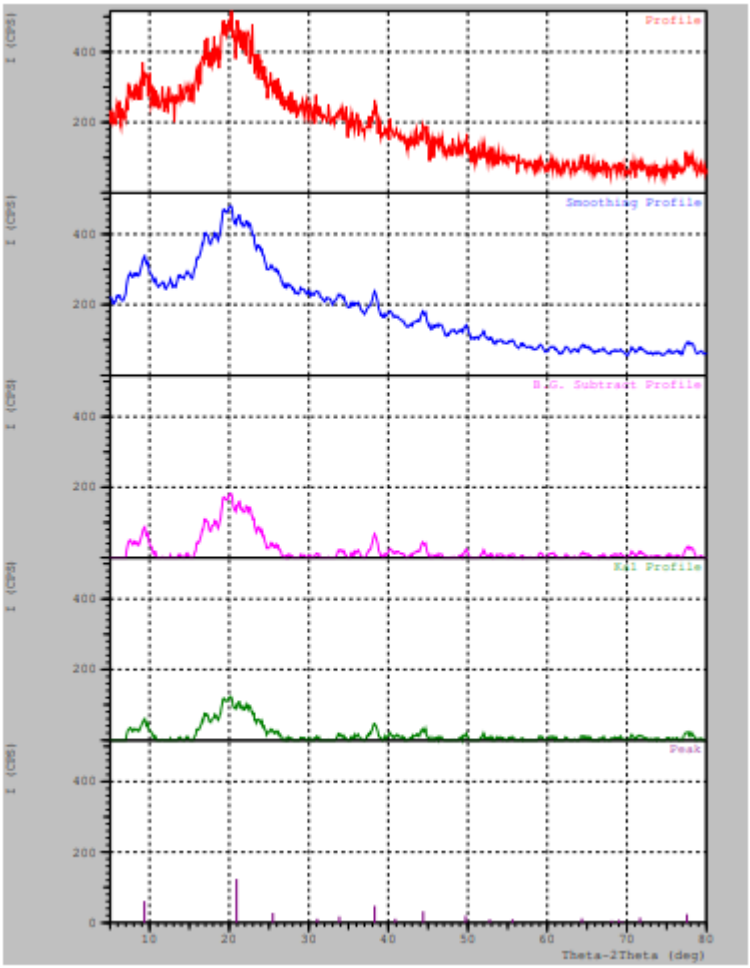

Fig 5.10.2 XRD for FMB

CHAPTER 6

CONCLUSION

BRB and FMB were successfully synthesized from Black rice and foxtail millet by using vinegar and glycerol. The **BRB** and **FMB** were characterized using various methods like, water solubility test, solubility test in various solvents, swelling ratio test, degradation in soil degradation in marine soil and several techniques such as **UV-VIS, FT-IR, ,TGA**.

- The solubility test in water shows that the solubility of BRB increases **8.35%** and FMB increases **7.25%** every 4 hours.
- The solubility test in various solvents shows that BRB has high solubility value of 67.2% in water, very low solubility of 1.25% of ethanol and medium solubility value of 35% in benzene.FMB has high solubility value of 64% in water, very low solubility of 1% in benzene and medium solubility value of 29% in benzene. This shows that the BRB and FMB has very good stability in water
- The swelling ratio test shows that the BRB and FMB has a swelling ratio of 104.84% and for BRB in 94.96% and FMB in 93.58%.
- The elongation at break of BRB was found to be 15.6 cm and FMB was found to be 13.8cm.
- The biodegradability test in the soil shows that the BRB and FMB completely decomposed after 30days.
- The biodegradability test in the marine soil shows that the BRB and FMB takes 12 days completely decomposed.
- The spectrum was recorded in the range 200-900nm. For BRB sample the maximum absorbance obtained at 560mm and the FMB sample the maximum absorbance obtained at 274nm this is similar to the UV absorption of starch based bioplastics. This indicates that the bioplastic absorbed UV light especially in the UV-A region.
- The FT-IR spectrum of BRB and FMB was shown in the fig. In the spectrum the sharp band at 1033.85 cm and 1018.41cm corresponding to the stretching vibration C-O bond. The band around 3294.42cmand 3302.13 is O-H stretching vibration for carbohydrate protein and polyphenols. The band around 2939.52 and 2931.80 cm^{1} can be referred to the C-H stretching vibration in presence of alkane.
- In BRB the first stage of weight loss 35.1% at 30–300 °C and the second stage of weight loss 43.9% at 300°C and 650 °C.For the initial phase of FMB weight loss with a

significantly average rate of weight loss and a total weight reduction of about 36.5%, the second stage of weight loss occurs between 10 to 270°C. Occurs, with a higher loss of 46.8%.The main cause of first-stage weight loss is the evaporation of some of the free water included in sample BRB and FMB. Thus the BRB and FMB possess good thermal stability.

CHAPTER7
REFERENCE

[1]. A.B.D. Nandiyanto et.al, Mechanical and biodegradation properties of cornstarch-Based bioplastic material**, 2020**

2. Ankita Shrestha and Bishnu Acharya, Biodegradation of Bioplastic using anaerobic digestion at retention time as per Industrial Biogas Plant and International Norms, **2020**

3. Esen Gökçe Özdamara and Murat Ateş Rethinking sustainability: A research on starch based bioplastic, Journal of Sustainable Construction Materials and Technologies, **2018**

4. Norhafezah Kasmuri, Muhammad Safwan and Abu Zait, Enhancement of Bio-plastic using Eggshells and Chitosan on Potato Starch Based, International Journal of Engineering & Technology**, 2018**

5. Edi Syafri et.al, Effect of Precipitated Calcium Carbonate on Physical, Mechanical and Thermal Properties of Cassava Starch Bioplastic Composites, International Journal on Advanced Science Engineering Information Technology, **2017**

6. Martin A. Hubbe et.al, Formulating Bioplastic Composites for Biodegradability, Recycling, and Performance. A Review, **2021**

7. Bayer et.al, direct transformation of edible vegetable waste into bioplastics Macromolecules**, 2014**

8. F.G. Nugroho, N. M. Nizardo and E. Saepudma, Synthesis of Citric Acid Crosslinked PVA/Tapioca Starch Bioplastic Reinforced with Grafted Cellulose, **2020**

9. Albuquerque PBS and Malafaia CB. Perspectives on the production, structural characteristics and potential applications of bioplastics derived from polyhydroxyalkanoates, International Journal of Biological Macromolecules. **2018**

10. Karthigeyan Chidambarampadmavathya, Obulisamy Parthiba Karthikeyana and Kirsten Heimanna Sustainable bio-plastic production through landfill methane recycling, 2016 11. Gerardo Coppola et al., Bioplastic from Renewable Biomass: A Facile Solution for a Greener Environment**, 2021**

12. Jürgen Liircks, Properties and applications of compostable starch-based plastic material, **1997**

13. Florian Felix Klein, Agnes Emberger-Klem and Klaus Menrad, Indicators of Consumers Preferences for Bio-Based Apparel: A German Case Study with a Functional Rain Jacket Made of Bioplastic, **2020**

14. Darshan Marjadi and Nishith Dharaiya, Bioplastic, A better alternative for sustainable Future, Everyman's science journal, **2010**

15. Ezgi Bezirhan Arıkan and H. Duygu Bilgen, Production of bioplastic from potato peel waste and investigation of its biodegradability, International Advanced Researches and Engineering Journal, **2019**

16. Francesco Razza and Francesco Degli Innocenti, Bioplastics from renewable resources: The benefits of biodegradability, Asia-Pacific Journal of Chemical Engineering, **2012**

17. Loh Guan Hong. Nor Yuliana Yuhana and Engku Zawawi, Review of Bioplastics as food packaging materials**, 2021**

18. S. Suleiman, A. Manut, and A. R. Nur Firdaus, "Starch Plastic Packaging and Agriculture

Applications," in ICIMT '09 International Conference, IEEE, pp. 513-516**, 2019**

19. R. Thiruchelvi, Aryaman Das Eesani sikdar, Bioplastics as better alternative to petro Plastic, Journal Material Today Proceedings, **2020**

20. Gaurav Kale et.al, Compostability of Bioplastic Packaging Materials: An Overview, 2007 21. Castillo Luciana A. et al., Food Packaging and Shelf Life, 14 Part B. 128-136, **2017**

22. Hasan Saygin and Asli Baysal, Degradation of subu-sized bioplastics by clinically important bacteria under sediment and seawater conditions: Impact on the bacteria responses, **2020**

23. Putri Rahma Wati, Effect of temperature and time for bioplastic from tapioca starch, **2019**

24. Maurizio Tosin et al., Laboratory test methods to determine the degradation of plastics in Marine environmental conditions, **2012**

25. M. Selvakumar and P.Sivakumar, Bioplastics -An Eco-Friendly Alternative to Petrochemical Plastics, Journal current world environment, **2019**

26. MehranGhasemloua et al Biodegradation of novel bioplastics made of starch. Polyhydroxyurethanes and cellulose Nano crystals in soil environment, **2018**

27. Jan-Georg Rosenboom. Robert Langer and Giovanni Traverso, Bioplastics for a circular economy**, 2022.**

28. Allan Calmont de Andrade Almeida et al. The sustainable cycle of a new cacao-based bioplastic from manufacturing to exploitable biodegradation products, RSC advances Journal**, 2021**.

29. Liqaa Hamid et.al. Fabricating Starch-Based Bioplastic Reinforced with Bagasse for Food Packaging, Circular Economy and Sustainability, **2021**

30. Genovesia et al, Comparative life cycle analysis of disposable and reusable tableware: The role of bioplastics, Cleaner Engineering and Technology**, 2022.**

31. I Risnasari, A Nuryawan, Delvian and Y S K Sekali, Use of bio polybag from tapioca starch and sawdust waste. IOP Conference Series: Earth and Environmental Science**, 2021.**

32. Jianlei Yang, Synthesis and characterization of starch/fiber-based bioplastic composites modified by citric acid-epoxidized palm oil oligomer with reactive blending**, 2021**

33. Mirko Cucina et.al, Degradation of bioplastics in organic waste by mesophilic anaerobic digestion, composting and soil incubation, **2021**

34. C. Lim et.al, Bioplastic made from seaweed polysaccharides with green production methods**, 2021**

35. Emma M.N. Polman et.al, Comparison of the aerobic biodegradation of biopolymers and the corresponding bioplastics: A review, **2021.**

36. Noorul Hidayah Yusoffa et.al, recent trends on bioplastics synthesis and characterizations: Polylactic acid (PLA) incorporated with tapioca starch for packaging applications, **2021**

37. Yacouba Zoungranan et.al, Influence of natural factors on the biodegradation of simple and composite bioplastics based on cassava starch and corn starch, Journal of Environmental Chemical Engineering, **2020.**

38.Katrin Jogi, Rajeev Bhat, Valorization of food processing wastes and by-products for bioplastic production, Sustainable Chemistry and Pharmacy, **2020**

39. Wen Yi Chia et.al, Algae for plasticbiodegradation and bioplastics production, Environmental Science and Eco technology, A Review **2020.**

40. Farinaz Ebrahimian et.al, Sustainable biofuels and bioplastic production from the organic fraction of municipal solid waste, **2020.**

41. Francesco Distant et.al, Current trends in the production of biodegradable bioplastics: The case of polyhydroxyalkanoates**, 2020**.

42. Vimudha Muralidharan et.al, Tannery trimming waste based biodegradable bioplastic: Facile synthesis and characterization of properties, **2020.**

43. Caesar Javier Lopez Rocha et.al, Development of bioplastics from a microalgae consortium from wastewater**, 2020.**

44. Masanori Yamada et.al, Preparation of bioplastic using soy protein, International Journal of Biological Macromolecules, **2019**

45. Olugbenga O. Oluwasina et.al, Influence of oxidized starch on physicomechanical, thermal properties, and atomic force micrographs of cassava starch bioplastic film, International Journal of Biological Macromolecules, **2019.**

46**.** M. Jim_enez-Rosado et.al, Bioplastics based on wheat gluten processed by extraction, **2019.**

47. Martina Nevoralov et.al, Controlled biodegradability of functionalized thermoplastic starch, based materials **2019.**

48. Shazia Tabasum et.al, a review on blending of corn starch with natural and synthetic polymers,

and inorganic nanoparticles with mathematical modeling **2019**.

An Inhibition Study of Hypertension α Blockers using Molecular Docking

A project submitted to

St. Mary's College (Autonomous), Thoothukudi

Affiliated to

MANONMANIUM SUNDARNAR UNIVERSITY

TIRUNELVELI

In partial fulfilment of the award of the degree of

MASTER OF SCIENCE IN CHEMISTRY

Submitted by

MUNIESHWARI. T

Reg. No: 21SPCH04

Under the Supervision and Guidance of

Dr. Mrs. C. ZOZIMUS DIVYA LOBO M.Sc., M.Phil, Ph.D.,

PG DEPARTMENT OF CHEMISTRY (SSC)

St. Mary's College (Autonomous), Thoothukudi

APRIL 2023

CERTIFICATE

This is to certify that this project work entitled **"An inhibition study of Hypertension α Blockers using Molecular Docking** " is submitted to St. Mary's College (Autonomous), Thoothukudi affiliated to **Manonmaniam Sundaranar University, Tirunelveli** in partial fulfilment for the award of the **Degree of Master of Science in Chemistry** and this work done during the year 2022 - 2023 by MUNIESHWRI. T (Reg. No: 21SPCH04)

Signature of the Guide

Dr. C. ZOZIMUS DIVYA LOBO
M.Sc., M.Phil, Ph.D.,
ASSISTANT PROFESSOR
DEPARTMENT OF CHEMISTRY
ST. MARY'S COLLEGE (AUTONOMOUS)
THOOTHUKUDI-628001. TAMILNADU

Signature of the Coordinator

5/4/23

Dr. J. ANTONY RAJAM, M.Sc., M.Phil., Ph.D., SET,
SSC Co-ordinator & Asst. Professor
PG Department of Chemistry
St. Mary's College (Autonomous)
Thoothukudi - 628 001.

Signature of the Director

Director
Self Supporting Courses
St. Mary's College (Autonomous)
Thoothukudi - 628 001.

Signature of Principal

Principal
St. Mary's College (Autonomous)
Thoothukudi - 628 001.

13/4/23

Signature of the Examiner

DECLARATION

I do hereby declare that the project entitled **"An inhibition study of Hypertension α Blockers using Molecular Docking** " submitted for the degree of Master of Science in Chemistry is my original work carried out under the guidance of **Dr. Mrs. C. ZOZIMUS DIVYA LOBO M.Sc., M.Phil., Ph.D. Assistant Professor, PG Department of Chemistry (SSC), St. Mary's College (Autonomous), Thoothukudi** and that it has not previously formed the basis for award of any Degree.

Station: Thoothukudi

Date: 05.04.23

T. Munieshwari

T. MUNIESHWARI

ACKNOWLEDGEMENT

I express my first and humble thanks to **GOD ALMIGHTY** for giving an opportunity to devote this work

I would like to express my sincere thanks to our Principal Dr. Sr. A.S.J. Lucia Rose, Secretary Dr .Sr. C. Shibana, Deputy principal Dr. Sr. S.Kulandi Therese, Director of SSC Rev. Sr. Josephine Jeyarani and Dr. J. Antony Rajam (SSC Coordinator), St Mary's College (Autonomous), Thoothukudi for providing the permission to complete the project work

I find it difficult for me to write something in short to acknowledge my guide **Dr. C. ZOZIMUS DIVYA LOBO** she taught me to think and solve the unconventional problems in a conventional way. Her constant inspiration, evaluable guidance tremendous patience and constructive criticism helped a lot to focus my views in the proper perspective I take this opportunity to express my deepest sense of gratitude and reference towards her for guiding me in the right direction throughout the course of this work.

I heartily express my sincere thanks to my parents and friends.

ABSTRACT

Molecular Docking Approach to Assess the Pharmacological Properties of Potential Natural Hypertension Treatments. Alpha-blockers used to treat hypertension are now the world's most common cause of disability and death, especially in low- and middle-income nations. Alpha blockers' advancement is mostly attributed to the risk factors associated with hypertension, which include genetic, behavioural, and environmental aspects. Blood pressure is one of the hereditary causes because it describes the pressure that blood applies to the artery walls as it travels through them. The ideal blood pressure range for a person is said to be a systolic blood pressure below 80 and a diastolic blood pressure under 120. In the current investigation, the ability of separated phytochemicals to bind to the intended protein was tested. In order to achieve this, the 3D structure of the current investigation, the ability of separated phytochemicals to bind to the intended protein was evaluated. For this, PyRx was used to replicate the target protein's (3-dimensional) structure (α -Blockers). The Ramachandra plot was then used to evaluate and confirm the 3D model. To predict the binding mechanisms of these drug-like compounds, the molecular docking of 32 phytochemicals described as α -blockers inhibitors was carried out using the PyRx software together with reference compounds. The findings showed that they were similar to reference ligands and had remarkable interactions with the target protein's active site residues. In summary, the current work gave the tested -blocker inhibitors a computational foundation. The discovery of innovative medicinal compounds for the treatment of should be aided by this information.

Keywords: Molecular docking, Protein, Ligand, Ramachandra plot, PyRx.

Content

CHAPTER 1

INTRODUCTION

HYPERTENSION

Blood pressure is one of the hereditary causes because it describes the pressure that blood applies to the artery walls as it travels through them [1]. The ideal blood pressure range for a person is said to be a systolic blood pressure below 80 and a diastolic blood pressure under 120 Alpha receptors, which are present in arteries and smooth muscle, are the targets that alpha blockers obstruct [2]. They prevent the hormone adrenaline from tightening the muscles and the smaller artery and venous walls by acting as they do. By stopping that effect, the blood arteries relax, resulting in an increase in blood flow. Alpha blockers, commonly known as alpha-adrenergic blocking drugs, function by preventing messages from travelling to particular areas of the body. Alpha blockers, like other "blocker" drugs, bind to molecules in the body that act decrease in blood pressure [3].

One of the most dangerous diseases to people's health is hypertension, which has a high incidence over the globe. The number of hypertension sufferers is rising every year, and by 2025, it is predicted that there will be 1.56 billion individuals worldwide. Only a small percentage of persons with hypertension who have the condition may successfully manage it. Heart disease, stroke, chronic renal disease, organ injury and a number of other secondary disorders that gravely endanger patients' lives are also caused by hypertension and have a negative impact on their quality of life. Therefore, it is crucial to create medications to manage hypertension [4].

Heart failure, ischemic heart disease, and left ventricular hypertrophy are among a group of illnesses collectively referred to as hypertension, which is increasingly recognised as a leading cause of high blood pressure-related death globally. It has been revealed that a number of genes, including WNK1, WNK4, Bp1, Bp2, AGT, and ACE, are implicated in the amount of hypertension. AGT gene mutations on chromosome 1 cause an imbalance in the generation of angiotensinogen, which ultimately results in hypertension. It was discovered that ACE (Angiotensin Converting Enzymes) plays a significant role in hypertension; its dysfunction is the condition's most frequent cause. The creation of the angiotensin II enzyme, which is created

from the conversion of angiotensin I by the action of is the most prevale biological cause of hypertension [5].

Types of Alpha Block

Certain alpha-blockers target only specific alpha-receptors. This is known as "selectivity," and it plays a role in the decision-making process when selecting an alpha-blocker to treat a condition. Alpha-blockers can be non-selective for A1 receptors or selective for them. There are no approved selective alpha-2 blockers as of yet [6].

Adverse effect

Nonselective alpha-blockers can cause hypotension, weakness, tachycardia and tremulousness. The inhibition of alpha-1 receptors causes vascular smooth muscle relaxation and vasodilation resulting in hypotension. The remaining negative effects result from increased norepinephrine release when alpha-2 receptors are simultaneously antagonised. This release causes beta receptor stimulation due to norepinephrine spill over, resulting in tremulousness and tachycardia [7].

Tachycardia and tremulousness are less common side effects of selective alpha-1 blockers. Although vasodilation and vascular smooth muscle relaxation can cause first-dose hypotension, syncope, dizziness, and headache. A sudden drop in blood pressure can cause reflex tachycardia [8].

Mechanism action

Alpha-blockers produce their pharmacological effects through alteration of the sympathetic nervous system. There are two types of alpha-adrenergic receptors: alpha-1 and alpha-2. Most of the alpha-1 adrenergic receptors are located on the vascular smooth muscle (in the skin, sphincters of the gastrointestinal system, kidney, and brain) and cause vasoconstriction when activated by catecholamine such as epinephrine and norepinephrine (NE) [9]. The vasoconstriction causes an increase in both systemic arterial blood pressure and peripheral resistance. Norepinephrine has a higher affinity for this receptor than epinephrine. Alpha-2 adrenergic receptors are located on peripheral nerve endings and inhibit the release of NE when activated; this provides a feedback mechanism for NE to inhibit its release [10].

Nonselective alpha-adrenergic antagonists cause vasodilation by blocking both alpha-1 and alpha-2 receptors. The blockage of alpha-2 receptors will increase the NE release, which

will reduce the force of the vasodilation induced by the blockade of the alpha-1 receptors. These medications work best when there is increased sympathetic activity such as during stress or when there is an increase in circulating catecholamine's, making these medications useful for patients with pheochromocytoma [11].

Selective alpha-1 adrenergic antagonists cause vasodilation by preventing NE from activating the alpha-1 receptor, resulting in a lowering of the blood pressure, allowing alpha-1 blockers to be used for hypertension. Alpha-1 blockers also cause relaxation of smooth muscle in the prostate, which can enable the urine to flow more freely thru the urethra, making the medications useful for the management of Benign Prostatic hyperplasia (BPH) [12]. Selective alpha-2 adrenergic antagonists inhibit negative feedback of NE, stimulating the sympathetic nervous system. However, there are limited findings on the significance of this mechanism of action in human medicine [13].

Contraindications

Alpha-blockers are contraindicated in individuals with hypersensitivity to alpha-blockers or any other component of the drug formulation. Caution is necessary when administering alpha-blockers in elderly patients or if previous cataract surgery [14]. These medications can complicate cataract surgery by inducing sudden iris prolapse and pupil constriction during the surgery - also known as "intraoperative floppy iris syndrome." [15].

Nonselective alpha antagonists have additional contraindications. Phenoxybenzamine and phentolamine are contraindicated in a breastfeeding mother. Clinicians should exercise caution if the patient has marked renal impairment, cerebrovascular disease, coronary artery disease, or current respiratory infection. These medications are not suitable for long-term use [16].

Toxity

Alpha-blockers are frequently prescribed in the elderly male population and toxicity is common in these individuals. The most common adverse effect is hypotension [17]. Extremely low blood pressure can cause ischemic insult to major organs and increase the fall risk. If toxicity suspected, general measures are necessary to optimize the blood pressure [18]. If a patient is hypotensive, he should be moved to a supine position until blood pressure and heart rate are acceptable. If the patient remains hypotensive, then the patient can be managed with

fluid resuscitation. If necessary, vasopressors could be administered as a last resort. There is no specific antidote availabl [19].

Common Alpha Blocker Names

- Alpha blockers come in a wide variety. Alpha-blockers that are frequently administered include:
- Cardura (doxazosin)
- Regitine (phentolamine)
- Tamsulosin, Flomax, and Hytrin (terazosin) [20].

Symptoms

Generally speaking, medications or other unexpected changes in your symptoms, particularly when side effects or symptoms interfere with your routine activities.

Hypertension can cause the following symptoms: fainting or passing out.

• Difficulty; Chest discomfort (angina).

• Breathing problems [21].

• Heart palpitations, or the uncomfortable sensation of having a fast or irregular heartbeat

• Privilege (an erection that lasts for at least four hours and is often painful [22].

DRUGS

Trials that have been conducted on different medication types in combination to treat hypertension have benefited from their complementary effects. The most widely used classes of antihypertensive drugs include angiotensin receptor blockers (ARBs), thiazide diuretics, alpha- and beta-blockers, calcium antagonists (CCBs), and angiotensin-converting enzyme inhibitors (ACEIs). Thiazide diuretics, CCBs, and combinations with rennin-angiotensin-aldosterone system (RAAS) blockers are all useful at lowering blood pressure [23]. There are several options for pairing an ACEI, ARB, and a diuretic or an ACEI with a CCB. The bulk of FDCs on the market right now are based on diuretics. Despite the unmatched safety and effectiveness of diuretics, current findings showing low-grade carcinogenicity has to be further examined [24].

A common treatment for renal and ureteral stones is shock wave lithotripsy (SWL). Stones are broken up into tiny bits, which can then naturally move down the ureter and into the bladder. Alpha-blockers might help to facilitate the passage of stone pieces, but it is still unclear how efficient they are [25]. To compare the effectiveness of alpha-blockers, a placebo, and standard care to standard care alone or standard care in adults receiving shock wave lithotripsy for renal or ureteral stones [26]. A common treatment for renal and ureteral stones is shock wave lithotripsy (SWL). Stones are broken up into tiny bits, which can then naturally move down the ureter and into the bladder. Alpha-blockers could help with promotion [27].

SIDE EFFECTS

The following side effects of selective alpha-blocking drugs are frequent, especially in people over 65 age. Reduced blood pressure (hypotension). Blood pressure can be effectively reduced by alpha-blockers. They do, however, sometimes function too effectively, leading to orthostatic hypotension, a dip in blood pressure that occurs when you stand up. This could make you feel lightheaded or woozy. If an A1-blocker is recommended, it's likely that your doctor will advise you to take it shortly before bed [28].

Initial -dose impact. The first dose of A1-blockers has a far greater impact on blood pressure than following doses, which is a very common side effect. Especially common symptoms of orthostatic hypertension include light-headedness, dizziness and fainting. Falling becomes more likely as a result, which can be quite dangerous for those who are older, have weaker bones, or are using blood thinners (because fall injuries can cause dangerous internal bleeding). The initial dose of an alpha-1 blocker is typically lower to reduce this impact [29].

The following are some common side effects associated with popular alpha blockers:

Orthostatic hypotension, also known as orthostatic, is a sudden drop in blood pressure that occurs shortly after standing or sitting up. This is more likely to happen with the first dose of this medication, any recent dose increase, or when combined with other antihypertensive agents or PDE-5 inhibitors [30].

Drowsiness or dizziness

- Fatigue
- Headache
- Retention of fluid
- Ejaculation that is abnormal

- ❖ Priapism is defined as a prolonged and painful erection lasting four hours or more.
- ❖ Angina (chest pain) [31].

Intra-operative floppy iris syndrome (IFIS), or poor pupil dilation during cataract surgery in alpha blocker patients. If IFIS occurs unexpectedly, it has the potential to derail cataract surgery [32].

MOLECULAR DOCKING

The completion of the human genome project has expanded the range of therapeutic targets in drug development. In parallel, structural data on protein-ligand and protein complexes has been provided by cutting-edge techniques such high-throughput crystallography, protein purification, and Nuclear Magnetic Resonance (NMR) spectroscopy. These developments led to the creation of molecular docking, commonly known as computer-aided drug design. Both ligand-based and structure-based techniques are used in molecular docking [33] When there is a lot of information about a ligand, ligand-based approaches like QSAR (quantitative structure-activity relationship) are recommended; otherwise, structure-based docking methods are utilised. Using a variety of computational techniques, molecular docking of known synthetic and natural ACE inhibitors was carried out in this study with the goal of finding the best inhibitor, which would ultimately serve as the basis for developing medications against hypertension by blocking ACE [34]. The structure-based docking method was chosen because ligand-based CADD makes use of the knowledge of known active and inactive molecules through chemically similar searches or the construction of predictive QSAR models, whereas structure-based CADD depends on the target protein structure knowledge to calculate interaction energies for all compounds tested. When there are high resolution structural data for the target protein, such as for soluble proteins that are easily crystallised, structure-based CADD is typically used [35]. Computational techniques have been developed in research to assess every factor involved in drug discovery and design [36].

Remedies for alpha blockers

Saw palmetto (Saw Palmetto) (Serena repens)

The palm saw palmetto is native to the southeaster United States. This plant's extract is a popular herbal supplement for the treatment of BPH. Saw palmetto is a 5-alpha-reductase inhibitor. It is also anti-inflammatory and has the ability to reduce the number of oestrogen and androgen (DHT) receptors [37].

Rye grass pollen (Secale cereal)

Some people use herbal supplements made from rye grass pollen to treat BPH symptoms and reduce prostate inflammation.

Cernilton is a well-known brand of rye grass pollen pharmaceutical. This medication may be effective in slowing or stopping prostate growth.

According to previous research, rye grass extract contains compounds that can inhibit prostatic cell growth and reduce inflammation. Reliable Source As a result, BPH symptoms such as frequent urination and nocturnal may be alleviated [38].

Stinging nettle

Stinging nettle contains antioxidant and anti-inflammatory compounds similar to pygeum and saw palmetto. In fact, nettle root and saw palmetto are frequently used in natural treatments for urinary disorders.

According to a 2019 study, nettle root extracts can effectively reduce BPH symptoms and improve the overall quality of life of people with the condition [39].

Lycopene

Lycopene is a naturally occurring pigment found in a variety of fruits and vegetables. A pilot study discovered that consuming lycopene-enriched extra virgin olive oil on a daily basis improved prostate health and decreased prostate-specific antigen levels.

Tomatoes are the richest source of lycopene available to most people, but a few other fruits and vegetables have lower levels of this antioxidant [40].

CHAPTER 2

LITERATURE SURVEY

- *Suwen Zaao et al., **(2021)*** studied "Ligands of Adrenergic Receptors: A Structural Point of View" Adrenergic receptors are G protein-coupled receptors for epinephrine and norepinephrine. They are targets of many drugs for various conditions, including treatment of hypertension, hypotension, and asthma. Adrenergic receptors are intensively studied in structural biology, displayed for binding poses of different types of ligands. Here, we summarized molecular mechanisms of ligand recognition and receptor activation exhibited by structure. We also reviewed recent advances in structure-based ligand discovery against adrenergic receptors.

- *Tapan Behl et el., **(2021)*** studied "Phytochemicals from Plant Foods as Potential Source of Antiviral Agents" To date, the leading causes of mortality and morbidity worldwide include viral infections, such as Ebola, influenza virus, acquired immunodeficiency syndrome (AIDS), severe acute respiratory syndrome (SARS) and recently COVID-19 disease, caused by the SARS-CoV-2 virus. Currently, we can count on a narrow range of antiviral drugs, especially older generation ones like ribavirin and interferon which are effective against viruses in vitro but can often be ineffective in patients. In addition to these, we have antiviral agents for the treatment of herpes virus, influenza virus, HIV and hepatitis virus. Recently, drugs used in the past especially against ebolavirus, such as remdesivir and favipiravir, have been considered for the treatment of COVID-19 disease. However, even if these drugs represent important tools against viral diseases, they are certainly not sufficient to defend us from the multitude of viruses present in the environment. This represents a huge problem, especially considering the unprecedented global threat due to the advancement of COVID-19, which represents a potential risk to the health and life of millions of people

- *Azimuth Azizi, et al., **(2021)*** studied"Phytochemicals with Anti 5-alpha-reductase Activity: A Prospective for Prostate Cancer Treatment" Prostate cancer (CaP) is one of the leading causes of death in men worldwide. Much attention has been given on its prevention and treatment strategies, including targeting the regulation of 5-alpha-Reductase (5αR) enzyme activity, aimed to limit the progression of CaP by inhibiting the conversion of potent androgen

dihydrotestosterone from testosterone that is thought to play a role in pathogenesis of CaP, by using the 5-alpha-Reductase inhibitors (5αRis) such as finasteride and dutasteride. However, 5αRis are reported to exhibit numerous adverse side effects, for instance erectile dysfunction, ejaculatory dysfunction and loss of libido. This has led to a surge of interest on plant-derived alternatives that might offer favourable side effects and less toxic profiles. Phytochemicals from plants are shown to exhibit numerous medicinal properties in various studies targeting many major illnesses including CaP. Therefore, in this review, we aim to discuss the use of phytochemicals namely phytosterols, polyphenols and fatty acids, found in various plants with proven anti-CaP properties, as an alternative herbal CaP medicines as well as to outline their inhibitory activities on 5αRs isozymes based on their structural similarities with current 5αRis as part of CaP treatment approaches.

- *Huda Mando et al., **(2021)*** studied "Flavonoids in Benign Prostate Hypertrophy: Identification in Herbal Preparations and Molecular Docking Approach" The benefits of phytotherapy in Benign prostatic hyperplasia (BPH) are of interest where they may lack side effects at long-term therapy. Through plant-derived preparations are Saw palmetto and Pumpkin seed oil. Evidence suggests that fatty acids, phytosterols, tocopherols, and flavonoids are the active components responsible for alleviating BPH symptoms. Flavonoids are reported to inhibit BPH through different mechanisms. Reducing inflammation and lowering reactive oxygen species are amongst the proposed mechanisms. In vitro studies highlighted the role of flavonoids in 5-alpha reductase II (5ARII) inhibitory activity. In this study, herbal preparations known to treat BPH were subjected to LC/MS/MS analysis integrated with multiple reaction monitoring (MRM) to identify the content of flavonoids. A molecular docking study was conducted on the assigned flavonoids to predict the binding mode and interaction with the targeted 3D- crystal structure of the human 5ARII enzyme. Results showed the existence of seven flavonoids and a polyphenol compound. Sakuranetin, Isorhamnetin, and Chlorogenic acid were not reported before. Molecular docking outcomes revealed that Astragalin, Isoquercitrin, Quercetin, and Chlorogenic acid have similar binding affinity to the reference Finasteride compound. These findings suggest flavonoids as potent potential inhibitors of 5ARII and could proceed to in vitro investigations.

- *Zhaowei Zhai et al., **(2021)*** studied "Network Pharmacology and Molecular Docking Combined to Analyze the Molecular and Pharmacological Mechanism of ternata in the Treatment of Hypertension" Hypertension is a cardiovascular disease that causes great harm to

health and life, affecting the function of important organs and accompanied by a variety of secondary diseases, which need to be treated with drugs for a long time. P. ternata alone or combination with western medicine has played an important role in traditional Chinese medicine. Although P. ternata is used clinically to treat hypertension, its functional molecular mechanism and pharmacological mechanism have not been elucidated. Therefore, in this study, the potentially effective components, and targets of P. ternata in the treatment of hypertension were screened by the method of network pharmacology, and the mechanism of P. ternata in the treatment of hypertension was analysed by constructing a component-target relationship network, PPI interaction network, targets' function analysis, and molecular docking. In the study, 12 potentially effective components and 88 targets were screened, and 3 potential protein modules were found and analysed after constructing a PPI network using targets. In addition, 10 targets were selected as core targets of the PPI network. After that, the targets were analysed by Gene Ontology (GO) enrichment analysis and Kyoto Encyclopedia of Genes and Genomes (KEGG) pathway analysis. Finally, the molecular docking method is used to study the interaction between the targets and the active components.

- *Ruidan Wang et al., **(2020)*** studied "Novel ACE Inhibitory Peptides Derived from Simulated Gastrointestinal Digestion in Vitro of Sesame (Sesamum indicum L.) Protein and Molecular Docking Study" The aim of this study was to isolate and identify angiotensin I-converting enzyme (ACE) inhibitory peptides from sesame protein through simulated gastrointestinal digestion in vitro, and to explore the underlying mechanisms by molecular docking. The sesame protein was enzymatically hydrolysed by pepsin, trypsin, and α-chymotrypsin. The degree of hydrolysis (DH) and peptide yield increased with the increase of digest time. Moreover, ACE inhibitory activity was enhanced after digestion. The sesame protein digestive solution (SPDS) was purified by ultrafiltration through different molecular weight cut-off (MWCO) membranes and SPDS-VII (< 3 kDa) had the strongest ACE inhibition. SPDS-VII was further purified by NGC Quest™ 10 Plus Chromatography System and finally 11 peptides were identified by Nano UHPLC-ESI-MS/MS (nano ultra-high performance liquid chromatography-electrospray ionization mass spectrometry/mass spectrometry) from peak 4. The peptide GHIITVAR from 11S globulin displayed the strongest ACE inhibitory activity (IC50 = 3.60 ± 0.10 μM). Furthermore, the docking analysis revealed that the ACE inhibition of GHIITVAR was mainly attributed to forming very strong hydrogen bonds with the active sites of ACE. These results identify sesame protein as a rich source of ACE inhibitory peptides and further indicate that GHIITVAR has the potential for development of new functional foods.

- *Afsun Sujayeva et al., (2020)* studied "Novel cyclic thiourea derivatives of amino alcohols at the presence of $Alcl_3$ catalyst as potent α-glycosidase and α-amylase inhibitors: Synthesis, characterization, bioactivity investigation and molecular docking studies" The article is devoted to the targeted synthesis and study of cyclic thiourea and their various new derivatives as new organic compounds containing polyfunctional group in the molecule. First time the reaction of the corresponding synthesized pyrimidinethione with 1,2-epoxy-3-chlorpropane at the presence of Alc_3 catalyst in 75–80% yield alkyl-1-(3-chloro-2-hydroxypropyl)-4-alkyl-6-phenyl-2-thioxo-1,2,5,6- tetrahydropyrimidine-5- carboxylates. In the next stage, new cyclic thiourea derivatives of amino alcohols were synthesised from the reaction of chlorinated derivatives of pyrimidinethiones with single amines and their structures were investigated by spectroscopic methods. In this study, a series of novel compounds were tested towards some metabolic enzymes including α-glycosidase (α-Gly) and α-amylase (α-Amy) enzymes. Novel compounds showed Kis in ranging of 10.43 ± 0.94–111.37 ± 13.25 μM on α-glycosidase and IC_{50} values in ranging of 14.38–106.51 μM on α-amylase. The novel cyclic thiourea derivatives of amino alcohols had effective inhibition profiles against all tested metabolic enzymes. Binding affinity and inhibition mechanism of the most active compounds were detected with in silica studies and have shown that 2-Hydroxypropyl and butan-1-aminium moieties play a key role for inhibition of the enzymes.

- *Walled A. M. A. El-Enanya et al., **(2019)*** studied "Synthesis and molecular docking of some new bis-thiadiazoles as anti-hypertensive α-blocking agents" Twelve bis-thiadiazole derivatives were synthesized in high yield via the reaction of 2, 20 -terephthaloyl bis(N-phenylhydrazine carbothioamide) with a variety of hydrazonoyl chlorides in ethanol containing catalytic amounts of TEA. All the newly synthesized compounds were characterized by physical and chemical tools (FT-IR, ^{1} H NMR, ^{13}C NMR, and Mass spectrometry). Moreover, all the novel synthesized derivatives were screened for their antihypertensive a-blocking efficacy against to assess their pharmaceutical significance. The encouraging promising results obtained from antihypertensive a-blocking activity studies on the newly synthesized derivatives make the synthesis of a new series of these compounds and studying of their pharmaceutical importance an active area for more and more investigations. The molecular docking of the most active derivative 15b against the human dopamine D3 receptor was performed by the Molecular Operating Environment (MOE 2014. 0901) program.

- *S. Aayisha et al., **(2019)*** studied "DFT, molecular docking and experimental FT-IR, FT-Raman, NMR inquisitions on "4-chloro-N-(4,5-dihydro-1H-imidazol-2-yl)-6- methoxy-2-methylpyrimidin-5-amine": Alpha-2-imidazoline receptor agonist antihypertensive agent" A molecule 4-chloro-N-(4,5-dihydro-1H-imidazol-2-yl)-6-methoxy-2-methylpyrimidin-5-amine plays a significant role in the treatment of hypertension and acts as a potential I 1 imidazoline receptor agonist. In this present work, the molecular structure of the title compound has been investigated using experimental (FT-IR, FT-Raman and NMR) and theoretical (DFT) techniques. R2 values of FR-IR, FT-Raman and bond lengths state the coherence between theoretical and experimental values. Asymmetric, symmetric stretching and bending vibrations were reported. The geometrical parameters obtained theoretically are in agreement with experimental values. Chemical activity region of the molecule (MEP), molecular stability, charge localization and delocalization (NBO), occupied and unoccupied molecular orbitals (HOMO-LUMO), dipole moment, polarizability and hyperpolarizability (NLO) have been calculated. There is a significant change in a net atomic charge distribution with a corresponding increase in the value of total dipole moment. Furthermore, the mulliken population analysis on atomic charges (electronic properties), thermodynamic parameters at various temperatures have also been calculated. To study the biological activity, different proteins for ligand have been taken and the results suggest that the compound might exhibit anti-hypertensive activity. Henceforth, Quantum mechanical calculations have been done for the title compound to get optimized structure and electronic energies for biological, physical, pharmaceutical and medicinal interest.

- *Praveen Kumar et al., **(2019)*** studied "Synthesis, anti-diabetic evaluation and molecular docking studies of 4-(1- aryl-1H-1, 2, 3-triazol-4-yl)-1, 4-dihydropyridine derivatives as novel 11-β hydroxysteroid dehydrogenase-1 (11β-HSD1) inhibitor" 11-Beta-Hydroxysteroid dehydrogenase-1(11β-HSD1) inhibitors are one of the emerging classes of molecules to fight against diabetic complications. A novel series of 4-(1-substituted-1H-1, 3-triazol-4-yl)-1, 4-dihydropyridine derivatives were synthesized and evaluated for their anti-diabetic activity. Two compounds showed antidiabetic activity very effectively. To clarify the mechanism of action of these compounds, the most potent compounds (5g and 5h) of the synthesized analogs were further studied by testing its 11-Beta Hydroxysteroid dehydrogenase-1 inhibitory activity through in vitro enzymatic experiments. The results showed that the 11βHSD1 inhibitory activity of compounds 5g and 5h was stable and efficient. Molecular docking studies revealed

compounds 5g (−9.758) and 5h (−8.495) to have a stable binding patterns to the human 11-BetaHydroxysteroid dehydrogenase-1.

- *Ufuk Atmacaa et al., **(2019)*** studied "Synthesis of oxazolidinone from enantiomerically enriched allylic alcohols and determination of their molecular docking and biologic activities" Enantioselective synthesis of functionalized cyclic allylic alcohols via kinetic resolution in transesterifcation with different lipase enzymes has been developed. The influence of the enzymes and temperature activity was studied. By determination of ideal reaction conditions, by-product formation is minimized; this made it possible to prepare enantiomerically enriched allylic alcohols in high ee's and good yields. Enantiomerically enriched allylic alcohols were used for enantiomerically enriched oxazolidinone synthesis. Using benzoate as a leaving group means that 1 mol % of potassium osmate is necessary and can be obtained high yields 98%. Inhibitory activities of enantiomerically enriched oxazolidinones (8, 10 and 12) were tested against human carbonic anhydrase I and II is enzymes (hCA I and hCA II), acetyl cholinesterase (AChE), and α-glycosidase (α-Gly) enzymes.

- *Sobhi M. Gomha et al., **(2019)*** studied "Synthesis and molecular docking of some new bis-thiadiazoles as anti-hypertensive α-blocking agents" Twelve bis-thiadiazole derivatives were synthesized in high yield via the reaction of 2, 20 -terephthaloyl bis (N-phenylhydrazine carbothioamide) with a variety of hydrazonoyl chlorides in ethanol containing catalytic amounts of TEA. All the newly synthesized compounds were characterized by physical and chemical tools (FT-IR, 1 H NMR, 13C NMR, and Mass spectrometry). Moreover, all the novel synthesized derivatives were screened for their antihypertensive a-blocking efficacy against to assess their pharmaceutical significance. The encouraging promising results obtained from antihypertensive a-blocking activity studies on the newly synthesized derivatives make the synthesis of a new series of these compounds and studying of their pharmaceutical importance an active area for more and more investigations. The molecular docking of the most active derivative 15 b against the human dopamine D3 receptor was performed by the Molecular Operating Environment (MOE 2014. 0901) program.

- *Noor Rahman et al., **(2019)*** studied "Molecular Docking of Isolated Alkaloids for Possible α-Glucosidase Inhibition" Diabetes mellitus, one of the most common endocrine-metabolic disorders, has caused significant morbidity and mortality worldwide. To avoid sugar digestion and postprandial hyperglycemia, it is necessary to inhibit α-glucosidase, a digestive enzyme

with an important role in carbohydrate digestion. The criteria for the selection of alkaloids are based on their in vitro and in vivo activities on glucose modulation. The current study assessed the bonding potential of isolated alkaloids with the targeted protein. For this purpose, the 3D structure of the target protein (α-glucosidase) was reproduced using MODELLER 9.20. The modeled 3D structure was then validated and confirmed by using the RAMPAGE, ERRAT, and Verify3D online servers. The molecular docking of 32 alkaloids reported as α-glucosidase inhibitors, along with reference compounds (acarbose and miglitol), was done through MOE-Dock applied in MOE software to predict the binding modes of these drug-like compounds. The results revealed that nummularineR and vindoline possess striking interactions with active site residues of the target protein, and were analogous to reference ligands. In conclusion, the current study provided a computational background to the α-glucosidase inhibitors tested. This novel information should facilitate the development of new and effective therapeutic compounds for the treatment of diabetes mellitus.

- *Muhammad Sahib Nawaz et al., **(2019)*** studied "A Molecular Docking Approach to Evaluate the Pharmacological Properties of Natural and Synthetic Treatment Candidates for Use against Hypertension" Cardiovascular diseases (CVDs) have become the leading cause of disability and death worldwide, particularly in low- and middle-income countries. Hypertension, a major cause of CVD progression, is widely attributable to genetic, behavioral, and environmental risk factors. Among the genetic reasons, angiotensin II enzyme, produced as a result of abnormal functioning of the renin–angiotensin system, is reported as the foremost cause of hypertension. A cascade of genes, including those encoding for WNK kinases (WNK1 and WNK4), Bp1, Bp2, angiotensinogen, and other enzymes, is involved in the conversion of angiotensin I to angiotensin II. However, the angiotensin-converting enzyme (ACE) plays a crucial role in this pathway. Therefore, ACE could be a potential therapeutic target in regulating the conversion of angiotensin I to angiotensin II and eventually controlling hypertension. In this study, a molecular docking-based approach was utilized for identifying and evaluating potential inhibitors of ACE present in herbs, other natural sources, and synthetic sources, on the basis of these compounds' binding affinities and other physicochemical features. In addition, the suitability of these inhibitors as drugs for biological systems, considering their adsorption, distribution, metabolism, and excretion (ADME), was predicted using Lipinski's rule. In conclusion, our study provides a novel and clearer insight into the interaction properties of known putative inhibitors of ACE.

- *Ammar Altemimi et al., **(2017)*** studied "Phytochemicals: Extraction, Isolation, and Identification of Bioactive Compounds from Plant Extracts" There are concerns about using synthetic phenolic antioxidants such as butylated hydroxytoluene (BHT) and butylated hydroxyanisole (BHA) as food additives because of the reported negative effects on human health. Thus, a replacement of these synthetics by antioxidant extractions from various foods has been proposed. More than 8000 different phenolic compounds have been characterized; fruits and vegetables are the prime sources of natural antioxidants. In order to extract, measure, and identify bioactive compounds from a wide variety of fruits and vegetables, researchers use multiple techniques and methods. This review includes a brief description of a wide range of different assays. The antioxidant, antimicrobial, and anticancer properties of phenolic natural products from fruits and vegetables are also discussed.

- *Atanas G. Atanasov et al., **(2014)*** studied "Natural product agonists of peroxisome proliferator-activated receptor gamma (PPARγ)" Agonists of the nuclear receptor PPARγ are therapeutically used to combat hyperglycaemia associated with the metabolic syndrome and type 2 diabetes. In spite of being effective in normalization of blood glucose levels, the currently used PPARγ agonists from the thiazolidinedione type have serious side effects, making the discovery of novel ligands highly relevant. Natural products have proven historically to be a promising pool of structures for drug discovery, and a significant research effort has recently been undertaken to explore the PPARγ-activating potential of a wide range of natural products originating from traditionally used medicinal plants or dietary sources. The majority of identified compounds are selective PPARγ modulators (SPPARMs), transactivating the expression of PPARγ-dependent reporter genes as partial agonists. Those natural PPARγ ligands have different binding modes to the receptor in comparison to the full thiazolidinedione agonists, and on some occasions activate in addition PPARα (e.g. genistein, biochanin A, sargaquinoic acid, sargahydroquinoic acid, resveratrol, amorphastilbol) or the PPARγ-dimer partner retinoid X receptor (RXR; e.g. the neolignans magnolol and honokiol). A number of *in vivo* studies suggest that some of the natural product activators of PPARγ (e.g. honokiol, amorfrutin 1, amorfrutin B, amorphastilbol) improve metabolic parameters in diabetic animal models, partly with reduced side effects in comparison to full thiazolidinedione agonists. The bioactivity pattern as well as the dietary use of several of the identified active compounds and plant extracts warrants future research regarding their therapeutic potential and the possibility to modulate PPARγ activation by dietary interventions or food supplements.

CHAPTER 3

SCOPE OF INVESTIGATION

- Alpha Blockers is a life threatening worldwide disease
- To find out target protein for Alpha Blockers
- To find the inhibitors for phytochemical compounds for Alpha Blockers
- To know the details about Alpha Blockers and its adverse effects of the world
- To identify a natural phytochemical compounds
- To find the high binding efficiency for protein ligand complex
- To recognize the good pharmacological activities of the phytochemical compounds in future

CHAPTER 4

MATERIALS AND METHODS

TARGET SELECTION

The X-ray crystal structure of 2AZ5 was retrieved from Protein Data Bank. The protein energy was analyzed through Ramachandran Plot. The protein energy minimized through the Swiss PDB minimizer and used for further docking studies.

RAMACHANDRA PLOT 2AZ5

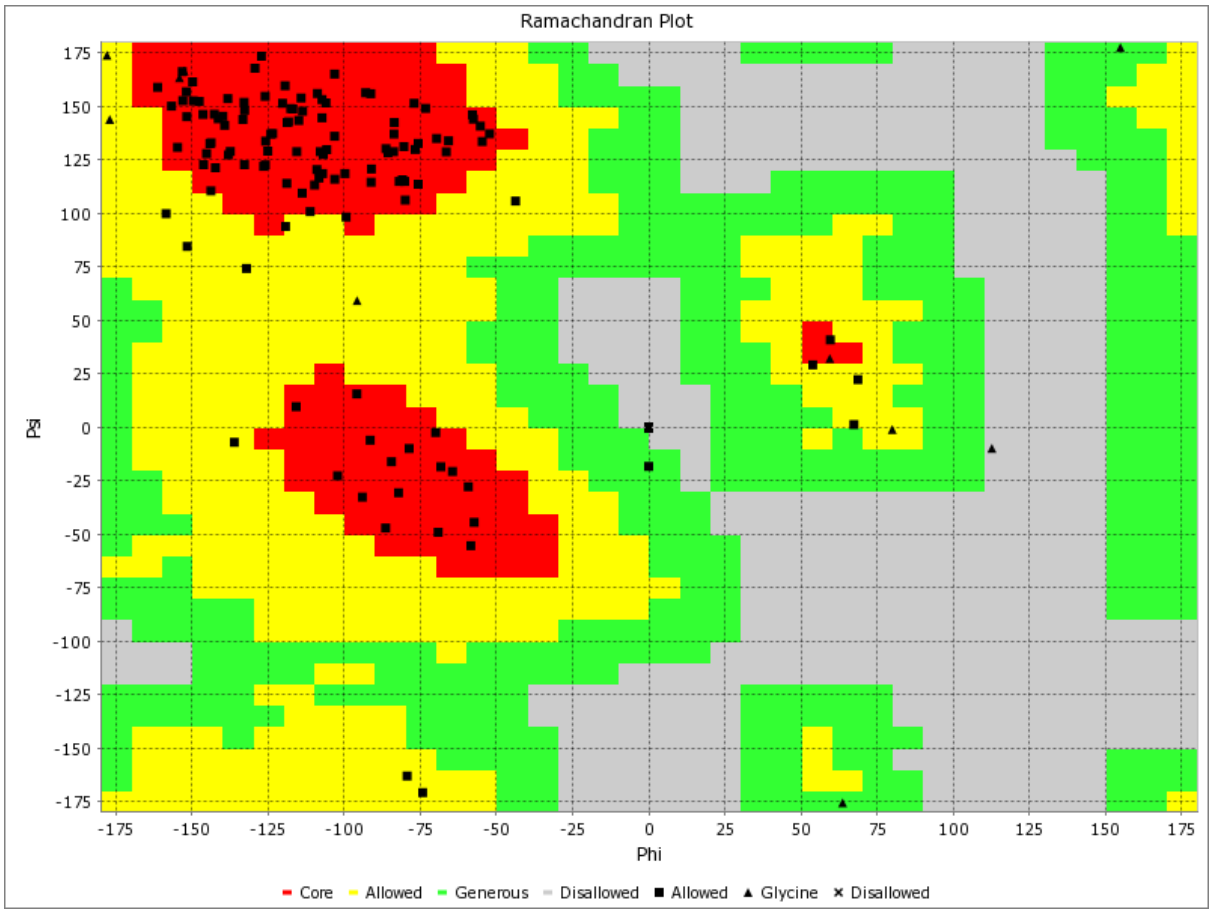

Figure 1Ramachandra plot

FASTA SEQUENCE

DKPVAHVVANPQAEGQLQWLNRRANALLANGVELRDNQLVVPSEGLYLIYS
QVLFKGQGCPSTHVLLTHTISRIAVSYQTKVNLLSAIKSPCQRETPEGAEAKPWYEPI
YLGGVFQLEKGDRLSAEINRPDYLDFAESGQVYFGIIAL

PROTEIN PREPARATION

Load the protein and apply the force field. For docking studies, the protein 2AZ5 loads from RCSB protein data bank (www.resb.org/pdb) and apply the force field. Field refers to the functional form parameter sets which are used to find out potential energy of a system. It includes parameter which is obtained through experimental works and quantum mechanics calculations. All molecules in a molecule system are made up of a number of components. Covalently bonded atoms take into consideration several parameters such as bond length, bond angle, dihedral angles etc., similarly there exist non bonded interactions such as Vanderwaals interactions, electrostatic interactions. Thus, the total potential energy of the system is calculated as follows.

$$E1 = E_{bond} + E_{angle} + E_{vanderwaals} + E_{electronic}]$$

LIGAND SELECTION

The SMILES notation of Thirty two phytochemical compounds including alkaloids and flavonoids from various medicinal plants were obtained by drawing their 2D structures in ACD-Chemsketch. The 3D structures of these compounds were generated in PUB Chem software and converted SDF format in to pdbqt by using on open babel and structure file generator.

LIGAND PREPARATION

The chemically synthesized individual ligand compounds were sketched using ACD/ChemSketch (12.0) software and saved in (.mol) file format. The saved ligand compounds were later imported in PyRx and go to Minimization studies using minimize. After minimized ligands go to ligand preparation, then go for docking studies with ligand fit.

BINDING SITE AND SITE PARTITION

The active site of a receptor can be represented in many ways, for example a sphere or a list of residues. The Binding Site definition is one such representation. A binding site is a set location, volume and shape of the binding site or all used in docking.

To define a binding site, the receptor is first mapped to a grid. Grid points within a given distance of the receptor atoms are marked as occupied by receptors and as undesirable as locations for ligand atoms. Two methods exist to identify a Binding Site. The first uses an

"eraser" algorithm to identify sites based on the shape of the receptor. The second uses the volume occupies by the known ligand force already in an active site.

VIRTUAL SCREENING

The 3D structures of all the selected fifty phytochemical compounds were virtually screened to reveal their binding efficiencies through docking in the predicted binding site using PyRx-Python Prescription (version 0.8). The docking was performed with the default parameters such as triangle matching base placements, zero, full score and no score contributions and threshold for full score and no score contributions of 30 and 70 respectively. Clash handling values of 2.9 Å and 0.6 for protein ligand clashes with maximum allowed overlap volume and in a ligand clash factors while considering the hydrogen in internal clash tests and 200 as the default docking values for maximum number of solutions per iteration and also per fragmentations.

DOCKING INTERACTION

The docking interactions revealing H-bond and Vanderwaals forces among the phytochemical compounds and the amino acid residues of were analyzed by PyRx-Python Prescription (PyRx).

PYRX DOCKING

PyRx is a Virtual Screening software for Computational Drug Discovery that can be used to screen libraries of compounds against potential drug targets. PyRx enables Medicinal Chemists to run Virtual Screening from any platform and helps users in every step of this process. From data preparation to job submission and analysis of the results. While it is true that there is no magic button in the drug discovery process, PyRx includes docking wizard with an easy-to-use user interface which makes it a valuable tool for Computer-Aided Drug Design. PyRx also includes chemical spreadsheet-like functionality and powerful visualization engine that are essential for structure-based drug design.

DOCKING ALOGRITHM

Select upper left button Load molecule to load your protein and ligand into PyRx workspace. Right click on ligands and click AutoDock to make ligand. Right click on protein and click AutoDock to Make Macromolecule. Now the protein and ligands files are ready for docking. Click on Start Here button under Vina Wizard. Select Local button under Vina

execution Mode. Click Start button. Select protein and ligands by simply clicking on them. Click forward to Run Vina. The grid box (white box with spherical handles) in the 3D scene as shown below. This grid box allows to select search space (Part of the protein, where the docking performs and it is typically known binding site) in the protein. To help locating the binding site (or active site) use binding site amino acids. Click molecules button under Navigator panel, then click on + button located in front of protein tab. After selecting the amino acids (use shift button to select multiple amino acids) click on the Toggle selection Spheres button to see the selected amino acids. Make sure you select the grid box size big enough to allow the ligand to move freely in the search space. Use the search space (Vina search space) values close the ones mentioned in the picture below, to get better results. Click the forward button to start Vina calculations. Once, the calculations are done, results will be populated as seen in the below table with the Binding Affinity (kcal/mol) values.

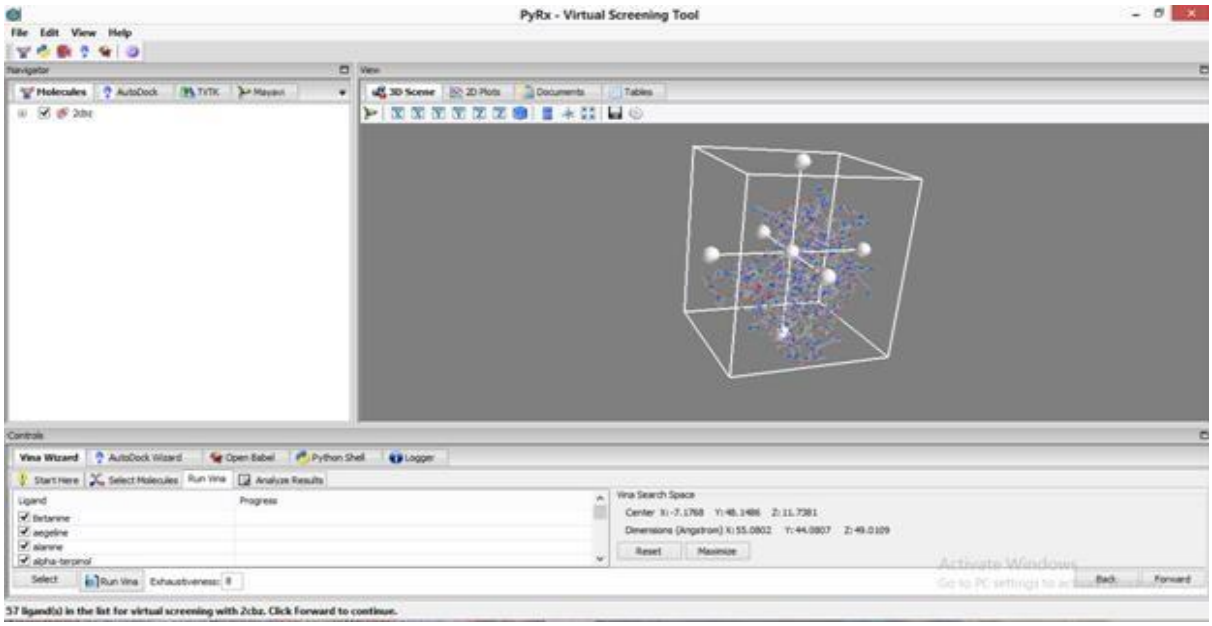

Figure 2Vina search space

More negative the binding affinity better the orientation of the ligand in the binding site. Results can be exported to other software programs like UCSF Chimera or PyMol or Discovery Studio for analysis. Click on Edit, go to Preferences. A pop-up window is opened. All your results will be saved in location specified as workspace. The protein folder contains three files (protein .pdbqt, ligand1_out.pdbqt and conf.txt), if you use only one ligand for docking. The ligand1_out.pdbqt contains 8 or 9 best poses (or orientations) of the ligand1 and conf.txt file contains search space (or grid box) parameters. Save this protein folder at your convenient

location for further analysis with Discovery studio. You are done with PyRx, now let's analyse the results by using Discovery studio. Open protein .pdbqt file followed by ligand1_out.pdbqt to analyse the results. Select the ligand by using upper sequence bar and click on select A (action)>find >Polar contacts >to any atoms..Now the result of PyRx docking is screened.

CHAPTER 5
RESULT AND DISCUSSION

TARGET SELECTION

The X- ray crystal structure of 2AZ5 was retrieved from Protein Data Bank .The protein energy was analysed through Ramachandra Plot. The protein energy and energy minimized through the SWISS PDB minimizer and used for further docking studies

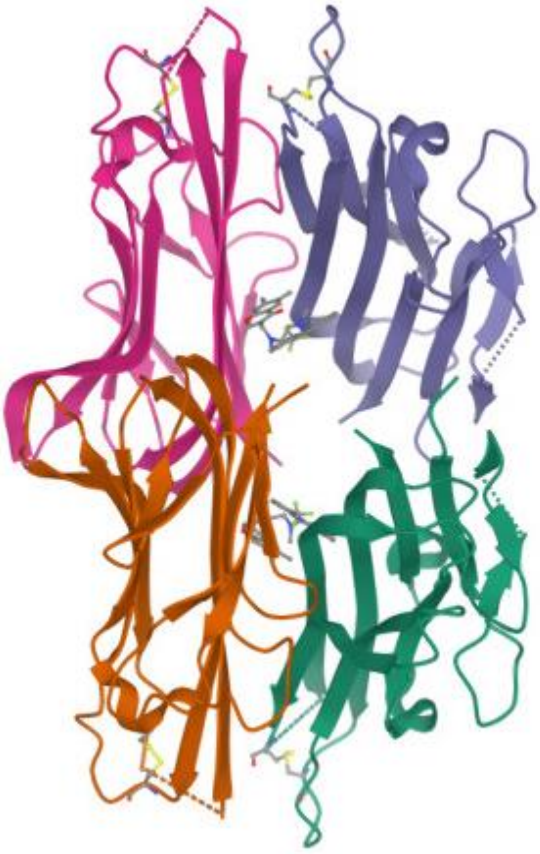

Figure 3 protein structure of 2AZ5

LIGAND SELECTION

The phytochemical compounds including alkaloids and flavonoids from various medicinal plants were obtained by drawing their 3D structures in ACD-Chemsketch (version 12.01). The 3D structures of these compounds were generated and converted into SDF format by using “OPEN BABEL ”convertor and structure file generator’ server.

A Phytochemical Compounds from different Plant Sources

COMPUOND NAME	CID NO.	*PLANT SOURCE*
Anaferine	443143	*Ashwagandha*
Apigenin	5280443	*Petroselinum crispum*
Arctigenin	64981	*Arctium Lappa*
Astilbin	119258	*Engelhardtiaroxb*
Bis_Demethoxy_Curcumin	5315472	*Curcuma longa*
Cosmosiin	5280704	*Diospyros Kaki*
Curcumin	969516	*Curcuma longa*
Cyanidin	128861	*Prunus avium*
Engeletin	6453452	*Engelhardtiaroxb*
Fisetin	5281614	*Fragaria ananassa*
Glycycoumarin	5317756	*Glycyrrhiza urallensis*
Glyasperin	480860	*Diospyros kaki*
Glycyrin	480787	*Glycyrrhiza urallensis*
Glycyrol	5320083	*Glycyrrhiza urallensis*
Hentriacontane	12410	*Withania somnifera*
Isoquercitrin	5280804	*Equisetum arvense*
Licoflavonol	5481964	*Diospyros Kaki*
Lignans	443013	*Larrea divaricate*
Liquiritigenin	114829	*Glycyrrhiza urallensis*
Luteolin	5280445	*Ailanthus excels*
Lycopene	446925	*Solanum lycopersicum*
Moexipril	91270	*Angiotension converting enzyme*
Oxalacetate	164550	*Albizia lebbeck*
Pelletierine	92987	*Punica granatum*
Physaguline-.	10100412	*Withania somnifera*
Adathoda vasica	5281727	*Pterocarpus marsupium*
Quinapril	54892	*Aegle marmelos*
Resveratrol	445154	*Vitis vinifera*
Rutin	5280805	*Ocimum basilium*
Silibinin	31553	*Silybum marianum*
Theophylline	2153	*Camellia sinensis*

Tylophorine	92114	*Tylophoraasthmatica*
Vasicine	667496	*Adathoda vasica*
Vasicinone	442935	*Adathoda vasica*
Vitamine E	14985	*Helianthus*

STRUCTURE OF PHYTOCHEMICAL COMPOUNDS

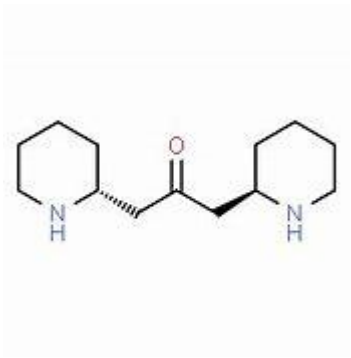

Anaferine

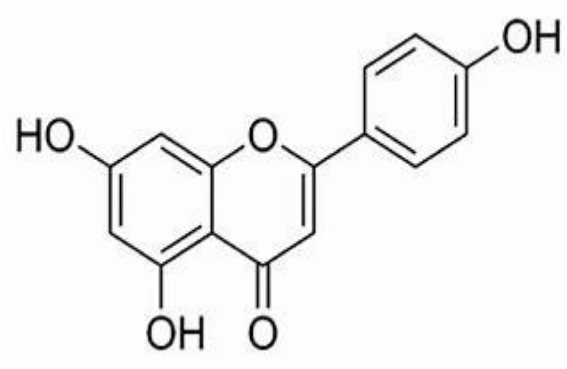

Apigenin

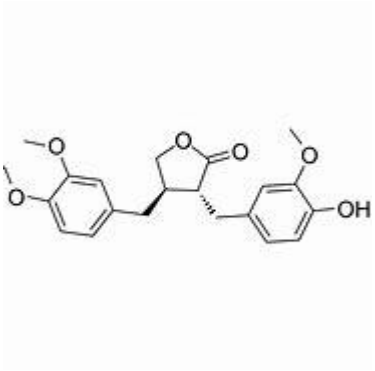

Arctigenin

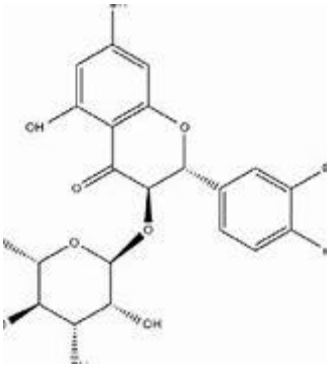

Astilbin

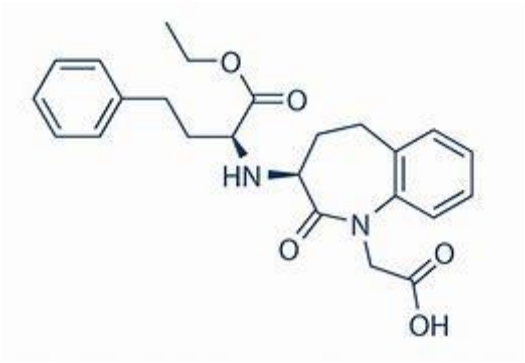

Benazepri

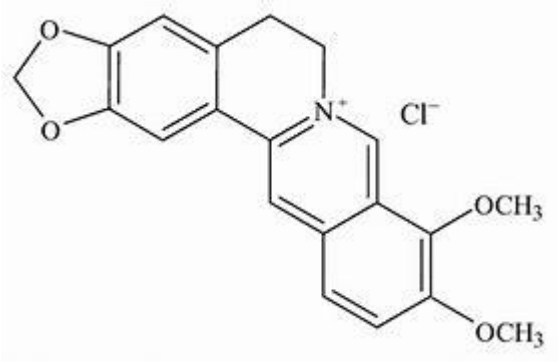

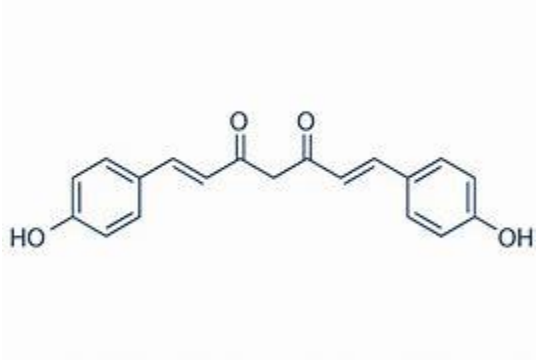

Bis_Demethoxy_Curcumin

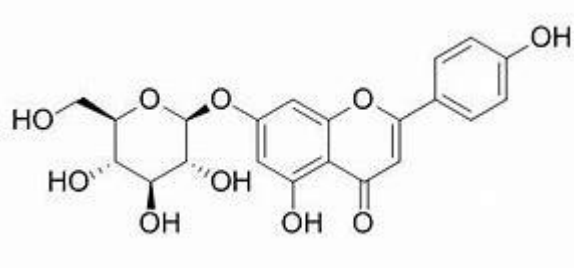

Cosmosiin

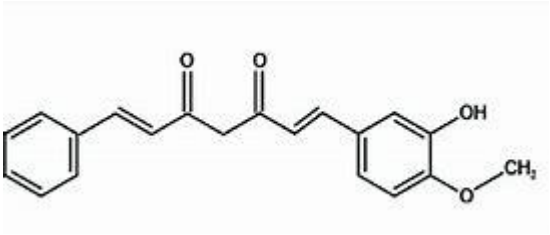

Curcimine

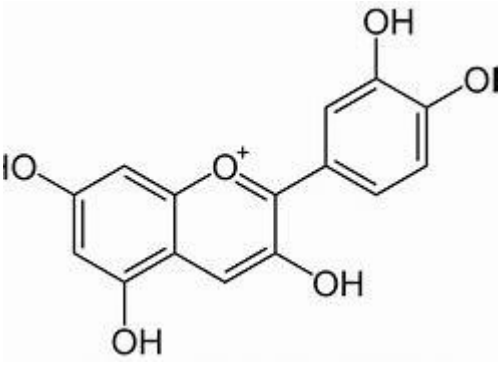

Cyanidin

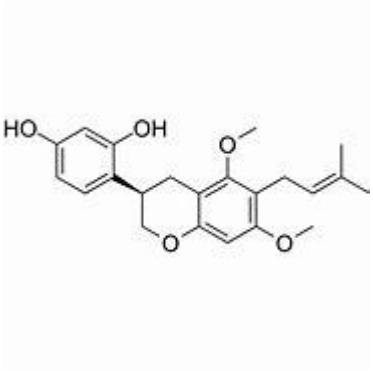

Glyasperin

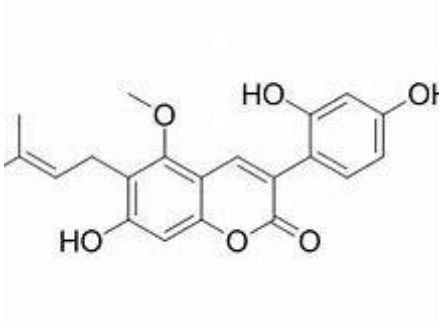

Glycycoumarine

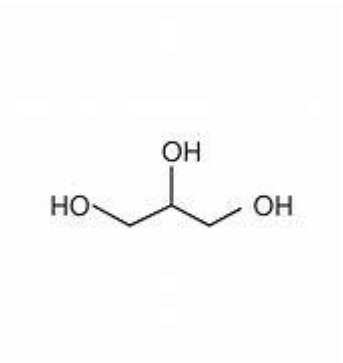

Glycyrin

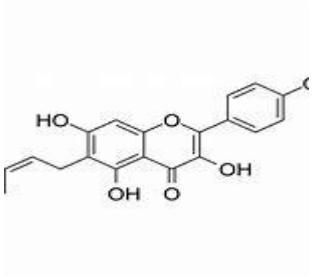

Licoflavonol

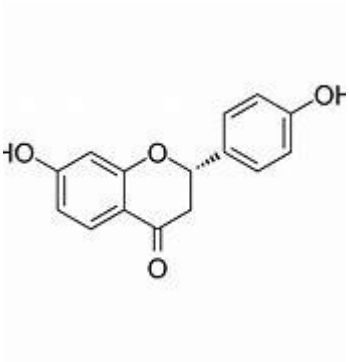

Liquiritigenin

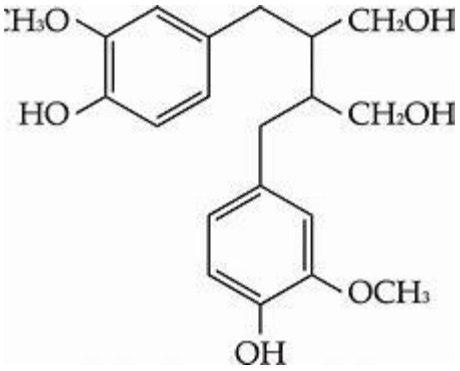

Lignans

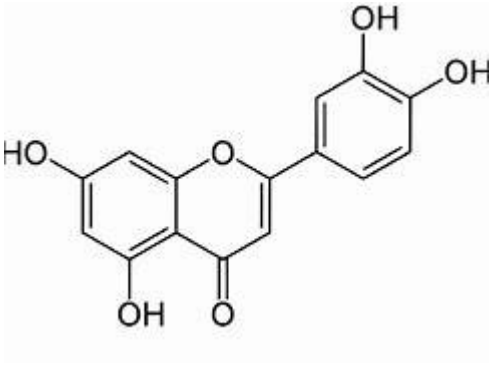

Luteolin

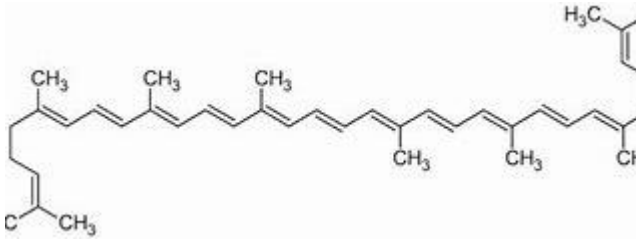

Lycopene

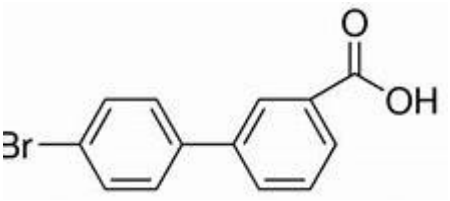

Moexipril

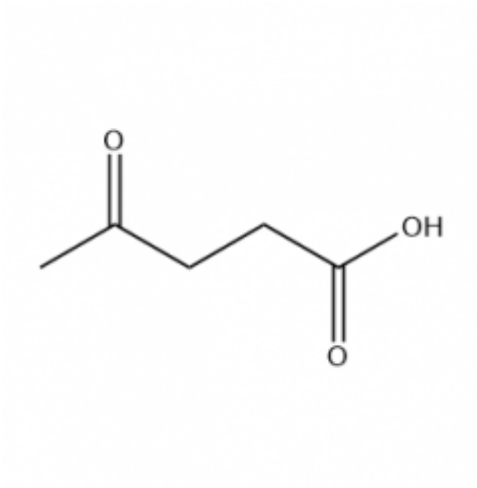

Oxalacetate

Pelletierine

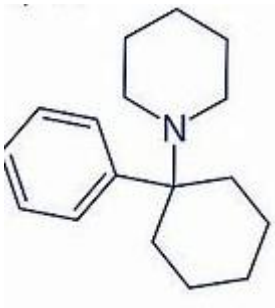

Physaguline-.

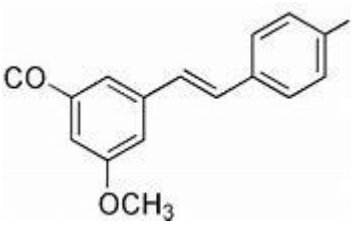

Pterostilbene

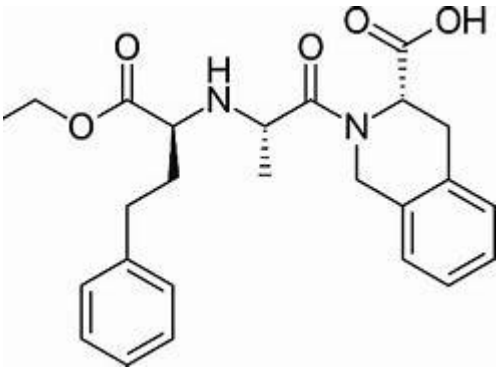

Quinapril

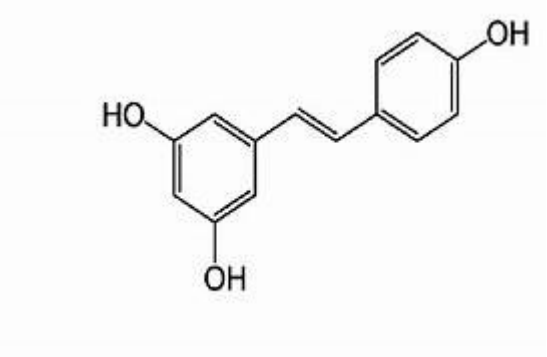

Resveratrol

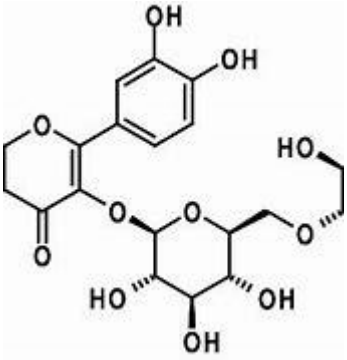

Rutin

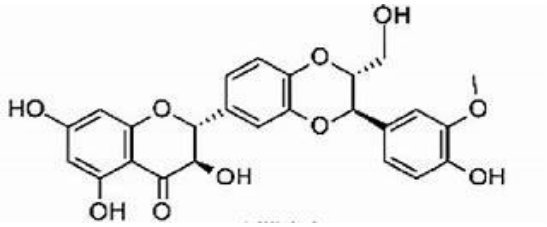

Silibinin

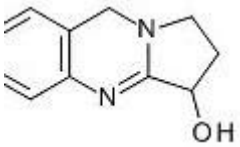

Vasicine

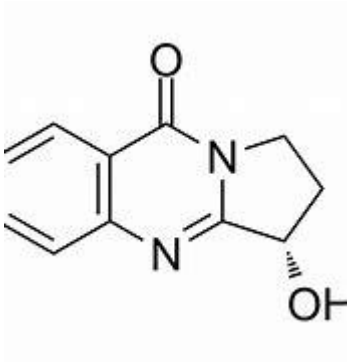

Vasicinone

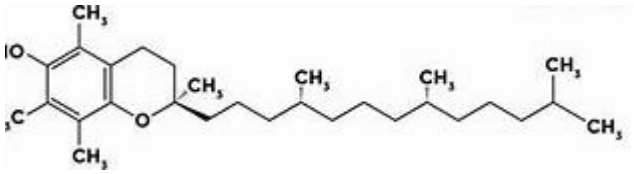

Vitamine E

BINDING SITE PREDICTION

The amino acid residues in binding site of 2AZ5 protein is defined by using the reference ligand complexed in the retrieved PDB file. The amino acid residues within 6 Å radius of reference ligand was included in the predicted binding site by using PyRx-Python Prescription (version 0.8).

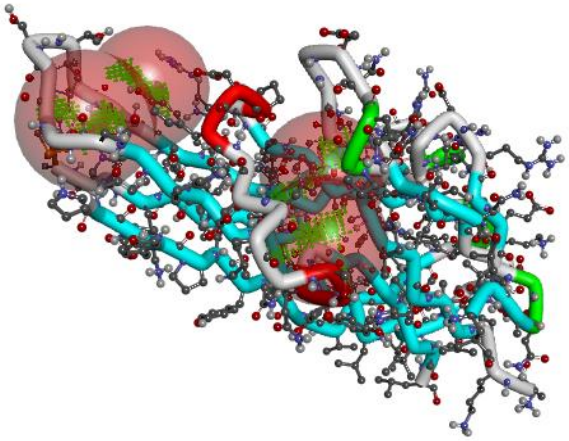

Figure 4 binding site prediction

VIRTUAL SCREENING

The 3D structures of all the selected phytochemical compounds were virtually screened to reveal their binding efficiencies through docking in the predicted binding site using PyRx Python Prescription. Docking values for maximum number of solutions per interaction and also per fragmentations. The binding affinity with their docking scores are given in table.

BINDING AFFINITIY OF PHYTOCHEMICAL BY USING PyRx

PHYTOCHEMICALS	BINDING ENERGY (Kcal/mol)
Apigenin	-8.4
Arctigenin	-8.3

Astilbin	-8.3
Benazepril	-7.5
Berberine	-10.1
Bis_Demethoxy_Curcumin	-7.9
Cosmosiin	-7.8
Curcumin	-7.7
Cyanidin	-7.6
Engeletin	-9.3
Fisetin	-7.4
Glyasperin	-7.4
Glycycoumarin	-7.8
Glycyrin	-8.3
Glycyrol	-7.3
Hentriacontane	-4.1
Isoquercitrin	-8.1
Licoflavonol	-7.4

Lignans	-8.3
Liquiritigenin	-9.2
Luteolin	-8.6
Lycopene	-5.1
Moexipril	-6.8
Oxalacetate	-3.7
Pelletierine	-5.2
Physaguline	-10.3
Pterostilbene	-7.8
Quinapril	-7.4
Resveratrol	-8
Rutin	-8.1
Silibinin	-8.6
Anaferine	-6.8

DOCKING INTERACTIONS

The docking interactions revealing H-bond and Vanderwaals forces among the phytochemical compounds and the amino acid residues of protein 2AZ5 were analyzed by PyRx-Python Prescription (version 0.8). PyRx is a Virtual Screening Software for

Computational Drug Discovery that can be used to screen libraries of compounds against potential drug targets. PyRx enables Medicinal Chemists to run Virtual Screening from any platform and helps users in every step of this process – from data preparation to job submission and analysis of the results. PyRx also includes chemical spreadsheet – like functionality and powerful visualization engine that are essential for structure-based drug design.

It excels at three-dimensional visualization of protein, ligand binding sites and surrounding amino acids of ligands were also visualized. Identified active sites were visualized in PYMOL visualization tool. The higher binding affinity of best ten phytochemical compounds are shown below.

Docking complex and interaction of PHYSAGULINE (10100412)

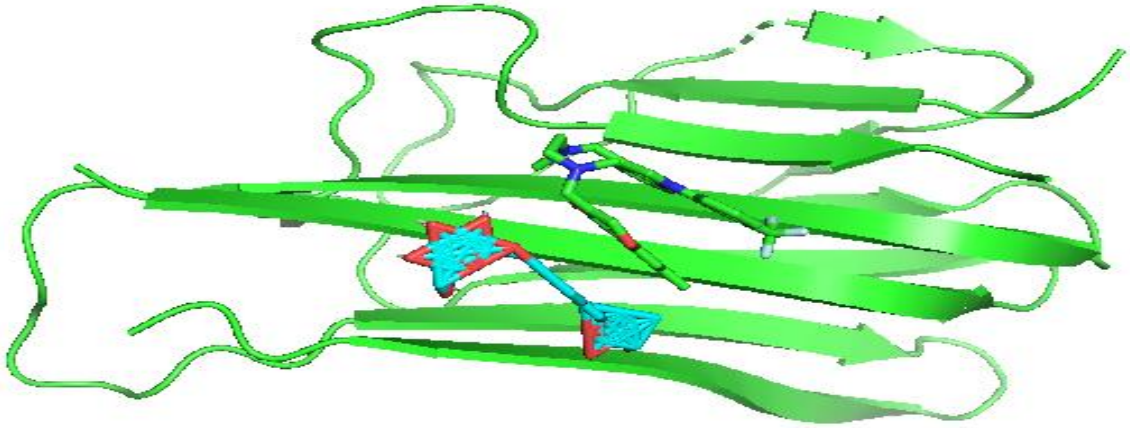

Docking complex and interaction of BERBERINE (CID No. 2353)

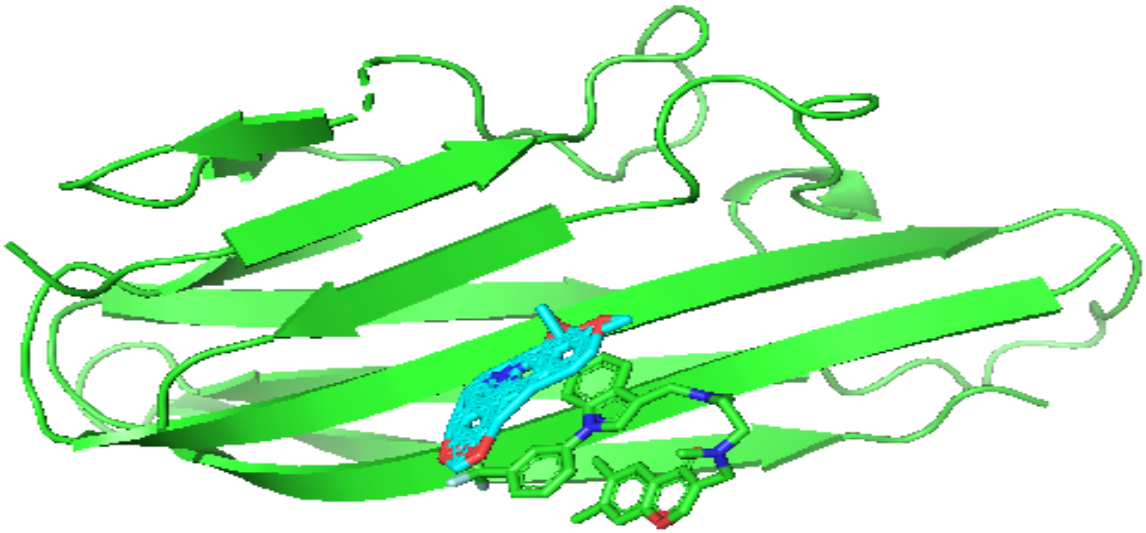

Docking complex and interaction of ENGELETIN (CID N0:6453452)

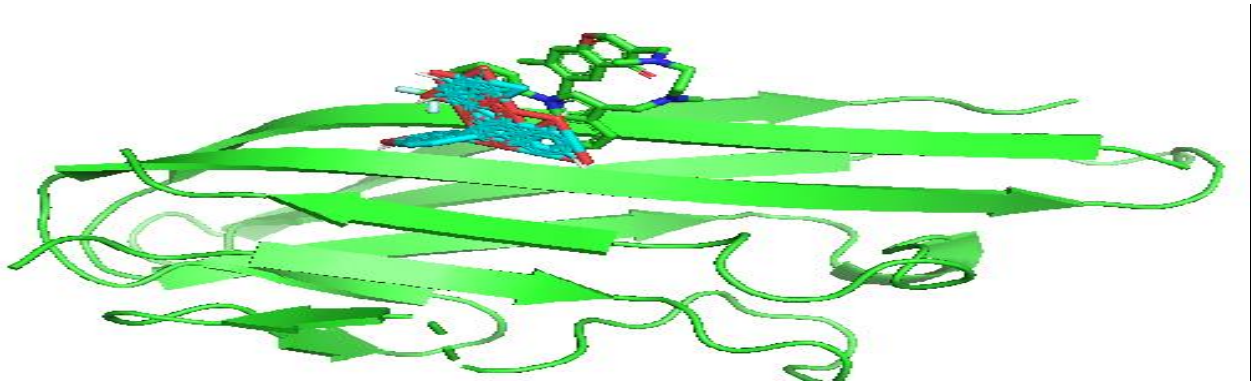

Docking complex and interaction of LIQUIRITIGENIN (CID N0.114829)

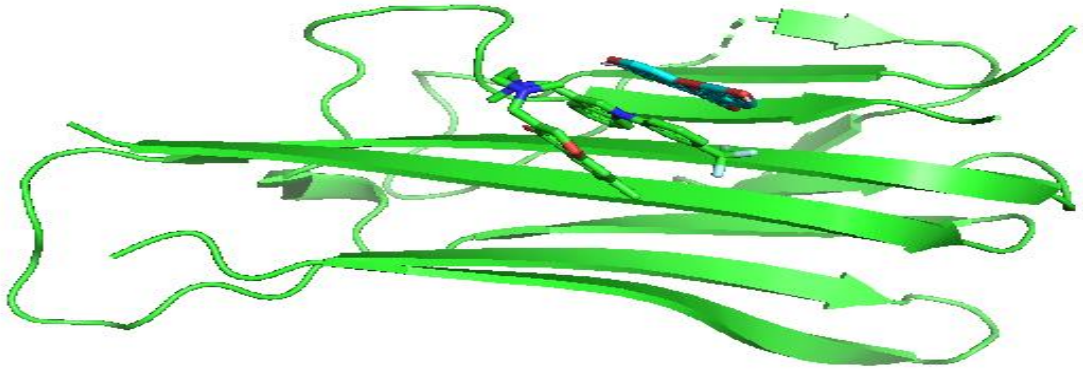

Docking complex and interaction of SILIBININ (CID NO.31553)

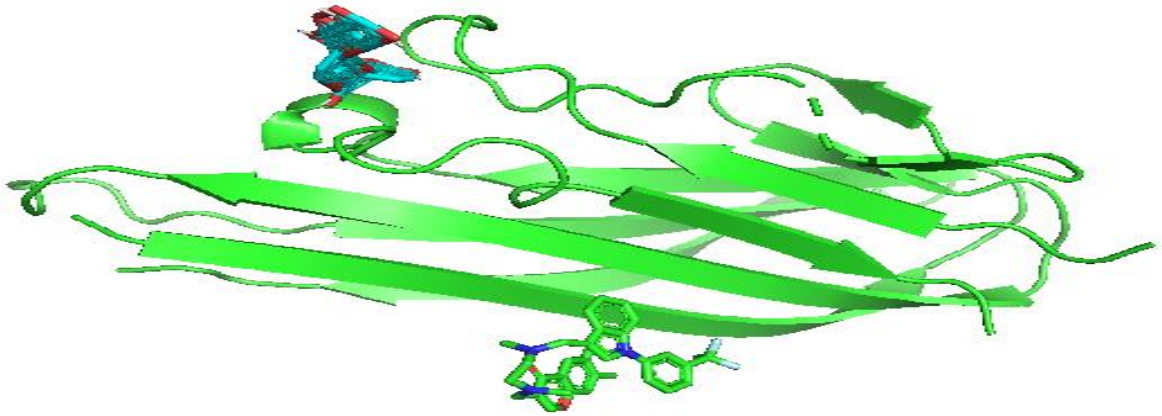

Docking complex and interaction of RUTIN (CID No.5280805)

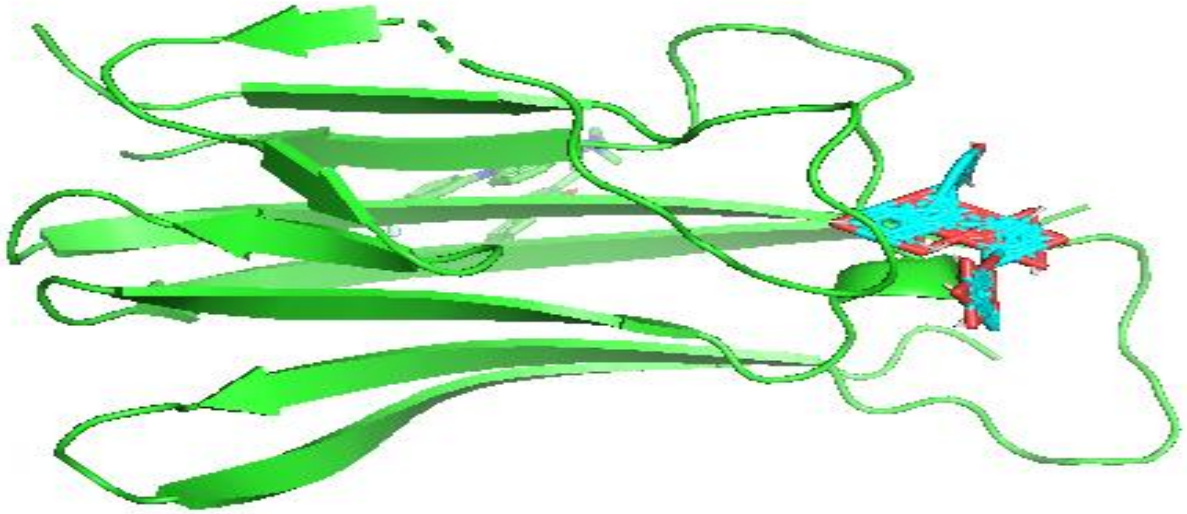

Docking complex and interaction of LUTEOLIN (CID NO.5280445)

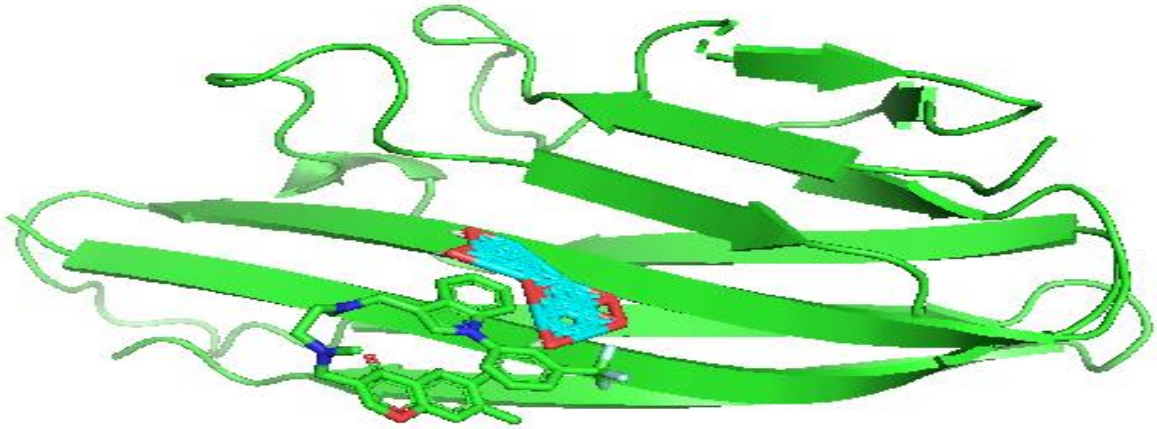

Docking complex and interaction of APIGENIN (CID NO.5280443)

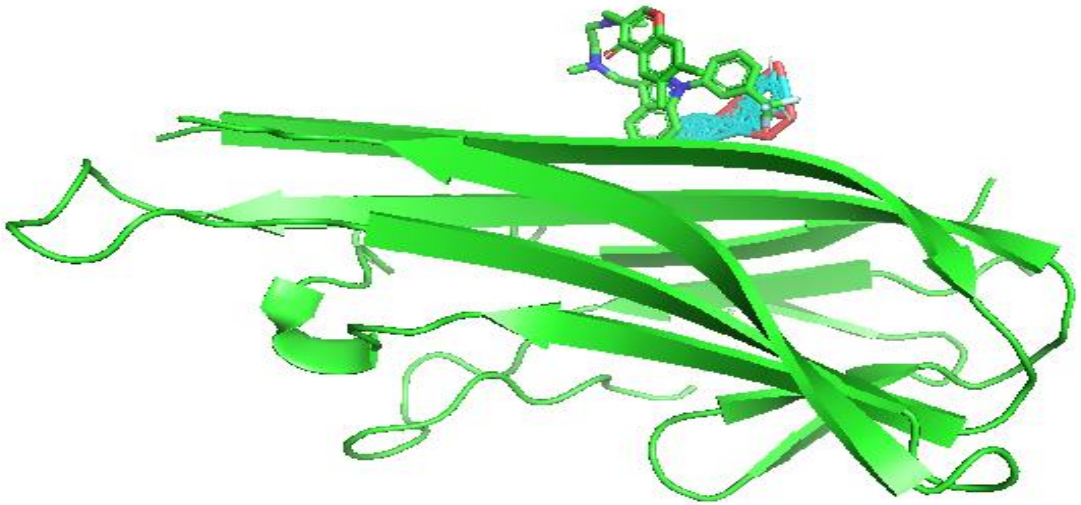

Docking complex and interaction of ARCTIGENIN (CID NO.64981)

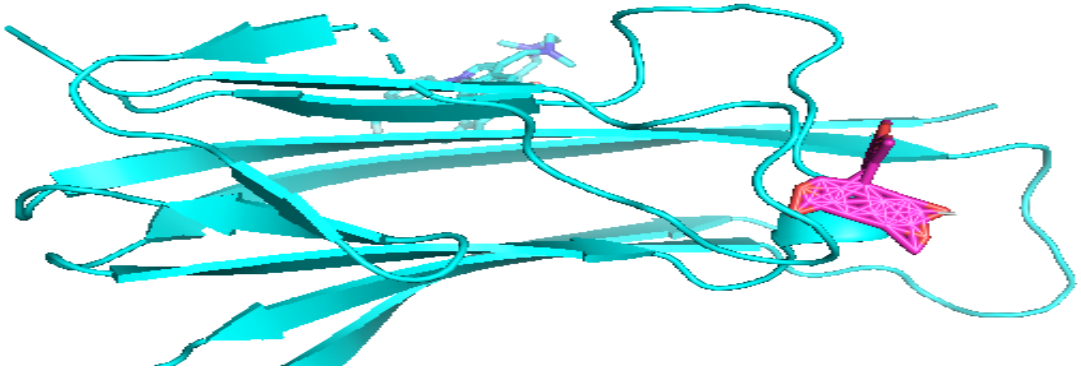

Docking complex and interaction of ASTILIBIN (CID NO.119258)

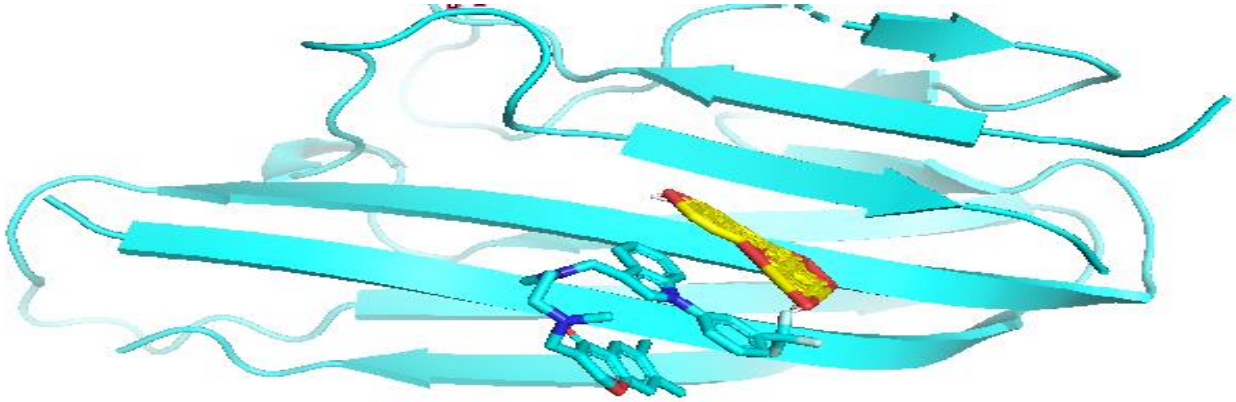

CHAPTER 6

CONCLUSION

The studies on the causes for the disease were conducted though docking in 2AZ5 protein. Phytochemical compounds were selected for protein. Some pounds were not docked and some compounds were docked successfully. Docking compounds are Arctigenin, Moexipril, Pterostilbene, Quinapril, Resveratrol etc. Docking compounds are Physaguline with dock score (-10.3 kJ/mol), Berberine with dock score (-10.1 kJ/mol), Engeletin with dock score (-9.3 kJ/mol), etc. Docking studies were sucessfully performed the ligand at the binding site of the receptor and thus inhibiting protein to express that causesHypertension in ALPHA BLOCKERS. The drug was constructed by modifying it to have less toxic effect and more efficient binding. It can be used as the potential drug helpful in curing ALPHA BLOCKERS. This drug can be made available commercially only after assing through the further studies of pharmacophore mapping and different phases of clinical tests.

CHEPTER 7

REFERENCE

1. Awais Attique , Muhammad Hassan, Muhammad Usman , Rana Muhammad Atif , Shahid Mahboob , Khalid A. Al-Ghanim , Muhammad Bilal and Muhammad Zohaib Nawaz, "*A Molecular Docking Approach to Evaluate the Pharmacological Properties of Natural and Synthetic Treatment Candidates for Use against Hypertension"*doi:10.3390/ijerph16060923, 2019.
2. Ruidan Wang, Xin Lu, Qiang Sun, Jinhong Gao, Lin Ma and Jinian Huang "*Novel ACE Inhibitory Peptides Derived from Simulated Gastrointestinal Digestion in Vitro of Sesame (Sesamum indicum L.) Protein and Molecular Docking Study"* doi: 10.3390/ijms21031059, 2020.
3. Chien-Hung Jhong1 Jirawat Riyaphan1 Shih-Hung Lin1 Yi-Chen Chia2 Ching-Feng Weng "*Screening alpha-glucosidase and alpha-amylase inhibitors from natural compounds by molecular docking in silico"* DOI No. 10.1002/biof.1219, 2015.
4. Waleed A. M. A. El-Enanya , Sobhi M. Gomhaa,b , Ahmed K El-Ziatyc , Wesam Husseinb , Mohamed M. Abdullad , Shaimaa A. Hassana , Hanan A. Sallamc , and Rania S. Ali. "*Synthesis and molecular docking of some new bis-thiadiazoles as anti-hypertensive a-blocking agents*" DOI: 10.1080/00397911.2019.1683207, 2019.
5. David O. Kennedy* and Emma L. Wightman "*Herbal Extracts and Phytochemicals: Plant Secondary Metabolites and the Enhancement of Human Brain Function"* doi:10.3945/an.110.000117, 2011.
6. Suzanne Oparil, Roland E. Schmieder "*New Approaches in the Treatment of Hypertension"*. DOI: 10.1161/CIRCRESAHA.116.303603. 2015.
7. Frishman WH, Kotob F. "*Alpha-adrenergic blocking drugs in clinical medicine. J Clin Pharmacol"*. 1999 Jan; 39(1):7-16. [PubMed]
8. Nash DT. "*Alpha-adrenergic blockers: mechanism of action, blood pressure control, and effects of lipoprotein metabolism"*. Clin Cardiol. 1990 Nov; 13(11):764-72. [PubMed]
9. Nash DT. "*Alpha-adrenergic blockers: mechanism of action, blood pressure control, and effects of lipoprotein metabolism"*. Clin Cardiol. 1990.

10. , Muhammad Hassan. "*National Institute of Diabetes and Digestive and Kidney Diseases; Bethesda (MD)"* Jan 8, 2018. Alpha 1 Adrenergic Receptor Antagonists. [PubMed]
11. Frishman WH, Kotob F "*Alpha-adrenergic blocking drugs in clinical medicine. J Clin Pharmacol"*. 1999 Jan; 39(1):7-16. [PubMed]
12. Ramirez J. "*Severe hypotension associated with α blocker tamsulosin"*. BMJ. 2013 Nov 05; 347:f6492. [PubMed]
13. Arnold AC, Raj SR. "*Orthostatic Hypotension: A Practical Approach to Investigation and Management"*. Can J Cardiol. 2017 Dec; 33(12):1725-1728. [PMC free article] [PubMed]
14. https://my.clevelandclinic.org/health/treatments/22321-alpha-blockers
15. Turner, S.; Myers, M.; Gadie, B.; Hale, S. A.; Horsley, A.; Nelson, A. J.; Pape, R.; Saville, J. F.; Doxey, J. C.; Berridge, T. L. J. Med. Chem. 1988, 31, 906. DOI: 10.1021/ jm00400a004.
16. Hansson L, Zanchetti A, Carruthers SG, Dahlöf B, Elmfeldt D, Julius S, Ménard J, Rahn KH, and Wedel H, Westerling S *"Effects of intensive bloodpressure lowering and low-dose aspirin in patients with hypertension: principal results of the Hypertension Optimal Treatment (HOT) randomized trial"*. Lancet 1998, 351:1755-1762.
17. Rouzaud-Laborde, C.; Lafitte, P.; Balardy, L.; Czosnyka, Z.; Schmidt, E.A. "*ICP and Antihypertensive Drugs"*. In Acta Neurochirurgica, Supplementum; Springer: Cham, Switzerland, 2018; Volume 126, pp. 163–165. ISBN 9783319657981
18. Shin-ichiro Miura1, 2, 3, Atsutoshi Okabe4, Yoshino Matsuo1, Sadashiva S Karnik3 and Keijiro Saku "*Unique binding behavior of the recently approved angiotensin II receptor blocker azilsartan compared with that of candesartan"* doi:10.1038/hr.2012.147 2022.
19. Huda Mando, Ahmad Hassan, Nathalie Moussa "*Flavonoids in Benign Prostate Hypertrophy: Identification in Herbal Preparations and Molecular Docking Approach*" doi.org/10.33263/BRIAC126.83078323. 2021.
20. https://www.bensnaturalhealth.com/blog/natural-alpha-blockers
21. Bajorath, J. "*Integration of virtual and high-throughput screening"*. Nat. Rev. Drug Discovery. 2002, 1, 882. [CrossRef]
22. Jorgensen, W.L. "*The many roles of computation in drug discovery"*. Science 2004, 303, 1813–1818. [CrossRef]

23. Kuntz, I.D.; Blaney, J.M.; Oatley, S.J.; Langridge, R.; Ferrin, T.E. "*A geometric approach to macromolecule-ligand interactions"*. J. Mol. Biol. 1982, 161, 269–288.
24. Kalyaanamoorthy, S.; Chen, Y.-P.P. "*Structure-based drug design to augment hit discovery"*. Drug Discovery. Today 2011, 16, 831–839. [CrossRef]
25. https://www.medicalnewstoday.com/articles/321231
26. Jayadeepa, R.M.; Sharma, S. "*Computational Models for 5αR Inhibitors for Treatment of Prostate Cancer: Review of Previous Works and Screening of Natural Inhibitors of 5αR2"*. Current computer-aided drug design 2011, 7, 231-237, https://doi.org/10.2174/157340911798260368.
27. Xiao, Q.; *Wang, L.; Supekar, S.; Shen, T.; Liu, H.; Ye, F.; Huang, J.; Fan, H.; Wei, Z.; Zhang, C. "Structure of human steroid 5α-reductase 2 with the anti-androgen drug finasteride"*. Nature Communications 2020, 11, https://doi.org/10.1038/s41467-020-19249-z.
28. Maestro 9.9. Schrödinger, LLC. New York: 2019. https://www.schrodinger.com/maestro. (Accessed on 15 September 2021).
29. Syed Sauban Ghani, S.S. *"A comprehensive review of database resources in chemistry"*. Eclética Química Journal 2020, 45, 57-68, https://doi.org/10.26850/1678-4618eqj.v45.3.2020.p57-68.
30. O'Boyle, N.M.; Banck, M.; James, C.A.; et al. Open Babel: An open chemical toolbox. J Cheminform 2011, 3, 33. https://doi.org/10.1186/1758-2946-3-33.
31. Harder, E.; Damm, W.; Maple, J.; Wu, C.; Reboul, M.; Xiang, J.Y. OPLS3*: "A force field providing broad coverage of drug-like small molecules and proteins"*. J. Chem. Theor. Comput. 2016, 12, 281–296, https://doi.org/10.1021/acs.jctc.5b00864.
32. . Storer, J.W.; Giesen, D.J.; Cramer, C.J.; Truhlar, D.G. Class IV charge models: "*A new semi empirical approach in quantum chemistry"*. J. Comput. Aided Mol. Des 1995, 9, 87–110, https://doi.org/10.1007/BF00117280.
33. Madhavi, S.G.; Adzhigirey, M.; Day, T.; Annabhimoju, R.; Sherman, W. "*Protein and ligand preparation: parameters, protocols, and influence on virtual screening enrichments"*, J. Comput. Aided Mol. Des. 2013, 27, 221–234, https://doi.org/10.1007/s10822-013-9644-8.
34. Xiao, Q.; Wang, L.; Supekar, S.; Shen, T.; Liu, H.; Ye, F.; Huang, J.; Fan, H.; Wei, Z.; Zhang, C. "*Structure of human steroid 5α-reductase 2 with the anti-androgen drug finasteride"*. Nature Communications 2020, 11, https://doi.org/10.1038/s41467-020-19249-z.

35. Friesner, R.A.; Banks, J.L.; Murphy, R.B.; Halgren, T.A.; Klicic, J.J.; Mainz, D.T.; Repasky, M.P.; Knoll, E.H.; Shelley, M.; Perry, J.K.; Shaw, D.E.; Francis, P.; Shenkin, P.S. Glide: "*A New Approach for Rapid, Accurate Docking and Scoring. 1. Method and Assessment of Docking Accuracy"*. Journal of Medicinal Chemistry 2004, 47, 1739-1749, https://doi.org/10.1021/jm0306430.
36. Wang, X.; Qian, Y.; Li, X.; Jia, X.; Yan, Z.; Han, M.; Qiao, M.; Ma, X.; Chu, Y.; Zhou, S.; Yang, W. "*Rapid determination of rosmarinic acid and its two bioactive metabolites in the plasma of rats by LC–MS/MS and application to a pharmacokinetics study. Biomed"*. Chromatogr. 2021, 35, https://doi.org/10.1002/bmc.4984.
37. Simirgiotis, M.J.; Benites, J.; Areche, C.; Sepúlveda, B. *"Antioxidant Capacities and Analysis of Phenolic Compounds in Three Endemic Nolana Species by HPLC-PDA-ESI-MS"*. Molecules 2015, 20, 11490-507, https://doi.org/10.3390/molecules200611490.
38. Chen, G.; Li, X.; Saleri, F.; Guo, M. "*Analysis of Flavonoids in Rhamnus davurica and Its Anti-proliferative Activities"*. Molecules 2016, 21, https://doi.org/10.3390/molecules21101275.
39. Tatar, G.; Salmanli, M.; Dogru, Y.; Tuzuner, T. *"Evaluation of the effects of chlorhexidine and several flavonoids as antiviral purposes on SARS-CoV-2 main protease: molecular docking, molecular dynamics simulation studies"*. Journal of Biomolecular Structure and Dynamics 2021, 1-10, https://doi.org/10.1080/07391102.2021.1900919.
40. Foddai, M.; Maldini, M.; Addis, R.; Petretto, G.L.; Chessa, M.; Pintore, G. "*Profiling of the Bioactive Compounds in Flowers, Leaves and Roots of Vinca sardoa"*. Natural Product Communications 2017, 12, https://doi.org/10.1177/1934578X1701200625.
41. Sun, J.; Liang, F.; Bin, Y.; Li, P.; Duan, C. "*Screening Non-colored Phenolics in Red Wines using Liquid Chromatography/Ultraviolet and Mass Spectrometry/Mass Spectrometry Libraries".* Molecules 2007, 12, 679- 693, https://doi.org/10.3390/12030679.
42. Xu, F.; Liu, Y.; Zhang, Z.; Yang, C.; Tian, Y. "*Quasi-MSn identification of flavanone 7-glycoside isomers in Da Chengqi Tang by high performance liquid chromatography-tandem mass spectrometry"*. Chinese Medicine 2009, 4, https://doi.org/10.1186/1749-8546-4-15.
43. Jung, U.J.; Kim, H.J.; Lee, J.S.; Lee, M.K.; Kim, H.O.; Park, E.J.; Kim, H.K.; Jeong, T.S.; Choi, M.S. "*Naringin supplementation lowers plasma lipids and enhances*

erythrocyte antioxidant enzyme activities in hypercholesterolemic subjects". Clinical Nutrition 2003, 22, 561-568, https://doi.org/10.1016/s0261- 5614(03)00059-1.

44. Renugadevi, J.; Prabu, S.M. "*Naringenin protects against cadmium-induced oxidative renal dysfunction in rats"*. Toxicology 2009, 256, 128-134, https://doi.org/10.1016/j.tox.2008.11.012
45. Den Hartogh, D.J.; Tsiani, E. "*Antidiabetic Properties of Naringenin: A Citrus Fruit Polyphenol"*. Biomolecules 2019, 9, 1–21, https://doi.org/10.3390/biom9030099.
46. www.pubchem.com.

Comparative study of green synthesised hydrogels, its characterization and antibacterial activity

A project submitted to

ST.MARYS COLLEGE (Autonomous), THOOTHUKUDI

Affiliated to

Mononmaniam Sundaranar University, Thirunelveli

In partial fulfilment of the award of the degree of

MASTER OF SCIENCE IN CHEMISTRY

Submitted by

PONSELVI.S

Reg No.21SPCH06

Under the supervision and guidance

Mrs. D. CAROLIN JENBIA RACHEL M.Sc., M.Phil, SET

PG DEPARTMENT OF CHEMISTRY (SSC)

St. Mary's College (Autonomous), Thoothukudi

April-2023

CERTIFICATE

This is to certify that this project work entitle "**Comparative study of green synthesised hydrogels, its characterization and antibacterial activity**" is submitted to **St. Mary's College (Autonomous), Thoothukudi** affiliated to **Manonmanium Sundaranar University Tirunelveli** in partial fulfillment for the award of the **Degree of Master of Science in Chemistry** and work done during the year 2021-2023 by **PONSELVI .S (Reg. No: 21SPCH06)**

5/4/23

Signature of the Guide

5/4/23

Signature of the Coordinator

Dr. J. ANTONY RAJAM, M.Sc., M.Phil., Ph.D., SET.
SSC Co-ordinator & Asst. Professor
PG Department of Chemistry
St. Mary's College (Autonomous)
Thoothukudi - 628 001.

Signature of the Director

Director
Self Supporting Courses
St. Mary's College (Autonomous)
Thoothukudi - 628 001.

Signature of the Principal

Principal
St. Mary's College (Autonomous)
Thoothukudi - 628 001.

Signature of the Examiner

13/4/23

DECLARATION

I do hereby declare that the project entitled "Comparative Study of green Synthesised hydrogels, its Characterization and Antibacterial activity"submitted for the degree of Master of Science in Chemistry is my original work carried out under the guidance of Under the supervision and guidance **Mrs. D. Carolin Jeniba Rachel M.Sc., M.Phil., SET., Assistant Professor, PG Department of Chemistry (SSC), St. Mary's College (Autonomous), Thoothukudi** and that it has not previously formed the basis for award of any degree.

S. Ponselvi

Ponselvi.S

Station: Thoothukudi

Date: 05.04.23

ACKNOWLEDGEMENT

I express my first and humble thanks to GOD ALMIGHTY for giving an opportunity to devote to this work.

I would like to express my sincere thanks to our secretary **Dr. Sr. C. SHIBANA** our Secretary, **Dr.Sr. A.S.J. LUCIA ROSE**, our Principal, **Rev. Sr. JOSEPHINE JEYARANI** Director of SSC, **Dr J.ANTONY RAJAM**, **M.Sc., M.phil, PhD**, Coordinator of SSC (Department of Chemistry), St. Mary's College (Autonomous), Thoothukudi for providing the permission to complete the project work.

I find it difficult for me to write something in short to acknowledge my guide **Mrs.D.CAROLIN JENIBA RACHEL M.Sc., M.phil, SET,** she taught me to think and solve the unconventional problem in a conventional way. Her constant inspiration, evaluable guidance tremendous patience and constructive criticism helped a lot to focus my views in the proper perspective. I take this opportunity to express my deepest sense of gratitude and reference towards her for guiding me in the right direction throughout the course of this work. My deep personal regards are due for her forever.

I would be ungrateful if I forget to thank **Dr.S.GURUSAMY,** V.O.C. College for giving full support and timely help during the course project.

My parents have given me a lot of love, care, encouragement, and financial help to finish my MSc project. I couldn't have completed my task as quickly as I did without the support of my friends. My parents and friends deserve my deepest gratitude.

CONTENT

ABSTRACT

Almond gum and Flax seed is documented as the world's oldest food source with exceptional medical, chemical, physical, and pharmaceutical values. They can be derived from natural or synthetic sources and are being extensively explored for their potential in tissue engineering , wound dressing , biosensors and drug delivery devices Polysaccharide base Hydrogel networks of cross-linked Hydrogel was synthesized through an redox initiating free radical polymerization utilizing almond gum and Flaxseed as a grafting backbone, Borax as the cross linker and Potassium persulphate, N,N,N',N'-tetramethyl ethylenediamine (TEMED) as the redox initiator pair. The both almond gum and Flax seed containing carbohydrates as a major component Hydrogel nanoparticals were characterized using several techniques such as UV-Visible, FT-IR, SEM, EDAX, XRD and TGA .The anti-bacterial study was also studied. The UV-Visible shows peak at 326nm for almond gum and 342nm for Flax seed. The SEM image shows the rocky structure of the prepared nanoparticle. The XRD result concludes the average size of Hydrogel nanoparticals as 2.4280nm and 2.4315nm respectively. The antibacterial effect studies show that the nanoparticle has good zone inhibition against the selected pathogens. The Hydrogel nanoparticle synthesis provides a simple, cost effective, reproducible, rapid, and safe method with numerous applications.

Keywords: Hydrogel nanoparticals, Flaxseeds and Almond gum.

CHAPTER 1

INTRODUCTION

1. HYDROGEL

Hydrogel, a polymeric material, has ability to incorporate large amounts of water in its three-dimensional networks. The first Hydrogel was reported in 1960 and prepared using 1, 2- ethanediol dimethacrylate and glycol methacrylate [1]. Smart Hydrogel has a strong response to volume, elasticity, viscosity, moisture, refraction index, colloidal stability, hardness, and other changes in terms of external conditions such as temperature, pH, ionic strength, pressure and electric field. Therefore, it has good application aspects in medical devices, tissue engineering, biosensors, separation systems and energy conversion systems [2]. If, as an interactive wound dressing, it can not only provide a moist condition, but also automatically adjust according to the physiological condition of the wound, forming a micro environment conducive to wound healing[3]. Generally, hydrogels can be synthesized via physical or chemical approach. The chemical approach may produce hydrogel with a higher mechanical strength compare to physicalapproach, of which cross-linking reaction is an effective chemical approach [4]. Hydrogel have been widely used in wound dressings, drug delivery, oil/water separation, sewage treatment, seedcultivation, and other fields for their good biocompatibility and biodegradability. The LCP super-absorbent hydrogels with excellent swelling and water retention properties are very promising for applications in the fields of commercial diapers, soil water retention and seed cultivation in agriculture, and dye pollutant removal [5]. Smart materials include hydrogel. The repeated monomers like photopolymers or copolymers containing hydrophilic polymer chains lead to the formation of hydrogel and these monomers are arranged in different ways, as shown in Figure1 .[6]

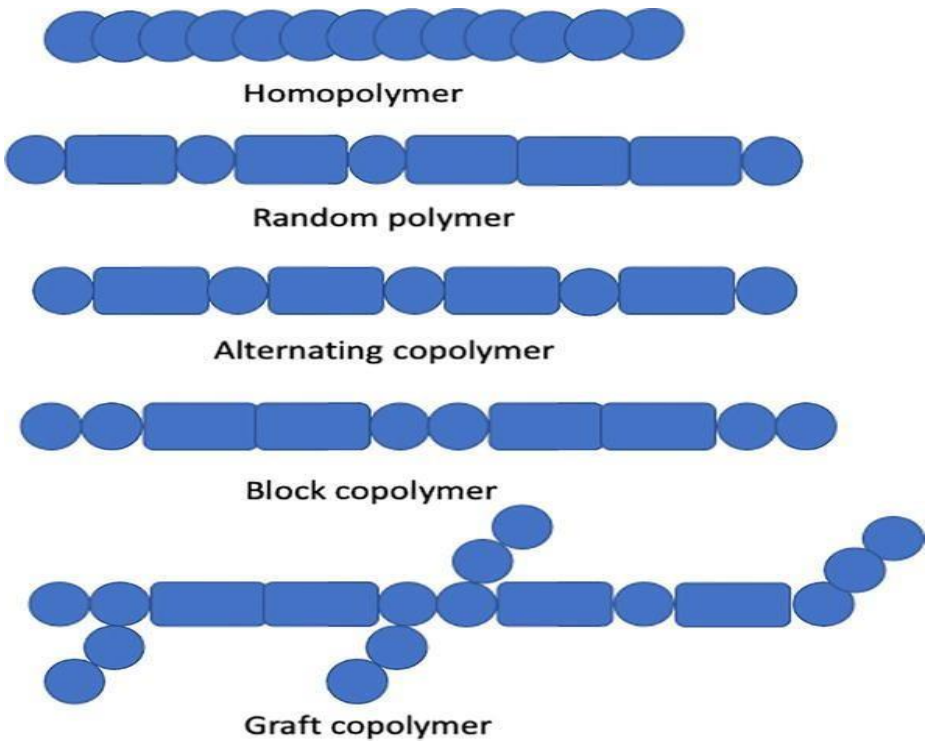

Fig 1.1 Different arrangement of monomer in hydrogel

1.2. Types of Hydrogel

- Physical Cross linked Hydrogel
- Chemically Cross linked Hydrogel
- Interpenetrating Network (IPN) Hydrogel

1.2.1. Physical Cross linked Hydrogel

Polymer networks should meet the following conditions to form hydrogel (a) strong inter-chain interactions in order to form a stable colligation in the molecular network, and (b) the polymer network must encourage the access and residence of water within the hydrogel.Hydrogel fulfilling these demands may, perhaps, be prepared by non-covalent approaches, such as electrostatic, hydrogen bonding, and hydrophobic forces among polymer

chains. The hydrogel formed by these interactions are solely physical gels and have high water sensitivity and thermo-reversibility [7].

1.2.2. Chemically Cross linked Hydrogel

The formation of physical gels through clustering of molecules causes formation of free chain loops and thus in homogeneity that signifies Short-lived network imperfections. Chemical cross linked hydrogel networks are easy to control as compared to physical hydrogel because their synthesis and applications are not only dependent on pHs. Chemical cross linking can be used to transform the physical properties of the hydrogel.[8]

1.2.3. Interpenetrating Network (IPN) Hydrogel

Cross linked polymer networks can be supplementary reinforced by interlocking secondary polymers within the entangled networks [9]. A polymer comprising of two or more networks, which are at least partially interlaced at a molecular scale but not covalently bonded toeach other and cannot be separated unless chemical bonds are broken, is known as an interpenetrating polymer network (IPN) [10].

1.3. Properties of hydrogel

The use of polymers (natural or synthetic) containing hydrophilic pendant groups' to synthesize hydrogel for biomedical applications is greatly advantageous because these hydrophilic groups not only facilitate ample water absorption but also assist in the interaction with biological tissues (epithelial tissues and mucous membranes. Normally, hydrogel in the fully swollen state are nearly viscoelastic, soft, rubbery, and low in interfacial angle withbiological fluids, which decreases the chances of a negative immune response. All these factors contribute to the biocompatibility of hydrogel. The hydrogel are also normally degradable to different extents, depending upon the type of cross linker involved. Furthermore, hydrogel have a swelling property, which is the most significant one in their existence. The swelling of hydrogel takes place in three steps [11] such as

1) Diffusion of water into the hydrogel network (water moving in is called primary bound water)
2) Relaxation of polymer chains (more water moving in is called secondary bound water).
3) Expansion of the hydrogel network (additional water moving in is termed as free water).According to the Flory–Reihner theory, swelling is a function of the elastic nature of the polymer chains and their compatibility with water molecules.

Hydrogel show different responses to changes in environmental stimuli, which may generally be categorized into (i) physical (temperature, light, etc.) (ii) chemical (pH and ionic strength) and (iii) biological (enzymes) stimuli. Chemical and biological stimuli are internal, whereas physical stimuli are external, except for temperature, which may be external or internal. Besides all this, there is a special type of stimulus-responsive smart hydrogel called shape memory hydrogel, with two characteristics: (i) permanent shape and (ii) a chemical or physical code that can help restore its original shape [12]

1.4. Hydrogel product sensitive to environmental conditions

As mentioned above, hydrogel as three-dimensional cross linked hydrophilic polymer networks are capable of swelling or de-swelling reversibly in water and retaining large volume of liquid in swollen state .Hydrogel can be designed with controllable responses as to shrink or expand with changes in external environmental conditions. They may perform dramatic volume transition in response to a variety of physical and chemical stimuli, where the physical stimuli include temperature, electric or magnetic field, light, pressure, and sound, while the chemical stimuli include pH, solvent composition, ionic strength, and molecular species (fig.2). The extent of swelling or de-swelling in response to the changes in the external environment of the hydrogel could be so drastic that the phenomenon is referred to as volume collapse or phase transition [13].

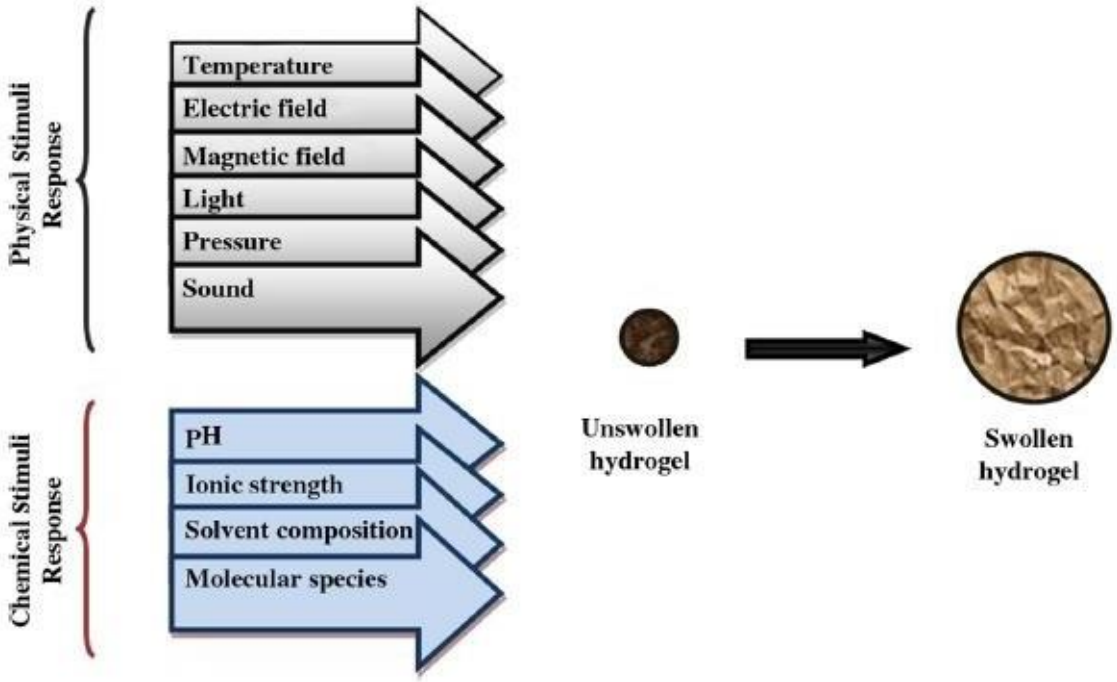

Fig1.2 Hydrogel preparation by different methods

1.5. Technologies adopted in hydrogel preparation

By definition, hydrogel are polymer networks having hydrophilic properties. While hydrogel are generally prepared based on hydrophilic monomers, hydrophobic monomers are sometimes used in hydrogel preparation to regulate the properties for specific applications .In general, Hydrogel can be prepared from either synthetic polymers or natural polymers. The synthetic polymers are hydrophobic in nature and chemically stronger compared to natural polymers. Their mechanical strength results in slow degradation rate, but on the other hand, mechanical strength provides the durability as well. These two opposite properties should be balanced through optimal design [14].Also, it can be applied to preparation of Hydrogel based on natural polymers provided that these polymers have suitable functional groups or have been functionalized with radically polymerizable groups . In the most succinct sense, a hydrogel is simply a hydrophilic polymeric network cross-linked in some fashion to produce an elastic structure. Thus, any technique which can be used to create a cross-linked polymer can be used to

produce a hydrogel. Copolymerization/cross-linking free-radical polymerizations are commonly used to produce hydrogel by reacting hydrophilic monomers with multifunctional cross-linkers.

Water-soluble linear polymers of both natural and synthetic origin are cross-linked to form hydrogel in a number of ways

1. Linking polymer chains via chemical reaction.
2. Using ionizing radiation to generate main-chain free radicals which can recombine as cross-link junctions.
3. Physical interactions such as entanglements, electrostatics, and crystallite formation [15]

Hydrogel are usually prepared from polar monomers. According to their starting materials, they can be divided into natural polymer hydrogel, synthetic polymer hydrogel, and combinations of the two classes From a preparative point of view, they can be obtained by graft polymerization, cross-linking polymerization, networks formation of water-soluble polymer, and radiation cross-linking, etc.There are many types of hydrogel; mostly, they are lightly cross-linked copolymers of acryl ate and acrylic acid, and grafted starch-acrylic acid polymers prepared by inverse suspension, emulsion polymerization, and solution polymerization. The polymerization techniques have been described below. [16]

1.5.1. Bulk polymerization

Many vinyl monomers can potentially be used for the productions of hydrogel. Bulk hydrogel can be formed with one or more types of monomers. The wide variety of monomers enables one to prepare the hydrogel with desired physical properties for a given application [17]. Usually, a small amount of cross-linking agent is added in any hydrogel formulation. The polymerization reaction is normally initiated with radiation, ultraviolet, or chemical catalysts. The choice of a suitable initiator depends upon the type of monomers and solvents being used. The polymerized hydrogel may be produced in a wide variety of forms including films and membranes, rods, particles, and emulsions (Fig. 3) [18].

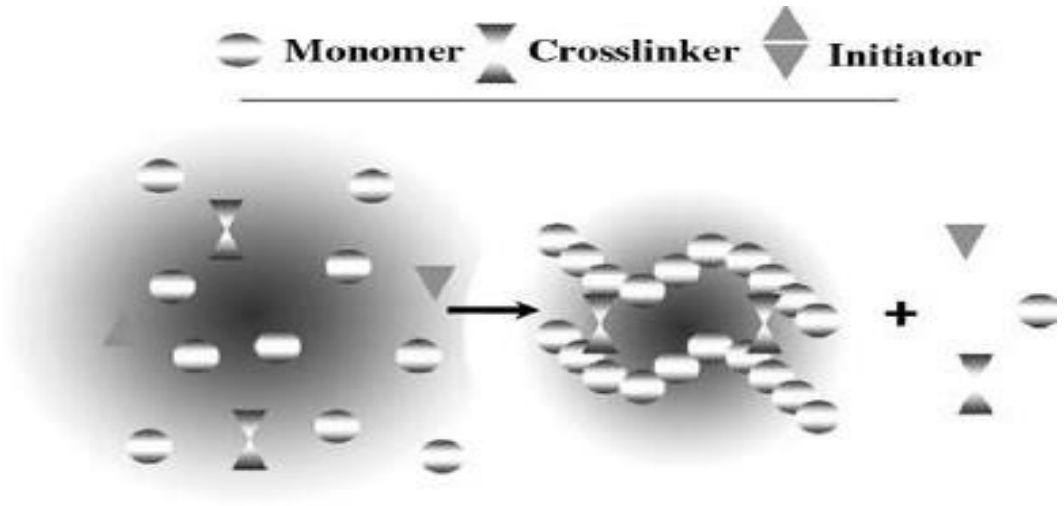

Figure 1.3 Schematic diagram of hydrogel preparation.

1.5.2. Solution polymerization/cross-linking

In solution copolymerization/cross-linking reactions, the ionic or neutral monomers are mixed with the multifunctional cross linking agent. The polymerization is initiated thermally by UV-irradiation or by a redox initiator system. The presence of solvent serving as a heat sink is the major advantage of the solution polymerization over the bulk polymerization. The prepared hydrogel need to be washed with distilled water to remove the monomers, oligomers, cross-linking agent, the initiator, the soluble and extractable polymer, and other impurities. Phase separation occurs and the heterogeneous hydrogel is formed when the amount of water during polymerization is more than the water content corresponding to the equilibrium swelling. Typical solvents used for solution polymerization of hydrogel include water, ethanol, water–ethanol mixtures, and benzyl alcohol. The synthesis solvent may then be removed after formation of the gel by swelling the hydrogel in water [19].

1.6. Hydrogel technical features

- ✓ The highest absorption capacity (maximum equilibrium swelling) in saline.
- ✓ Desired rate of absorption (preferred particle size and porosity) depending on the application requirement.

- ✓ The highest absorbency under load (AUL).
- ✓ The lowest soluble content and residual monomer.
- ✓ The lowest price.
- ✓ The highest durability and stability in the swelling environment and during the storage.
- ✓ The highest biodegradability without formation of toxic species following the degradation.
- ✓ PH-neutrality after swelling in water.
- ✓ Colorlessness, absolute non-toxic and photo stability.
- ✓ Re-wetting capability (if required) the hydrogel has to be able to give back the imbibed solution or to maintain it depending on the application requirement (e.g., in agricultural or hygienic applications).[20]

1.7. Almond Gum

A natural gum, Almond Pisin, is obtained from an almond tree. Also known as almond gum and Almond gondh, Almond Pisin has myriad health benefits. Indigenous to Southwestern Asia and Iran, the sweet almond tree from which Almond Pisin is extracted is found in India and Pakistan. Among the natural polymers, polysaccharides in particular have some remarkable characteristics and considerable research has been directed towards them for the production of hydrogel [21].

Fig 1.4 Almond Gum

Carbohydrates of the almond gum are mainly constituted of arabinose, xylitol, galactose and uronic acid with traces of rhamnose, mannose and glucose, thus suggesting an arabinogalactan structure of the gum. It is cheap and has many properties that have generated interest in its use such as water binding capacity, biodegradability biocompatibility, non-toxicity,bioactivity, metal uptake & fat binding capacity and antimicrobial activity [22].

1.8. Flaxseed

Flaxseed comes from the flax plant (also known as *Linum usitatissimum*), which grows to be about 2 feet tall. It likely was first grown in Egypt but has been cultivated all around the world. Flaxseed gum, i.e. a by-product of the flaxseed oil industry, has received much attention as an emerging hydrocolloid due to its techno functional versatility, environmental sustainability,low cost, as well as high biocompatibility and biodegradability [23].

Fig 1.5 Flax seed

Although the chemical composition and structure conformational properties of flaxseed gum can vary on its genotypic and phenotypic characteristics, the extraction, isolation and purification conditions are also well known for impacting its proximate and acidic composition and consecutively, its techno functional profile Hitherto, flaxseed gum has been successfully employed in producing food composites due to its prevalent thickening and gelling capacity In protein-rich hydrogel-based food systems, the stabilizing, structurising and texturising effectiveness of flaxseed gum depends on its colloidal interactions with proteins as influenced by extrinsic factors such as the ionic strength, pH and temperature [24].

CHAPTER 2

LITERATURE SURVEY

- Kang Liu et al., (2021) studied "Research progress on polysaccharide/protein hydrogels: Preparation method, functional property and application as delivery systems for bioactive ingredients" [9] some bioactive ingredients in foods are unstable and easily degraded during processing, storage, transportation and digestion. To enhance the stability and bioavailability, some food hydrogels have been developed to encapsulate these unstable compounds. In this paper, the preparation methods, formation mechanisms, physicochemical and functional properties of some protein hydrogels, polysaccharide hydrogels and protein-polysaccharide composite hydrogels were comprehensively summarized. Since the hydrogels have the ability to control the release and enhance the bioavailability of bioactive ingredients, the encapsulation and release mechanisms of polyphenols, flavonoids, carotenoids, vitamins and probiotics by hydrogels were further discussed. This review will provide a comprehensive reference for the deep application of polysaccharide/protein hydrogels in food industry.

- Yicheng Wang,et al (2021) studied "Preparation of shaped non-polyelectrolyte hydrogel particles with decomposable and recyclable performance by vortex ring freezing"[25] The vortex-ring derived particles are new type of non-spherical hydrogel particles, which are prepared by imitating the process of vortex-ring in nature. However, the traditional existing vorticity ring derived hydrogel particles were prepared by dropping polyelectrolyte solution into contra-ion coagulation bath, which limited the choice of materials. In this paper, a strategy of preparation non-spherical hydrogel particles by using non-polyelectrolyte polyvinyl alcohol through the method of vortex ring was proposed. Based on the principle that the boraciated polyvinyl alcohol solution could be quickly gelled under alkaline condition, the spherical and various derivative shapes (red cell, bowl, dish, ring) of polyvinyl alcohol vortex-ring derived hydrogel particles (PVHP) were prepared. The hydrogel particles have the ability to assemble into different modules by dynamic borate bond in the hydrogel particles. Also, this dynamic

borate bond endowed the PVHP decomposable and recyclable performances. In addition, two-compartments, three-compartments and magnetic PVHP were also prepared, endowing PVHP with several functions. which opens up a new environmentally friendly way for the preparation of multifunctional particles.

- Vasanthi Sethu et al (2020) studied " Performance study of chia seeds, chia flour and *Mimosa pudica* hydrogel as polysaccharide-based superabsorbent polymers for sanitary napkins" [1] This research reports the development and characterisation of three types of natural polysaccharide-based Superabsorbent polymers (SAPs) for application in sanitary napkins, namely chia seeds (*Salvia hispanica* L.), chia flour and *Mimosa pudica* hydrogel (MPH). Physical properties and performances of the materials were tested to determine the absorbing capacity, swelling capacity, absorbency under load and re-wet under load capacities. Antibacterial tests against *Staphylococcus aureus* and *Escherichia coli* and biodegradability tests were also carried out. Characterisation was carried out with Fourier transform infrared spectroscopy, field emission scanning electron microscope, energy dispersive X-ray spectroscopy and thermo gravimetric analysis. The results reveal that MPH had the highest absorbing capacity, at 5.24 g/g and lowest re-wet value, at 1.58 g, indicating MPH is a better SAP compared to chia seeds and chia flour. Scanning electron images of MPH revealed the macroporous structure of MPH with hollow channels that allow quick transportation of liquid. Antibacterial tests and biodegradability tests results indicate that MPH has potential antibacterial properties and biodegradability. Results of this work indicate that MPH has the highest potential to be used as SAP in sanitary napkins whencompared to chia seeds and chia flour.

- Bo Jiang et al (2020) studied "Preparation of gelatin/poly (γ-glutamic acid) hydrogels with stimulated response by hot-pressing preassembly and radiation crosslinking"[26] The conventional preparation method of natural polymers is low in strength, which limits the application ofmulti stimuli responsive hydrogels as intelligent wound dressings. In this work, interpenetrating gelatin and γ-polyglutamic acid (γ-PGA) hydrogels with good biocompatibility, biodegradability and mechanical properties were prepared by hot-pressing pre-gelation of gelatin/γ-PGA and synergistic with gamma irradiation. The effects of radiation crosslinking

dosage on gel fraction, swelling ratio, tensile strength and surface morphology were investigated. The biocompatibility of radiation cross-linked hydrogel was evaluated by aseptic test, hemolysis test, cytotoxicity test, delayed hypersensitivity reaction as well as in vivo degradation studies from in vitro to in vivo. The optimized hydrogel irradiated by 25 kGy has good water retention and biodegradability, especially the stimulation of temperature, pH value, salt species and concentration. The mechanical strength, biocompatibility and responsive properties of the hydrogel indicate that the intelligent hydrogel prepared by this method is a good hydrogel biomaterial for developing interactive wound dressing.

- Bao Zhang at al(2020) studied "Preparation, characterization, and encapsulation capability of the hydrogel cross-linked by esterified tapioca starch" [27]The modified starch-based hydrogels were prepared by crosslinking modified starch with sodium trimetaphosphate. Modified starch was obtained by esterification of tapioca starch with maleic anhydride. The degree of substitution (DS) increased significantly from 0.078 to 0.258 as the content of maleic anhydride increased from6.67% to 33.33%. Fourier transforminfrared spectroscopy demonstrated that starchwas successful esterified. In addition, the thermal properties of modified starch-based hydrogels were investigated by differential scanning calorimeter and thermogravimetry analysis,which proved that hydrogels had better thermal stability. Esterified starch-based hydrogels showed excellent pH sensitivity bymeasuring of swelling degree.When DS was 0.250, the adsorption capacity and encapsulation efficiency of starch-based hydrogels were
  399.23 μg/g and 80%, respectively, which exhibited satisfactory embedding properties for curcumin. Therefore, esterified tapioca starch-based hydrogels could be as the encapsulatingmaterials to protect bioactive substances, which provided a theoretical basis for their application in food field and pharmaceuticals industry

- Hirofumi Satani, at al (2020) studied "Simple and environmentally friendly preparation of cellulose hydrogels using an ionic liquid" [28] In this study, we developed an easy process for the production of cellulose hydrogels over a wide concentration range by using an ionic liquid/DMSO mixed solution that can easily be recycled at room temperature and has low environmental impact. Cellulose was completely dissolved at 6 to 20 wt% with respect to the [BMIm][OAc]/DMSO mixed solution at room temperature and ambient pressure. Placing the cellulose solution in a mold and immersing it in deionized water caused solvent replacement of the [BMIm][OAc]/DMSO mixed solution with deionized water, making it easy to obtain a cellulose hydrogel without using a crosslinking agent. Approximately 80% of the ionic liquid could be reused by constructing a system that recovers the ionic liquid discharged from the cellulose solution during solvent replacement. The pore size, water content and mechanical strength of the cellulose hydrogel strongly depended on the concentration of the cellulose solution prepared using the [BMIm][OAc]/DMSO mixture. However, the crystallinity and thermal stability did not show a concentration dependence.

- Andrew Zannettinob et al (2020) studied " Hydrogel-based preparation of cell aggregates for biomedical applications"[29] Cell aggregates are widely used either as *in-vitro* models for drug screening, fundamental studies on disease progression and developmental biology, as well as *in-vivo* injectable cells for tissue regener- ation. Compared to single-cell suspensions, cell aggregates retain superior cell viability, mimic *in-vivo* microenvironments and enhance functional properties, such as superior anti-inflammatory properties of mesenchymal stem/stromal cell aggregates or enhanced albumin production by hepatocyte aggregates. Cell aggregates can be either prepared by conventional spontaneous aggregation, or advanced substrate- based and technology-assisted methods, which have been well described in previous reviews. However, hydrogel-based preparation of cell aggregates is a novel, hitherto rarely considered method compared to conventional preparation of cell aggregates, such as hanging drops and commercial AggreWell TM plates. This review will mainly focus on two- dimensional (2D) hydrogel surface -based and three-dimensional (3D) hydrogel embedding- based preparation of cell aggregates by revealing the underlying mechanisms and highlighting some of their potential biomedical applications

- Changkun Liu et al (2020) studied "Simple preparation of external-shape and internal-channel size adjustable porous hydrogels by fermentation for efficient solar interfacial evaporation" [30] Solar interfacial evaporation is a promising technology for the purification of seawater and polluted water using sustainable solar energy. An adjustable shape and internal-channel size of photothermal evaporation material are essential for regulating heat utilization and water supply rate to three-dimensional (3D) evaporation device. However, a simple method for the preparation process is rarely reported to date. Inspired by bread making, a straightforward fermentation method is applied to the preparation of adjustable porous hydrogel as photothermalevaporation materials. It only takes 40 min to ferment and three simple freeze-thawing cycles to construct the final hydrogel materials. A mold can be used to easily adjust the external shape of the fermentation porous hydrogels (FPHs). The internal-channel size of FPHs can be simply tuned by the fermentation time. The flexible porous structure endows FPHs with excellent photothermal evaporation capability and makes it easy to meet the requirements of water supplyrates under the light intensity of different latitudes for water treatment.

- Osman Duman, et al (2020) studied "Preparation and characterization of environmentally friendly agar/κ- carrageenan/montmorillonite nanocomposite hydrogels"[31] In the present study, for the first time, agar/κ-carrageenan and agar/κ-carrageenan/montmorillonite hydrogel materials were prepared by the free-radical crosslinking reaction of agar and κ-carrageenan in the presence of triethylene glycol divinyl ether (TEGDE) as the crosslinker agent. Here, montmorillonite (MMT) modified with phenylalanine was used as additive agent. Agar/κ- carrageenan hydrogel materials with and without MMT wer characterized by FTIR, SEM and XRD analyses. The effect of free radical initiator (ammonium persulfate, APS) concentration, crosslinking agent (TEGDE) concentration, reaction temperature, polysaccharide ratio and MMT concentration on the swelling performance and surface property of hydrogel material wasinvestigated and optimum reaction conditions were determined. Maximum equilibrium swelling capacity of the agar/κ-carrageenan hydrogel was found to be 2523 % under the optimum conditions ([APS]=5×10−4 M [TEGDE]=5×10−4 M, T=70 °C and magar:mκ- carrageenan=1:4). An increase of the MMT content within hyrogel matrix led to a decrease in

the swelling values of hydrogels. All of the hydrogels prepared in various formulations exhibited non-Fickian swelling behavior. New hydrogel materials obtained from this study could be potential candidates for biomedical applications.

- N. Ramadhan et al (2019) studied "Preparation of Chitosan-EDTA hydrogel as soil conditioner for soybean plant (Glycine max)" [32] Research on preparation of chitosan hydrogel cross linked with Ethylenediaminetetraacetic acid (EDTA) as soil conditioner for soybean (*Glycine* max L.) plants was successfully carried out. The aims of study are to determine the characteristics and effect of composition comparisons in preparation of hydrogels and to determine the physicochemical properties of soil such as humidity, temperature, pH, absorbed potassium levels, C-organic content and cation exchange capacity. The characterization was carried out using FTIR and SEM. FTIR analysis showed specific the presence of functional groups, O-H (3450.65), CH3 (2924.09), COOH (1382.96), N-H2 (1587.42), and C– – O amide (1635.64). SEM analysis shows the hydrogel surface in each composition and concentration of chitosan-EDTA of different pore or cavity sizes so that it influences the degree of swelling and crosslinking degree. The application of chitosan-EDTA hydrogel for the improvement of soybean plants with a composition of CHITA225 can have a significant influences on the 75th day of measurement. The soil pH values between 7.6 and 7.9, humidity of 31%, soil temperature of around 26–29 C, absorbed potassium levels of 11.29 ppm, soil organic contentof 2.56%, and cation exchange capacity of 17.22 meq/100 g. In addition, the effect of hydrogel use on soybean plants shows the maximum number of leaves measured at 60 days, 98.2 cm and 25 strands. The results showed that the hydrogel synthesized by chitosan and EDTA has the potential as soil conditioner.

- Yasuhiko Tabata et al (2019) studied "Preparation of fibrin hydrogels to promote the recruitment of anti-inflammatory macrophages"[33] Macrophages play an important role in regulating inflammation and tissue regeneration. In the present study, uniform fibrin hydrogel scaffolds were engineered in millimeters. These scaffolds induced anti-inflammatory macrophages to digest and infiltrate the scaffold. The culture conditions of the fibrin hydrogels decreased the secretion of tumor necrosis factor-a (TNF-a), a pro-inflammatory cytokine, and

increased the secretion of interleukin-10 (IL-10), an anti-inflammatory cytokine, in mouse bone marrow-derived macrophages. Similar results were also observed in human monocyte-derived macrophages (HMDMs). In addition, most of cells that infiltrated the fibrin hydrogels were macrophages expressing CD163, CD204, and CD206, which are anti-inflammatory macrophages markers, both in mice and in human cells. Therefore, to induce increased macrophage infiltration, we attempted to combine fibrin hydrogels with SEW2871, a monocyte/macrophage recruitment agent that is known to be a sphingosine-1 phosphate receptor 1 agonist, solubilized in water by micelle formation with a cholesterol-grafted gelatin. However, the fibrin hydrogels alone retained the same monocyte migration activity as the hydrogels with SEW2871-incorporated micelles in the hydrogel-bearing mouse model. These findings indicate that fibrin hydrogels have a strong promoting effect on the recruitment of anti- inflammatory macrophages. Therefore, fibrin hydrogels may be an optimal biomaterial in the design of medicines for macrophage-induced regenerative therapies.

- Kyoung Min Lee et al (2019) studied "One-step preparation of hydrogel particles that show rapid detection of hydrogen peroxide: The dual role of new methylene blue"[35] We report a synthetic platform that offers a facile preparation route for stimuli-responsive hydrogels via redox radical initiation. The initiation mechanism has been efficiently used for the formation of many synthetic hydrogels since the redox reaction readily generates radical species and polymerizes monomers. In this conceptual study, we have created stimuli-responsive hydrogel particles using a new methylene blue dye that plays a significant dual role as a radical activator and a reactive site. Therefore, the dye not only facilitated redox radical initiation for the formation of hydrogel particles, but also imparted them with sensing capability. Furthermore,wecould obtain the dye-labelled, micron-sized particles through inverse suspension polymerization, and use them for the rapid sensing of hydrogen peroxide as designed. The response of particles was found to be much faster (> 1100%) than that of free dye molecules, and also the distinct colour change visualized the detection reaction. As a proof of concept, the hydrogel particles were able to detect the evolution of hydrogen peroxide from glucose that underwent enzymatic oxidation.

- Danyuan Xu et al (2019) studied "Facile preparation of biomass lignin-based hydroxyethyl cellulose super-absorbent hydrogel for dye pollutant removal"[36] The severe preparation process, poor swelling properties and mechanical properties of traditional cellulose and polyvinyl alcohol (PVA) composite hydrogels heavily limited their practical applications. To solve these issues, we use long-chain hydroxyethyl celluloses (HECs) as framework backbones, short-chain PVAs as branched chains, lignin molecules as extended crosslinkers and epichlorohydrin molecules as crosslinkers to prepare the lignin-based hydroxyethyl cellulose- PVA (LCP) super-absorbent hydrogels in the alkaline aqueous solution under mild reaction conditions, demonstrating high swelling ratio of up to 1220 g/g. The LCP hydrogels could take up large amounts of positively charged dyes rhodamine 6G, crystal violet and methylene blue with uptakes of 153, 184 and 196 mg/g, respectively. The LCP super-absorbent hydrogels also present excellent water retention, biodegradability and excellent swelling properties, which are very promising for applications in the fields of commercial diapers, soil water retention and seed cultivation in agriculture, and dye pollutant removal.

- Toshihisa Mizunoa, et al (2019) studied "Synthesis and characterization of chemically-reactive solubilization surfactants for membrane proteins and preparation of membrane protein hydrogel microfibers" [37] We herein report the synthesis and characterization of unique chemically reactive solubilization surfactants Alk-DKDKC12K and Bis-alk-DKDKC12K that consist of the DKDKC12K unit, previously reported to function as a novel class of lipopeptide-based solubilization surfactant for membrane proteins such as photosystem I (PSI) derived from cyanobacteria, and one or two alkyne groups at the N- and/or C-terminal sides, which could react with bis-azide crosslinker *via* Huisgen cycloaddition reaction. By a stepwise *in situ* crosslinking of PSI solubilized in a buffer, containing Alk-DKDKC12K and Bis-alk- DKDKC12K, with a set of crosslinkers (the first one is bis azide compounds and the second is formylated dextran), we succeeded in preparing hydrogel microfibers encapsulating PSI withoutdamage to the original photophysical functions.

- Jingfa Yangb et al (2019) studied "Preparation of composite graphene hydrogels adsorbent with special-shaped ZnO and TiO2" [38] Graphene-based hydrogels (GH) have exhibited prominent

performances in wastewater treatment. Herein, Specialshaped ZnO tetrapods and TiO2 nanosheets were introduced to the preparation of GH via a one-step hydrothermal reduction method. The ZnO-GH and TiO2-GH composite hydrogel with a uniform 3D network structure and good mechanical properties can be used as an adsorbent for printing and dyeing wastewater. The optimum doping amount of ZnO and TiO2 in the composite hydrogel and the adsorption regularity to rhodamine B (RhB) with different concentrations were discussed. The cyclic adsorption performance and adsorption kinetics were briefly discussed. When the doping ratio of ZnO to graphene oxide (GO) is 5:8, ZnO-GH has the best adsorption rate, which is 71.7%. The best degradation rate appears at a ZnO doping ratio of 1:2, which also shows the best total removal rate of RhB of approximately 82.20%. When the doping ratio of TiO2 to GO is 3:4, the photocatalytic degradation rate is 30.3%, and the total removal rate of RhB reaches 99.1%, which indicates that RhB can be almost completely removed by TiO2-GH through adsorption and degradation. After five cycles, the adsorption capacity of ZnO-GH and TiO2-GH for the low RhB concentration is still good. The addition of ZnO and TiO2 improves not only the adsorption and degradation properties of the composite hydrogel but also its recycling performance as a result of the increase in mechanical stability.

- Shige Wang et al (2019) studied "Preparation of therapeutic-laden konjac hydrogel for tumor combination therapy" [39] Featured with three-dimensional network structure, polymer hydrogels have found tremendous applications in biomedical fields. In this study, therapeutic- laden Konjac glucomannan (KGM) hydrogel was prepared by injecting polydopamine (PDA)/5-fluorouracil (5-FU)/calcium folinate (CF)/KGM alkaline solution to the target area, for the synergistic tumor photothermal and chemotherapy. In alkaline solution, dopamine can be synchronously polymerized to form PDA, while KGM can be hydrolyzed and transformed intoa thermally irreversible KGM hydrogel. Besides, the alkaline condition can increase the solubility of 5-FU. The hydrogel matrix can control the release of 5-FU and CF. PDA renders the composite hydrogel excellent tumor photothermal therapy ability. Moreover, CF can be usedas a synergist to enhance the tumor chemotherapy efficiency of 5-FU. With convenient handling, excellent photothermal conversion ability and high biocompatibility, the

multifunctional hydrogel system is anticipated to find a promising translational potential in clinical therapeutic applications.

- Anna Marinopouloua, et al (2019) studied "Preparation of model starch complex hydrogels" [40] Amylose can form molecular inclusion complexes by forming a helix around ligands and thus protecting them and increasing their bioavailability. Hydrogels are biomaterials that have been used in drug and nutrient delivery. In this study, we have used a simple method to fabricate 3-D porous hydrogels using starch inclusion complexes as the structural material. Native maize starch and myristic acid as a model ligand were complexed and subsequently cross-linked with trisodium trimetaphosphate (TTP) to synthesize the hydrogels and pores were created after freeze-drying. X-ray diffraction and DSC thermal analysis verified the presence of amylase inclusioncomplexes in the hydrogels matrix. The starch complex hydrogels had 70% porosity with pores ranging from approximately 50 μm–250 μm that swelled up to approximately 600 μm upon hydration. As a result, the equilibrium water content and the degree of swelling of the hydrogels were 66.8% and 191.7%, respectively, while Young's modulus of elasticity of the hydrogels was 56.6 kPa. The starch complex hydrogels had a slow degradation rate in the presence of α-amylase and lost~38% of their weight after 36 days of incubation at 37 °C.

- Dhamodharan Raghavachari et al (2019) studied "Facile preparation of biocompatible macroporous chitosan hydrogel by hydrothermal reaction of a mixture of chitosan-succinic acid-urea"[41] The facile preparation of macroporous, super water absorbing, biocompatible hydrogels of chitosan involving the hydrothermal reaction of a mixture of chitosan (CH), succinic acid (SA) and urea (UR), all of which are sustainable materials, is reported. The structure of the dry CHSAUR was ascertained by CP MAS-SS NMR spectroscopy, Fourier transform infrared (FTIR) spectroscopy, powder x-ray diffraction analysis (PXRD), and thermogravimetric analysis (TGA). The principle role of UR in the synthesis was identified as the source of ammonia, which increased the pH of the acidic chitosan solution with reaction time, leading to the formation of the insoluble hydrogel of chitosan accompanied by the

formation of pores of different sizes and volumes. In addition, a small fraction of urea participated in chemical reaction with the primary hydroxyl groups in the sixth position of the glucosamine repeat units of chitosan resulting in carbamate linkages. The as-prepared hydrogel, following workup and methanol extraction, was found to be chitosan crosslinked with succinic acid through electrostatic interaction. It was macroporous with percentage porosity varying between 49.4% to 64.2%. It also exhibited different extents of water uptake with the maximum of 760 ± 20 g/g being for the one prepared with the weight ratio of 1: 4: 4 of chitosan: succinic acid: urea. The absorption of water is found to arise out of the porosity as well as presence of water attracting chitosan ammonium cation-succinate electrovalent bonds that are formed by thereaction between SA and ammonium cation of the chitosan backbone. The absorption of salin water was relatively poor suggesting that the saline water absorption might be arising largely due to the presence of micropores and specific interaction. The hydrogels exhibited Herschel- Bulkley rheological behavior. The extraction of CHSAUR with 0.1 N NaOH in methanol resulted in the removal of the physical crosslinks, consisting of succinate anions; the presence of chitosan with porous morphology was confirmed additionally by copper (+2) adsorption. In contrast to the widely reported method of preparing microporous chitosan scaffold of cylindricalshape that takes several days to a week, the present method offers a simple means of preparing macroporous chitosan of any shape and size in very large scale with soft foam-like morphology.With its biocompatibility towards mouse fibroblast cells it could find applications in drug delivery, biodegradable super water absorbency and haemostatic applications.

- Jianping Deng et al (2019) studied "Chiral, thermal-responsive hydrogels containinghelicalhydrophilic polyacetylene: preparation andenantiodifferentiatingrelease ability"[42] In this contribution, a chiral*N*-propargylamide monmer (R and S) was synthesized and used as comonomer to preparehydrophilic polyacetylene (HPA) bearing polymerizable vinyl groups in the presence of(nbd)Rh+B (C6H5)4. The obtained HPA chains could form single-handed helical structure in water and showed intense optical activity. Taking advantage of the hydrophilic and polymerizable moieties, HPA was further used as macromer to prepare hydrogels in deionized water via free radical polymerization, using *N*-isopropylacrylamide (NIPAm) as comonomer, *N*,*N*-methylenebisacrylamide (BIS) as crosslinker, ammonium

persulphate (APS) and *N*,*N*,*N*,*N*-tetramethylethylenediamine (TEMEDA) as redox initiator. The asprepared hydrogels exhibited optical activity, thermal responsibility and biocompatibility. More interestingly, the hydrogels showed enantio-differentiating release ability towards mandelic acid enantiomers, demonstrating the potential applications of the novel optically active hydrogels in chiral drug delivery fields.

- Junli Ren et al (2019) studied "A one-pot strategy for preparation of high-stren strength carboxymethyl xylan-g-poly(acrylic acid) hydrogels with shape memory property"[43] High strength hydrogels open new possibilities in the fields of bioengineering and biomedical. In this paper, a highly efficient one-pot strategy was developed to prepare carboxymethyl xylan-g-poly (acrylicacid) (CMX-g-PAA) hydrogels with high compression strength, high elongation and high elasticity by using the metal coordination and the reinforcement of hydroxylate multi-walledcarbon nanotubes (HCNTs). Prepared hydrogels were characterized by means of FTIR, XRD, SEM, rheological measurements as well as their swelling and mechanical properties. Results showed that the Fe3+-carboxyl coordination and HCNTs imparted hydrogels with high strength and good rapid recovery properties, in which the maximum high compressive strength and elongation at break were achieved to 10.4 MPa and 1032%, and the shape of hydrogels almost returned to the original shape after the external force was removed after 30 cycles of compression. These hydrogels also exhibited Fe3+-triggered shape memory properties. Therefore, as-prepared hydrogels possessing high strength, rapid recovery and shape memory properties, could broaden access for application in intelligent toys, electronic skin, biosensing, and tissue engineering.

- Yu Chen et al (2019) studied "Preparation of chitosan-Cu2+/NH3 physical hydrogel and its properties" [44] Chitosan (CTS) physical hydrogels crosslinked under gaseous ammonia atmospheres have attracted considerabl attentions for their abilities tomaximize the biological activities of CTSwhile maintaining their biocompatibility. However, poor mechanical properties significantly limit their application. The CTS-metal ion complexing hydrogels showed better mechanical properties. However, the formation process is uncontrollable, and the high dosages of metal ions used may cause cytotoxicity. In the present work, CTS-Cu2+/NH3 physical

hydrogel with excellent comprehensive properties was prepared by ammonia fumigation and metal ion complexation. Its formation mechanism and structure were investigated. The above physical hydrogel revealed excellent mechanical properties with the mechanical strength up to 0.30 MPa, significantly higher than CTS/NH3 hydrogel, seven at much lower Cu2+ contents. And CTS-Cu2+/NH3 hydrogel is more thermal stable than CTS/NH3 hydrogel. In addition, it exhibited specific killing effects on Pseudomonas aeruginosa. These results suggest that CTS-Cu2+/ NH3 physical hydrogel has a great application potential as a wound dressing.

- Andrew Zannettinob et al (2018) studied " Hydrogel-based preparation of cell aggregates for biomedical applications"[45] Cell aggregates are widely used either as *in-vitro* models for drug screening, fundamental studies on disease progression and developmental biology, as well as *in-vivo* injectable cells for tissue regener- ation. Compared to single-cell suspensions, cell aggregates retain superior cell viability, mimic *in-vivo* microenvironments and enhance functional properties, such as superior anti-inflammatory properties of mesenchymal stem/stromal cell aggregates or enhanced albumin production by hepatocyte aggregates. Cell aggregates can be either prepared by conventional spontaneous aggregation, or advanced substrate- based and technology-assisted methods, which have been well described in previous reviews. However, hydrogel-based preparation of cell aggregates is a novel, hitherto rarely considered method compared to conventional preparation of cell aggregates, such as hanging drops and commercial AggreWell TM plates. This review will mainly focus on two- dimensional (2D) hydrogel surface -based and three-dimensional (3D) hydrogel embedding- based preparation of cell aggregates by revealing the underlying mechanisms and highlighting some of their potential biomedical applications.

- Alireza Shakeria et al (2018) studied "Preparation of polymer-carbon nanotubes composite hydrogel and its application as forward osmosis draw agent" [46] In this study, we functionalized multiwall carbon nanotube with polar groups including eCOOH and eOH groups (F.MWCNT) and synthesized composite polymer hydrogel via dispersion in monomer solution and by using a simple poly (acrylic acid-co-maleic anhydride) (PAA-co-PMA) crosslinking

reaction. Incorporation of the F.MWCNT phase into the PAA-co-PMA hydrogel network was verified using Fourier transformation infrared spectroscopy (FTIR) and scanning electron microscopy (SEM) analysis. The physico-chemical properties of the composite polymer hydrogels were investigated and compered to pure hydrogel. In addition, the effect of F.MWCNT incorporation on polymer hydrogels performance as forward osmosis draw agent was studied. The results indicated that the addition of F.MWCNT (1.2 wt %) within the polymer hydrogel enhanced the water adsorbing capacity of the composite hydrogel as expected. Furthermore, the composite hydrogel (1.2 wt% of incorporated F.MWCNT) displayed a much higher water flux compared with the pure PAA-co-PMA polymer hydrogel during the FO test. The facile and efficient preparation of the F.MWCNT incorporated PAA-co-PMA composite hydrogel means it will have potential applications as a novel draw agent.

- V. Jaisankar et al (2017) studied "An eco-friendly synthesis, characterisation and antibacterial applications of novel almond gum – poly(acrylamide) based hydrogel silver nanocomposite" [47] Polysaccharide based semi interpenetrating hydrogel (SIH) networks of cross-linked poly(acrylamide) was synthesised through an redox initiating free radical polymerization utilizing almond gum as a grafting backbone, N,N'– methylenebisacrylamide (MBA) as the crosslinker and ammonium persulphate (APS) – N,N,N',N'-tetramethyl ethylenediamine (TEMED) as the redox initiator pair. Silver ions were introduced into the hydrogel matrix and silver nanoparticles of invariable size were developed insitu of the swollen hydrogel by the reduction of silver ions (Ag^+) using azadirachta indica (neem) leaf extract. The prepared hydrogel - silver nanocomposite (HSN) was characterized by UV – visible diffused reflectance spectroscopy (DRS), fourier transform infrared spectroscopy (FT-IR), high resolution scanning electron microscopy (HR-SEM), energy dispersive X-ray analysis (EDX) and thermogravimetric analysis (TGA). The influence of pH on the swelling behavior of HSN was studied and theantibacterial activity of the developed nanocomposite was evaluate.

- Hiroki Hashimoto, et al (2017) studied "Preparation of chitosan hydrogel and its solubility in organic acids" [48] The increase of the stability of chitosan (CS) in the solution is extremely important for the applicationof CS in various fields. In this study, we describe that the

hydrogelation of CS can solve this problem. CS hydrogel was readily prepared by addition of a sodium hydroxide solution to a CS acetic acid solution. The CS hydrogel was stable in the wet state and could maintain its molecular weight for a long period oftime at room temperature. The obtained CS hydrogel could be readily dissolved with addition of acids,such as acetic acid and other organic acids, as determined by measuring the pH and transmittance of the solutions. Dissolution of the CS hydrogel indicated that the amount of carboxylate ion per amino group of CS was only 0.5 molar equivalents. Moreover, the binding state between the acetic acid and aminogroups of CS in an aqueous solution is discussed using results from1H NMR spectroscopy. The methylsignals attributed to free acetic acid, acetic acid in an ionic bond, and the acetamido group of the N-acetylglucosamine residue was clearly observed, and the strength of each peak changed quantitatively with the addition of acetic acid.

CHAPTER 3

SCOPE OF THE WORK

The purpose of this study is to create and assess various hydrogel qualities utilizing natural items that are readily available locally. Biological processes including the delivery of medications or cells, the regeneration of hard and soft tissues, as well as other applications like agriculture, have drawn the attention of several researchers in recent years. As a result, the current study was done to environmentally friendly synthesis hydrogel using resin and flax seeds.

The following are the investigation's goals:

- Using locally sourced, environmentally friendly plant materials as reducing agents/capping agents in the synthesis of hydrogel would, presumably, replace the pricey chemicals previously utilized.
- To engage synthesized Hydrogel nanoparticals with optical properties by UV-Visible spectroscopy.
- To examine the functional groups of synthesized nanoparticles using Fourier Transform Infrared Spectroscopy (FTIR).
- To determine the size and nature of hydrogel nanoparticles by X-ray diffraction (XRD)
- To confirm the elemental composition by Energy Dispersive Analysis of X-rays (EDAX)
- To analyze the surface morphology of nanoparticles by SEM.
- To study the thermal stability of hydrogel nanoparticles using TGA, DTG and DTA.
- To determine the microbial activity of hydrogel nanoparticles using by Antibacterial activity (Disc diffusion method)
- To know the absorbance capacity and swelling ratio of hydrogel nanoparticle by absorbance test.

CHAPTER 4

MATERIALS AND METHODS

4.1 MATERIALS

Almond gum (RS), Flaxseeds (FS), Borax powder, Potassium persulphate (PPS), N, N, N', N'-tetramethyl ethylenediamine (TEMED), Double distilled water (DDW) was used for the synthesis of hydrogel and for the preparation of solutions required in this study.

4.2 Methods

4.2.1 Synthesis of Hydrogel using Almond gum and Flax seeds

The gum was dried well and powdered using mortar and pestle. It was soluble in double distilled water and concentrated by heating. The concentrated gum was precipitated in an ice Cold ethanol. The precipitated gum was separated and dried at 60 ºC. The pure gum was finely Grained and stored in air tight container. AG (0.1 g) was mixed in 5 mL of DDW to get a homogeneous solution. AM (1.0 g) was dissolved in 6 ml of DDW followed by initiator PPS (0.005 g in 1 mL of DDW) and cross-linker Borax powder (0.01 g in 1mL of DDW). Both the solutions were mixed and TEMED (0.02 mL in 1 mL of DDW) was added which, together with PPS, acts as redox-initiating pair and initiates free radical polymerization. The reaction mixture was stirred and heated at 60 ºC for 5 minutes. The polymerization reaction results in theformation of hydrogel within 10 minutes of reaction time. The formed hydrogel was equilibrated with water for 3 days to remove unreacted monomers and reagents. The hydrogel was dried in hot air oven to constant weight.

4.4ANTIBACTERIAL ACTIVITY

4.4.1 Antibacterial Activity of synthesized Hydrogel

Antibacterial Activity was performed by disc diffusion method (Kirby amp; Bauer, 1966)

4.4.2 Procedure for the disc diffusion method

The test bacteria was inoculated in peptone water and incubated for 3 – 4 hours at 35 ºC. Mueller hinton agar plates was prepared and poured in sterile petriplates. 0.1 mL of bacterial culture was inoculated on the surface of Mueller hinton agar plates and spread by using L-rod. The inoculated plates were allowed to dry for five minutes. The disk loaded with samples Concentration 1000 µg/mL was placed on the surface of inoculated petriplates using sterile Technique. The plate was incubated at 37 ºC for 18-24 hours. The plate was examined for Inhibitory zone and the zone of inhibition was measured in mm.

4.5 Absorbing capacity

The primary purpose of Hydrogel is to absorb saline solution, disperse it quickly, and able to retain the absorbed solution without re-wetting the surface (Shanmugasundaram et al., 2010). Absorbing capacity of RS and FS hydrogel were determined using the procedure given in US 1.0 g of RS and FS was weighed and recorded as W1 to be taken into the teabag and sealed. An empty teabag was also prepared to act as the blank. A plastic container was prepared and filled with saline solution up to 4 cm depth. The RS and FS were distributed uniformly throughout the teabag. Teabags with RS, FS and without Flax seeds were held horizontally and laid on the surface of the saline solution to wet the surface of teabags for 1 min before they were submerged into the saline solution. After soaking for 60 min., the teabags were removed from thesaline solution and hung on the retort stand to allow it to drip for 15 min. The weight of teabag with flax seeds was weighed and recorded as W3. Empty teabag was also weigh and recorded as W2. Same procedures were repeated to test the absorbing capacity of RS and FS. The absorbing capacity was calculated using the below equation.

$$\textbf{Absorbing capacity (g/g)} = \frac{(w3-w2)-w1}{w1}$$

4.6 Swelling capacity

Swelling capacity is very important to determine the swelling of hydrogel and also help to determine the swelling mechanism of the Hydrogel. 1.0 g of RS & FS were measured and put into a measuring cylinder. The cylinder was tapped by finger for 100 times and the volume of the RS & FS was recorded (V_1). Distilled water was added into the measuring cylinder to fill up the volume to 100 mL. At consecutive time intervals (0.5 min., 1 min., 10 min., 30 min., 1 h, and 8 h), the sediment volume of the swollen hydrogel was observed and recorded as V_2. Same procedures were repeated to test the swelling capacity of RS &FS. The swelling capacity was calculated as a ratio of swollen volume to tapped volume, using the below equation.

$$\textbf{Swelling capacity (cm3/cm3)} = V_2/ V_1$$

4.7. CHARACTERIZATION TECHNIQUES

Computer controlled JASCO V-650 was used to study UV-Vis spectral behavior. The FT-IR spectra were recorded using a MIRacle 10 FTIR instrument, XRD measurements were made by out by Quantax 200 with X-Flash-Bruker. Analytical X'Pert Powder XCelerator Diffractometer, measurement range: 10 to80 degrees in 20 and particle size was calculated using Scherer's equation.Themal stability was studied by Themobalence. And surface morphology found by scaning electronic microscopy.

4.7.1. UV Spectroscopy

UV spectrophotometer principle follows the Beer-Lambert Law. This law states that whenever a beam of monochromatic light is passed through an absorbing Substance, the decreasing rate of the radiation intensity of the absorbing solution 1sproportional to the concentration of the solution and the incident radiation. This law is expressed through this equation:

$$A \log (l_0/I) = ECL$$

A- absorbance, $\mathbf{l_0}$- intensity of light upon a sample cell, **I** -intensity of light departing the sample cell, **C** - concentration of the solute, **L** - length of the sample cell and **E**- molar absorptive.

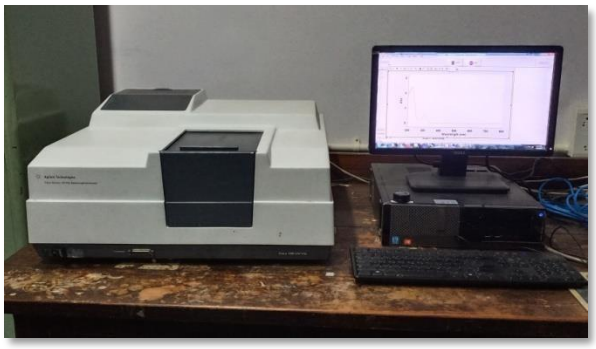

Fig 4.7.1 UV -Visible

Spectroscopy4.7.1.(a) WORKING

There are many parts in the instrumentation of the UV-Vis spectroscopy system, which are indispensable in the functioning of the UV-Vis spectrophotometer. Ultraviolet-visible spectrophotometer system focuses electromagnetic radiation from the light source to the sample. Depending on the configuration set in the system, light is transmitted through the sample or reflected off it. Then, the light is collected from the sample through reading.

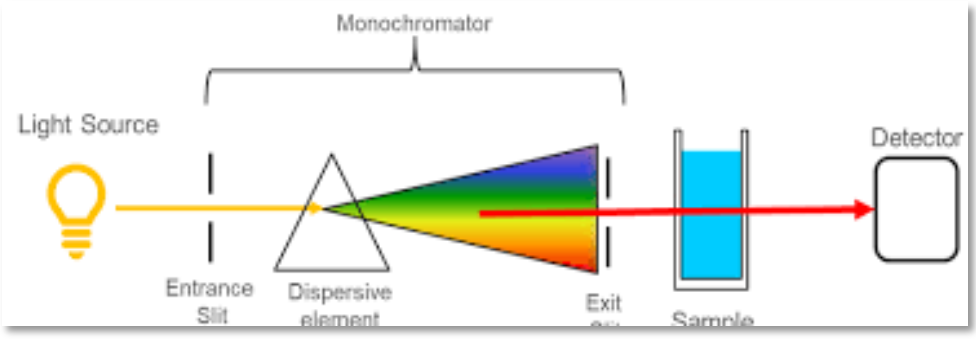

Fig 4.7.2a Instrumentation of UV Spectroscopy

Initially, light is focused into the entrance slit of the monochromatic from the source. Monochromator uses dispersing elements, namely optical grating to separate the light by wavelength. The light is passed into a charged coupled device (CCD), which is made up of

individual tiny detectors; hence the intensity of light at each wavelength will be measured. CCD is read-off to a computer and the result obtained is a spectrum, which shows the intensity of each wavelength of light. Spectrophotometers are able to measure the electromagnetic radiation from ultraviolet to infrared. Spectrum will show the intensity of light versus the wavelength.

4.7.2. FT -IR Spectroscopy

FTIR (Fourier Transform Infra-Red Spectroscopy) is a sensitive technique particularly for identify1ng organic chemicals. It can also characterize some inorganic. It is a particularly useful tool in isolating and characteriz1ng organic contamination.

- The region from o.8 u to 2.5u is called Near IR,
- 2.5u to 15u is called Mid IR or Ordinary IR
- 15 to 200u is called Far IR

Lambert-Beer's Law-The concentration of a sample can be estimated by:

$$A= \varepsilon.C.D$$

ε is the molar absorption coefficient.

C is the sample concentration.

D is the sample thickness.

Fig 4.7.2 FT - IR Spectroscopy

4.7.2 a WORKING

. FTIR analysis measures the range of wavelengths in the infrared region that are absorbed by a material. This is accomplished through the application of infrared radiation (IR) to samples of a material. The sample's ability to absorb the infrared light's energy at various wavelengths is measured to determine the material's molecular composition and structure. Unknown materials are identified by searching the IR spectrum against a database that has a wide range of reference spectra. Materials can be quantified using the FTIR materials characterization technique as long as a standard curve of known concentrations of the component of interest can be created. Fourier Transform Infrared Spectroscopy Analysis can be used to identify unknown materials, additives within polymers, surface contamination on a material, and more. The results of the tests can pinpoint a sample's molecular composition and structure. A simple device called an interferometer is used to identify samples by producing an optical signal with all the IR frequencies encoded into it. The signal can be measured quickly. Then, the signal is decoded by applying a mathematical technique known as Fourier transformation. This computer-generated process then produces a mapping of the spectral information. The resulting graph is the FTIR spectrum which is then searched against reference libraries for identification.

4.7.3. FESEM

FESEM - Field Emission Scanning Electron Microscope. A FESEM is microscope that works with electrons instead of light. It is used to visualize very small topographic details on the surface or entire or fractioned objects. Electrons are liberated from a field emission source and accelerated in a high electrical field gradient. These electrons are liberated by a field emission source. The object is scanned by electrons according to a zigzag pattern.

4.7.3 a WORKING

The electron beam is focused by the electro-magnetic lenses (condenser lens. scan coils. stigmator coils and objective lens) and the apertures in the column to a tiny sharp spot.The current in the condenser determines the diameter of the beam: a low current result in a small diameter, a higher current in a larger beam A narrow beam has the advantage that the resolution

is better, but the disadvantage that the signal to noise ratio is worse. The situation is reversed when the beam has a large diameter

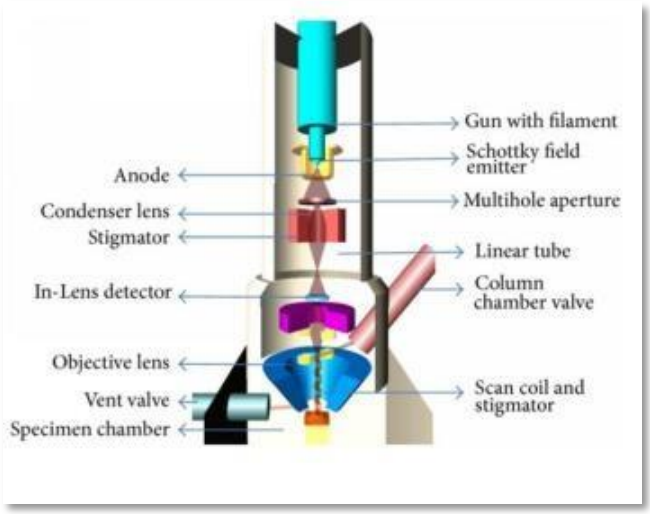

Fig 4.7.3 Instrumentation of FESEM

The scan coils deflect the electron beam over the object accord1ng to a zigzag pattern. The formation of the image on the monitor occurs in synchrony with th1s scan movement The scan velocity determines the refreshing rate on the screen and the amount of noise in the image. The smaller the scanned region on the object, the larger the magnification becomes at a constant window size. Scan coils often consist of upper and lower coils, which prevent the formation of a circular shadow at low magnification

The stigmator coils are utilized to correct irregularities in the x and y deflection of the beam and thus to obtain a perfectly round-shaped beam. When the beam is not circular. But ellipsoidal, the image looks blurred and stretched.

The objective lens is the lowest lens in the column. The the electron beam on the objective focuses object At a short working distance the objective lens needs to apply a to deflectthe electron greater force beam. The shortest working distance produces the best smallest beam diameter, the resolution, but also the poorest depth of field

4.7.4. EDAX

Energy Dispersive Analysis of X-rays (EDAX) is an analytical Technique used for elemental analysis or chemical characterization of a sample it based on the investigation of a sample through interactions between electromagnetic radiation and matter, analyzing X-rays to being hit with the electromagnetic radiation. Its characterization response to capabilities is due in large part to the fundamental principle that each element has a unique at atomic structure; be identified uniquely from each other.

Fig 4.7.4 Instrumentation of EDAX

4.7.4 a WORKING

EDAX systems are most commonly found on Scanning electron microscopes and electron microprobes. Scanning electron microscopes are equipped with a cathode and magnetic lenses to create and focus a beam of electrons. The energy of the electron beam has to be selected to give a compromise between the requirements of resolution and X-ray production efficiency. The X-radiation excited in the specimen was analyzed in two fully focusing crystal spectrometers. The EDS X-ray detector measures the relative abundance of emitted rays versus their energy. The detector is typically lithium drifted silicon Solid state device. When an incident X-ray strikes the detector, it creates charge pulse that is proportional to the energy of X-ray. The charge pulse is converted to a voltage pulse by a reamplifier. The charge-sensitive signal is then sent to a multichannel analyzer where the pulses are sorted by voltage

4.7.5. XRD

X-ray Powder Diffraction (XRD) is inefficient analytical technique used determination of grain size, composition of solid solution, lattice constants, and agrees of crystalline in a mixture of amorphous and crystalline substances X-ray diffraction based on constructive interference of monochromatic X-rays ad a crystalline sample. These X -rays are generated by acathode ray tube filtered to produce monochromatic radiation, collimated to concentrate, and directed toward the sample.

4.7.5 a WORKING

X-rays are generated in a cathode ray tube by heating a filament to produce electrons, accelerating the electrons toward a target by applying a voltage and bombarding the target material with electrons. When electrons have sufficient energy to dislodge inner shell electrons of the target material, characteristic X-ray spectra are produced.

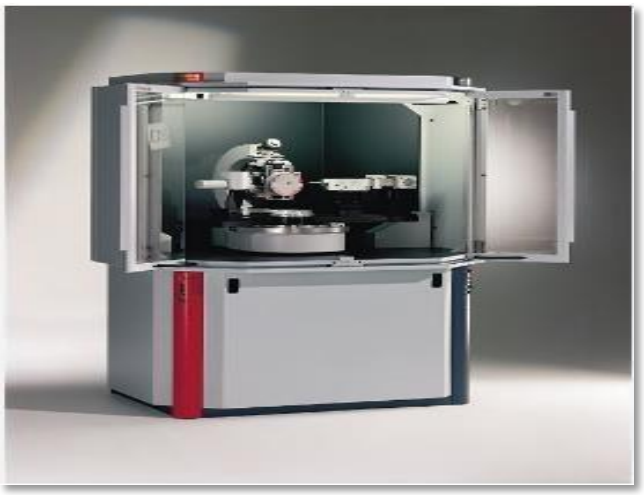

Fig 4.7.5 Instrumentation of XRD

Copper is the most common target material for single-crystal diffraction. These X-rays are collimated and directed onto the sample. As the sample and detector are rotated, the intensity of the reflected X-rays is recorded. When the geometry of the incident X-rays impinging the Sample sat1sfies the Bragg Equation, constructive interference occurs and a peak in intensity occurs.

Detector records and processes this X-ray signal and converts the signal account rate which is then output to a device such as a printer or computer monitor. The geometry of an X- ray diffractonmeter is such that the sample rotates in the path of the collimated X-ray beam at angle 0 while detector the X-ray is mounted on an arm to collect the diffracted X-rays.

4.7.6 TGA

In thermo-gravimetric analysis, the sample is heated in a given environment (air, N2, CO2, He, Ar, etc.) at controlled rate. The change in the weight of the substance is recorded as a function of temperature or time. The temperature is increased at a constant rate for a known initial weight of the substance and the changes in weights are recorded as a function of temperature at different time interval. This plot of weight change against temperature is called thermo-gravimetric curve or thermo-gram; this is the basic principle of TGA

Fig 4.7.6 a TGA instrument

4.7.6a WORKING

A typical thermogravimetric analyzer consists of a precision balance with a sample pan located inside a furnace with a programmable control temperature. The temperature is generally increased at constant rate (or for some applications the temperature is controlled for a constant mass loss) to incur a thermal reaction. The thermal reaction may occur under a variety of atmospheres including: ambient air, vacuum, inert gas, oxidizing/reducing gases, corrosive gases, carburizing gases, vapors of liquids or "self-generated atmosphere"; as well as a varietyof pressures including: a high vacuum, high pressure, constant pressure, or a controlled pressure.

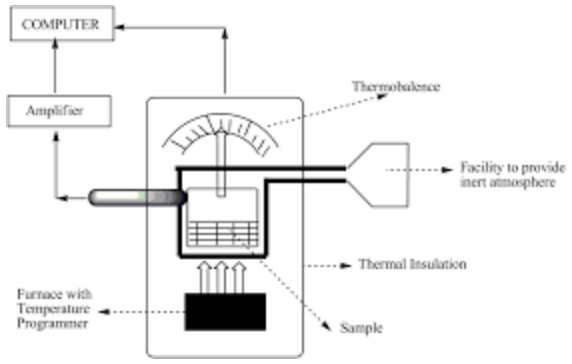

Fig 4.7.6b instrumentation of TGA

The thermogravimetric data collected from a thermal reaction is compiled into a plot of mass or percentage of initial mass on the y axis versus either temperature or time on the x-axis. This plot, which is often smoothed, is referred to as a TGA curve. The first derivative of the TGA curve (the DTG curve) may be plotted to determine inflection points useful for in-depth interpretations as well as differential thermal analysis.

CHAPTER 5

RESULT AND CONCULSSION

5.1 UV-Analysis

The UV -Visible spectra observed for RS and FS in the range 200- 900 nm. The particle shows three absorption peaks at **212nm, 224nm, and 326nm** for RS and **214nm, 222nm, 342nm** for FS (5.1.a). The band gap energy in nanomaterials could be obtained from absorption maxima. The band gap energy for RS peaks 5.8eV, 5.53eV and 3.62eV respectively. And the band gap energy for FS peak is 5.79eV, 5.5eV, 3.6eV respectively (5.1.b).The transition state for the above energy is list out in the table 5.1[49].

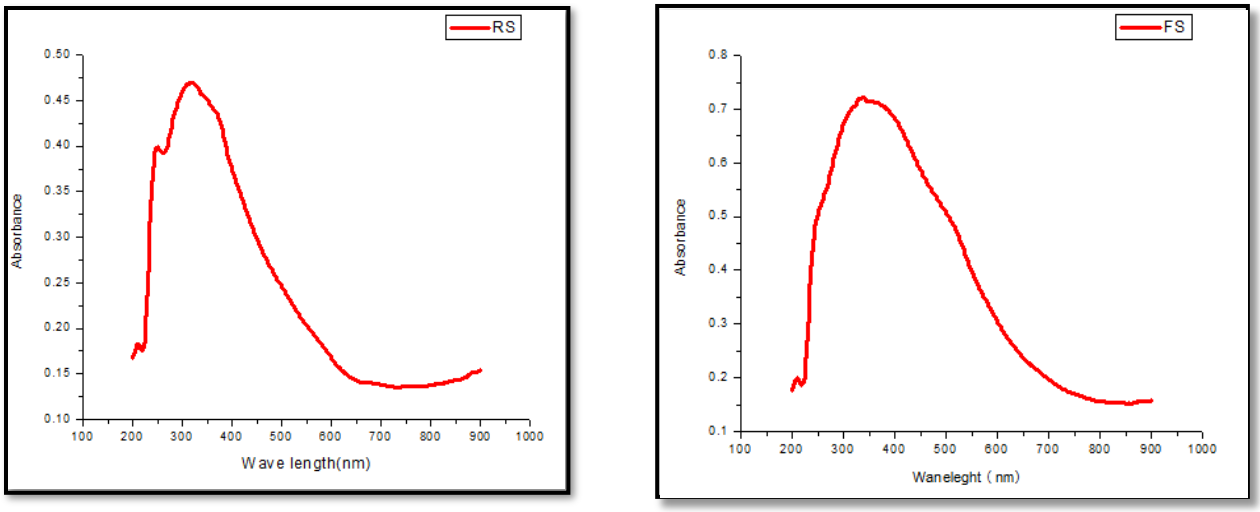

Fig 5.1.a UV-Visible Spectra of RS and FS (Absorbance Vs Wavelength)

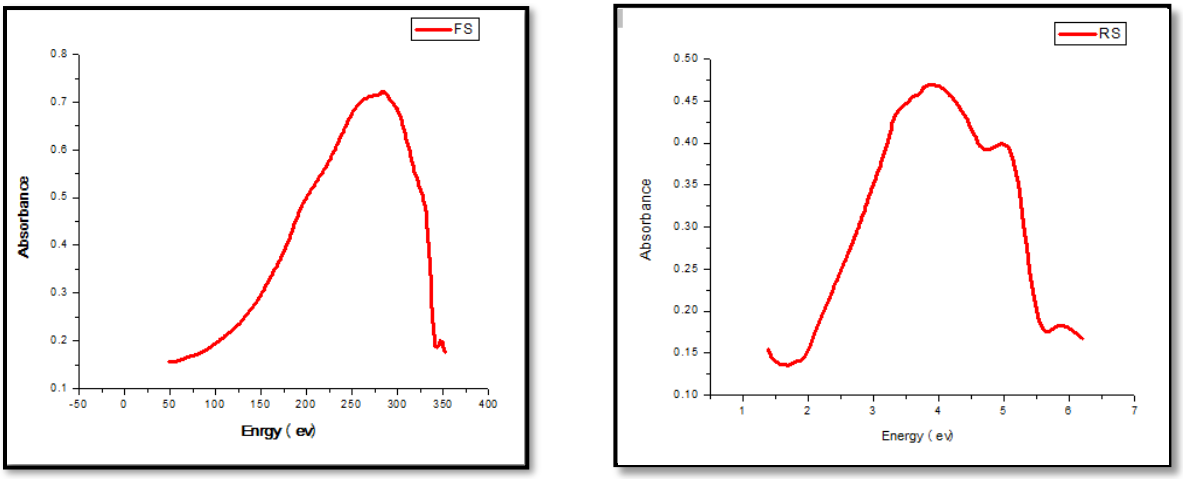

Fig 5.1.b UV-Visible spectra for RS and FS (Absorbance Vs Energy)

Table 5.1 UV-Visible Spectrum for RS and FS

Sample	Absorbance	Wavelength λ (nm)	Energy (eV)	Transition type
RS	0.182618	212	5.9047	σ- π*
	0.187709	224	5.5357	π-π*
	0.467665	326	3.8036	π-π*
FS	0.190513	214	5.7943	σ- π*
	0.190073	222	5.5855	π-π*
	0.718036	342	3.6257	π-π*

5.2 FT-IR studies

The hydrogel synthesis from RS and FS was recognized using FT-IR. Samples were measured between 400cm^{-1} and 4000 cm^{-1}(Fig 5.2.a &5.2.b). The peak stretching in RS and FS 3842.20 cm^{-1}, 3711.04 cm^{-1}, could be interpreted as an O-H bond [49]. The CHO group-induced bond at RS at 1728 cm^{-1}[50] .The aromatic skeletal vibration can be observed in the wide bond of RS and FS at positions 1597 cm^{-1} and 1589 cm^{-1} respectively[51]. Bands 1338 cm^{-1} in RS and 1334.74 cm^{-1} in FS display an aliphatic band for CH, CH_2[52]. Polysaccharide is seen in the bands 1072.42 cm^{-1} in RS and 1087.85 cm^{-1} in FS [53]. Moreover, the oxygen in the hydroxyl group causes the bands 1026.13 cm^{-1} in RS and 1018.47 cm^{-1} in FS. The peak in 455 cm^{-1},447.49cm^{-1} at the RS and FS, respectively, displays a C=C twist[54].

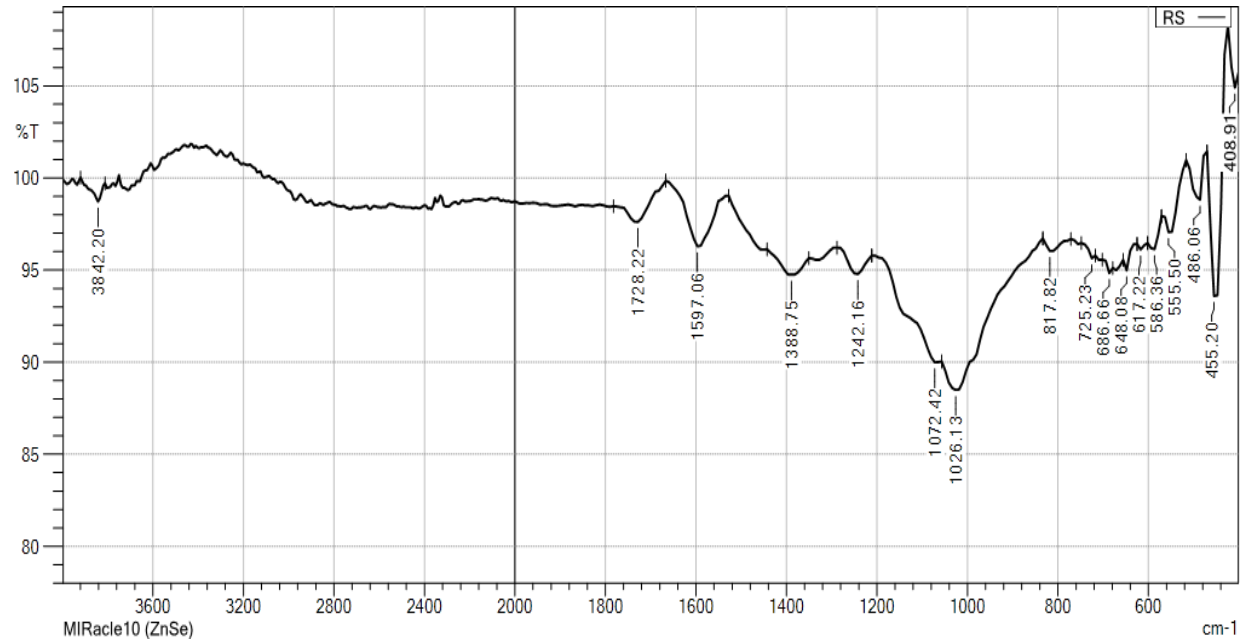

Fig 5.2.a FT-IR Spectrum of sample RS

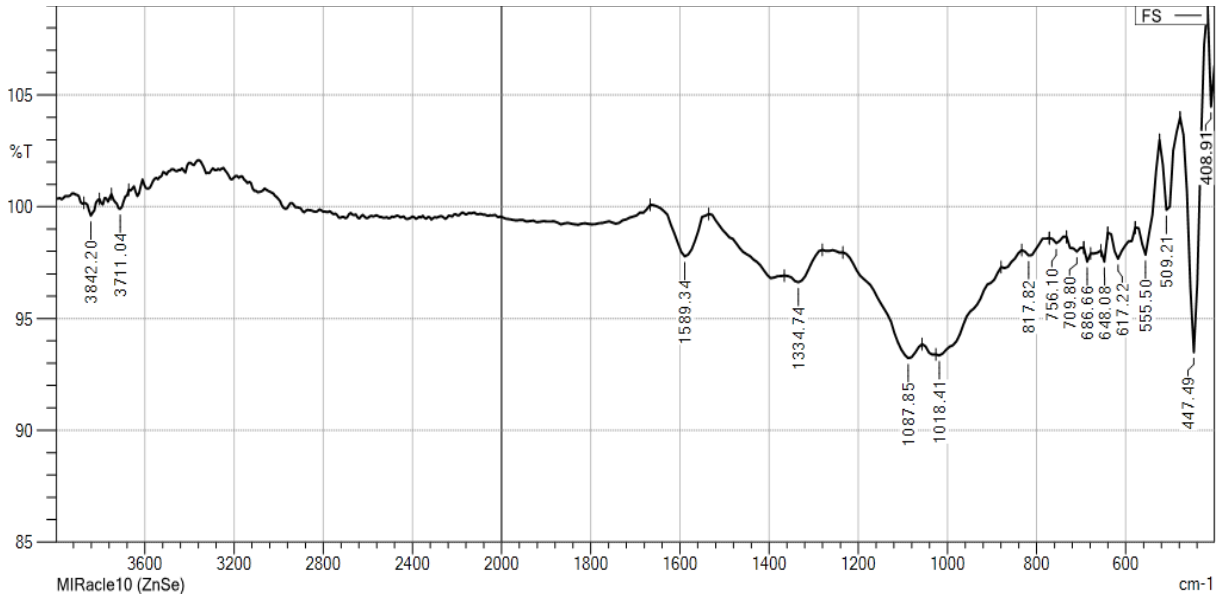

Fig 5.2.b. FT-IR Spectrum of sample FS

Table 5.2 The Spectrum of FT-IR data of the Samples

Vibration	**RS**	**FS**
	Wave number λ(cm^{-1})	**Wave number λ(cm^{-1})**
O-H stretching	3842.20 cm^{-1}	3842.20 cm^{-1}
Aromatic skeletal	1597.06 cm^{-1}	1589.34 cm^{-1}
polysaccharide	1072.42 cm^{-1}	1087.85 cm^{-1}

C=C twist	455.20 cm^{-1}	447.49 cm^{-1}
Oxygen in hydroxyl group	1026.13 cm^{-1}	1018.41 cm^{-1}
C≡N amide bond	1338.75 cm^{-1}	1334.74 cm^{-1}

5.3 TGA CALCULATION

TGA is a precise method for examining the decomposition pattern and thermal stability of hydrogel. The TGA and DTG, DTA of RS, FS hydrogel were revealed in Fig 5.3.c & 5.3.d. Useful data from TGA results include handling, storage, and shelf life of RS and FS at various temperatures. The sample weight loss is displayed as a function of temperature on the TGA curve [55]. From the observation, the weight loss was generally associated with two stages. In FS(Fig 5.3.a) the first stage of weight loss 26.1% at 30–270 ℃ and the second stage of weight loss 22.0% at 300℃ and 780 °C [56]. For the initial phase of RS (Fig 5.3.b) weight loss with a significantly average rate of weight loss and a total weight reduction of about 26.3%, the second stage of weight loss occurs between 300 and 780 ℃. Occurs, with a higher loss of 35.8%.The main cause of first-stage weight loss is the evaporation of some of the free water included in sample RS and FS. The disintegration of the polysaccharide structure was the primary cause of the weight loss for the second stage. According to TGA studies, hydrogel from RS and FS all decompose slowly and at a high temperature, suggesting exceptional thermal stability [54].

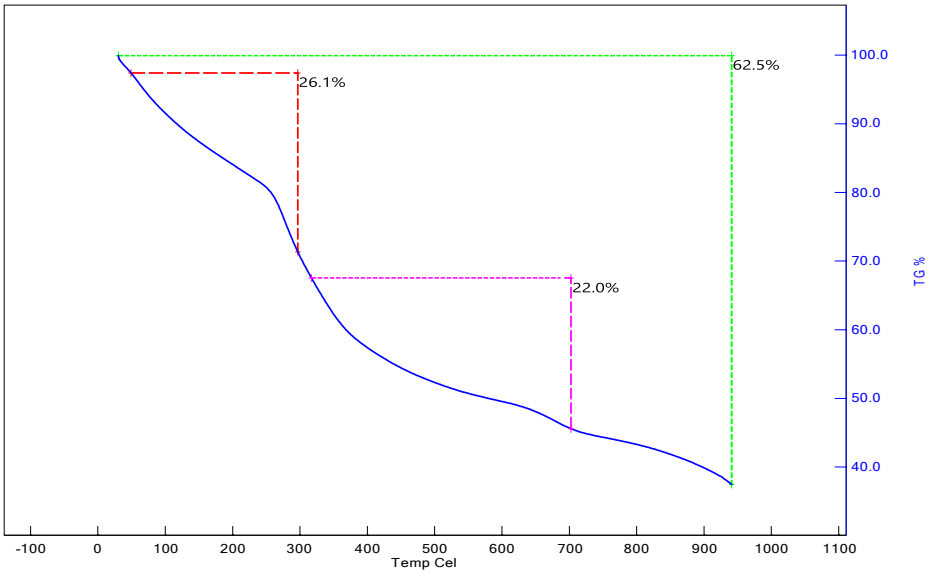

Fig 5.3.a TGA of FS curve

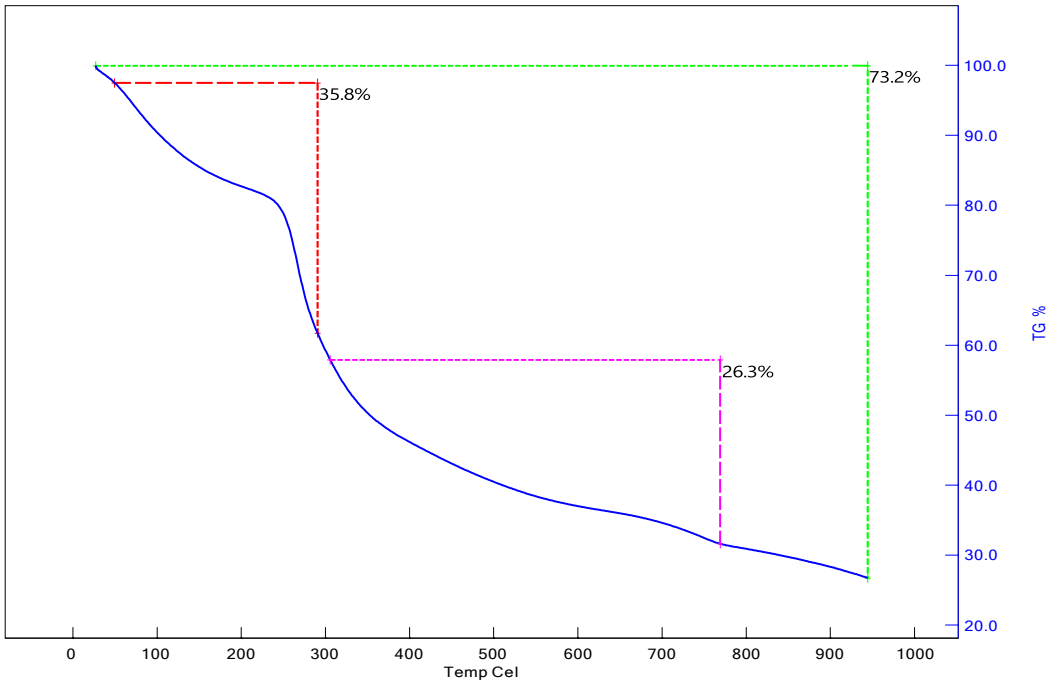

Fig5.3.b TGA of RS curve

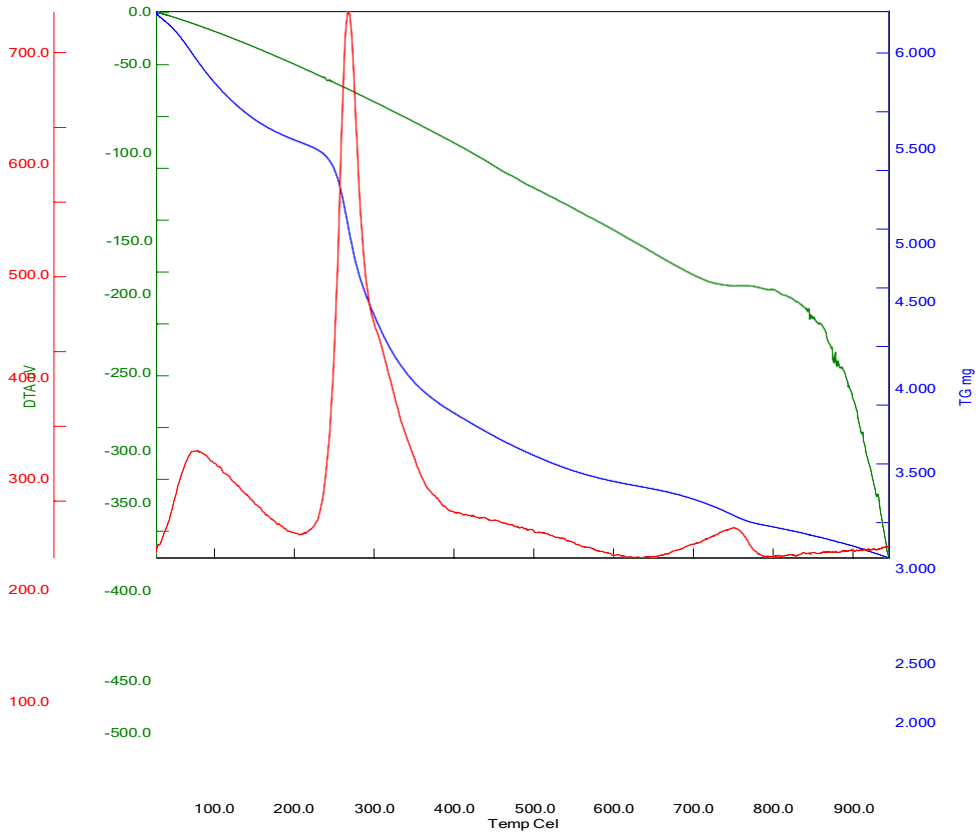

Fig 5.3.c Comparison of TGA, DTA and DTG for FS

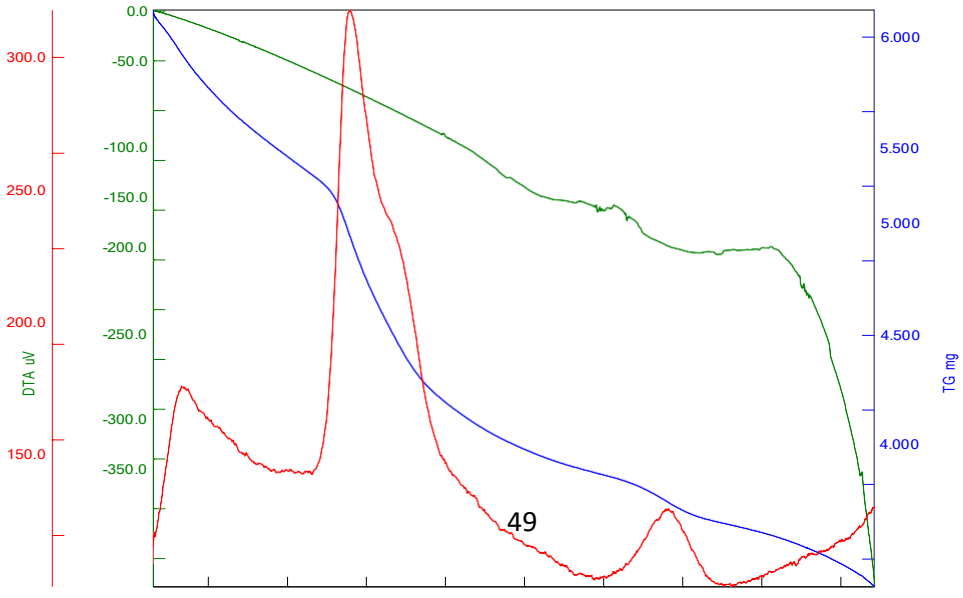

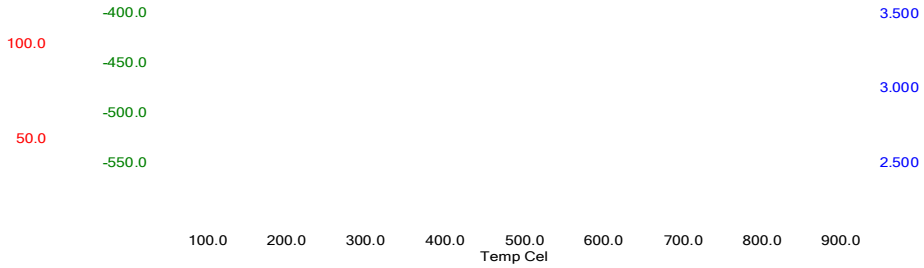

Fig 5.3.d Comparison of TGA, DTA and DTG for RS

5.4 XRD Calculation

The average crystallite size (D) was calculated using the well known Scherer's formula

$$D = K\lambda / \beta\cos\theta$$

Where D is the average crystalline diameter in nanometer (nm),

k is the Scherer constant equal to 0 .94

λ is the wavelength of the X ray radiation used and is equal to 1.5406A

θ is the Bragg diffraction angle of the concerned diffraction peak

$$\beta = (\pi /180)\ 2\theta$$

β is the full width at half maxima ('FWHM) intensity of the diffraction peak [56]. Average crystallite size (D) of synthesized nanoparticle **RS** and **FS** was found to be **2.4280nm** and **2.4315nm** respectively.

Table 5.3.a To Calculate Average crystalline size (D)

Sample	2θ	Θ	Cosθ	B	D(nm)
RS	31.7732	0.5867	0.9999	0.5542	2.6629
	30.7100	0.4200	0.9999	0.5351	2.7062
	44.5900	0.3800	0.9999	0.7770	1.9151
	Average = 2.428nm				
FS	31.4453	0.2013	0.9999	0.5471	2.6772
	30.3366	0.1766	0.9999	0.5278	2.7379
	44.2900	0.1838	0.9999	0.7706	1.8794
	Average = 2.4315nm				

Sample	2θ	Θ	Sin^2 θ	Sin^2 θ/2	Sin^2 θ/3	Sin^2θ /4	Sin^2 θ/5	Sin^2 θ/6	Sin^2 θ/7	Sin^2 θ/8
RS	31.773	15.88	0.0749	0.0374	0.0249	0.018	0.014	0.012	0.010	0.009
	30.710	15.35	0.0699	0.0349	0.0233	0.017	0.013	0.011	0.009	0.008
	44.590	22.29	0.1439	0.0719	0.0479	0.036	0.028	0.023	0.020	0.017
										K = 0.017
FS	31.445	15.722	0.0738	0.0369	0.0246	0.018	0.014	0.012	0.010	0.009
	30.336	15.166	0.0684	0.0342	0.0228	0.01	0.013	0.011	0.009	0.008
	44.290	22.145	0.1142	0.0542	0.0386	0.028	0.022	0.019	0.016	0.014
										K = 0.014

Table 5.3.c To select appropriate pattern of $h^2+l^2+K^2$ values and to identify the bravis lattice

Sample	2θ	Θ	Sin^2 θ	Sin^2 θ/K	$h^2+l^2+k^2$	hkl
RS	31.7732	15.886	0.07494	4.4082	3	111
	30.7100	15.355	0.0699	4.1117	3	111
	44.5900	22.295	0.1439	8.4647	6	200
FS	31.4453	15.722	0.0738	5.2771	3	111
	30.3366	15.166	0.0684	4.8857	3	111
	44.2900	22.145	0.1142	8.1571	6	200

For RS, the lattice value $a = \frac{\lambda}{2\sqrt{K}}$

a = 1.5406/2√0.017

a = 5.9079 $A°$

For FS,he lattice value $a = \frac{\lambda}{2\sqrt{K}}$

a = 1.5406/2√0.014

a = 6.5102 $A°$

The lattice value as for the synthesized nanoparticals RS & FS was to be 5.9079$A°$, 6.5102 $A°$the XRD result. The Structure of RS and FS Corresponds to the Face centre cubic (FCC) [51].

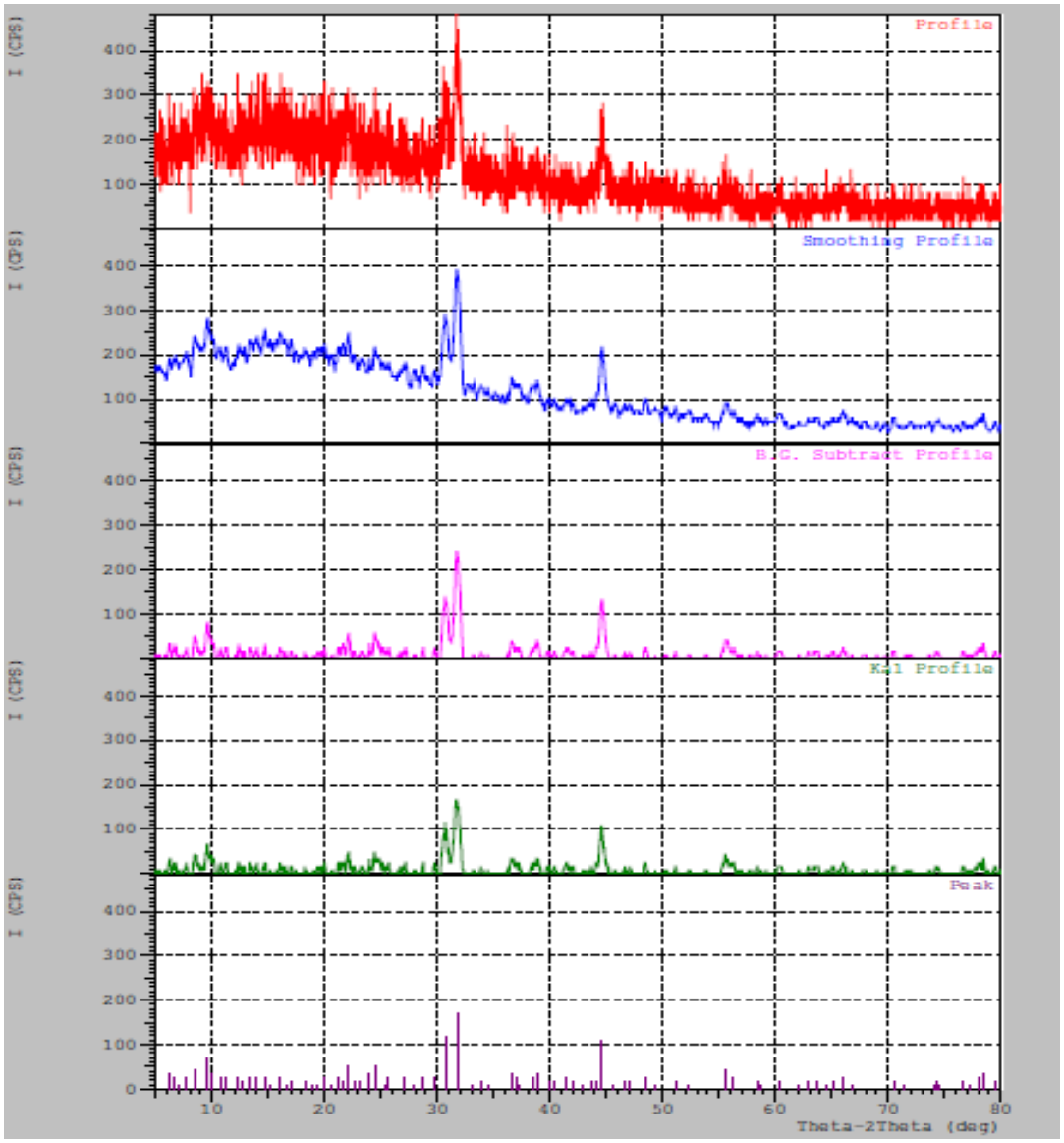

Fig 5.4.1(a) XRD Spectrum of RS

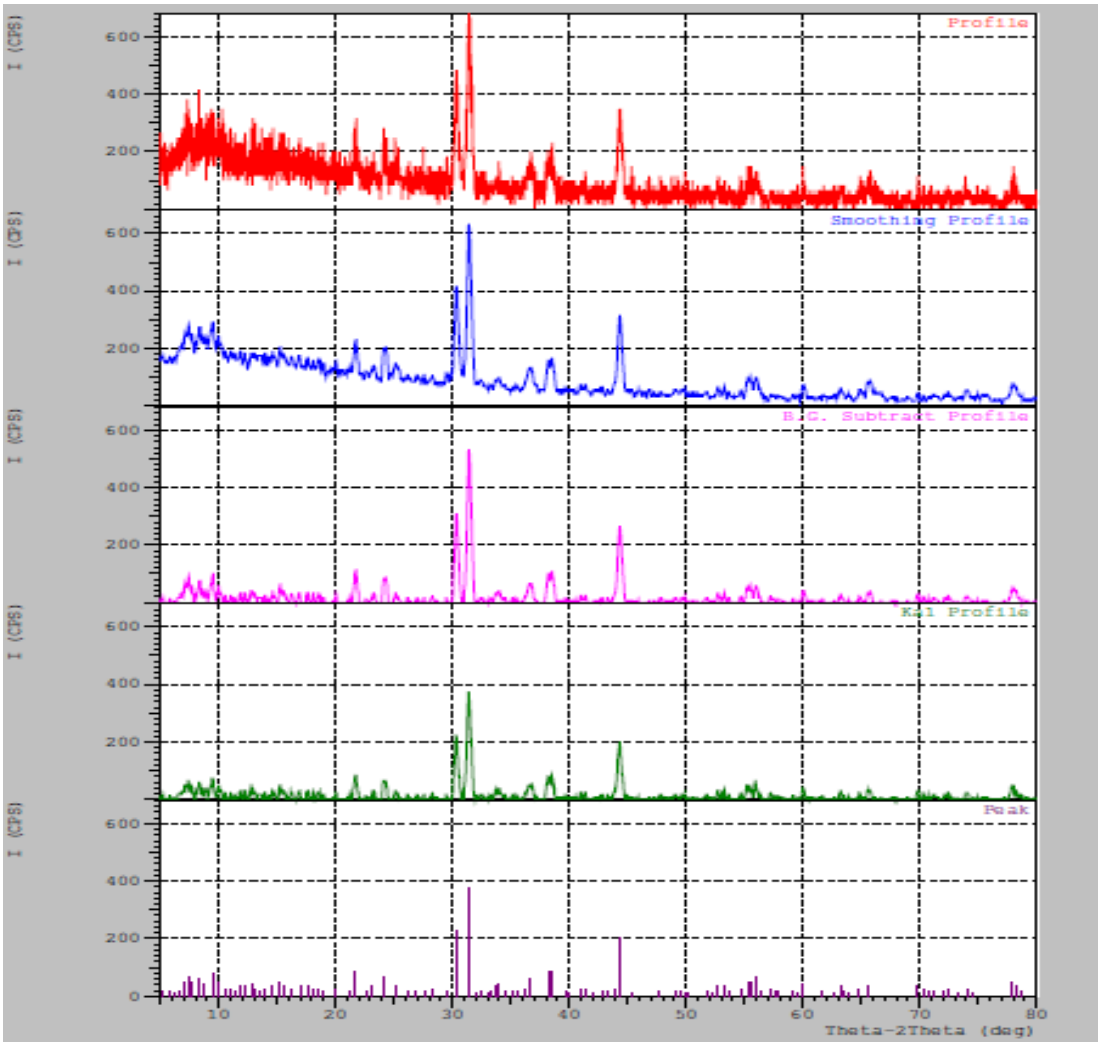

Fig 5.4.1(b) XRD Spectrum of FS

5.5 SEM Characterization

The morphology and size distribution of the RS and FS nanoparticals can be measured by the Field Emission Scanning Electron (FE-SEM) using MIRA3 TESCAN equipment. The average size range from 20um -500nm.The shape of the particles is rocky in structure and they are well separated from each other, where no coagulation is noticed [52]. The SEM images for

sample RS and FS show the different magnification such as 5µm, 2µm, 1µm and 10µm in 5.5.1(a,b,c,d) and Fig 5.5.2 (a,b,c,d) respectively.

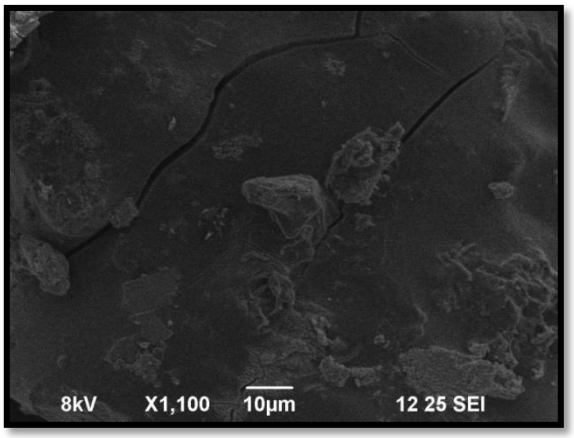

Fig 5.5.1(a)

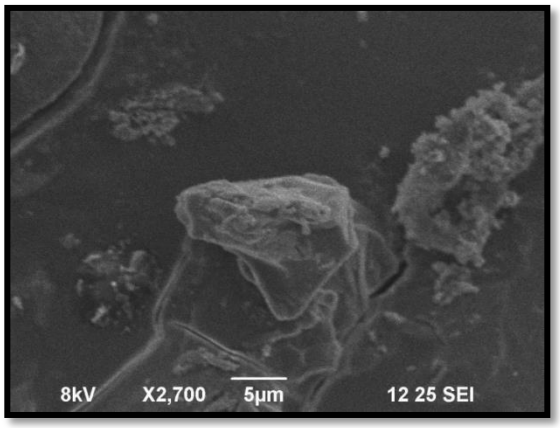

Fig 5.5.1 (b)

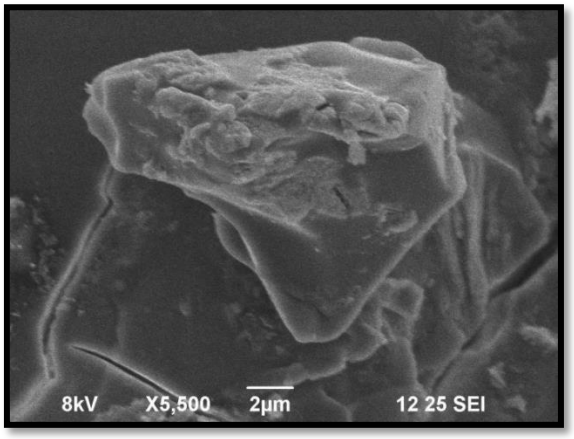

Fig 5.5.1 (c)

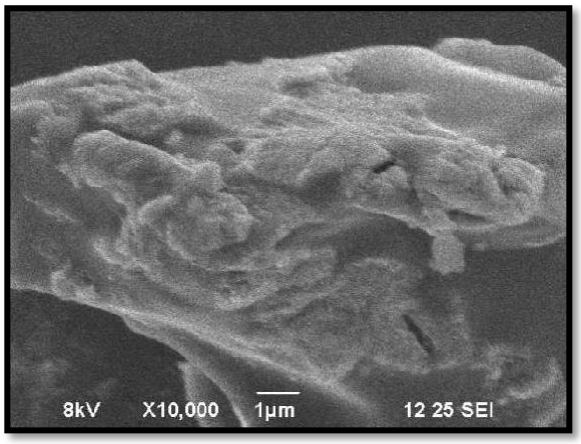

Fig 5.5.1 (d)

Fig 5.5.1 a, b, c, d SEM images of RS at various magnifications such as 10µm, 5 µm, 2 µm, and 1µm.

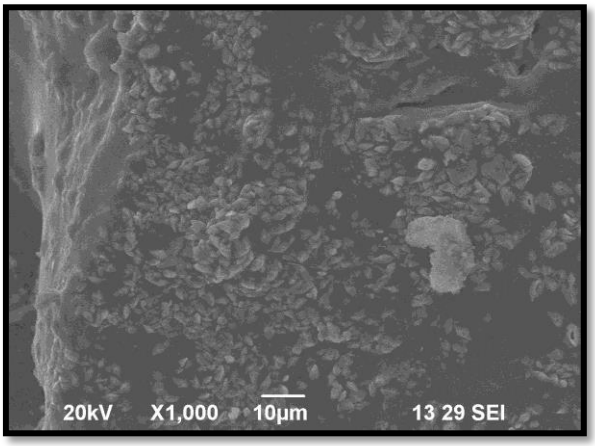

Fig 5.4.2(a)

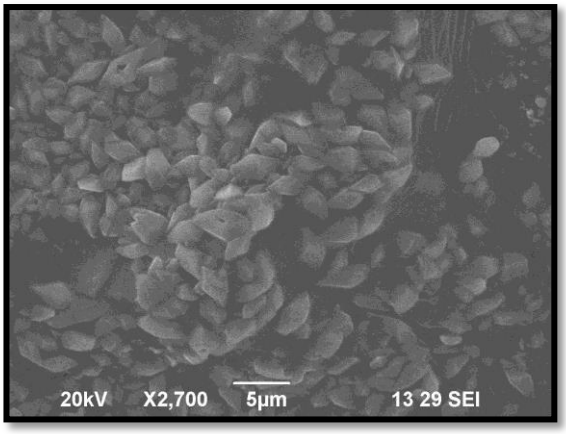

Fig 5.4.2(b)

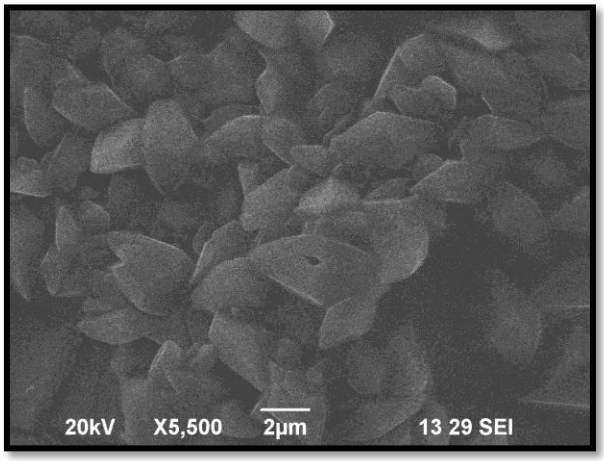

Fig 5.4.2(a)

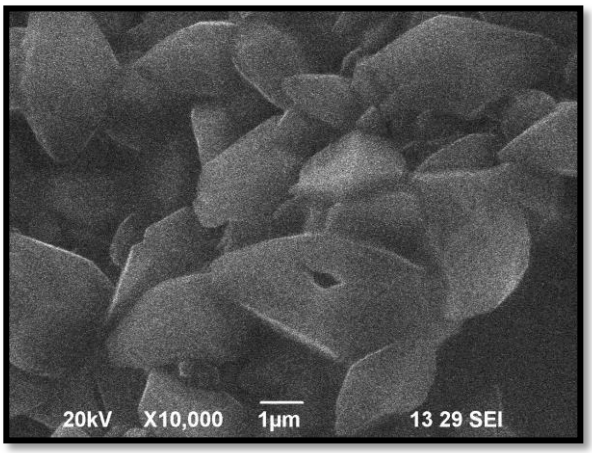

Fig 5.4.2(a)

Fig 5.4.2 a, b, c, d SEM images of FS at various magnifications such as 10µm, 5µm, 2µm, and 1µm.

5.5. EDAX Analysis

The composition of Hydrogels in two samples is idenfied by the Energy Dispersive X-Ray Spectroscopy (EDAX) in Fig 5.5.1 & 5.5.2. The results clearly indicate the presence of the elements Carbon in high concentration compare to others.

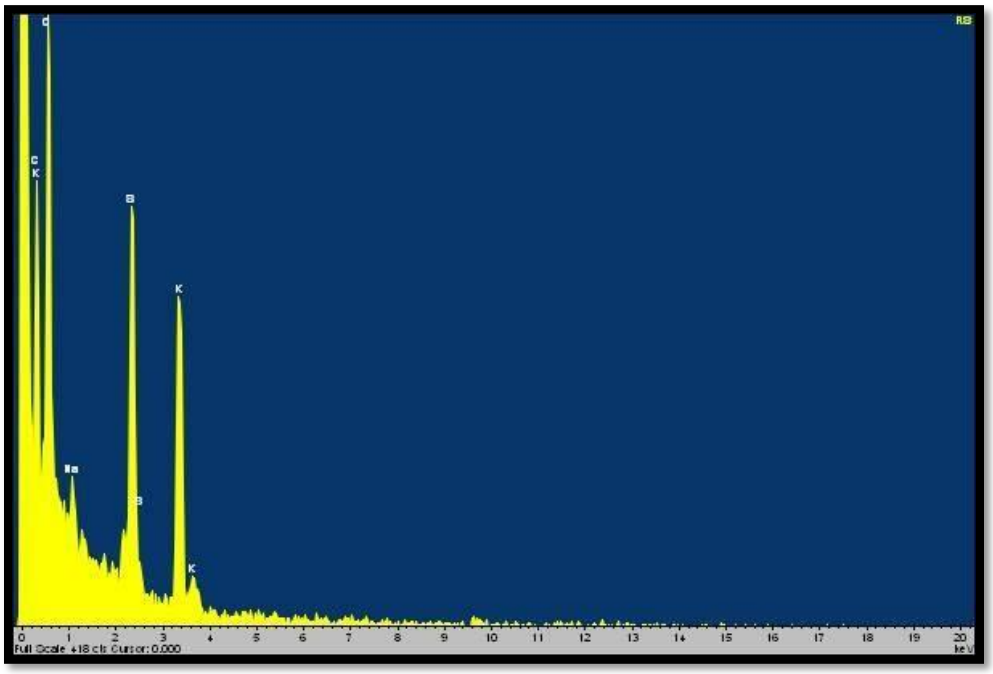

Fig 5.5 (a) EDAX for RS

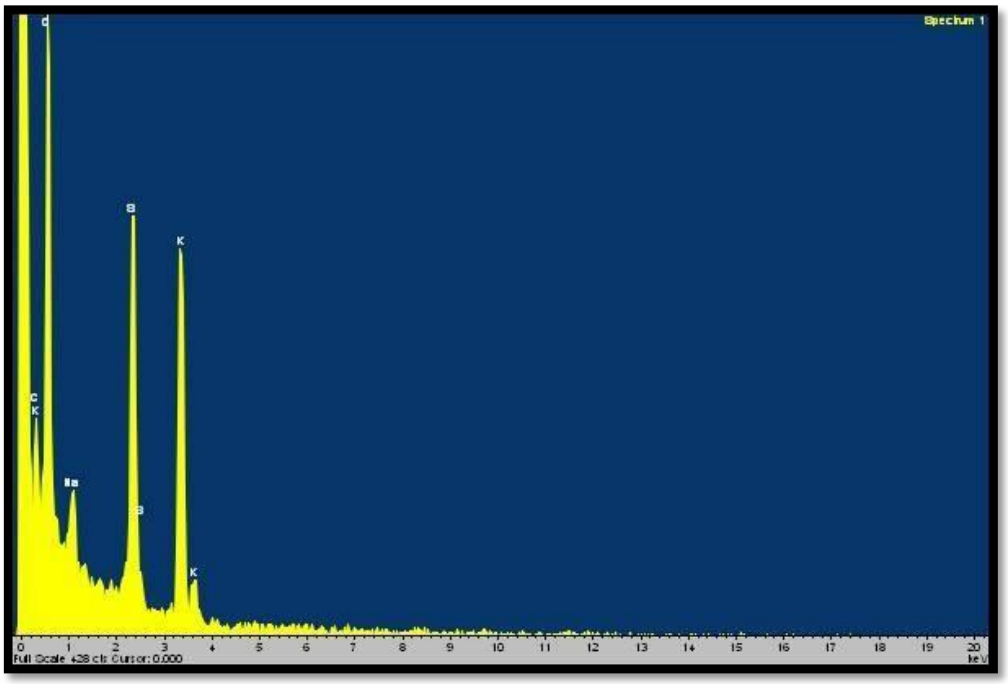

Fig 5.5 (b) EDAX for FS

5.7. Absorption capacity

Absorbing capacity of the RS & FS Hydrogels were measured and analyzed. The results indicate that RS have the lowest absorbing capacity at 6.9517 g/g compared to FS. FS has a slightly higher absorbing capacity at 7.4074 g/g compared to RS, indicating FS is the best absorbing material compared RS.

Table 5.7 Comparison of Absorption Capacity for RS & FS

S. No	Time(min)	RS	FS
1	1	3.1225	3.1415
2	5	5.0998	4.5958
3	10	5.8331	6.1053
4	20	6.7597	6.9709
5	30	6.9517	7.4074

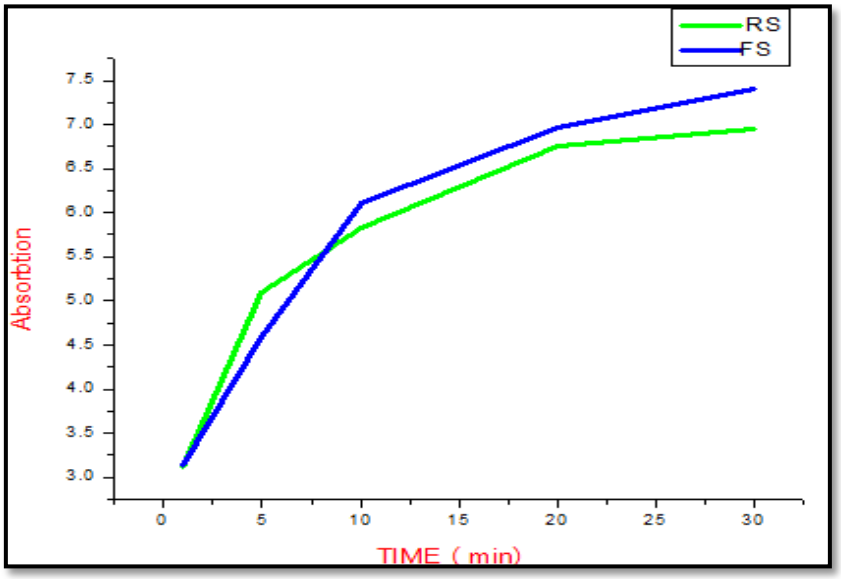

Fig 5.7 Absorption capacity for RS &FS

5.8. Swelling Ratio

Swelling capacity of RS and FS MPH measures the ability to swell inside a known amount of solution. It is determined by the amount of solution that can absorbed by it. While FS has the lowest swelling capacity no matter in a longer or shorter period of time . This result is different from the absorbing capacity result, in which RS has the highest absorbing capacity. Theresults are not comparable because of the different swelling mechanism of RS and FS. While the swelling mechanism of RS and FS seeds depends on the presence of hydrophilic functional groups cross-linking levels, porosity of the polymers and network flexibility [53].

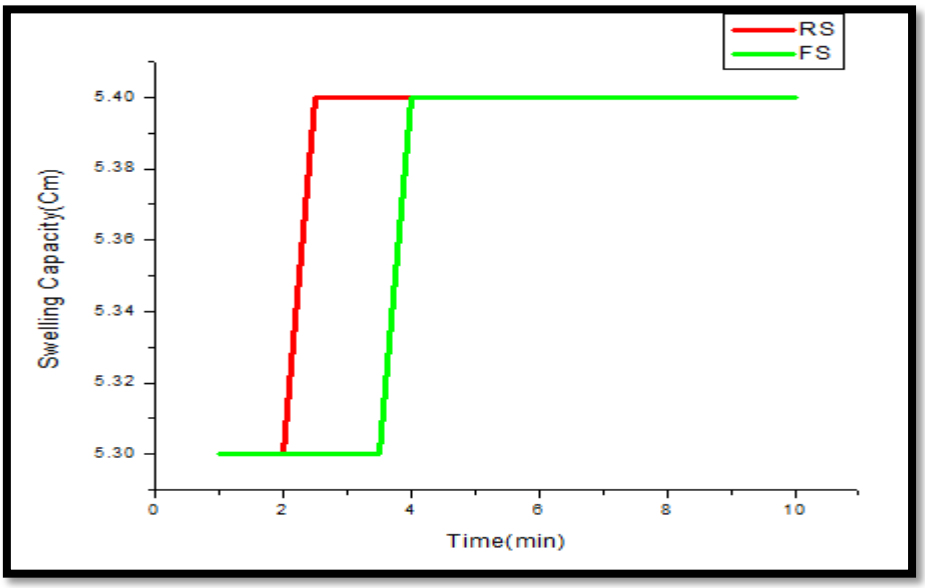

Fig 5.8 Swelling capacity of RS & FS

5.9 Antibacterial activity

5.9.1. Composition of Muller Hinton Agar Media

Beef Extract : 02.00 g

Acid Hydrolysate of Casein : 17.50 g

Starch : 01.50g

Agar : 17.00 g

PH : 7.3 0.1

Table 5.9 Antibacterial Activity of RS and FS

Test Pathogens	**Zone of inhibition (mm)**		
	Ampicillin (Std)	**RS**	**FS**
Escherichia coli	14	10	11
Staphylococcus aureus	15	11	9
Bacillus subtilis	12.5	10	16.5
Bacillus cereus	20.5	9	13.5
Pseudomonas aeruginosa	14	13	14.5

Both Gram negative (*Pseudomonas aeruginosa and Escherichia coli)* and Gram positive (*Staphylococcus aureus, Bacillus subtilis, Bacillus cereus)* bacteria were used for this study. On comparing both samples, the sample FS shows higher anti bacterial activity than the sample RS for *Pseudomonas aeruginosa, Escherichia coli, Bacillus subtilis and Bacillus cereus*. For *Staphylococcus aureus*, the sample RS have high activity than FS. Among the five pathogens, *Bacillus subtilis* shows the maximum inhibition up to 16.5mm for FS.

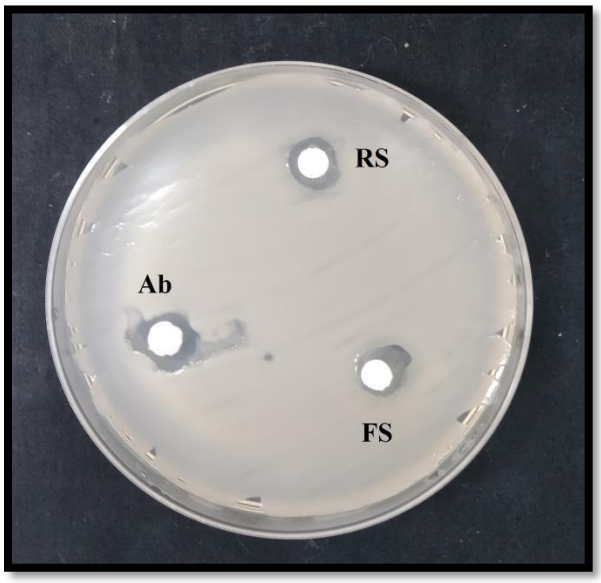

Fig 5.9 (a)

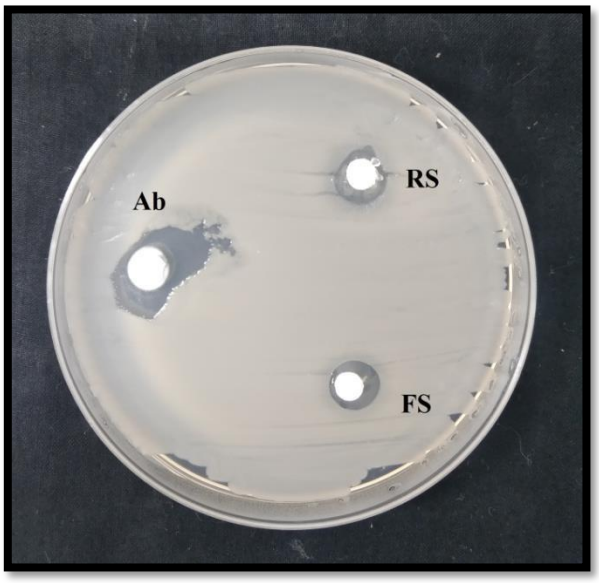

Fig 5.9 (b)

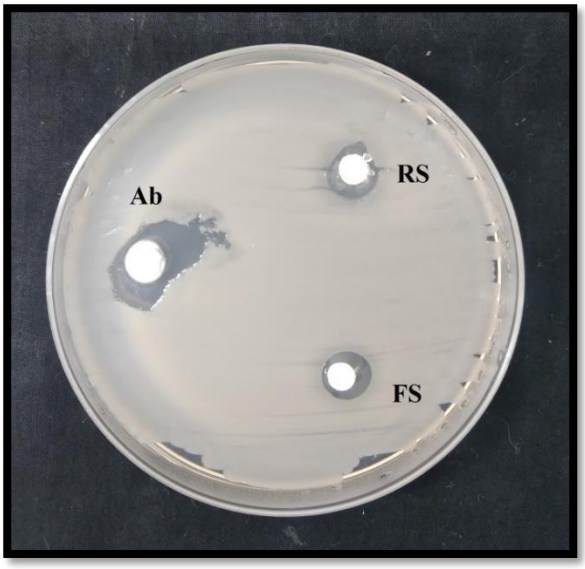

Fig 5.9 (c)

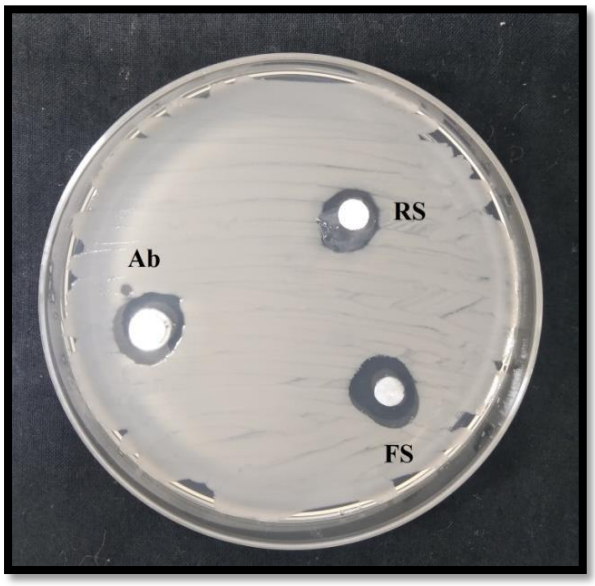

Fig 5.9(c)

The Fig 5.9 a, b, c, d shows, *Escherichia coli, Staphylococcus, Bacillus subtilis, Pseudomonas aeruginosa*

CHAPTER 6

CONCLUSION

Hydrogel were synthesized by green method using natural sources Almond gum and Flax seed. Hydrogel was characterized by UV, FTIR, and SEM with EDAX, TGA, and XRD. And also determine the Microbial activity of Hydrogel nanoparticle using by Antibacterial activity (Disc diffusion method).

- The UV-Visible absorption peaks indicates σ- π^*, π-π^* transition state of RS and FS.
- The FT-IR Studies shows O-H stretching ,Aromatic skeletal ,polysaccharide in the sample RS and FS
- In XRD shows the synthesized Hydrogels amorphous as well as crystalline in nature. The crystalline size of RS and FS is 2.4280nm and 2.4315nm respectively. So that it confirms the hydrogel synthesized is in nanosize.
- TGA found the thermal stability of hydrogel. In FS first stage of weight loss at 26.1% and the second stage of weight loss 22.0%. RS First stage of weigh loss 26.3%, the second stage of weight loss 35.8%.
- The SEM results shows surface morphology of RS and FS have a flax and flower bud.
- EDAX analysis found carbon, oxygen element present in the RS & FS.
- The antibacterial activity explains clearly that the prepared RS & FS has inhibition with the 5 pathogens studied.
- The synthesized hydrogel have significant properties, such as mechanical strength, biocompatibility, biodegradability, swelling capacity, and absorbing capacity.
- The synthesized hydrogel was used for deliver drugs or cells, regenerate hard and soft tissues, adhere to wet tissues, prevent bleeding, provide contrast during imaging, protect tissues or organs during radiotherapy, and improve the biocompatibility of medical implants.

sCHAPTER 7

REFERENCE

[1] Vasanthi Sethu et al, "*Performance study of chia seeds, chia flour and Mimosa pudica hydrogel as polysaccharide-based superabsorbent polymers for sanitary napkins"* Materials Today Communications https://doi.org/10.1016/j.mtcomm.2020.101712, **2020.**

[2] K. Kabiri, M. Zohuriaan-Mehr, "*Superabsorbent hydrogel composites"*, Polymer Advanced Technology, https://doi.org/10.1002/pat.356, **2003**.

[3] S. Kiatkamjornwong, et al, "*Synthesis and property characterization of cassava starchgrafted polyacrylamide-co-(maleic acid) superabsorbent via γ-irradiation*", Polymer 43 3915– 3924, https://doi. org/10.1016/s0032-3861, **2002.**

[4] K.Buchanan, Hird, T. Letcher, *"Cross linked poly sodium acrylate Hydrogel"*, Polymer. Bull. 15(4). https://doi.org/10.1007/bf00254851, **2006.**

[5] A. Zamani et al, "*Extraction and precipitation of chitosan from cell wall of zygomycetes Fungi by dilute sulfuric acid"*, Biomacromolecules 3786–3790, https://doi.org/10.1021/ bm700701, **2007.**

[6] L.P´erez-´Alvarez et al, "*Polysaccharide-based superabsorbent: synthesis, properties, and applications"*. Polymers and Polymeric Composites: A Reference Series,1393–1431, https://doi.org/10.1007/ 978-3-319-77830-3 ,**2019**.

[7] T.Yoshimura et al, "*Synthesis and characterization of novel biodegradable superabsorbent Hydrogels based on chitin and succinic anhydride"*, Carbohydr. Polym. 61 (3) 322–326, https: //doi.org/10.1016/j. carbpol.**2005**.

[8] J. Dutkiewicz, "*Superabsorbent materials from shellfish waste*?" A review,J. Biomed.Mater. Res.63 (3) 373–381, https://doi.org/10.1002/jbm.10231,**2002.**

[9] Xue-Qiang Zha et al, "*Research progress on polysaccharide/protein Hydrogels: Preparation method, functional property and application as delivery systems for bioactive ingredients*" Kang doi.org/10.1016/j.foodres.2021.110542, **2021.**

[10] G. Muhammad et al, Polysaccharide based superabsorbent hydrogel from Mimosa pudica: swelling–deswelling and drug release, RSC Adv. 6(28)23310–23317, https://doi.org/10.1039/c5ra23088h, **2016**.

[11] R. Marineli et al, "*Antioxidant potential of dietary chia seed and oil (Salvia hispanica L.) inducedobeserats,Food",*Res.Int.766667667https://doi.org/10.1016/j.foodres.2015.07.039, **2015**.

[12] A. Pourjavadi et al, "*Optimization of synthetic conditions CMC-g-poly (acrylic acid)/Celite composite superabsorbent by Taguchi method and determination of its absorbency under load"*, Express Polym. Lett. 1 (8) 488–494, https://doi.org/10.3144/expresspolymlett.2007.69, **2007**

[13] J. Febrianto et al, "*Equilibrium and kinetic studies in adsorption of heavy metals using biosorbent: a summary of recent studies"*, J. Hazard. Mater.162 (2–3) 616–645, https://doi.org/ 10.1016/j.jhazmat.2008.06.042,**2009**.

[14] F. Bouaziz et al, "*Purification, structural data and biological properties of polysaccharide from Prunus amygdalus gum"*, Int. J. Chem. Tech Res. 50 578–584, **2014.**

[15] Sébastien Cambier et al, "*Exploration of the co-structuring and stabilising role of flaxseed gum in whey protein isolate based cryo-hydrogels",* Microbiol.74 4264–4270, **2008**.

[16] Yoshimura et al, "*Synthesis and characterization of novel biodegradable superabsorbent hydrogel based on chitin and succinic anhydride"*, Carbohydr. Polym. 61 (3) 322–326, https://doi.org/10.1016/j. carbpol.2005.06.014, **2005.**

[17]. Fruitworldmedia, "*A Genius Solution For Fighting Drought In Fruit Production"* – Fruitworldmedia [online] Available at: https://fruitworldmedia.com/index.php/ featured/genius-solution-fighting-drought-fruit-production/ [Accessed 2 May 2020], **2017**.

[18] S. Siebrecht et al, "*What's happening in the Chia Market?"* [Online] NewFoodMagazine. Available at: https://www.newfoodmagazine.com/article/96460/the-chia-market / [Accessed 28 July 2020], **2019**.

[19] T. Pongjanyakul et al, "*Xanthan–alginate composite gel beads: molecular interaction and in vitro characterization",* Int.J.Pharm.331(1) 61–71, https://doi.org/10.1016/j.ijpharm.2006.09.011 **2006**.

[20] M. Cerqueira et al, "*A. Vicente, Structural and thermal characterization of galactomannans from non-conventional sources"*, Carbohydrate. Polym. 83 (1) 179–185, https://doi.org/ 10.1016/j.carbpol.2010.07.036,**2011**.

[21] Emiliano Carretti et al, "*A new family of high viscosity polymeric dispersions for cleaning easel paintings*", Journal of Cultural Heritage, https://doi.org/10.1016/j.culher.2010.04.002, **2010**.

[22] K. Lee, E.A. Silva, D.J. Mooney, "*Growth factor delivery-based tissue engineering: general approaches and a review of recent developments"*, J. R. Soc. Interface 8153–170, https://doi.org/10.1098/rsif.2010.0223, **2011**.

[23] A.M. Ziemba, R.J. Gilbert, "*Biomaterials for local, controlled drug delivery to the injured spinal cord"*, Front. Pharmacol. 8 1–20, https://doi.org/10.3389/ fphar.2017.00245, **2017.**

[24] J. Elisseeff et al, "*Controlled-release of IGF-I and TGF-b1 in a photopolymerizing hydrogel for cartilage tissue engineering"*, J.Orthop. Res.19 1098–1104, https://doi.org/10.1016/S0736-0266(01)00054-7, **2001**.

[25] Xiaoqun Zhu et al.,"*Preparation of shaped non-polyelectrolyte hydrogel particles withdecomposable and recyclable performance by vortex ring freezing"* Journal of Industrial and Engineering Chemistry, https://doi.org/10.1016/j.jiec.2021.07.039,**2021.**

[26] Vasanthi Sethu et al.," *Performance study of chia seeds, chia flour and Mimosa pudica hydrogel as polysaccharide-based superabsorbent polymers for sanitary napkins*" Materials Today Communications , https://doi.org/10.1016/j.mtcomm.2020.101712 ,**2020**

[27] Bo Jiang et al .,*"Preparation of gelatin/poly (γ-glutamic acid) hydrogels with stimulated response by hot-pressing preassembly and radiation cross linking*" Materials Science & Engineering C ,https://doi.org/10.1016/j.msec.2020.111259, **2020.**

[28] Bao Zhang at al "*Preparation, characterization, and encapsulation capability of the hydrogel cross-linked by esterified tapioca starch*",International Journal of Biological Macromolecules, https://doi.org/10.1016/j.ijbiomac.2020.03.141 **2020.**

[29] Hirofumi Satani, at al.,*"Simple and environmentally friendly preparation of cellulose hydrogelsusinanionicliquid"*Pre-proof,https://doi.org/10.1016/j.carres.2020.108054,**2020.**

[30] Andrew Zannettinob et al.,*"Hydrogel-based preparation of cell aggregates for biomedical applications"* Food Research International , https://doi.org/10.1016/j.foodres.2021.110542 ,**2020.**

[31] Changkun Liu et al.,"*Simple preparation of external-shape and internal-channel size adjustable porous hydrogels by fermentation for efficient solar interfacial evaporation"* industrialandEngineeringChemistry,https://doi.org/10.1016/j.jiec.2021.07.039,**2020.**

[32] Osman Duman, et al *"Preparation and characterization of environmentally friendly agar/κ-carrageenan/montmorillonite nanocomposite hydrogels"* Carbohydrate Polymers, https://doi.org/10.1016/j.carbpol.2018.05.033, **2020.**

[33] N.Ramadhan et al "*Preparation of Chitosan-EDTA hydrogel as soil conditioner for soybean plant(Glycine max)"*, Journal of Water Process Engineering, https://doi.org/10.1016/j.jwpe.2018.04.018,**2019.**

[34] Yasuhiko Tabata et al., "*Preparation of fibrin hydrogels to promote the recruitment of anti-inflammatory"* Applied Materials Today, https://doi.org/10.1016/j.apmt.2020.100747**, 2019.**

[35] Kyoung Min Lee et al*., "One-step preparation of hydrogel particles that show rapid detection of hydrogen peroxide: The dual role of new methylene blue"* Solar Energy https://doi.org/10.1016/j.solener.2020.08.038, **2019.**

[36] Danyuan Xu et al .,"*Facile preparation of biomass lignin-based hydroxyethyl cellulose super-absorbent hydrogel for dye pollutant removal"* Colloids and Surfaces A, https://doi.org/10.1016/j.colsurfa.2020.124987, **2019**

[37] Toshihisa Mizunoa, et al.,"*Synthesis and characterization of chemically-reactive solubilization surfactants for membrane proteins and preparation of membrane protein hydrogel microfibers"* Groundwater for Sustainable Development https://doi.org/10.1016/j.gsd.2019.100277 **,2019.**

[38] Anna Marinopouloua, et al*., "Preparation of model starch complex hydrogels" Amylose can form molecular inclusion complexes by forming a helix around ligands and thus protecting*

them and increasing their bioavailability, International Journal of Biological Macromolecules, https://doi.org/10.1016/j.ijbiomac.2019.06.234,**2019.**

[39] Dhamodharan Raghavachari et al.,*"Facile preparation of biocompatible macroporous chitosan hydrogel by hydrothermal reaction of a mixture of chitosan-succinic acid-urea"* Colloid and Interface Science Communications**,** https://doi.org/10.1016/j.colcom.2019.100199**2019.**

[40] Jianping Deng et al "*Chiral, thermal-responsive hydrogels containinghelicalhydrophilic polyacetylene: preparation andenantiodifferentiatingrelease ability*" Colloids and Surfaces A Colloids and Surfaces A**,** https://doi.org/10.1016/j.colsurfa.2019.123783**201**

[41] Junli Ren et al .,"*A one-pot strategy for preparation of high-stren strength carboxymethyl xylan-g-poly(acrylic acid) hydrogels with shape memory property*" Chemical Engineering Journal, https://doi.org/10.1016/j.cej.2019.122048,**2019.**

[42] Yu Chen et al .,"*Preparation of chitosan-Cu2+/NH3 physical hydrogel and its properties"* **,** Food Hydrocolloids, https://doi.org/10.1016/j.foodhyd.2019.05.046**2019.**

[43] Andrew Zannettinob et al.,"*Hydrogel-based preparation of cell aggregates for biomedical applications",* Materials Science & Engineering C, https://doi.org/10.1016/j.msec.2019.109845, **2018.**

[44] Alireza Shakeria et al *.,"Preparation of polymer-carbon nanotubes composite hydrogel and its application as forward osmosis draw agent*" Polymer Chemistry, DOI: 10.1039/x0xx00000x , **2018**.

[45] V. Jaisankar et al., *"An eco-friendly synthesis, characterisation and antibacterial applications of novel almond gum – poly(acrylamide) based hydrogel silver nanocomposite"* Journal of Colloid and Interface Science, https://doi.org/10.1016/j.jcis.2018.12.023, **2017.**

[46] Hiroki Hashimoto, et al, *Preparation of chitosan hydrogel and its solubility in organic acids",* International Journal of Biological Macromolecules, https://doi.org/10.1016/j.ijbiomac.2019.03.011, **2017**.

[47] Y. Zuo, J. Gu, L. Yang, Z. Qiao, H. Tan, Y. Zhang, Int. J. Preparation and characterization of dry method esterified starch/polylactic acid composite materials Biol. Macromol. 64 174–180**, 2014.**

[48] X.-M. Li, J. Zhu et al Fabrication and characterization of pickering emulsions stabilized by octenyl succinic anhydride -modified gliadin nanoparticle, Food Hydrocoll. 90 19–27, **2019.**

[49] B. Zhang, B. Wei et al, Preparation and characterization of carboxymethyl starch microgel with different crosslinking densities Carbohydr. Polym. 124 245–253, **2015.**

[50] J. Sahari, S.M. Sapuan, E.S. Zainudin, M.A. Maleque, Carbohydr. Polym. Thermmechanical behaviors of thermoplastic starch derived from sugar palm tree (*Arenga pinnata*) 92 1711–1716**, 2013**.

[51] H. Liu et al, Facile fabrication of redox/pH dual stimuli responsive cellulose hydrogel Carbohydr. Polym. 176 299–306, **2017**.

[52] F. Alavi et al,, Cold gelation of curcumin loaded whey protein aggregates mixed with k-carrageenan: Impact of gel microstructure on the gastrointestinal fate of curcumin Food Hydrocoll. 85 267–280,**2018.**

[53] L.F. Wang **et al**,, S.Y. Pan, H. Hu, W.H. Miao, X.Y. Xu, Synthesis and properties of carboxymethyl kudzu root starch Carbohydr. Polym. 80 174–179, **2010.**

[54] J.R. Dontulwar et al,, An esteric polymer synthesis and its characterization using starch, glycerol and maleic anhydride as precursor Carbohydr. Polym. 65 207–210**, 2006**.

[55] J. Chen et al, The synergistic gelation of okra polysaccharides with kappa-carrageenan and its influence on gel rheology, texture behaviour and microstructures Food Hydrocoll. 87 425– 435**,** 2019**.**

[56] B. Biduski et al, Starch hydrogels: The influence of the amylose content and gelatinization method Int. J. Biol. Macromol. 113 443–449, **2018.**

[57] Gao-Xin Xu et al., *"Preparation, characterization, and encapsulation capability of the hydrogel cross-linked by esterified tapioca starch*" International Journal of BiologicalMacromolecules https://doi.org/10.1016/j.ijbiomac.2020.03.141,**2020**